TURUN
YLIOPISTO
UNIVERSITY
OF TURKU

New Molecular Mechanisms in Castration-Resistant Prostate Cancer

Verneri Virtanen

TURUN YLIOPISTON JULKAISUJA – ANNALES UNIVERSITATIS TURKUENSIS
SARJA – SER. D OSA – TOM. 1955 | MEDICA – ODONTOLOGICA | TURKU 2026

TURUN
YLIOPISTO
UNIVERSITY
OF TURKU

NEW MOLECULAR MECHANISMS IN CASTRATION-RESISTANT PROSTATE CANCER

Verneri Virtanen

TURUN YLIOPISTON JULKAISUJA – ANNALES UNIVERSITATIS TURKUENSIS
SARJA – SER. D OSA – TOM. 1955 | MEDICA – ODONTOLOGICA | TURKU 2026

University of Turku

Faculty of Medicine
Institute of Biomedicine
Department of Medical Biochemistry and Genetics
Turku Doctoral Programme of Molecular Medicine (TuDMM)

Supervised by

Docent Maria Sundvall, M.D., Ph.D.
Cancer Research Unit, Institute of Biomedine
University of Turku and
Department of Oncology
Turku University Hospital
Turku, Finland

Reviewed by

Docent Ville Paakinaho, Ph.D.
Institute of Biomedicine
University of Eastern Finland
Kuopio, Finland

Docent Tuomas Mirtti, M.D., Ph.D.
Finnish Cancer Institute and
Helsinki University Hospital
Department of Pathology
Helsinki, Finland

Opponent

Professor Cory Abate-Shen, Ph.D.
Department of Molecular Pharmacology and Therapeutics
Columbia University
New York, NY, United States

The originality of this publication has been checked in accordance with the University of Turku quality assurance system using the Turnitin OriginalityCheck service.

ISBN 978-952-02-0582-9 (PRINT)
ISBN 978-952-02-0583-6 (PDF)
ISSN 0355-9483 (Print)
ISSN 2343-3213 (Online)
Painosalama, Turku, Finland 2026

UNIVERSITY OF TURKU
Faculty of Medicine
Institute of Biomedicine
Department of Medical Biochemistry and Genetics
VERNERI VIRTANEN: New molecular mechanisms in castration-resistant prostate cancer
Doctoral Dissertation, 179 pp.
Turku Doctoral Programme of Molecular Medicine (TuDMM)
May 2026

ABSTRACT

Prostate cancer (PCa) is a major cause of cancer morbidity and mortality among men. Common therapy involves the reduction of circulating androgens to castrated levels. However, after the initial response, PCa eventually starts growing despite castrate levels of androgens, thereby becoming castration-resistant PCa (CRPC). There are no curative treatments for CRPC, and once PCa develops metastases, it becomes lethal. Therefore, elucidating the mechanisms of survival, growth, and metastasis in CRPC is necessary to develop improved therapies against CRPC.

In this thesis, I have investigated new molecular mechanisms in CRPC, specifically, the interplay between androgen receptor (AR) signaling and BRCA1, the role of the BRCA1 protein in PCa, and metastasis formation regulation by the stress fiber contraction regulator caldesmon (CaD). We described AR-mediated activation of NRF2 via BRCA1 in CRPC by assaying PCa cell lines, murine xenografts, and patient samples. Moreover, this study showed that the dynamic regulation of BRCA1 by AR signaling may predispose to genetic alterations and promote castration resistance via enhanced reactive oxygen species defense. Additionally, we found that silencing *CALD1* reduced metastasis in zebrafish PCa xenografts and spheroids in 3D culture. Our experimental and bioinformatic analyses suggest that CaD correlates with metastasis-associated epithelial-to-mesenchymal transition in PCa. We discovered that antiandrogen resistance gives rise to cell populations expressing CaD and glucocorticoid receptor (GR), and found that GR upregulated CaD in PCa using a castration-resistant murine xenograft. Furthermore, we explored the potential for CaD as a drug target by characterizing a *cald1* mutant zebrafish, which exhibited a non-lethal phenotype with a mild neural defect.

This thesis demonstrated that different AR signaling states have the capacity to induce transient genomic instability and enhance defense against ROS via regulation of *BRCA1* and BRCA1-mediated NRF2-activation. In this thesis, we have also identified the oncogenic properties of CaD as a mediator of PCa metastasis. Additionally, we found that *cald1* mutations were tolerated and non-lethal in early zebrafish development, suggesting potential for CaD as a drug target.

KEYWORDS: Castration-resistant prostate cancer, metastasis, personalized medicine, caldesmon, BRCA1, DNA repair

TURUN YLIOPISTO
Lääketieteellinen tiedekunta
Biolääketieteen laitos
Lääketieteellinen biokemia ja genetiikka
VERNERI VIRTANEN: Kastraatioresistentin eturauhassyövän uudet molekyylimekanismit
Väitöskirja, 179 s.
Molekyylilääketieteen tohtoriohjelma
Toukokuu 2026

TIIVISTELMÄ

Eturauhassyöpä aiheuttaa merkittävää sairastavuutta ja kuolleisuutta. Yleinen hoito perustuu miessukuhormonien laskemiselle kastraatiotasolle. Alkuvaiheen jälkeen eturauhassyöpä kuitenkin saa kyvyn kasvaa kastraatiotasosta huolimatta. Kastraatioresistenttiin eturauhassyöpään ei ole parantavia hoitoja. Etäpesäkkeitä kehittänyt tauti on kuolemaan johtava sairaus. Siksi on tärkeää selvittää tekijöitä, jotka mahdollistavat kastraatioresistentin syövän kasvun ja etäpesäkkeiden muodostumisen. Näiden mekanismien tunteminen on edellytys tehokkaampien hoitojen kehittämiselle.

Tässä väitöskirjassa selvitin uusia molekyylimekanismeja kastraatioresistentissä eturauhassyövässä, erityisesti miessukuhormonireseptori-signaloinnin ja BRCA1:n vuorovaikutusta, BRCA1-proteiinin roolia eturauhassyövässä sekä caldesmonin (CaD) roolia etäpesäkkeiden muodostumisessa. Osoitimme miessukuhormonin aktivoivan NRF2:a BRCA1-välitteisesti hyödyntämällä solumalleja, hiiri-xenografteja ja potilasnäytteitä. Tutkimuksemme osoitti, että BRCA1:n dynaaminen säätely eturauhassyövässä voi altistaa geneettisille muutoksille ja edistää kastraatioresistenssiä antioksidanttipuolustuksen kautta. *CALD1*:n hiljentäminen eturauhassyöpäsoluissa vähensi niiden kykyä muodostaa etäpesäkkeitä seeprakala-xenografteissa sekä pienoiskasvaimia 3D-ympäristössä. Havaitsimme, että CaD osallistuu säätelemään muutosta epiteelisoluista mesenkymaalisoluiksi. Havaitsimme kastraatioresistentteissä hiiri-xenografteissa solupopulaatioita, jotka ilmensivät sekä CaD:a että glukokortikoidireseptoria (GR). Lisäksi osoitimme, että GR säätelee CaD:n ilmentymistä eturauhassyövässä. Kuvailimme myös *cald1*-mutaatioiden vaikutukset seeprakalassa. Mutanttien fenotyyppi ei ollut letaali ja ilmentyi korkeintaan lievänä hermoston kehityshäiriönä.

Tässä väitöskirjassa tunnistettiin, että erilaiset miessukuhormoni-signaloinnin tilat voivat aiheuttaa ohimenevää geneettistä epävakautta ja vahvistaa antioksidanttipuolustusta BRCA1:n ja NRF2-aktivoinnin kautta. Lisäksi väitöskirja osoitti CaD:n aiheuttavan etäpesäkkeitä eturauhassyövässä ja että seeprakalat sietävät hyvin *cald1*-mutaatioita varhaisessa kehityksessä, mikä viittaa CaD:n olevan mahdollinen lääkekohde.

AVAINSANAT: Kastraatioresistentti eturauhassyöpä, yksilöllistetty lääketiede, caldesmon, BRCA1, etäpesäkkeet, DNA:n korjaus

Table of Contents

Abbreviations

AD	androgen deprivation
ADT	androgen deprivation therapy
AKT	protein kinase B
ANOVA	analysis of variance
AP-N	aminopeptidase N
AR	androgen receptor
ATM	ataxia telangiectasia mutated
ATP	adenosine triphosphate
ATR	ataxia telangiectasia and Rad3-related
BCR	biochemical recurrence
BMI1	B lymphoma Moloney murine leukemia virus insertion region 1
BSA	bovine serum albumin
BRCA1	breast cancer type 1 susceptibility protein
BRCA2	breast cancer type 2 susceptibility protein
BRD4	bromodomain-containing protein 4
CaD	caldesmon
CAF	cancer-associated fibroblast
CAMKK2	calcium/calmodulin-dependent kinase kinase 2
cAMP	cyclic adenosine monophosphate
CAR	chimeric antigen receptor
CARN	castration-resistant Nkx3.1-expressing cell
CBP	cAMP response element-binding-binding protein
CDK1	cyclin-dependent kinase 1
CDK2	cyclin-dependent kinase 2
CDK8	cyclin-dependent kinase 8
CENPF	centromere protein F
cGMP	cyclic guanosine monophosphate
ChIP-seq	chromatin immunoprecipitation sequencing
CITED2	CBP/p300-interacting transactivator 2
CNA	copy number alteration
COMPASS	complex of proteins associated with Set1

CPT-1a	carnitine palmitoyltransferase-1a
CRISPR	clustered regularly interspaced short palindromic repeats
CRPC	castration-resistant prostate cancer
CTC	circulating tumor cell
ctDNA	circulating tumor DNA
CtIP	C-terminal–binding protein–interacting protein
CYP17A1	cytochrome P450 steroid 17α-hydroxylase
CXCL	C-X-C motif chemokine ligand
CXCR	C-X-C motif chemokine receptor
DAB2IP	disabled homolog 2-interacting protein
DDR	DNA damage response
DHEA	dehydroepiandrosterone
DHT	dihydrotestosterone
DMEM	Dulbecco's modified Eagle's medium
DMSO	dimethyl sulfoxide
DNMT	DNA methyltransferase
EAU	European Association of Urology
ECM	extracellular matrix
EED	embryonic ectoderm development
EMT	epithelial-to-mesenchymal transition
ERG	E26 transformation-specific–related gene
ERK	extracellular signal-regulated kinase
ETS	E26 transformation-specific
EZH2	enhancer of zeste homolog 2
FDG	fluorodeoxyglucose
FGF	fibroblast growth factor
FTH1	ferritin heavy chain 1
FOXA1	forkhead box protein A1
FOXM1	forkhead box protein M1
FOXO1	forkhead box protein O1
GO:BP	Gene Ontology: Biological Process
GR	glucocorticoid receptor
GSTP1	gluthathione S-transferase P
HGF	hepatocyte growth factor
HIF-1α	hypoxia-inducible factor 1-alpha
HK2	hexokinase 2
HOXB13	homeobox protein B13
HR	homologous recombination
HRP	horseradish peroxidase
h-CaD	high-molecular weight caldesmon

KLK2	kallikrein-related peptidase 2
KMT2D	lysine methyltransferase 2D
LH	luteinizing hormone
LSD1	lysine-specific histone demethylase 1A
l-CaD	low-molecular weight caldesmon
MAPK	mitogen-activated protein kinase
mCRPC	metastatic castration-resistant prostate cancer
MCT	monocarboxylate transporter
MLL	mixed-lineage leukemia
MRI	magnetic resonance imaging
mTOR	mechanistic target of rapamycin
N-MYC	neuroblastoma-derived v-myc avian myelocytomatosis viral related oncogene
NCOA2	nuclear receptor coactivator 2
NDRG3	N-Myc downstream-regulated gene family member 3
NEPC	neuroendocrine prostate cancer
NSD2	nuclear receptor binding SET domain protein 2
NF-κB	nuclear factor kappa-light-chain-enhancer of activated B cells
NRF2	nuclear factor erythroid 2-related factor 2
ONECUT2	one cut homeobox 2
OSR1	protein odd-skipped related 1
PALB2	partner and localizer of BRCA2
PAP	prostatic acid phosphatase
PBRM1	protein polybromo-1
PBS	phosphate-buffered saline
PCa	prostate cancer
PET	positron emission tomography
PI3K	phosphoinositide 3-kinase
PKC	protein kinase C
PKGIβ	protein kinase G type I beta
POU3F2	Pit-Oct-Unc domain, class 3, transcription factor 2
PPP1CA	serine/threonine-protein phosphatase PP1-alpha catalytic subunit
PRC2	polycomb repressive complex 2
PSA	prostate-specific antigen
PSMA	prostate-specific membrane antigen
PTEN	phosphatase and tensin homolog
PTU	1-phenyl-2-thiourea
PTZ	pentylenetetrazole
RAF	rapidly accelerated fibrosaroma
ROS	reactive oxygen species

RNF6	ring finger protein 6
RREB-1	Ras-responsive element-binding protein 1
RTK	receptor tyrosine kinase
RUNX2	runt-related transcription factor 2
SCD-1	stearoyl-CoA desaturase-1
SD	standard deviation
SEM	standard error of the mean
SIAH2	seven in abstentia homolog 2
SMARCA2	SWI/SNF-related matrix-associated actin-dependent regulator of chromatin subfamily A member 2
SMARCA4	SWI/SNF-related matrix-associated actin-dependent regulator of chromatin subfamily A member 4
SOX2	Sex-determining region Y-box 2
SPINK1	serine protease inhibitor Kazal-type 1
SWI/SNF	SWItch/Sucrose Non-Fermentable
TBST	Tris-buffered saline with Tween-20
TET2	Ten-Eleven Translocator 2
TGF-β	transforming growth factor beta
TME	tumor microenvironment
TRIM24	tripartite motif–containing 24
VEGF	vascular endothelial growth factor
Wnt	Wingless/Integrated
ZIP1	zinc transporter 1
ZEB1	zinc finger E-box-binding homeobox 1
ZMYND11	zinc finger Myeloid–Nervy–Deformed Epidermal Autoregulatory Factor 1 type containing 11
γH2Ax	phosphorylated histone H2A.X

Gene names are given using standardized HUGO symbols and not written out in full.

List of Original Publications

This dissertation is based on the following original publications, which are referred to in the text by their Roman numerals:

I Sriraman S*, Virtanen V*, Kukkula A, Toriseva M, Lumiainen A, West G, Poutanen M, Taimen P, Sundvall M. Androgen receptor-mediated regulation of BRCA1 modulates the antioxidant defense in prostate cancer. *The Journal of Pathology*, 2025;267(4): 385–398.

II Virtanen V, Paunu K, Kukkula A, Niva S, Junila Y, Toriseva M, Jokilehto T, Mäkelä S, Huhtaniemi R, Poutanen M, Paatero I, Sundvall M. Glucocorticoid receptor-induced non-muscle caldesmon regulates metastasis in castration-resistant prostate cancer. *Oncogenesis*, 2023; 12(1): 42.

III Virtanen V, Paunu K, Niva S, Sundvall M*, Paatero I*. Effect of caldesmon mutations in the development of zebrafish embryos. *Biochemical and Biophysical Research Communications*, 2023; 669: 10–18.

*Shared contribution. The original publications have been reproduced with the permission of the copyright holders.

1 Introduction

Prostate cancer (PCa) is the most commonly diagnosed cancer among men in Europe and the United States. Its increasing incidence and prevalence largely reflect more sensitive diagnostic practices and increased life expectancy. While many PCas are indolent and unlikely to progress within a patient's lifetime, a subset of cases follows a more aggressive clinical course progressing toward a lethal metastatic disease.

Hormonal therapy, or androgen deprivation therapy (ADT), has been the backbone of systemic treatment for advanced PCa since the discovery in 1941 by Charles Huggins that prostate tumors regress in response to castration or estrogen administration (Huggins & Hodgens, 1941). Although ADT initially induces tumor regression in almost all patients, the disease invariably progresses to a state known as castration-resistant PCa (CRPC), which remains incurable.

CRPC arises through a range of molecular adaptations that allow cancer cells to survive and proliferate despite undergoing ADT. These adaptations involve both genetic and non-genetic mechanisms, including reactivation of androgen receptor (AR) signaling, reprogramming of intracellular pathways, and changes in the tumor microenvironment (TME). Although many of these resistance mechanisms have been well-characterized, several key regulators remain incompletely understood.

This thesis investigates PCa mechanisms at the junction between dynamically progressing AR signaling states and the DNA damage response (DDR), metastasis, and reactive oxygen species (ROS) defense. We discovered that caldesmon (CaD) and breast cancer type 1 susceptibility protein (BRCA1) can contribute to disease progression and the development of resistance at various points during PCa evolution from early lesions to lethal metastatic disease. Specifically, this study explored the regulation of epithelial-to-mesenchymal transition (EMT) and oxidative stress responses and evaluated how these processes contribute to metastasis and resistance to therapeutic targeting of the AR pathway in PCa. Additionally, this study showed the effect of CaD in a broader context of healthy tissues which is necessary to assess its potential in therapeutic settings.

2 Review of the Literature

2.1 Clinical overview of PCa

PCa is a malignancy that arises from transformed epithelial cells within the prostate gland. The prostate is a glandular organ named after the ancient Greek term *prostátēs* (the one standing before), referring to its anatomical location situated immediately anterior to the bladder. The term entered English medical usage in the 17th century (Marx & Karenberg, 2009). The prostate drains into the urethra and encloses the junction between the vasa deferentia, seminal vesicles, and urethra (McNeal, 1981). Epithelial cells are separated by stroma consisting of the extracellular matrix (ECM), fibroblasts, smooth muscle cells, myofibroblasts, endothelial cells of both blood and lymph vasculature, neuronal cells, and immune cells (Tuxhorn et al., 2002).

This chapter outlines PCa epidemiology and management strategies. The molecular background is addressed later in chapters 2.2–6.

2.1.1 Prevalence and clinical heterogeneity of PCa

PCa is estimated to be diagnosed in one in eight men in the United States during their lifetime (Siegel et al., 2025). Autopsy studies revealed that the histologic prevalence of PCa in men under 30 years is 5% and increases by a factor of 1.7 per decade, reaching 59% (CI: 48–71%) in men over 79 years (Bell et al., 2015). These findings underscore the high prevalence of subclinical low-grade indolent PCa. This is further reflected in the excellent prognosis of localized PCa, with a 5-year survival rate exceeding 99%, compared to only 34% for metastatic PCa (Siegel et al., 2025). When including all PCa stages, the 5-year and 10-year survival for the Finnish 2019–2023 cohort in the NORDCAN database were 94.3% and 90.9%, respectively (Engholm et al., 2010). Taken together, these data highlight that high rates of non-lethal disease are being diagnosed and most likely overtreated, whereas therapeutic strategies for aggressive disease remain insufficiently effective.

2.1.2 Etiological factors and risk determinants in PCa

A Nordic prospective twin study estimated the heritability of PCa, defined as the proportion of variance in cancer risk attributable to interindividual genetic differences, at 57% (CI: 51–63%), compared to 33% (CI: 30–37%) for overall cancer risk (Mucci et al., 2016). Hereditary PCa manifests with earlier disease onset whereas the clinical course does not appear to differ from non-hereditary PCa (Hemminki, 2012; Randazzo et al., 2016). However, the extensive genetic heterogeneity of PCa is likely to obscure additional putative differences in phenotype beyond disease onset, as more than 100 common susceptibility loci for aggressive PCa risk have been identified (Amin Al Olama et al., 2015; Gulati et al., 2017).

The most prevalent germline variants linked to PCa risk and aggressivity affect DDR genes and are observed in 4.6% of localized PCa and 11.8% of metastatic PCa with the most commonly affected genes being *BRCA2* (44% of affected DDR genes in metastatic PCa), *ATM* (13%), and *CHEK2* (12%) (Pritchard et al., 2016). The DDR is reviewed in detail in chapter 2.5. Additionally, *HOXB13*, a hox gene family member, is the most commonly germline mutated single gene associated with PCa risk outside DDR genes in PCa, with 1.12% prevalence (Ewing et al., 2012; Karlsson et al., 2014; Kote-Jarai et al., 2015; Lynch et al., 2016; Nicolosi et al., 2019). Hox genes are critically involved in large-scale regulation of anatomical development. Homeobox protein B13 (HOXB13) expression persists in the adult prostate and is not recurrently mutated in other cancers. Furthermore, HOXB13 interacts with the AR (C. Jung et al., 2004; Norris et al., 2009).

Several factors, including smoking, alcohol use, and diet, have been associated with minor changes in PCa risk and prognosis (Kenfield et al., 2016). The significance of environmental context was exemplified by a study showing that immigrating from Japan to the United States resulted in a 3.6-fold increase in the incidence rate of PCa (H. Shimizu et al., 1991). However, no widely accepted dietary recommendations specifically for PCa prevention have been established (Kenfield et al., 2016; Mottet et al., 2021).

Interestingly, several medications targeted at abnormal metabolism, such as SGLT2 inhibitors, which reduce glucose levels, and statins, which reduce LDL cholesterol, have demonstrated a protective effect on the risk of PCa in patients with metabolic morbidities such as type 2 diabetes and atherosclerosis (Van Rompay et al., 2019; J. Zheng et al., 2024). However, glucose levels alone, as measured by HbA1c, have not shown a causative link with PCa risk (J. Zheng et al., 2024). Therefore, the exact PCa-relevant mechanism of action remains unclear. Alternatively, cancer cells may directly express target molecules of these drugs, thus putatively allowing the exertion of metabolic changes at both systemic and cellular level.

Notably, metrics associated with optimal cardiovascular health have also been linked to lower overall cancer incidence (Rasmussen-Torvik et al., 2013). Adherence to favorable lifestyle factors has been estimated to have the potential of preventing up to 36% of early PCa deaths in the highest genetic risk groups (Plym et al., 2024).

2.1.3 Management of localized PCa

Localized PCa is often asymptomatic but may sometimes manifest with lower urinary tract symptoms as a consequence of the expanding tumor altering the urethral flow or by bleeding into the urethra (Wilt & Ahmed, 2013). Digital rectal examination alone can detect 55.8% of primary PCa, including 17.3% that would be missed with prostate-specific antigen (PSA) testing of blood samples alone (Schröder et al., 1998).

PSA is expressed and secreted by luminal cells (discussed in chapter 2.2.1) in response to AR activation (J. Kim & Coetzee, 2004). Although measurement of PSA levels in blood is widely used for PCa detection, it is not specific for cancer as it increases due to benign hyperplasia, and PSA screening is also responsible for overdiagnosis of indolent disease (Etzioni et al., 2002; Grossman et al., 2018). However, PSA level remains an indispensable tool for disease monitoring and follow-up (Lilja et al., 2008). Importantly, PCa can already invade outside the prostate while no symptoms are evident (Rebello et al., 2021). Metastatic disease is discussed in the chapter 2.3.

Risk assessment is based on the histological analysis of tumor tissue by a pathologist who assigns a Gleason score (Gleason & Mellinger, 1974). The ISUP grade group system, which is widely adopted in clinical practice, is directly derived from the Gleason score (Epstein et al., 2016). The European Association of Urology (EAU) risk group for biological recurrence of localized or locally advanced PCa based on ISUP is further adjusted by clinically examined tumor size, location, and spread, as well as serum PSA and possible nodal involvement indicated by computer tomography/bone scan (Cornford et al., 2025).

PCa is a highly heterogeneous disease, both between patients and within individual patients, often marked by multifocality, with multiple distinct tumor foci arising in the same prostate. There is also significant heterogeneity within tumors (Haffner et al., 2021). This emphasizes the importance of acquiring representative samples for histological risk assessment. Notably, magnetic resonance imaging (MRI) improves the selection of biopsy targets and may in some cases help to identify which patients might safely avoid biopsy altogether (Cornford et al., 2024). The improved sensitivity of MRI-targeted biopsy over systematic biopsy is reflected in the fact that patients classified into lower ISUP grades by systematic biopsy have worse survival, suggesting undergrading caused by the underdetection of higher-

grade lesions, which are more reliably identified by MRI-targeted biopsy (Ploussard et al., 2020).

Based on the EAU risk stratification (Cornford et al., 2025) and considering the patient's frailty and life expectancy due to other conditions, patients are assigned to one of the following management strategies: watchful waiting, active surveillance, radical prostatectomy, or radiotherapy (Cornford et al., 2024; Hamdy et al., 2023). In the ProtecT trial, the 15-year PCa–specific mortality was low across active monitoring, surgery, and radiotherapy, highlighting the indolent course of many localized cases and the importance of avoiding overtreatment (Hamdy et al., 2023). Notably, the trial included patients with initial PSA between 3.0–20.0 µg/l, resulting in study groups with 76.3–77.6% Gleason score 6 and 1.8–2.6% Gleason score 8 or higher as determined by systematical biopsies, suggesting that predominantly ISUP 1 cases were included (Lane et al., 2014). At median follow-up of 15 years, the mortality across groups was 2.2–3.1% (Hamdy et al., 2023).

In patients without nodal involvement, radiotherapy is most commonly delivered as external-beam radiotherapy, although it may also be administered as brachytherapy or in combination with ADT. In contrast, in cases of nodal involvement or two of the following criteria in the absence of nodal involvement: extraprostatic extension, ISUP 4–5, or PSA ≥ 40 µg/l, radiotherapy is generally administered in combination with ADT and abiraterone (Cornford et al., 2024). Although surgical treatment in cases of clinically localized PCa usually results in undetectable levels of PSA, some PSA is expected to remain after radiotherapy because the remaining benign prostate cells continue to secrete PSA (Schellhammer et al., 1993).

The AR inhibitor enzalutamide with or without ADT is recommended for patients with high-risk local biochemical recurrence (BCR) as defined by PSA doubling time ≤ 9 months and PSA ≥ 2 and 1 µg/l above nadir after radiotherapy and radical prostatectomy, respectively (Freedland, de Almeida Luz, et al., 2023; Freedland, Gleave, et al., 2023; Tilki et al., 2024). For other patients initially treated with radical prostatectomy, salvage radiotherapy with or without hormonal therapy is recommended for local BCR. If the initial treatment was radiotherapy, local salvage therapy, such as brachytherapy, is recommended only for highly selected patients with preferentially biopsy-proven local BCR (Tilki et al., 2024).

Biochemical recurrence in patients who have undergone radical prostatectomy or radiotherapy precedes metastases detected by conventional imaging such as bone scan and abdominopelvic computed tomography (CT) by a median of eight years (Pound et al., 1999; Zagars & Pollack, 1997). However, the emergence of more sensitive imaging modalities, particularly prostate-specific membrane antigen (PSMA) positron emission tomography (PET)/CT, has allowed for the earlier detection of metastases. Other PET-based techniques, such as fluciclovine and

choline PET/CT, have been previously used but have largely been supplanted by PSMA-based imaging because of their superior sensitivity and specificity (Hofman et al., 2020). Imaging for distant metastases should only be performed if it may affect the selection of management strategy (Tilki et al., 2024).

2.1.4 Management of metastatic PCa

Metastatic disease is the leading cause of cancer-related mortality. Disseminating tumor cells can impair the function of invaded organs, leading to a progressive decline across multiple organ systems. Eventually, the body becomes unable to compensate for or recover from organ failure or additional insults such as infection (Boire et al., 2024; Valastyan & Weinberg, 2011). Clinically, metastases can be asymptomatic or present with both systemic symptoms and site-specific complications, which in the case of PCa commonly manifest as bone pain (Coleman, 2001).

The overarching goal of treatment is to prevent mortality from metastatic progression, while balancing adverse effects and alleviating symptoms. Although radical prostatectomy and radiotherapy offer curative potential for localized PCa, no curative treatments exist for advanced or metastatic disease (Rebello et al., 2021). In the absence of curative options, therapy aims to delay progression long enough for patients to die of unrelated causes or at least increase survival, while preserving optimal quality of life.

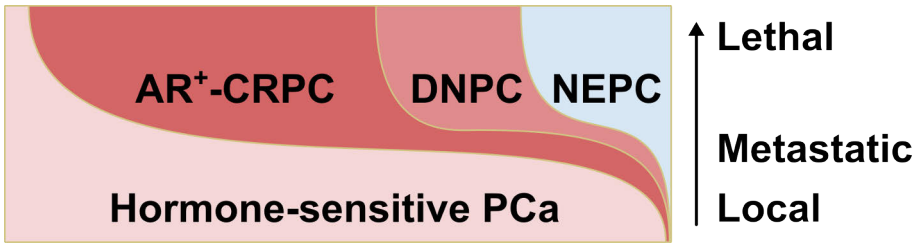

Figure 1. AR signaling status relative to the progression of PCa. PCa can be subtyped based on its AR signaling state to hormone-sensitive (castration-sensitive) PCa and CRPC. CRPC is very rare in untreated tumors but inevitably develops in response to therapeutic targeting of AR signaling. CRPC is further categorized into AR-positive (AR-dependent) and AR-negative or AR-low subtypes. A significant proportion of AR-negative or AR-low PCa exhibits a neuroendocrine-like gene expression and histology and is termed neuroendocrine PCa (NEPC), whereas non-neuroendocrine-like AR-negative PCa is termed double-negative PCa (DNPC). Notably, in this figure the timescale from localized to lethal disease is not depicted proportionally, as progression from local to metastatic takes significantly longer than mortality following the development of metastases. Instead, the scale is intentionally skewed to complement and highlight the evolution of AR signaling subtypes. AR = androgen receptor, PCa = prostate cancer, CRPC = castration-resistant PCa, AR+-CRPC = AR-positive CRPC.

Systemic therapy is required to treat distant metastasis. ADT remains the cornerstone for the first-line treatment of hormone-naïve metastatic PCa (i.e., disease not yet exposed to androgen-altering or AR-targeting therapies) and is now routinely combined with other agents to improve outcomes (Tilki et al., 2024). Castration resistance rarely develops without undergoing ADT, but will eventually develop in almost all patients receiving ADT (Figure 1). Consequently, the earlier use of ADT as an adjuvant therapy with certain regimens of radiotherapy for localized PCa, may increase the chance of castration resistance being present at the time of first metastasis (Cornford et al., 2024).

2.1.4.1 Management of hormone-sensitive metastatic PCa

ADT has been the cornerstone and standard of care for patients with metastatic PCa for several decades. Currently, ADT is also combined with chemotherapy or AR-targeted agents, including the androgen biosynthesis inhibitor abiraterone or the AR inhibitors apalutamide and enzalutamide, as a doublet therapy when applicable (Tilki et al., 2024). In addition, triplet therapy with ADT, chemotherapeutic docetaxel, and either abiraterone or the AR inhibitor darolutamide is recommended for high-risk patients suitable for the regimen (Fizazi et al., 2022; Hussain et al., 2023; Smith et al., 2022; Tilki et al., 2024). ADT, which lowers testosterone in blood to castrate levels (<1.7 nnmol/l or <50 ng/dl), can be achieved by performing orchiectomy or by utilizing drugs that disrupt the secretion of pituitary hormones, particularly the secretion of luteinizing hormone (LH), that stimulate hormone synthesis in the testis (Tilki et al., 2024). This is most commonly achieved using LH-releasing hormone analogues, typically administered as long-acting depot injections. The following paragraphs briefly discuss AR inhibitors, abiraterone and docetaxel, and their mechanistic rationale for therapeutic potential in PCa.

AR inhibitors bind the ligand-binding domain of AR and compete with DHT for receptor binding, thereby inhibiting ligand-dependent AR activation. Thus, AR inhibitors strengthen androgen blockade, thereby increasing selective pressure against AR signaling. Bicalutamide is a first-generation non-steroidal AR antagonist, but it can exert partial agonism in tumors with adapted AR signaling (Culig et al., 1999). Enzalutamide is a second-generation AR antagonist with five-fold greater binding affinity than bicalutamide and does not exhibit known agonism (Tran et al., 2009). Apalutamide, structurally related to enzalutamide, offers improved pharmacokinetics and efficacy in preclinical models (Clegg et al., 2012). Darolutamide, the most recently FDA-approved agent among these, has a higher affinity for AR and improved blood–brain barrier selectivity, potentially reducing central nervous system side effects (Moilanen et al., 2015). Proteolysis-targeting chimeras (PROTACs) that induce AR degradation are currently being investigated

as potential next-generation strategies (L. Chen et al., 2021; Kregel et al., 2020; S. Lee et al., 2024; Neklesa et al., 2019; Rathkopf et al., 2025; W. Zhang et al., 2024).

Abiraterone targets androgen production in adrenals via inhibition of the key androgen biosynthesis enzyme cytochrome P450 17-alpha-hydroxylase (CYP17A1; Barrie et al., 1994) and thus, further lowers the androgen concentrations available to PCa cells (Attard et al., 2009). Prednisolone is given together with abiraterone to substitute for the reduced cortisol production associated with abiraterone (Fizazi et al., 2016). Abiraterone metabolites may also directly target AR (Z. Li et al., 2016).

Docetaxel and other taxanes primarily promote apoptosis by arresting the cell cycle through microtubule stabilization. However, they have also been shown to inhibit AR nuclear translocation by interfering with microtubule-mediated transport, potentially contributing to their efficacy in PCa (Sousa-Pimenta et al., 2023).

Despite effectively delaying PCa progression for up to several years, metastatic CRPC (mCRPC) usually inevitably develops even under ‘triplet therapy’ (Fizazi et al., 2022; Hussain et al., 2023; Smith et al., 2022). Notably, therapy-induced genomic adaptations in AR inhibition occur predominantly as amplifications of *AR* or its enhancer or *AR* mutations, which is consistent with strong selective pressure (Herberts et al., 2022; Visakorpi et al., 1995). In contrast, many genomic alterations present in untreated primary PCa are only modestly enriched in CRPC (Cancer Genome Atlas Research Network, 2015), suggesting that they arise largely independently of treatment and may reflect intrinsic tumor biology rather than therapy-driven evolution. This emphasizes the importance of non-genomic mechanisms in resistance to the therapeutic targeting of AR signaling. The genomic and non-genomic mechanisms involved in progression to CRPC are reviewed in detail in chapter 2.4.

2.1.4.2 Management of mCRPC

Patients commonly undergo several therapies including ADT before developing mCRPC. Therefore, treatment selection will depend on previous regimens (Tilki et al., 2024). This section discusses the available agents not covered under hormone-sensitive disease and briefly outlines the molecular rationale for their use.

Genetic testing may guide treatment selection in mCRPC, as first-line combination treatment with a poly(adenosine diphosphate-ribose) polymerase (PARP) inhibitor and either an AR inhibitor or abiraterone has shown survival benefits, particularly in patients with BRCA-deficient tumors (Agarwal et al., 2023; Chi et al., 2023; Clarke et al., 2022; Fizazi et al., 2023; Saad et al., 2023). PARP enzymes sense DNA damage and are involved in recruiting repair factors. Inhibition of PARP therefore increases unresolved DNA damage, leading to cytotoxicity in cells deficient in homologous recombination (HR; Figure 2; Virtanen et al., 2019).

These regimens are most effective in BRCA-deficient tumors but have also been approved for broader HR-deficient populations and, in some regions, for unselected patients (Tilki et al., 2024). Olaparib and Rucaparib are additionally approved as monotherapies for later-line treatment in patients with specific HR gene mutations (de Bono et al., 2020; Fizazi et al., 2023; Hussain et al., 2020). Recently, the PARP inhibitor niraparib in combination with abiraterone acetate plus predinisone showed benefit also in hormone-sensitive metastatic PCa, marking their future application in earlier disease settings (Attard et al., 2025).

Chemotherapy remains an option for the treatment of mCRPC. Docetaxel can be followed up with cabazitaxel chemotherapy. However, sequencing of AR-targeting drugs is not recommended (de Bono et al., 2010; de Wit et al., 2019; Tilki et al., 2024). For patients with symptomatic bone metastases who have received docetaxel, radium-223 radionuclide treatment may be considered (Cornford et al., 2024; Parker et al., 2013). Radium-223 mimics calcium and is incorporated into areas of osteoblastic activity, which are characteristic of PCa bone metastasis. Once incorporated, it emits alpha particles that locally destroy adjacent tumor cells (Morris et al., 2019).

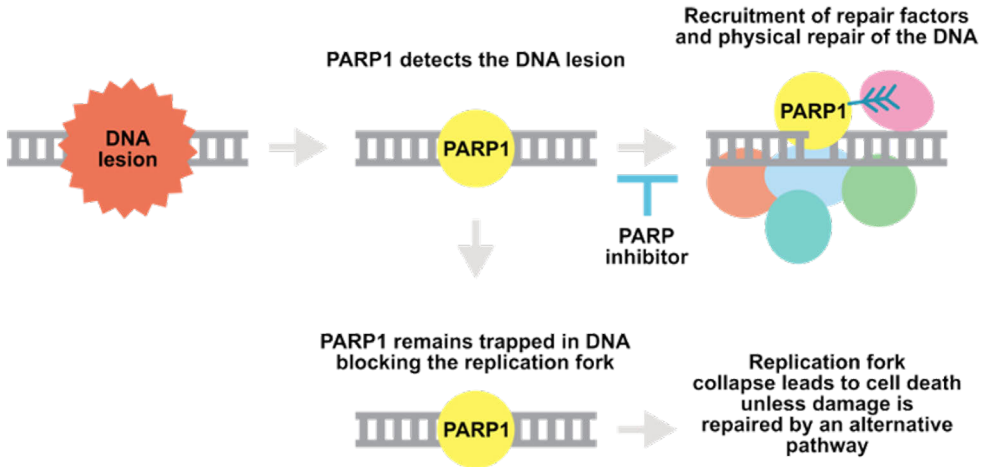

Figure 2. A schematic illustrating the molecular rationale for PARP inhibition. Whereas PARP1 is involved in the repair of multiple DNA lesion types, its main function is in the detection single-strand DNA breaks. PARP inhibitors not only block the catalytic activity of PARP enzymes but also trap PARP on DNA at sites of damage by preventing its dissociation. These cytotoxic PARP–DNA complexes stall replication forks and give rise to replication-associated DNA lesions, which cannot be efficiently resolved without HR. As a result, these lesions accumulate and induce cell death in HR repair–defected cells. PARP = poly(adenosine diphosphate-ribose) polymerase, HR = homologous recombination. Illustration adapted from Virtanen et al., Genes 2019.

Targeting PSMA, which is highly expressed in CRPC and metastatic lesions, offers a promising approach for the detection and targeted treatment of metastatic disease. PSMA is a transmembrane receptor with enzymatic activity in its extracellular domain and is internalized upon ligand binding, allowing targeted delivery of cytotoxic agents. These therapies include lutetium-177-PSMA-617, which has been approved for patients with PSMA-positive mCRPC who have received prior therapy (Cornford et al., 2024). PSMA-targeting strategies under development include new forms of radioligand therapy, antibody–drug conjugates, bispecific T cell engagers, and chimeric antigen receptor (CAR) T cells (Figure 3; Hyväkkä et al., 2021). Diagnostic imaging with PSMA PET tracers also allows for the sensitive detection of lesions (Hofman et al., 2020), but AR-negative or AR-low CRPC subtypes may lack PSMA expression (Bakht et al., 2023). In such cases, fluorodeoxyglucose (FDG) PET may offer better sensitivity by detecting tumors with high glucose metabolism, consistent with Warburg effect activation in AR-independent PCa (Kelloff et al., 2005; Xian et al., 2015).

Treatment approaches that target other oncogenic pathways have also been investigated. The phosphoinositide 3-kinase (PI3K)–protein kinase B (AKT) pathway, which is frequently activated in PCa, can be targeted with AKT inhibitors. In patients with phosphatase and tensin homolog (PTEN) deficiency identified by IHC, the AKT inhibitor ipatasertib combined with abiraterone showed improved progression-free survival but did not confer an overall survival benefit and showed no efficacy in unselected populations (de Bono et al., 2025). The broader implications of PI3K-AKT signaling are discussed in chapters 2.2–4.

Immunotherapy has shown limited success in PCa patients. Sipuleucel-T is an autologous immune therapy unavailable in Europe with demonstrated overall survival benefit in mCRPC (Kantoff et al., 2010; Tilki et al., 2024). During this treatment, the patient's peripheral immune cells are collected and exposed ex vivo to a fusion protein containing prostatic acid phosphatase (PAP) and immune-activating domains, thereby priming the immune system to recognize tumor cells (Kantoff et al., 2010). Immune checkpoint inhibitors have had limited efficacy in PCa, which is considered an immunologically "cold" tumor with few cytotoxic lymphocytes and a predominance of myeloid-derived suppressor cells (Stultz & Fong, 2021). PSMA-directed CAR T cell therapies are under investigation (Narayan et al., 2022), although their clinical efficacy in solid tumors remains modest compared to hematologic malignancies (Cappell & Kochenderfer, 2023). Additionally, bispecific T cell engagers targeting kallikrein-related peptidase 2 (KLK2) have shown favorable safety profiles and PSA responses in 42% of participants in early trials (Stein et al., 2025).

Finally, radiotherapy or surgical ablation may be considered for palliative purposes or, in selected cases, for oligometastatic diseases (Tilki et al., 2024). These

local interventions can alleviate symptoms or delay disease progression when applied to limited metastatic sites.

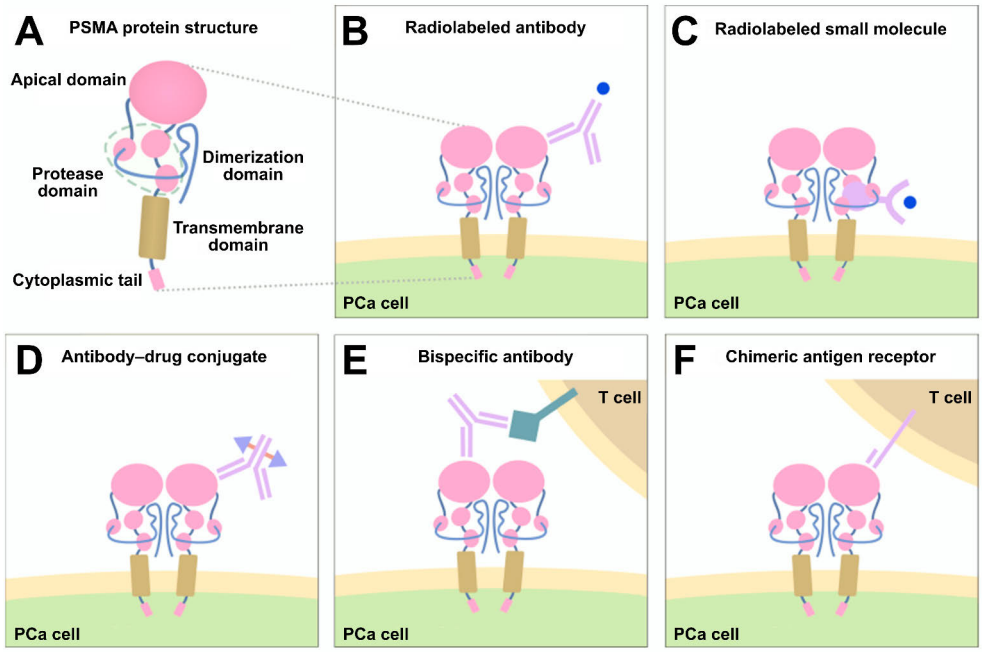

Figure 3. Illustrative depiction of PSMA structure and a schematic illustration of PSMA-targeting agents as examples of molecules against surface proteins. (A) PSMA is a transmembrane protein with its enzymatically active protease domain exposed extracellularly. (B) PSMA-targeting radioligand therapy can be achieved by conjugating a radionuclide to a PSMA-specific antibody. (C) Alternatively, small-molecule PSMA ligands linked to radionuclides can be used for targeted radiotherapy. (D) PSMA-directed antibody–drug conjugates deliver cytotoxic agents to PSMA-expressing cells. (E) Bispecific antibodies can recruit T cells to PSMA-positive tumor cells by co-engaging T cell receptors (e.g., CD3 or CD28). (F) Chimeric antigen receptor (CAR)-engineered T or natural killer cells can be programmed to target PSMA. PSMA = prostate-specific membrane antigen, PCa = prostate cancer. Illustration adapted from Hyväkkä et al., Cancers 2021.

2.2 Molecular mechanisms contributing to PCa initiation and progression

This chapter, together with chapters 2.3 and 2.4, provides a broader discussion of the molecular and cellular mechanisms relevant to PCa biology, including tissue organization, signaling pathways, metabolic adaptations, TME changes, metastasis, and castration resistance. It begins with an overview of prostate epithelial lineages and their relevance to tumor initiation, followed by a discussion of molecular alterations and regulatory processes that shape prostate tumor evolution. While

chapters 2.5 and 2.6 focus more directly on DNA damage repair and BRCA1, as well as the role of *CALD1* in actomyosin contractility and cancer, this chapter also examines PCa alterations and processes not directly addressed in the experimental work. This broader context is intended to situate the findings within the complex and multifactorial nature of PCa.

2.2.1 Tissue architecture of the prostate and PCa

Considering the plasticity and dynamic phenotype shifts characteristic of PCa, this chapter reviews the epithelial cell types of benign prostate.

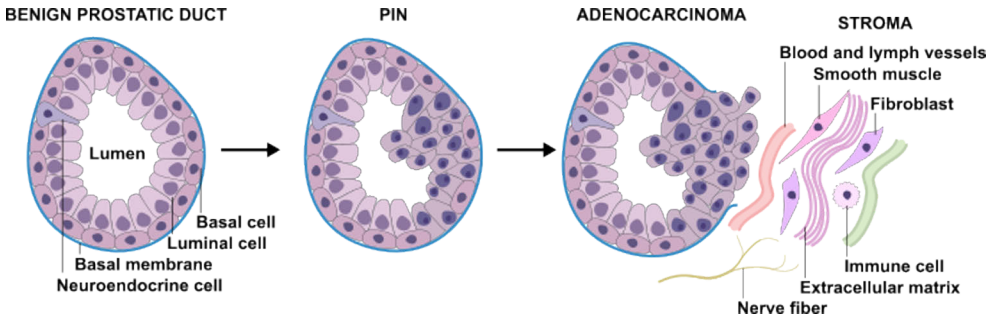

Figure 4. Schematic illustration of prostate acinar architecture during tumorigenesis. In benign prostate tissue, luminal cells secrete into the lumen and form an organized layer, while basal cells lie adjacent to the basement membrane, which separates the glandular epithelium from the prostate stroma. Androgen-independent neuroendocrine cells, the rarest of the three cell types, are also present in the benign prostate. Prostatic intraepithelial neoplasia is a premalignant condition in which the cells exhibit dysplastic abnormalities. However, these dysplastic cells do not invade beyond the basement membrane, although they may show an infiltrative growth pattern within its confines. In a malignant lesion, malign cells invade outside the basement membrane. Additionally, stroma is affected by and affects the tumor evolution as well as the benign state. Prostate stroma includes smooth muscle cells, fibroblasts, immune cells, endothelial cells, and nerve-associated cells. PIN = Prostatic intraepithelial neoplasia.

The prostate epithelium consists of three main cell types: luminal, basal, and neuroendocrine (Figure 4). Luminal cells are the major cell type present in the epithelium and are located facing the lumen, whereas basal cells are located closer to the basement membrane (Signoretti & Loda, 2006). Luminal cells are AR-dependent and thus express the AR target gene PSA, the presence of which in the serum thereby serves as an indirect clinical marker for the quantity of luminal cells (Bonkhoff & Remberger, 1996). The basal cell type expresses lower AR compared to the luminal cell type, and the neuroendocrine type does not express AR (Shen & Abate-Shen, 2010). Neuroendocrine cells are significantly rarer and their influence on PCa progression remains unclear.

Notably, benign neuroendocrine epithelial cells are not considered the origin of cancer cells with the neuroendocrine histological phenotype observed in AR-independent CRPC (Figure 1), such as neuroendocrine PCa (NEPC). Instead, NEPC arises through phenotypic plasticity driven by epigenomic reprogramming and clonal evolution under therapeutic pressure resulting in neuroendocrine-like features (Beltran et al., 2016; Romero et al., 2024).

Importantly, stromal AR, expressed in smooth muscle cells, fibroblasts, and myofibroblasts plays a key role in maintaining a benign prostate epithelial architecture, as shown in genetically engineered mouse models with stroma-specific *Ar* deletion (Singh et al., 2014; Wen et al., 2015; Yu et al., 2012). Similarly, rare neuroendocrine cells may contribute to the maintenance of a benign epithelial ecosystem, potentially through paracrine signaling.

High-grade prostatic intraepithelial neoplasms (PINs) are premalignant lesions that are fully located within the epithelium and are considered the main precursor lesions for prostate adenocarcinoma (Figure 4; Montironi et al., 2002). As an alternative hypothesis, inflammation-induced lesions of proliferative inflammatory atrophy have been suggested to precede PINs or independently precursor adenocarcinoma (De Marzo et al., 2007). PINs appear with aberrated epithelial architecture, sustained basal cell presence, and cell atypia (Montironi et al., 2002). Although it is possible that multiple lesion types contribute to prostate carcinogenesis, for the sake of clarity, this thesis will use the term PIN to refer generically to precursor lesions.

PCa most commonly appears as adenocarcinoma, which is characterized by the absence of basal cells (Figure 4). It is not known whether basal cell's disappearance is independent of luminal cell activity, or a consequence of luminal cells becoming more aggressive. This suggests that either basal cells transform into luminal-like cells or luminal cells act as cells of origin. α-Methylacyl-CoA racemace (AMACR) is a luminal cell–associated peroxisomal enzyme overexpressed in prostate adenocarcinoma that can be stained to aid histopathological diagnosis (Shen & Abate-Shen, 2010).

Although there is a basal stem cell lineage in PCa, it has been shown that a subset of luminal cells can regenerate and act as bipotential progenitors. These stem-like luminal progenitor cells are marked by Nkx3.1 expression under castrate conditions and are therefore termed castration-resistant Nkx3.1-expressing cells (CARNs; X. Wang et al., 2009). Mouse studies have shown that PCa consistently favors a luminal origin over a basal origin, although a basal origin has been observed in renal grafts, suggesting that human PCa likely also originates from luminal cells, while other possibilities are still being investigated (Z. A. Wang et al., 2014).

Additionally, rare epithelial populations resembling lung club and hillock cells have been identified in the prostatic urethra and collecting ducts; however they are

largely absent from the anatomical zones where PCa usually develops (Henry et al., 2018). More recently, transcriptional profiles associated with club-like cells have been detected in tumor-associated regions of the prostate (Kiviaho et al., 2024). Importantly, this transcriptional program closely resembles that of the castration-resistant Nkx3.1-expressing luminal progenitor cells identified in mouse models, suggesting a possible human counterpart to the CARN population (Chua et al., 2014; Karthaus et al., 2020; X. Wang et al., 2009). Interestingly, this human transcriptional phenotype is marked by the expression of C-X-C motif chemokine ligand (CXCL)-family cytokines, which have been implicated in the maintenance of myeloid-derived suppressor cell infiltration in PCa (C. Guo et al., 2023; Kiviaho et al., 2024).

Taken together, luminal or luminal-like cells are the predominant lineage in PCa, with basal and luminal features arising through acquired plasticity to support progression events such as metastasis and resistance via androgen-independence. Luminal origin is supported by the prevalence and relevance of luminal markers such as NKX3-1 and PSA throughout PCa progression.

2.2.2 Emergence of malignancy through evolutionary selection

Cancer is characterized by clonal evolution as a natural consequence of differences in fitness between benign and malignant cells, and later among malignant subclones (Nowell, 1976). From the perspective of clonal evolution, benign tissues can be viewed as actively maintaining an equilibrium under selective pressure. From this perspective, cancer is an iterative process in an adaptive tissue ecosystem that escapes the equilibrium by acquiring genomic alterations (Greaves & Maley, 2012). The serial genomic events emerging in this process provide surviving clones with attributes that can collectively be called hallmarks of cancer. The ‘hallmarks of cancer’ framework serves as a heuristic tool aiming to outline what are the phenotypic aberrations that define a cancer cell (Hanahan, 2022; Hanahan & Weinberg, 2000).

The latest edition of hallmarks of cancer, including emerging hallmarks and enabling characteristics, includes the acquired capabilities for sustaining proliferative signaling, evading growth suppressors, resisting cell death, enabling replicative immortality, inducing/accessing vasculature, genome instability and mutation, activating invasion and metastasis, reprogramming cellular metabolism, avoiding immune destruction, tumor-promoting inflammation, unlocking phenotypic plasticity, nonmutational epigenetic reprogramming, polymorphic microbiomes, and senescent cells (Hanahan, 2022). The following chapters discuss the conditions under which these attributes arise and review the identified genetic and regulatory factors that support their emergence in PCa. The most common

somatic alterations, including E26 transformation-specific (ETS) fusions, *PTEN* loss, *SPOP* mutations, and *TP53* alterations are discussed separately in more detail, whereas the less common alterations are reviewed more briefly. The germline events contributing to PCa are reviewed in chapter 2.1.2.

2.2.3 Copy number aberrations in primary PCa

Recurrent somatic genomic events in PCa are predominantly chromosomal rearrangements and copy number alterations (CNAs), whereas point mutations or small indels are heterogeneous and less consistently shared across patients (Ciriello et al., 2013). Moreover, the CNA burden is an independent prognostic factor in PCa and is associated with higher PSA and Gleason scores in PCa (Cancer Genome Atlas Research Network, 2015; Hieronymus et al., 2018). Arm-level CNAs are common in PCa and often reflect early clonal events, whereas focal alterations are also recurrent. Recurrent chromosomal alterations are listed here along with their respective putative genetic drivers, which are discussed further in this chapter.

Frequently lost arm-level regions include, 8p (*NKX3-1*), 10q (*PTEN*), 13q (*RB1*, *BRCA2*), 16q, and 18q, whereas gains are common on 7q and 8q (*MYC*, *NCOA2*). Some regions, such as 7q and 18q, are recurrently altered at the arm level, but lack a consistently identified focal driver. This highlights the gaps in our understanding of the selective pressures that drive certain CNAs. Recurrent focal deletions and gains are summarized in Table 1 (Cancer Genome Atlas Research Network, 2015).

Table 1. Common focal CNAs in PCa. CNA: copy number alteration.

LOCATION	Putative relevant gene(s) affected	CNA
2q22.1	*SPOPL*	deletion
3p13	*FOXP1*, *RYBP*, and *SHQ1*	deletion
3p26	*FANCD2*	deletion
5q11.2	*MAP3K1*	deletion
5q15–q21	*CHD1*	deletion
6q12–q22	*MAP3K7*	deletion
12p13.1	*CDKN1B*	deletion
17p13.1	*TP53*	deletion
21q22.3	Region between *TMPRSS2* and *ERG* (secondary to fusion gene)	deletion
8p11.23	*FGFR1* and *WHSC1L1*	gain
8q24.21	*MYC*	gain
11q13.2	*CCND1*, *PPP1CA*	gain

2.2.4 Oncogenic ETS fusion protein

Gene fusions involving members of the ETS transcription factor family and androgen-responsive promoter elements are more common than point mutations in PCa (Tomlins et al., 2005). The borrowed promoter allows cancer cells to use prostate-sustaining androgen signal as fuel for cancer-promoting levels of ETS proteins. The most frequently involved ETS genes in PCa are *ERG*, *ETV1*, *ETV4*, and *FLI1*, whereas androgen-regulated promoters typically originate from *TMPRSS2*, *SLC45A3*, or *NDRG1*, with the *TMPRSS2-ERG* fusion being the most prevalent fusion. ETS genes are rarely expressed independently of androgen-regulated promoters, and such expression may occur via epigenomic activation (Cancer Genome Atlas Research Network, 2015). The loss of ETS repressor *ERF* may induce similar oncogenic effects by relieving repression at ETS target sites, and is therefore mutually exclusive with ETS fusions (Bose et al., 2017; F. W. Huang et al., 2017).

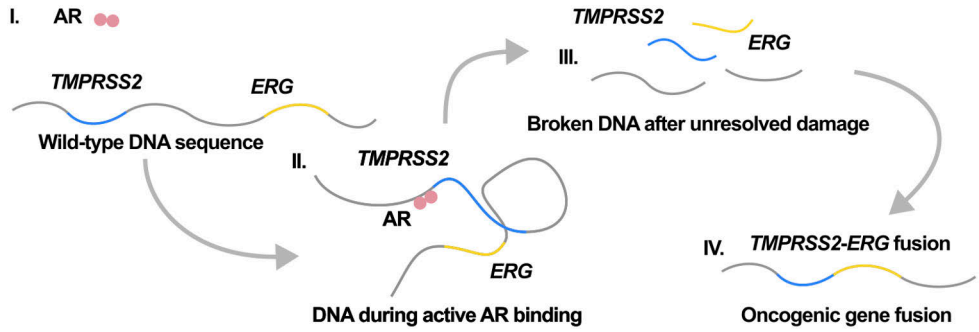

Figure 5. A schematic drawing depicting the sequence of chromosomal movement proposed to induce the formation of ETS fusion gene in PCa using *TMPRSS2* and *ERG* as examples. I. *ERG* is located in 21q22.2 and *TMPRSS2* is located in 21q22.3. Upon activation by androgen, AR forms a homodimer and locates to the nucleus. II. AR homodimer promotes the transcription of target genes such as *TMPRSS2*. AR binding DNA in the proximity of *TMPRSS2* alters the conformation of DNA. This induced conformation brings *ERG* and *TMPRSS2* closer to each other. III. Transcription and DNA conformation may modulate the susceptibility for DNA double-strand breaks at specific sites. IV. Broken DNA can be erroneously repaired to form a fusion gene. Moreover, interstitial genes can be lost due to erroneous repair. ETS = E26 transformation-specific, PCa = prostate cancer, AR = androgen receptor.

Depending on ancestry, the prevalence of ETS fusions in PCa patients is 27–50%, with highest frequency observed in men of European descent (Blackburn et al., 2019; Magi-Galluzzi et al., 2011; Tomlins et al., 2005; Tomlins, Laxman, et al., 2008).

Induced *Erg* expression in genetically engineered mouse models (GEMMs) is sufficient to produce prostate neoplasia but only after prolonged latency of up to 26

months (L. T. Nguyen et al., 2015), whereas ETS fusion produces no phenotype at 18 months (Carver et al., 2009). These findings suggest that ETS activity is oncogenic particularly when triggered by aging or accumulation of cooperative alterations.

Interestingly, the specificity of the ETS fusion gene to PCa appears to be driven not only by selective pressure but also by functional susceptibility, as AR signaling has been shown to physically induce chromatin proximity between fusion partners in PCa (Figure 5; Mani et al., 2009). ETS fusion proteins have also been shown to promote DNA damage (Ruzanov et al., 2024). Moreover, ETS fusion is associated with the altered expression of genes involved in lipid metabolism, suggesting increased fatty acid synthesis (Sinha et al., 2019). Interestingly, deletion of interstitial genes between *TMPRSS2* and *ERG* has also been suggested to contribute to PCa progression (Linn et al., 2016).

2.2.5 Activation of growth and survival signaling via PI3K-AKT pathway in PCa

The PI3K-AKT pathway is a major transductor of signals in cellular proliferation and survival while being intertwined with several other pathways (Cantley & Neel, 1999; Crumbaker et al., 2017). Consequently, several pathological alterations that lead to the acquisition of cancer hallmarks involve genes related to this pathway.

A classic vulnerability in the pathway commonly utilized by cancer is the loss of PTEN (J. Li et al., 1997). This phosphatase limits phosphorylation of the AKT enzymes, which are kinases capable of activating hundreds of possible targets upon phosphorylation. When lost, PTEN can no longer dephosphorylate phosphatidylinositol 3,4,5-trisphosphate, resulting in sustained AKT phosphorylation and the uncontrolled activation of downstream targets.

PTEN is deleted or mutated in 17% of primary PCa and additionally, alterations are observed in *PIK3CA*, *PIK3CB*, *AKT1,* and *MTOR* (Cancer Genome Atlas Research Network, 2015). Interestingly, *Pten* loss overrides *Ar* loss effects in both luminal and basal lineages, underscoring the fundamental interdependence between the PI3K/AKT pathway and AR signaling in PCa (Carver et al., 2011; Mulholland et al., 2011; Xie et al., 2017). In GEMMs *PTEN* loss induces PINs that can progress to invasive adenocarcinoma (S. Wang et al., 2003), which has served as a foundation for later GEMM studies combining *Pten* loss with additional genetic alterations. Elevated PI3K/AKT, mitogen-activated protein kinase/extracellular signal-regulated kinase (MAPK/ERK), and receptor tyrosine kinase (RTK) activity has been observed in PCa, with only a weak correlation to canonical genomic alterations, suggesting that these pathways may be broadly activated through non-canonical mechanisms (Cancer Genome Atlas Research Network, 2015).

2.2.6 *SPOP* mutations in primary PCa

SPOP is found mutated in 6–15% of PCa and encodes speckle-type POZ (SPOP), a protein that enables ubiquitination by Cullin3-RING complex, thus contributing to protein degradation (Barbieri et al., 2012; Zhuang et al., 2009). AR is among the proteins ubiquitinated by SPOP, which promotes the degradation of the AR protein. Consequently, *SPOP* functions as a tumor suppressor, the loss of which stabilizes the AR protein levels (An et al., 2014; Bernasocchi et al., 2021; Gan et al., 2015). This aligns with the observation that *SPOP* mutant PCa exhibits higher AR transcriptional activity than other genomic subtypes (Cancer Genome Atlas Research Network, 2015).

Interestingly, *SPOP*-mutated PCa often lacks ETS fusions, and as both alterations are associated with distinct alteration patterns, they can be considered to form the two major genomic subtypes of PCa (Barbieri et al., 2012). Mutual exclusivity is likely a consequence of ETS-related gene (ERG) increasing SPOP protein levels which in turn facilitates zinc finger Myeloid–Nervy–Deformed Epidermal Autoregulatory Factor 1 type containing 11 (ZMYND11) degradation. This degradation is needed to allow the transcription of relevant ERG targets, thereby creating a selective pressure against *SPOP* mutations after ETS-rearrangements in PCa (Bernasocchi et al., 2021).

SPOP has been shown to be essential for DNA-protein cross-link repair in PCa; thus, *SPOP* loss also contributes to increased DNA damage (Watanabe et al., 2020). Moreover, *SPOP* loss promotes both PI3K and the mechanistic target of rapamycin (mTOR) pathway and AR signaling, while also uncoupling the reciprocal feedback regulation of these pathways in PCa (Blattner et al., 2017). *SPOP* mutations appear to contribute to an immunosuppressive TME by being associated with reduced $CD3^+$ and $CD8^+$ T cell infiltration (L. Zhang et al., 2018).

Clinically, *SPOP* mutations are more common in primary PCa than in mCRPC and are associated with a more favorable prognosis in mHSPC, suggesting that they represent a more treatment responsive phenotype, although they do also occur in lethal mCRPC PCa (Swami et al., 2020). This is consistent with the rationale that *SPOP* mutations produce a phenotype reliant on stabilized AR, which could make these subclones more susceptible to therapies targeting AR signaling.

2.2.7 Activated MYC, Immune evasion and hypoxia

Activation of MYC is common early event in PCa with up to 50–76% PIN lesions showing positive staining. Interestingly, protein expression in early PCa does not correlate with 8q24 amplifications suggesting that while recurrent amplifications are common later on, early activation is mediated by regulators discussed further (Gurel et al., 2008). Furthermore, induced overexpression of *Myc* in GEMMs initiates PCa

characterized by loss of *Nkx3.1* and upregulation of the serine/threonine kinase *Pim-1* (Ellwood-Yen et al., 2003). Finally, high MYC expression dimishes canonical AR target expression and alters the AR transcriptional program. This shift contributes to PCa initiation and progression, and correlates with metastasis risk, AR inhibitor treatment failure, and mortality (Qiu et al., 2022).

A subset of aggressive localized PCa ranging from 15–52% presents with >5% programmed death-ligand 1 (PD-L1)-positive staining together with increased $CD8^+$ T cell infiltration despite the absence of clinical responses to immune checkpoint blockade. Interestingly, these tumors were enriched with *RB1* (91% vs. 64%), *BRCA2* (55% vs. 27%), and *CHD1* (36% vs. 1–18%) deletions. Although the enriched genes were linked to genomic integrity, the study did not observe significant differences in tumor mutational burden or the proportion of genomic alterations between the immunogenic and non-immunogenic foci (Calagua et al., 2021).

Hypoxia correlates with early biochemical relapse after local treatment in PCa (Lalonde et al., 2014). Moreover, hypoxia correlates with *TP53* mutations, *PTEN* loss, higher somatic single nucleotide variant burden, catastrophic chromothriptic events, higher CNA burden, and mitochondrial genome mutations in PCa (Bhandari et al., 2019).

These findings highlight that PCa commonly presents with MYC activation, whereas additional features such as hypoxia and distinct immune phenotypes may further contribute to aggressive disease in subsets of tumors.

2.2.8 Other recurrently mutated and deleted genes in primary PCa

This chapter summarizes the remaining common and well-studied somatic gene alterations in primary PCa, along with their related dysregulated genes. These include common oncogenic events across cancer types, such as loss of particular tumor suppressors, which can often be relatively rare in primary PCa but become enriched in castration-resistant or metastatic PCa. In contrast, some of the most common PCa alterations are less broadly observed across other cancer types and in many cases these alterations appear to either support or modulate AR signaling. Metabolic changes are discussed in the following chapter.

The *NKX3-1* homeobox gene (Bova et al., 1993; Bowen et al., 2000) and pioneer transcription factor *FOXA1* (Cancer Genome Atlas Research Network, 2015; Eyunni et al., 2025; Gerhardt et al., 2012; J. Li et al., 2020; Sahu et al., 2011; C. Zhang et al., 2011) are principal prostate-relevant transcription factors that modulate AR signaling, and whose alterations enable its oncogenic reprogramming.

Additionally, several factors, including the nuclear receptor binding SET domain protein 2 (NSD2; Parolia et al., 2024), odd-skipped related 1 (OSR1; W. K. Kim et

al., 2022), p300, cyclic adenosine monophosphate (cAMP) response element-binding-binding protein (CBP; Welti et al., 2021), *ATAD1*, *MINPP1* (Sinha et al., 2019), and *CHD1* (Boysen et al., 2018; Burkhardt et al., 2013; Z. Zhang et al., 2020; D. Zhao et al., 2017) have been suggested to enhance AR signaling or alter the AR transcriptome, when altered or dysregulated.

MAPK pathway-related alterations are present in 25% of primary PCa, but this prevalence is driven largely by the heterozygous loss of *MAP3K7* present in up to 18% of patients. However, canonical MAPK mutations, namely *BRAF*, *HRAS*, *RRAS2*, and *RAC1*, are only observed at low frequencies up to 2% (Cancer Genome Atlas Research Network, 2015). *MAP3K7* loss is mutually exclusive with ETS fusions, but is enriched with *CHD1* loss (Jillson et al., 2021), and is associated with advanced tumor stage, high Gleason grade, lymph node metastases, and early biochemical recurrence (Kluth et al., 2013).

TP53 is a central tumor suppressor gene involved in regulating cell fate in response to stress, and is the most frequently altered gene across cancers (Donehower et al., 2019; Levine et al., 1991). In PCa, *TP53* is mutated in 6–8% of primary tumors (Barbieri et al., 2012; Cancer Genome Atlas Research Network, 2015), with alterations becoming increasingly enriched during disease progression, reaching 53% in mCRPC (Hamid et al., 2019; Nientiedt et al., 2020; Robinson et al., 2015). Accordingly, *TP53* is further discussed in later chapters.

In addition to serving as a biomarker, PSA is a serine protease that may contribute to PCa pathogenesis by breaking down ECM and adhesion proteins, activating signaling molecules, and regulating angiogenesis (Koistinen et al., 2021). Interestingly, serine protease inhibitor Kazal-type 1 (SPINK1), a serine protease inhibitor overexpressed in 10% of primary PCa, is enriched in AR-independent PCa (Räsänen et al., 2016). This suggests that PSA protease activity could directly contribute to the pathogenesis of AR-dependent PCa.

Other less common factors potentially contributing to PCa tumorigenesis include rapidly accelerated fibrosaroma (RAF) fusions, *SPINK1* outlier overexpression, *IDH1* mutations, and *MED12* mutations (Barbieri et al., 2012; Cancer Genome Atlas Research Network, 2015; Palanisamy et al., 2010; Tomlins, Rhodes, et al., 2008). Commonly hypermethylated genes in PCa include *GSTP1*, *SHF*, *FAXDC2*, *ZNF154*, *STAT6*, *HEXA*, and *KLF8* (Cancer Genome Atlas Research Network, 2015). Additionally, mutations in mitochondrial DNA have been observed in primary PCa, and some of these mutations tend to co-occur with MYC amplifications. This co-occurrence has been linked to more aggressive disease and poorer prognosis (Hopkins et al., 2017).

Whereas the factors described above are present in most tumors, up to one-fourth of tumors lack a canonical driver (Cancer Genome Atlas Research Network, 2015). The remaining cases may be explained by undetected structural variants, epigenetic

changes, noncoding driver mutations, or dysregulation of noncoding RNAs. Common identified non-genetic changes are reviewed in the following chapter.

Indeed, noncoding RNAs, which produce functional RNA that can have enzymatic and regulatory roles, contribute to PCa initiation and progression alongside protein-coding genes (L. Ding et al., 2021). This is exemplified by the high diagnostic accuracy of microRNA-based assays on serum samples in research settings, which surpasses PSA testing in terms of specificity while maintaining comparable sensitivity (Urabe et al., 2019).

Importantly, patients may harbor multiple somatic alterations that are not known to be oncogenic in isolation. However, their combinatorial functional effects could still contribute to tumorigenesis. Assessing the oncogenic contribution of such rare synergistic constellations is challenging and their extreme rarity, potentially being unique to a single patient, limits the feasibility and clinical impact of studying them.

2.2.9 Increased ROS and altered metabolism

More than 90% of PCa shows hypermethylation of the *GSTP1* promoter, resulting in the loss of *GSTP1* expression. *GSTP1* encodes a protein functioning as a catalyst for detoxification reactions (W. H. Lee et al., 1994). In preclinical PCa models, restoration of gluthathione S-transferase P (GSTP1) expression did not produce a marked phenotype. This led to the proposal that *GSTP1* loss is an early event that increases susceptibility to oxidation and DNA damage, thereby facilitating further oncogenic changes (Mian et al., 2016).

Another highly common non-genetic early event, occurs similarly in more than 90% of PCa, is downregulation of zinc transporter 1 (ZIP1) via repression mediated by Ras-responsive element-binding protein 1 (RREB-1) (Costello & Franklin, 2006, 2016). In benign prostate epithelial cells, high intracellular zinc levels inhibit the tricarboxylic acid (TCA) cycle enzyme mitochondrial aconitase, preventing citrate oxidation. This results in citrate accumulation and a reduced adenosine triphosphate (ATP) yield from an estimated 38 to 14 per glucose molecule (B. Chen et al., 2024; Costello & Franklin, 2006). In contrast, the TCA cycle is active in PCa because the downregulated ZIP1 no longer supplies zinc to the cells (Costello & Franklin, 2006). This metabolic shift is further evidenced by a global upregulation of TCA cycle enzymes, which occurs mainly at the protein level rather than at the transcriptional level (Latonen et al., 2018). Moreover, ZIP1 downregulation also removes the inhibition of nuclear factor kappa-light-chain-enhancer of activated B cells (NF-κB) signaling and hypoxia-inducible factor 1-alpha (HIF-1α), PSA, aminopeptidase N (AP-N), and vascular endothelial growth factor (VEGF) expressions inducted by zinc in prostate cells (B. Chen et al., 2024). In summary, citrate secretion is a characteristic feature of benign prostate epithelium, highly regulated by zinc, but

actively discarded during tumorigenesis to restore full oxidative metabolism, consequently increasing energy efficiency by approximately 2.7-fold (Costello & Franklin, 2006).

This early metabolic reprogramming is notable because it contrasts with the Warburg effect, a common metabolic phenomenon in which cancer cells favor the rapid acquisition of 2 ATP molecules per glucose via aerobic glycolysis over the full TCA cycle, which produces an estimated 38 ATP molecules per glucose (Warburg et al., 1927). Interestingly, the Warburg effect has been reported in both localized PCa and advanced and metastatic PCa (Pujana-Vaquerizo et al., 2024). This indicates that oxidative phosphorylation and aerobic glycolysis can coexist in PCa metabolism from its earliest stages, rather than representing mutually exclusive metabolic states.

IHC analysis of lipid metabolism–associated enzymes as surrogate markers of the Warburg effect in radical prostatectomy samples demonstrated a correlation between ISUP histology grade and stearoyl-CoA desaturase-1 (SCD-1) expression in patients with total cholesterol > 200 mg/dL as well as a correlation between biochemical recurrence and carnitine palmitoyltransferase-1a (CPT-1a). These findings suggest that the activation of the Warburg effect can be a pre-ADT event in aggressive PCa (Russo et al., 2023). Indirect evidence of early glycolytic pathway activation was also observed in *Trp53*-null and *Pten*-null GEMMs, with monocarboxylate transporter (MCT) activation already present in PINs when *Pten* was lost (Pertega-Gomes et al., 2015). Moreover, it has been shown that *PTEN*-/*TP53*-deficient PCa requires the Warburg effect to grow, and that it initiates this metabolic shift through deficiency-specific mechanisms that involve the upregulation of hexokinase 2 (HK2; L. Wang et al., 2014). Together, these studies suggest that the Warburg effect and altered lipid metabolism may be features in subsets of aggressive PCa.

Therefore, primary PCa is commonly characterized by deviations from the benign prostate epithelium, including shifts in cellular energy metabolism and increased susceptibility to oxidative DNA damage.

2.3 Molecular mechanisms in PCa metastasis

PCa cells have a unique propensity to metastasize to bone (84% of metastatic patients) and to form lesions with osteoblastic features in contrast to strictly osteolytic lesions seen commonly for bone metastases occurring in other cancer types (Gandaglia et al., 2014; Riihimäki et al., 2018). Other PCa metastasis sites include the lymph nodes, liver, lungs, and rarely the brain. Visceral metastases are associated with poor outcomes and are more frequently observed in CRPC and NEPC (J. Kang et al., 2022).

Genomic alterations associated with the transformation to metastatic PCa include mutations in *MYC*, *FOXA1*, and *TP53* and CNAs affecting *MYC*, *BRCA2*, *CDK12, PTEN*, and *CHD1* (Abida et al., 2017; Grasso et al., 2012; Gundem et al., 2015; Hieronymus & Sawyers, 2012; Mateo et al., 2020; Robinson et al., 2015). Moreover, *AR*, *TP53*, *PTEN* and *FOXA1* alterations are enriched in bone metastases, but their contribution to bone tropism remains to be demonstrated (J. Kang et al., 2022; van Dessel et al., 2019). In contrast, *SPOP* mutations have shown mixed associations with metastasis in different cohorts. In paired sample analysis between primary and metastatic tumors, mCRPC showed a decrease in copy numbers of *TP53*, *RB1*, and *PTEN*, increased *MYC* copy numbers, and increased *CTNNB1* and *APC* mutations. Notably, DDR mutations showed no difference between paired samples although they were generally enriched in mCRPC. Indeed, there was a trend of lower copy numbers of DDR genes in mCRPC, which may suggest that while DDR alterations predispose to the development of metastases, DDR alteration accumulation is not as directly tied to the process of tumor evolution to metastatic disease as strongly as other genomic alterations identified in the study (Mateo et al., 2020).

A study examining the phylogenics of PCa metastasis by analyzing the subclonal structure of metastases in 10 patients found that half of the studied patients showed a polyclonal origin. Both monoclonal and polyclonal metastases were seeded from subclones carrying CRPC-associated alterations. Although the observation of greater genetic similarity between metastases than between the primary tumor and metastases may suggest metastasis-to-metastasis seeding, it does not fully rule out dissemination from an undetected primary tumor subclone or the possibility of parallel evolution driven by similar selective pressures (Gundem et al., 2015).

A recent pan-cancer whole-genome analysis comparing separate cohorts revealed that PCa metastases are exceptionally clonal compared to primary tumors. Rather than contradicting earlier evidence of polyclonal seeding, this observation underscores the high degree of heterogeneity in primary PCa and suggests that metastatic subclones emerge relatively late in tumor evolution. This study also found a significant increase in apolipoprotein B mRNA-editing enzyme catalytic polypeptide-like (APOBEC) mutational patterns as well as single base substitution (SBS) mutational signatures SBS1 and SBS5/SBS40 in metastatic PCa samples (Martínez-Jiménez et al. Nature 2023). SBS1 is a clock-like signature because it usually correlates with age in normal tissues and cancer (Alexandrov et al., 2015). The study found that in PCa metastases the pattern corresponded to the equivalent of an additional 71 years of clock-like accumulation on average, which was interpreted to be partly attributable to a higher cell turnover (Martínez-Jiménez et al., 2023).

Building on these broader insights, several specific molecular contributors to the metastatic progression of PCa have been identified. Below, I summarize the selected molecular findings linked to metastasis before turning to more detailed thematic discussions of the invasion–metastasis cascade, EMT, and TME.

Although not enriched in mCRPC, ETS rearrangements, *KRAS* mutations, and *FBXL4* loss have been shown to promote bone tropism (Deplus et al., 2016; Stankiewicz et al., 2017; Weng et al., 2019). Similarly, in GEMMs, *Kras* mutations accompanied by *Nkx3-1* mutations and *Pten* loss increase susceptibility to bone metastasis compared to *Nkx3-1* mutations and *Pten* loss alone. Interestingly, the *Kras*-mutant, *Nkx3-1*-mutant, and *Pten* loss genotype induces a MYC/KRAS activation that is similarly present particularly in metastatic patient samples (Arriaga et al., 2020).

Additional GEMM studies have identified alternative pathways toward metastatic progression. Expressing the SV40T antigen via a cryptdin-2 promoter induced a neuroendocrine cell–specific expression of p53- and Rb1-inhibiting proteins, which led to the development of androgen-independent tumors that metastasized at 6 months with significant bone tropism (Garabedian et al., 1998). Telomerase reactivation following telomere dysfunction also leads to bone metastasis in GEMMs (Z. Ding et al., 2012). The rationale behind this is that while telomere dysfunction fuels the acquisition of new somatic events, telomerase reactivation attenuates DNA damage and permits the selection of cooperative events necessary for metastasis. In that study, such events included the deregulation of the transforming growth factor beta (TGF-β) pathway and triple inactivation of *p53*/*Pten*/*Smad4* which produced an aggressive and metastatic PCa phenotype in GEMMs (Z. Ding et al., 2011, 2012). However, loss of *Smad4* in GEMMs shows relatively low bone tropism, and *SMAD4* mutations in CRPC and metastatic PCa are rare (J. Kang et al., 2022).

Likewise, functional screening has identified additional regulators of metastasis. In vivo genome-wide clustered regularly interspaced short palindromic repeats (CRISPR) screening identified multiple genes biologically relevant for PCa metastases, and verified the potential of *CITED2*, a transcriptional modulator of pathways including p53, MYC, TGF-β, and hypoxia, as a target by showing that inhibition of cbp/p300-interacting transactivator 2 (CITED2) impaired bone metastases in a highly metastatic GEMM (Arriaga et al., 2024). ATPase family AAA domain-containing protein 2 (ATAD2) was shown to be enriched in metastases when compared to primary tumors and was associated with MYC pathway activation (Dutta et al., 2025).

Forkhead box protein M1 (FOXM1) and centromere protein F (CENPF) are upregulated in one-third of PCa and approximately 90% of metastatic PCa (Aytes et al., 2014). FOXM1 has also been implicated in docetaxel resistance via the induction

of 5' adenosine monophosphate-activated protein kinase (AMPK)/mTOR-mediated autophagy (Lin et al., 2020).

PI3K/AKT signaling has broad effects, including key functions that promote metastasis upon activation, namely, by enhancing motility, reducing intercellular adhesion, and supporting neovascularization (Y. He et al., 2021). Therefore, PI3K/AKT pathway activation and/or *PTEN* loss is enriched across cancer metastases, including metastatic PCa (Whang et al., 1998). Additionally, one mechanism by which *PTEN* loss may promote invasion in PCa involves activation of Runt-related transcription factor 2 (RUNX2). Mechanistically, this is achieved by loss of *PTEN* hyperactivating AKT signaling, which prompts AKT to inhibit forkhead box protein O1 (FOXO1), which in turn releases its inhibition of RUNX2 (H. Zhang et al., 2011). Calcium/calmodulin-dependent kinase kinase 2 (CAMKK2) has also been implicated in promoting fatty acid synthesis in PCa while being associated with proliferation, migration, invasion, and inhibition of AR activity (Penfold et al., 2018). Furthermore, CAMKK2 is upregulated in both hormone-naïve PCa and CRPC, acting as a master regulator of metabolic processes downstream of the AR (Massie et al., 2011). Interestingly, in triple-negative breast cancer CAMKK2 is highly correlated with tumor invasiveness, and its inhibition suppresses metastasis via the loss of stress fibers (D. Mukherjee et al., 2023).

Epigenetic regulators also contributed to this phenomenon. Downregulation of *DAB2IP* by enhancer of zeste homolog 2 (EZH2) induces the activation of Ras and NF-κB, while promoting EMT and metastasis. Homolog 2-interacting protein (DAB2IP) staining is inversely correlated with Gleason scores, suggesting that the downregulation associates with high-grade PCa. Moreover, DAB2IP staining is already reduced at the PIN stage compared with normal tissue. (Min et al., 2010).

A range of other mediators have also been implicated, including *AKA12P*, *SDF-1*/*CXCL12*, *ANXA2*, *CXCR4, SPINK1*, integrin αvβ3, and neuroblastoma-derived v-myc avian myelocytomatosis viral related oncogene (N-MYC) downstream-regulated gene family member 3 (NDRG3; Barthel et al., 2013; De et al., 2003; Y. Jung et al., 2015; G. Y. Lee et al., 2018; Leinonen et al., 2013; McCabe et al., 2007; Shiozawa et al., 2011; Su et al., 2006; Taichman et al., 2002).

In summary, multiple contributing factors with metastatic potential have been identified, yet only a few gene alterations have been consistently associated with metastases. Notably, many of the identified contributors converge on pathways, such as Ras signaling, which are rarely genetically altered in PCa. Ras has been observed to cooperate with MYC, which in contrast is broadly activated in PCa (Gurel et al., 2008). Together, these observations raise the possibility that even non-genetic transient pathway activation may contribute to metastatic progression when cooperative genetic alterations provide a permissive background.

2.3.1 Invasion-metastasis cascade and EMT

The invasion-metastasis cascade model views metastasis as a multistep process with successive bottlenecks. The cascade consists of local invasion, intravasation, survival in circulation, extravasation, and colonization of a new organ or tissue (Lambert et al., 2017).

To disseminate, cancer cells must loosen epithelial and ECM adhesions and acquire motility in order to enter the blood or lymphatic circulation, exit them, and survive in new tissue contexts (J. Kang et al., 2022). Motility relies on the dynamic assembly and disassembly of intracellular protein networks, primarily those of the actin cytoskeleton (K. M. Yamada & Sixt, 2019). Once in circulation, tumor cells face shear stress and immune elimination, notably by natural killer cells (Labelle & Hynes, 2012; Lambert et al., 2017; Pereira-Veiga et al., 2022).

Importantly, there is no substantial clonal expansion during the metastatic cascade prior to colonization. Thus, unlike primary tumor growth, the cascade does not involve iterative cycles of clonal expansion and selection. Instead, it operates as a selective filter, in which only subclones with phenotypic states compatible with each step progress further. Consequently, genetic alterations observed in metastases are not necessarily metastasis-specific adaptations per se but rather represent a contingent subset of alterations that evolved under distinct selective pressures during primary tumor growth and were subsequently filtered for compatibility with the metastatic cascade.

Accordingly, alterations observed in metastases and in primary tumors appear to represent a largely overlapping set of driver alterations, and despite extensive efforts no consistent metastasis-specific alterations have been identified (Naxerova, 2025). Nonetheless, lineage studies in PCa evidence that not all subclones have the same potential for metastasis, indicating that the multistep accumulation of mutations gives rise to genotypes that have an increased propensity to undergo the metastatic cascade (Gundem et al., 2015).

Thus, while genetic events may prime cells for dissemination, actual traversal of the invasion-metastatic cascade is largely governed by non-genetic, reversible programs such as EMT/partial-EMT, stemness, dormancy, immune evasion, and niche interactions (Lambert et al., 2017).

EMT is a cell program that is physiologically triggered during embryogenesis and is later activated during wound healing and fibrosis. In cancer, EMT is associated with metastasis and cancer stem cell behavior. Stem cells are characterized by the ability to self-renew and the capacity to differentiate, and cancer cells that enhance these properties through EMT are often described as exhibiting increased stemness (S. A. Mani et al., 2008; Morel et al., 2008). EMT has also been suggested to have potential roles in the initiation of cancer in some contexts. EMT orchestrates a reversible transformation toward a mesenchymal cell state and is activated by the

transcription factors *TWIST*, *SNAIL*, *SLUG*, and *ZEB1/2* (Dongre & Weinberg, 2019; Y. Kang & Massagué, 2004; Lambert et al., 2017).

EMT allows cells to become more motile and equips them with mesenchymal-like capabilities, such as invading and degrading the ECM. During EMT, epithelial cells lose their apical–basal polarity and their cytoskeleton is dynamically reshaped. A hallmark of this transition is the formation of actin stress fibers, while cytokeratin levels are reduced and replaced by vimentin as the principal intermediate filament of the mesenchymal cell state (Lamouille et al., 2014).

Although the epithelial and mesenchymal states are often presented as a dichotomy, they represent the theoretical extremes of a spectrum. Cells undergoing EMT commonly adapt partial phenoypes, retaining some epithelial traits while acquiring mesenchymal features (Lambert et al., 2017; Nieto et al., 2016).

A classic EMT feature is the destabilization of adherens junctions via downregulation of E-cadherin, leading to the loss of epithelial cell–cell junctions when co-occuring with other EMT-associated events. E-cadherin downregulation is often accompanied by a reciprocal increase in N-cadherin levels, enabling cells to adhere to mesenchymal cells (Lamouille et al., 2014). However, in PCa, E-cadherin is co-expressed with the EMT-regulator zinc finger E-box-binding homeobox 1 (ZEB1), which typically represses E-cadherin in other cancers. Notably, E-cadherin levels in PCa are correlated with aggressiveness and are higher in bone metastases (Putzke et al., 2011).

Sustained E-cadherin levels during the EMT have been proposed to serve as a mechanism for collective cell migration, allowing groups of cells to move together (Lambert et al., 2017). Supporting this idea, a recent methodological study isolating circulating tumor cells (CTCs) from blood samples reported that a high proportion of metastatic PCa samples (9 of 12) contained clusters of CTCs, suggesting that PCa metastases may arise from both single-cell or multicellular seeding (Magnusson et al., 2024).

Whereas, aggressive PCa appears to retain E-cadherin expression, loss of *Cdh1* (gene encoding E-cadherin) in a GEMM induces PIN-like lesions and co-loss with *PTEN* leads to adenocarcinoma with goblet cell metaplasia, which is not typically seen in patients (Olson et al., 2019).

TGF-β family proteins induce EMT by activating multiple signaling pathways including mothers against decapentaplegic homologs (SMAD), PI3K, MAPK, and Rho family guanosine triphosphatases (Rho GTPases). These pathways converge to enhance the expression of key regulators of EMT. Growth factors acting through RTKs can also induce EMT partly by activating the PI3K and MAPK pathways. In addition, several other signaling pathways, including Wingless/Intergrated (Wnt), Hedgehog, HIF1α, and Notch, have been associated with EMT (Lamouille et al., 2014).

After arrival at the metastasis site, most cells die or enter long-term dormancy (Luzzi et al., 1998). Successful colonization usually requires stem-like properties and a mesenchymal-to-epithelial transition, which is consistent with the epithelial appearance of most metastases (Lambert et al., 2017).

2.3.2 PCa TME in metastasis

The TME comprises ECM and all the cell types present, excluding malignant epithelial cells. These include smooth muscle cells, fibroblasts, immune cells, endothelial cells, and nerve-associated cells in the context of the prostate. The ECM includes proteins, such as collagen, laminin, fibronectin, and hyaluronate, which are predominantly synthesized and secreted by fibroblasts (J. Kang et al., 2022). Tumor evolution also transforms the TME, as demonstrated by single-cell RNA sequencing of PCa stroma. Stromal transcriptional states shaped by the tumor genotype predict the risk of metastasis (Pakula et al., 2024).

Smooth muscle cells are the most common cells in the normal prostate stroma, while cancer-associated fibroblasts (CAFs) are the most common cell in the primary PCa TME (Chiarugi et al., 2014; Tuxhorn et al., 2002). In PCa, CAFs transition from fibroblasts into myofibroblasts, which co-express α-smooth muscle actin and vimentin in contrast to fibroblasts that only express vimentin (Gabbiani, 2003).

Several mechanisms allow molecular crosstalk between tumor cells and TME. Virtually all cells release cell membrane–bound vesicles, known as exosomes, which, in the case of tumor cells, can home to and fuse with target organ cells guided by tumor-specific integrin-patterns on exosomes. Thereby exosomes allow the exhange of non-secreted lipids, proteins, RNA (Yáñez-Mó et al., 2015), and even DNA (Lázaro-Ibáñez et al., 2014) between the tumor cells and the pre-metastatic niche as well as the local TME (Hoshino et al., 2015). In PCa, exosomal TGF-β has been identified to promote fibroblast transformation via SMAD pathway in the local TME (J. Webber et al., 2010; J. P. Webber et al., 2015). Moreover, osteoblasts can be reprogrammed by PCa-derived exosomes to support bone tropism and metastatic growth (J. Kang et al., 2022). Interestingly, a study has shown that PCa exosomes can deliver PSA mRNA and protein to infiltrating T cells, highlighting the potential of tumor–immune crosstalk, although the significance of this phenomenon remains unclear (S. Chen et al., 2021).

Evidence shows that PCa transforms its TME into an osteomimetic TME (J. Kang et al., 2022). In addition, decreased expression of AR in the stroma is associated with poor prognosis and early disease progression (J. Kang et al., 2022; Ricciardelli et al., 2005; Singh et al., 2014; Wikström et al., 2009). Notably, the bone marrow stroma readily expresses significant AR compared to other metastasic target organs (Mantalaris et al., 2001).

In summary, these data highlight that while no metastasis-specific driver alterations have been conclusively established, PCa metastasis arises from the permissive states generated by clonal evolution in the primary tumor, together with non-genetic programs such as EMT, plasticity, and microenvironmental reprogramming.

2.4 Molecular mechanisms of CRPC

PCa represents a genetically C-class cancer in contrast to M-class cancer meaning that PCa is characterized by a relatively small mutational burden and an increasing number of CNAs (Ciriello et al., 2013; Fraser et al., 2017; Sinha et al., 2019). Interestingly, mutation rates are relatively similar between hormone-naïve and CRPC (0.9–1.5 vs. 2.0 mutations per megabase) whereas CNAs are significantly enriched in CRPC (Berger et al., 2011; Taylor et al., 2010).

PCa progresses during castrate levels of circulating androgens most commonly through AR-dependent mechanisms (Figure 6; Virtanen et al., 2020; Watson et al., 2015). This means that paradoxically, testosterone-independent growth in PCa often occurs via enhanced AR signaling. *AR* is the single most altered gene in CRPC and is the central driver of resistance to ADT (Abida et al., 2019). However, AR-independent clones form a significant subtype, and such phenotypes, such as NEPC, are thought to emerge from the increasing plasticity and genomic instability assigned to the late evolution of CRPC (Figure 1). In the era of potent AR inhibition, AR-independent phenotypes have become more prevalent in mCRPC (Bluemn et al., 2017).

2.4.1 Restored AR signaling

Somatic *AR* mutations are present in approximately 10–15% of CRPC tumors, whereas they are rare (<1%) in untreated primary PCa (Grasso et al., 2012; Robinson et al., 2015). The most frequently observed mutations cluster in the ligand-binding domain, conferring ligand promiscuity that allows activation by other steroid hormones or antiandrogens (Joseph et al., 2013; Korpal et al., 2013). Other recurrent alterations enable activation by glucocorticoids and broaden the steroid specificity (Azad et al., 2015; Lallous et al., 2016). Together, these mutations facilitate persistent AR signaling despite therapy and contribute to treatment resistance.

AR amplification is observed in up to 70% of CRPC but is rarely observed in untreated PCa (Koivisto et al., 1997; Quigley et al., 2018). Docetaxel and cabazitaxel treatments did not increase *AR* copy number (Conteduca, Jayaram, et al., 2019; Conteduca, Oromendia, et al., 2019). Amplifications of the *AR* upstream enhancer

region often co-occur with *AR* amplification, are seen in up to 80% of CRPC, and have been shown to upregulate *AR* expression (Quigley et al., 2018; Takeda et al., 2018; Viswanathan et al., 2018). Amplified *AR* has been shown to appear as extrachromosomal DNA, which may catalyze a faster copy number gain process (Zivanovic et al., 2023).

Alterations in AR coregulators can restore or enhance AR transcriptional output under androgen-deprived conditions. Silencing of the AR coactivators *NCOA1* and *NCOA2* reduces PSA levels in AR-positive cell lines, indicating their role in sustaining AR-driven transcription (Agoulnik et al., 2005, 2006). Moreover, nuclear receptor coactivator 2 (NCOA2) levels were significantly higher in post-ADT samples than in pre-ADT samples, suggesting selection for enhanced AR coactivation during ADT (Agoulnik et al., 2006). In contrast, impaired corepressor function may lower the transcriptional threshold for AR activation, and mutations in the nuclear receptor corepressors *NCOR1* and *NCOR2* are observed in 2.5% and 1.9% of CRPC, respectively (Armenia et al., 2018).

B lymphoma Moloney murine leukemia virus insertion region 1 (BMI1) prevents AR degradation via MDM2-mediated ubiquitination, is upregulated in PCa, and is associated with a worse prognosis (Glinsky et al., 2005; Zhu et al., 2018). Interestingly, SPOP is able to ubiquitinate BMI1, thereby promoting its degradation, which may in part increase the selective pressure toward *SPOP* loss (Hernández-Muñoz et al., 2005). Additionally, the PI3K/AKT pathway is frequently coactivated with BMI1 and mediates its phosphorylation (Nacerddine et al., 2012).

The mixed-lineage leukemia (MLL) complex interacts with the AR directly via the menin-MLL subunit and functions as a transcriptional coactivator by facilitating chromatin states permissive for AR-driven gene expression. Consistently, menin expression is higher in CRPC than in hormone-naïve PCa, compatible with an increased MLL-mediated epigenetic facilitation of AR activity in CRPC (Malik et al., 2015).

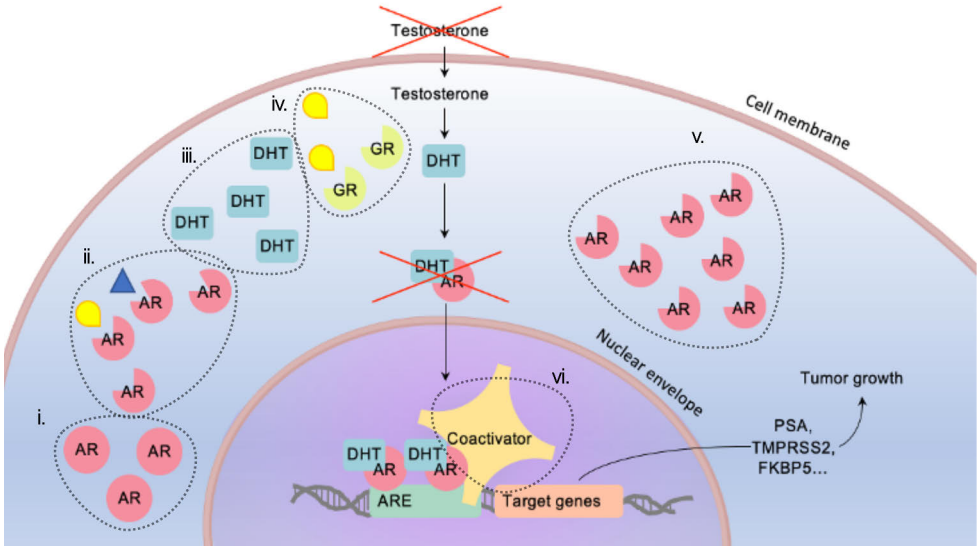

Figure 6. Mechanisms of resistance to therapeutics targeting AR signaling in PCa. PCa cell with disrupted testosterone availability has several potential mechanisms of regaining capability for tumor growth including ligand-independent activation (i.), ligand promiscuity (ii.), increased ligand availability (iii.), alternative nuclear receptor signaling (iv.), AR overexpression (v.), and altered coactivator expression (vi.). AR-V7 (i.) is an alternatively spliced variant of the androgen receptor that lacks the ligand-binding domain. As a result, AR-V7 can activate androgen receptor target gene transcription in a ligand-independent manner, leading to constitutive signaling regardless of androgen availability. The same outcome of constitutive ligand-independent activation can result from an *AR* mutation (i.). *AR* mutations can also lead to ligand promiscuity (ii.). Intratumoral de novo androgen synthesis would also be expexted to confer resistance (iii.). As therapies do not necessarily fully deplete availability of androgen, cancer cells can increase sensitivity to the remaining ligands via *AR* amplification (v.). Alternatively, another nuclear receptor (iv.), the most studied and observed of which being GR, can partly take over AR's cistrome to sustain tumor growth. Additionally, coactivator levels (vi.) have been shown to be enriched in CRPC, further enhancing AR signaling efficiency. Notably, AR signaling can be restored to similar levels even in the absence of direct *AR* alterations underscoring the high selective pressure for restoration. AR = androgen receptor, PCa = prostate cancer, GR = glucocorticoid receptor, CRPC = castration-resistant PCa, DHT = dihydrotestosterone, ARE = androgen response element, PSA = prostate-specific antigen, TMPRSS2 = transmembrane protein, serine 2, FKBP5 = FK506-binding protein 5. Adapted from Virtanen et al. Duodecim 2020.

The altered expression of AR variants is considered to contribute to castration resistance. The most studied variant, AR-V7, is already expressed in benign prostate cells but is highly expressed in some castration-resistant cells. The variant is constitutively activated and thus allows AR signaling to be retained independently of testosterone levels and the presence of ligand-binding-inhibiting agents (Figure 6). Accordingly, detectable levels of AR-V7 in circulating tumor cells have been associated with reduced responses and shorter survival in patients treated with AR

inhibitors (Antonarakis et al., 2014; Armstrong et al., 2019). Notably, the ligand binding end of the AR protein is important for several interactions (B. He et al., 2002) and thus cells relying on AR-V7 activity are expected to lack several interaction–dependent AR functions, which would likely alter the AR transcriptional program. On this basis, high AR-V7 expression is likely to reflect a distinct AR-dependent CRPC state.

Additionally, AR transcriptional activity can be enhanced by multiple accessory factors that modulate AR stability, chromatin accessibility, or transcriptional complex assembly, thereby amplifying AR output even under androgen-deprived conditions. Such factors include ring finger protein 6 (RNF6), seven in absentia homolog 2 (SIAH2), DNA-dependent protein kinases, bromodomain-containing protein 4 (BRD4), tripartite motif–containing 24 (TRIM24), insulin, and keratinocyte growth factor, all of which have been shown to promote AR-driven transcription (G. Wang et al., 2018).

Interestingly, a study observed similar AR signaling output between *AR*-amplified and copy number–neutral metastases in a patient with no reported *AR* mutations, suggesting that mechanisms outside *AR* alterations can compensate AR signaling with similar efficiency. (Hasan et al., 2023). Moreover, a study investigating prognostic factors for survival under enzalutamide or abiraterone acetate plus prednisone treatment found that no single *AR* perturbation was associated with prognosis (De Laere et al., 2019; Rebello et al., 2019).

A longitudinal circulating tumor DNA (ctDNA) study has suggested that gene structural rearrangements affecting the *AR* ligand-binding domain emerge under selective pressure imposed by AR inhibitors (Annala et al., 2021). Sequential ctDNA study further showed that under antiandrogen treatment, 62% of patients developed additional copy number increases in *AR* gene body and/or *AR* enhancer and/or new ligand-binding domain mutations. Interestingly, no other common alterations were observed in the cohort, suggesting that selective pressure under AR inhibition is highly specific (Herberts et al., 2022). This selective pressure is underscored, for example, by the VCaP cell line derived from a patient who had received flutamide, an early generation AR inhibitor, after ADT, which contains *AR* amplification with up to 20 copies of the gene (Germain et al., 2023).

AR degraders are being studied with the rationale that by eliminating the AR protein rather than merely antagonizing it, degraders may overcome the resistance created by ligand-binding domain mutations or splice variants (L. Chen et al., 2021; Kregel et al., 2020; S. Lee et al., 2024; Neklesa et al., 2019; W. Zhang et al., 2024). Early clinical trials on AR degraders have shown promising responses in patients who have progressed on ADT, one or more AR inhibitors, and taxane chemotherapy. Fitting the rationale, responders with *AR* ligand binding domain mutations have also been observed (Rathkopf et al., 2025).

CTC analysis revealed an androgen-driven luminal-like transcriptional phenotype expressing high proliferation markers that correlated with early progression under lutetium-177-PSMA-617, independent of *FOLH1* expression. Strikingly, the overall survival in this group was comparable to that in neuroendocrine-like phenotypes, indicating that transition to an AR-low or neuroendocrine-like state is not a prerequisite for aggressive disease (Sharifi et al., 2025).

2.4.2 Steroid supply under castration

During ADT, steroid synthesis independent of pituitary regulation by LH continues to provide molecules capable of activating nuclear receptor signaling in PCa tissue. In particular, adrenals produce dehydroepiandrosterone (DHEA) and DHEA sulfate, steroid hormone precursors with weak androgenic activity (Watson et al., 2015). PCa cells express and upregulate all enzymes necessary for de novo androgen synthesis during CRPC progression (Locke et al., 2008; Stanbrough et al., 2006).

Notably, inhibition of this pathway via cytochrome P450 steroid 17α-hydroxylase (CYP17A1) blockade with abiraterone paradoxically increases intratumoral CYP17A1 expression, suggesting that suppression of AR signaling in the CRPC context may actively drive the compensatory upregulation of de novo androgen synthesis (Cai et al., 2011).

It is of note that, while ADT effectively reduces serum testosterone by approximately 98%, intraprostatic dihydrotestosterone (DHT) decreases by approximately 75%, which highlights the importance of adrenal androgens like DHEA in sustaining DHT synthesis (Nishiyama et al., 2004). However, surgical ablation of adrenal androgens via bilateral adrenalectomy was already explored soon after the discovery of ADT with unencouraging responses, and it has not been revisited even after the mechanistic rationale became clearer, likely because emerging pharmacological strategies showed greater promise (West et al., 1952).

2.4.3 AR bypass via alternative nuclear receptor activation

The GR protein is encoded by the *NR3C1* gene and belongs to the family of 3-ketosteroid nuclear receptors, together with the mineralocorticosteroid receptor (*NR3C2*), progesterone receptor (*NR3C3*), and AR (*NR3C4*). Importantly the DNA binding domain in these receptors is highly conserved, and consequently, the hormone-responsive elements share similarities, which provides a rationale for AR bypass signaling by GR (Hiltunen et al., 2024). Moreover, in a physiological environment, AR represses GR via EZH2, and consequently, ADT or inhibition of AR signaling mechanistically induces GR de-repression via a downregulated AR

signal (Arora et al., 2013; Shah et al., 2017). Indeed, GR has been shown to be induced by AR inhibition and has an overlapping transcriptome with AR in CRPC (Figure 6; Arora et al., 2013). GR is expressed in normal prostate cells and downregulated during PCa initiation but may again reach levels seen in benign cells during metastasis (Puhr et al., 2018). Moreover, neuroendocrine and AR-low PCa have higher GR expression than AR positive-PCa (Tang et al., 2022). However, the interplay between the AR and GR in PCa is highly complex and has not yet been fully explored.

FOXA1, as discussed earlier as a regulator of AR DNA binding, also regulates GR by modulating both its expression and DNA binding. GR prefers to bind to DNA preoccupied by FOXA1, although its binding is inhibited by bound AR. Moreover, FOXA1 represses *NR3C1* via corepressor transducin-like enhancer protein 3 (TLE3). Thus, reduced FOXA1 promotes GR signaling but alters GR binding sites (Helminen et al., 2024).

Interestingly, cells with *CHD1* loss were re-sensitized to enzalutamide upon GR inhibition, suggesting that their enzalutamide resistance is partly GR-driven (Z. Zhang et al., 2020).

2.4.4 Epigenetic adaptations and chromatin remodeling

Integrative multi-omics studies in PCa have shown that, on a per-gene basis, protein levels correlate most strongly with H3K27Ac enrichment at gene-associated regulatory regions, followed by DNA methylation and CNAs with mRNA having the weakest correlation of the four (Sinha et al., 2019). This highlights that epigenomic features and CNAs are more specifically and predictively associated with measurable protein level changes than overall mRNA expression in PCa.

Histone hypermethylation appears early in PCa tumor evolution but appears to play a role also later in mCRPC. *EZH2* is overexpressed in mCRPC (Varambally et al., 2002). EZH2 catalyzes the trimethylation of histone H3 (H3K27me3) as a subunit of polycomb repressive complex 2 (PRC2). This specific type of histone methylation is increased in PCa compared to that in benign prostate, whereas global levels of histone methylation are generally reduced in PCa (Sugiura et al., 2021). This may, in part, result from the overexpression of histone demethylases, such as *LSD1*, which targets H3K4me1/2 (Crea et al., 2012).

Interestingly, lysine-specific histone demethylase 1A (LSD1) also promotes AR independence by regulating the expression of several genes outside its methylation function, effectively causing antitumor effects when LSD1 functions other than demethylation are inhibited (Sehrawat et al., 2018).

Furthermore, both EZH2 and embryonic ectoderm development (EED), another subunit of PRC2, have been shown to interact with AR. Silencing *EZH2* or *EED*

reduced PSA in AR-positive cell lines, although AR levels did not significantly decrease in all cell lines (Q. Liu et al., 2019). Interestingly, PRC2 deposits the repressive H3K27me3 histone mark at regulatory regions of neuroendocrine marker genes in both luminal- and neuroendocrine-like PCa cells, whereas in NEPC these loci also exhibit enrichment of the activating H3K4me3 mark. This bivalent chromatin state helps explain why NEPC fails to undergo phenotype reversal via EZH2 inhibition, and instead contributes to maintenance of a terminally differentiated state (Venkadakrishnan et al., 2024). PRC2 and lysine methyltransferase 2D-complex of proteins associated with Set1 (KMT2D-COMPASS), two chromatin-modifying complexes, have been shown to function as critical regulators of the epithelial state, with their loss unlocking distinct EMT trajectories (Y. Zhang et al., 2022).

Although EZH2 protein is enriched in NEPC, its inhibition does not revert the phenotype back to adenocarcinoma, but instead seems to further promote the expression of NEPC markers, suggesting the induction of terminal differentiation (Venkadakrishnan et al., 2024). While targeting histone deacetylases or epigenetic methylation pathways as monotherapies has not shown promise, mechanistic studies indicate that such interventions may be more effective when used to modulate lineage-specific vulnerabilities or combined with other targeted approaches (Ferrari et al., 2019; Venkadakrishnan et al., 2024). This may suggest that treatments targeting epigenetic methylation pathways or histone acetylation reach their peak potential when used as modulators of another therapy or as a way to prevent the development of treatment resistance.

Moreover, one-fifth of mCRPC cases are associated with DNA hypermethylation patterns involving *TET2*, *DNMT3B*, *IDH1*, and *BRAF*, possibly driven by *AR*, *MYC*, and *ERG* expression (S. G. Zhao et al., 2020). Since Ten-Eleven Translocator 2 (TET2) is a demethylation enzyme, its repression by AR may directly contribute to this hypermethylation (Nickerson et al., 2017; Takayama et al., 2015).

Targeting DNA methylation is currently being investigated in clinical trials. Given that DNA methylation-driven adaptations have been implicated in the development of resistance to various therapies, there is a strong rationale for prioritizing combination studies with agents whose efficacy is limited by therapy resistance. Pretreatment with DNA methyltransferase (DNMT) inhibition followed by docetaxel in patients whose disease progressed during or after docetaxel therapy, suggests that targeting DNA methylation may partially reverse docetaxel resistance in some patients, but no further clinical trials have been reported (Singal et al., 2015). Furthermore, DNMT inhibition in mice has been shown to induce the re-expression of methylated markers, such as B7-H3, in NEPC and *RB1*-deficient CRPC, thereby potentially broadening the repertoire of druggable targets in late-stage disease (Y. Yamada et al., 2023).

The SWItch/Sucrose Non-Fermentable (SWI/SNF) chromatin remodeling complex modulates DNA accessibility via ATP hydrolysis (Kassabov et al., 2003). SWI/SNF-related matrix-associated actin-dependent regulators of chromatin subfamily A member 2 (SMARCA2) and member 4 (SMARCA4) are mutually exclusive ATPase subunits of the SWI/SNF complex, meaning that only one is incorporated per assembly. Dual degradation of SMARCA2/4 and protein polybromo-1 (PBRM1) attenuated the transcription of key PCa drivers, AR, FOXA1, MYC, and ERG. Although SWI/SNF is a fundamental chromatin regulator in most cell types, CRPC becomes particularly dependent on it because of aberrant, enhancer-driven transcription orchestrated by multiple oncogenic factors (Xiao et al., 2022). This provides a promising rationale for therapeutic targeting of SWI/SNF in CRPC.

Although p300 and cAMP response element-binding protein-binding protein (CBP) likely modulate the AR transcriptome in hormone-sensitive PCa, they clearly support CRPC, as demonstrated by reduced growth under inhibition with concurrent deactivation of AR and C-MYC signaling (Welti et al., 2021).

2.4.5 Metabolic and redox adaptations

ADT increases oxidative stress in PCa cells (Blatt et al., 2023). By diverting pyruvate away from the TCA cycle, the Warburg effect indirectly lowers mitochondrial ROS production, which would otherwise arise from oxidative phosphorylation (J. Kim et al., 2016). Thus, reliance on the Warburg effect may serve as a survival mechanism to limit ROS in CRPC despite the high energy demands. Supporting this notion, silencing *LDHA* in AR-negative cell lines induced apoptosis, suggesting that AR-independent CRPC could be particularly dependent on the Warburg effect (Xian et al., 2015).

Loss of *KEAP1* via mutation or promoter DNA hypermethylation in PCa can activate nuclear factor erythroid 2-related factor 2 (NRF2) expression, as Kelch-like ECH-associated protein 1 (KEAP1) promotes the degradation of NRF2 (P. Zhang et al., 2010). NRF2 is a master regulator of antioxidant defense and therefore provides another mechanism for reducing ROS (Rojo de la Vega et al., 2018; Sies & Jones, 2020).

2.4.6 The *CDK12* tandem duplicator phenotype

Tandem duplicator phenotype is associated with the co-loss of *BRCA1* and *TP53*, but this co-loss is rare in PCa (Menghi et al., 2018). Instead, in PCa *CDK12* inactivation or loss causes a distinct pattern of genomic instability marked by focal tandem duplications, often in coding regions. These alterations can lead to gene

fusions and other coding sequence rearrangements (Y.-M. Wu et al., 2018). *CDK12* is altered in 5–7% of multiple cancer types, with its highest frequency observed in mCRPC, whereas alterations are relatively rare in primary PCa. *CDK12* loss tends to be mutually exclusive with ETS fusions and alterations in *PTEN, SPOP*, *TP53*, *BRCA2*, and *ATM* (Antonarakis et al., 2020; Y.-M. Wu et al., 2018). This is consistent with CRPC-associated tandem duplication phenotype samples being mutually exclusive of ETS fusions (Viswanathan et al., 2018).

FGF3 and *FGF4* alterations are also associated with the tandem duplication phenotype in CRPC, and commonly co-occur with *CDK12* alterations (van Dessel et al., 2019). Although *CDK12* has been proposed as a HR defect gene, it is distinct from canonical HR defect profiles, and interestingly non-*BRCA2*/*ATM* HR deficiency alterations appear to be enriched in *CDK12*-altered tumors. *CDK12* carriers have shown inferior responses to docetaxel and, PARP-inhibitors (Antonarakis et al., 2020). Responses to immune checkpoint blockade with ipililumab and nivolumab are also limited in this subgroup, mirroring the marginal responses observed in unselected mCRPC cohorts (C. B. Nguyen et al., 2024).

2.4.7 Drivers converging on androgen-independence

Analyses classifying tumor phenotypes as basal or luminal based on transcriptional profiling, which reflect the current state and not necessarily the cell of origin, have associated basal expression profiles with worse survival, likely reflecting the aggressive phenotype of subclones with attenuated AR signaling (Aggarwal et al., 2021).

MYCN amplifications have been shown to contribute to neuroendocrine differentiation in CRPC, especially in co-operation with *AURKA* overexpression (Beltran et al., 2011). Notably, up to 83% and 86% of metastatic NEPCs harbor *MYCN* and *AURKA* amplifications, respectively (Mosquera et al., 2013). Overexpression of N-MYC increases neuroendocrine markers and EZH2 abundance, thus downregulating *AR* via H3K27me3 repression (Dardenne et al., 2016). Interestingly, the amplifications only appear in 5% of unselected PCa, while they are already present in 65–70% of primary tumors from patients that later develop metastatic NEPC, possibly suggesting that, in the majority of NEPC cases, molecular alterations such as *MYCN* and *AURKA* amplification reflect an early bias or partial commitment toward the neuroendocrine lineage, preceding pressure by ADT (Mosquera et al., 2013).

Moreover, the activation of Wnt/β-catenin signaling has been linked to AR-negative PCa, and this signaling promotes *MYCN* and *FOXA2*, which has also been linked to neuroendocrine transdifferentiation (Formaggio et al., 2021).

However, a clinical phase II trial exploring AURKA inhibition in patients with metastatic CRPC and suspected NEPC components based on histology, NE markers, or metastatic patterns demonstrated variable clinical responses. In this cohort, the frequency of AURKA amplification was lower than expected, highlighting the need for more precise molecular selection criteria to guide targeted therapy (Beltran et al., 2019). Interestingly, N-MYC transcriptionally activates DDR expression, including *PARP1*/*2* and *BRCA1* (W. Zhang et al., 2018).

Although *AR* perturbations were not associated with prognosis under enzalutamide or abiraterone acetate plus prednisone treatment, *TP53* alterations harbored independent prognostic value (De Laere et al., 2019). Whether this is caused by modulation of AR signaling, increased plasticity or adaptability, or simply by increased aggressiveness, remains unknown.

Interestingly, AURKA, MYCN, p53, and RB1 regulate each other, possibly forming a network in which the factors promote broader interconnected oncogenic processes, leading to a vicious cycle (Formaggio et al., 2021). Notably, genetic and epigenetic profiling of CRPC has shown that while genomic alterations do not consistently distinguish NEPC from adenocarcinoma, epigenomic subtypes segregate clearly and align with this dichotomy, suggesting that diverse genetic alterations can converge on similar epigenomic states that promote NEPC (Beltran et al., 2016).

Interestingly, a study examining alterations appearing during ADT found that *TP53*, *SPOP*, and *FOXA1* were particularly unchanged during the course of treatment, which was interpreted as suggesting that alterations pertaining to these genes may often occur as early events prior to ADT instead of being treatment-emergent (Annala et al., 2021).

Sex-determining region Y-box 2 (SOX2), a pioneer transcription factor associated with NEPC and a common marker for stemness and pluripotency, promotes plasticity in *TP53*- and *RB1*-deficient CRPC (Mu et al., 2017). The combination of *TP53* and *RB1* deficiency notably induces transdifferentiation of luminal-like to AR-negative neuroendocrine-like cells under ADT, mechanistically activating epigenetic reprogramming via EZH2 and SOX2 (S. Y. Ku et al., 2017; Mu et al., 2017). However, 40% of CRPC with co-loss retained *AR* expression, suggesting that other factors partake in determining whether transdifferentiation is induced (Nyquist et al., 2020).

AR signaling suppresses the master neural transcription factor Pit-Oct-Unc domain, class 3, transcription factor 2 (POU3F2, commonly known as BRN2), which modulates SOX2 activity and is required for neuroendocrine transdifferentiation, thus establishing a mechanism by which decreased AR signaling promotes a neuroendocrine-like transcriptional program (Bishop et al., 2017).

Myc has been shown to induce rapid formation of PINs in GEMMs (Ellwood-Yen et al., 2003). *Myc* overexpression, together with *Pten* loss, induced metastasizing GEMMs using Hoxb13 transcriptional control elements (Hubbard et al. Cancer Res 2016). When accompanied by *Pten* loss, ectopic *N-Myc* expression induces neuroendrocrine PCa (Dardenne et al., 2016). Additionally, a mouse model with prostate-targeted *Pten* loss and expression of mutant *Kras* developed bone metastases. Interestingly, bone metastatic cells in this model exhibited enrichment of a *MYC* gene expression signature (Arriaga et al., 2020). *KRAS* is amplified in 2% of primary tumors and up to 20% of metastases. Similarly, *MYC* is amplified in 31% of primary tumors and 70% of metastases (Abida et al., 2019; Arriaga et al., 2020; Cancer Genome Atlas Research Network, 2015).

Cell populations that survive docetaxel therapy are marked by the activation of Notch and Hedgehog signaling pathways (Domingo-Domenech et al., 2012). Additionally, Notch signaling has also been suggested to contribute to enzalutamide resistance (Farah et al., 2019). Notch and Hedgehog pathways intersect with PI3K/AKT and NRF2 signaling, which together contribute to cancer cell survival, stemness, and therapy resistance (Xia et al., 2022). Interestingly, Notch signaling has been shown to suppress neuroendocrine-like differentiation in PCa (S.-Y. Ku et al., 2024).

2.4.8 MAPK/ERK activation

One cut homeobox 2 (ONECUT2) is a transcription factor that suppresses AR activity genome-wide by antagonizing FOXA1-dependent chromatin programs and is active in up to one-third of CRPC (Rotinen et al., 2018). *FOXA1* expression is reduced in NEPC, and reduced FOXA1 promotes neuroendocrine transdifferentiation by suppressing *CXCL8* expression, thereby stimulating MAPK/ERK pathway activation and the expression of *ENO2* (J. Kim et al., 2017).

MAPK pathway activation together with active fibroblast growth factor (FGF) signaling has been implicated in double-negative PCa, which is negative for both markers of NEPC and AR (Bluemn et al., 2017). Double-negative PCa is reported to account 7–23% of CRPC, thus possibly being more common than NEPC (Bluemn et al., 2017; W. K. Kim et al., 2024). Other studies have reported that double-negative PCa is driven by hepatocyte growth factor (HGF) and Wnt activation (W. K. Kim et al., 2024).

PPP1CA is amplified in 17–25% of mCRPC and only 7% of primary PCa. *PPP1CA* encodes the serine/threonine-protein phosphatase PP1-alpha catalytic subunit (PPP1CA), which promotes MAPK/ERK pathway activation by dephosphorylating the B-Raf inhibitory phosphorylation sites in PCa (M. Chen et al., 2018).

Despite the low frequency of canonical MAPK pathway activating mutations in primary PCa (Cancer Genome Atlas Research Network, 2015), amplification of MAPK pathway members is present in 32% of mCRPC. Moreover, transcriptomic and phosphoproteomic analyses showed even broader MAPK/ERK pathway activation in mCRPC (Nickols et al., 2019). Interestingly, the induction of oncogenic RAS has been shown to render LNCaP cells androgen-independent, suggesting that MAPK pathway activation can promote androgen-independency (Voeller et al., 1991). Moreover, culturing LNCaP cells in androgen-depleted conditions produced neuroendocrine-like cells with an activated MAPK pathway and elevated receptor-type protein-tyrosine phosphatase alpha (RPTPα) protein levels (X.-Q. Zhang et al., 2003). Moreover, increased RAF-1 expression has been associated with CRPC (R. Mukherjee et al., 2005).

PI3K/AKT and MAPK/ERK signaling can each sustain, and together synergistically augment, AR-mediated growth under ADT, indicating that aggressive PCas can be driven by multiple, parallel pathways rather than a single dominant route (Gao et al., 2006). In PTEN-deficient PCa, AR and PI3K signaling are reciprocally coupled; therefore, the inhibition of one axis reactivates the other, providing a strong preclinical rationale for combination blockade (Carver et al., 2011; Mulholland et al., 2011). However, clinical trials have only shown modest potential with no significant overall survival effects in combinatory settings despite a sound biological rationale (de Bono et al., 2025; Rescigno et al., 2024; Sweeney et al., 2021). Moreover, subjecting PTEN-null LNCaP cells to increasingly severe AR pathway suppression generated an AR-negative cell line that exhibited undetectable pAKT levels and elevated activity of the FGF and MAPK pathways (Bluemn et al., 2017). Together, this highlights that the PI3K, MAPK, and AR pathways appear to form a plastic, compensatory network, where pathway reliance shifts with disease context, which explains why combinatorial targeting has so far produced only modest clinical benefits.

2.4.9 Activation of CAF and myeloid support programs

Stromal changes are deeply intertwined with epithelial evolution in CRPC. Stromal AR modulates the epithelial response to ADT, as loss of *AR* in the stromal compartment has been shown to attenuate castration-induced epithelial apoptosis (Kurita et al., 2001).

Moreover, ADT-induced epigenetic activation of the MAPK pathway in CAFs reprograms them to provide metabolic support for tumors. By secreting glutamine, CAFs fuel mTOR activity and neuroendocrine transdifferentiation in epithelial cells, and may also facilitate metastasis through systemic glutamine elevation (Mishra et al., 2018).

Although *SMAD4* is infrequently altered in clinical PCa, functional studies in mouse models have revealed that SMAD4 acts as a potent barrier for progression and metastasis. Dual loss of *Pten* and *Smad4* drives fully penetrant, invasive adenocarcinoma with frequent lymph node and lung metastases, partly through upregulation of cyclin D1 and osteopontin, and critically, via yes-associated protein 1 (YAP1)-dependent secretion of CXCL5, which recruits C-X-C motif chemokine receptor 2 (CXCR2)-positive myeloid-derived suppressor cells. (Z. Ding et al., 2011; G. Wang et al., 2016). However, when low *SMAD4* mRNA expression is grouped with *SMAD4* deletions, these alterations can collectively make up as much as 54% of cases in metastatic cohorts, which implies clinical relevance (Miller et al., 2024).

Targeting myeloid-derived inflammation using CXCR2 inhibitors to block senescence-associated tumor-elicited chemotaxis has shown early potential for reversing antiandrogen resistance. The study also reported worse survival for higher expression of CXCL1, CXCL2, and CXCL8. Non-responders in the early trial appeared to be associated with *TP53* and *CDKN1B* alterations, suggesting that cell cycle bypass is a possible rationale for resistance to CXCR2 inhibition (C. Guo et al., 2023). Club cells have been proposed to participate in immune cell recruitment to the TME, as *CXCL1*, *CXCL2*, *CXCL8*, and *CXCL16* are enriched in regions containing club cell populations (Kiviaho et al., 2024).

2.5 Cellular mechanism of DDR

Cells rely on DDR to detect DNA lesions, activate checkpoint signaling, and engage in appropriate repair pathways to maintain genomic stability. DDR signaling coordinates DNA repair with cell-cycle progression, enforcing G1/S, intra-S, and G2/M checkpoints to allow time for repair before replication or mitosis proceeds (Flynn & Zou, 2011; Shiloh, 2003). If lesions remain unrepaired, the cells may undergo apoptosis, senescence, or mitotic catastrophe. In cancer, these checkpoint controls are often attenuated, allowing continued proliferation despite persistent DNA damage and promoting genomic instability (Groelly et al., 2023).

Importantly, DDR is not limited to DNA repair. Many components intersect with transcription, replication, chromatin remodeling, and signaling networks (Jackson & Bartek, 2009; Ljungman & Lane, 2004). This intertwining of genome maintenance with broader cellular programs means that partial DDR deficiencies not only have the potential to increase the mutational burden but also reshape transcriptional plasticity, lineage states, and therapy response.

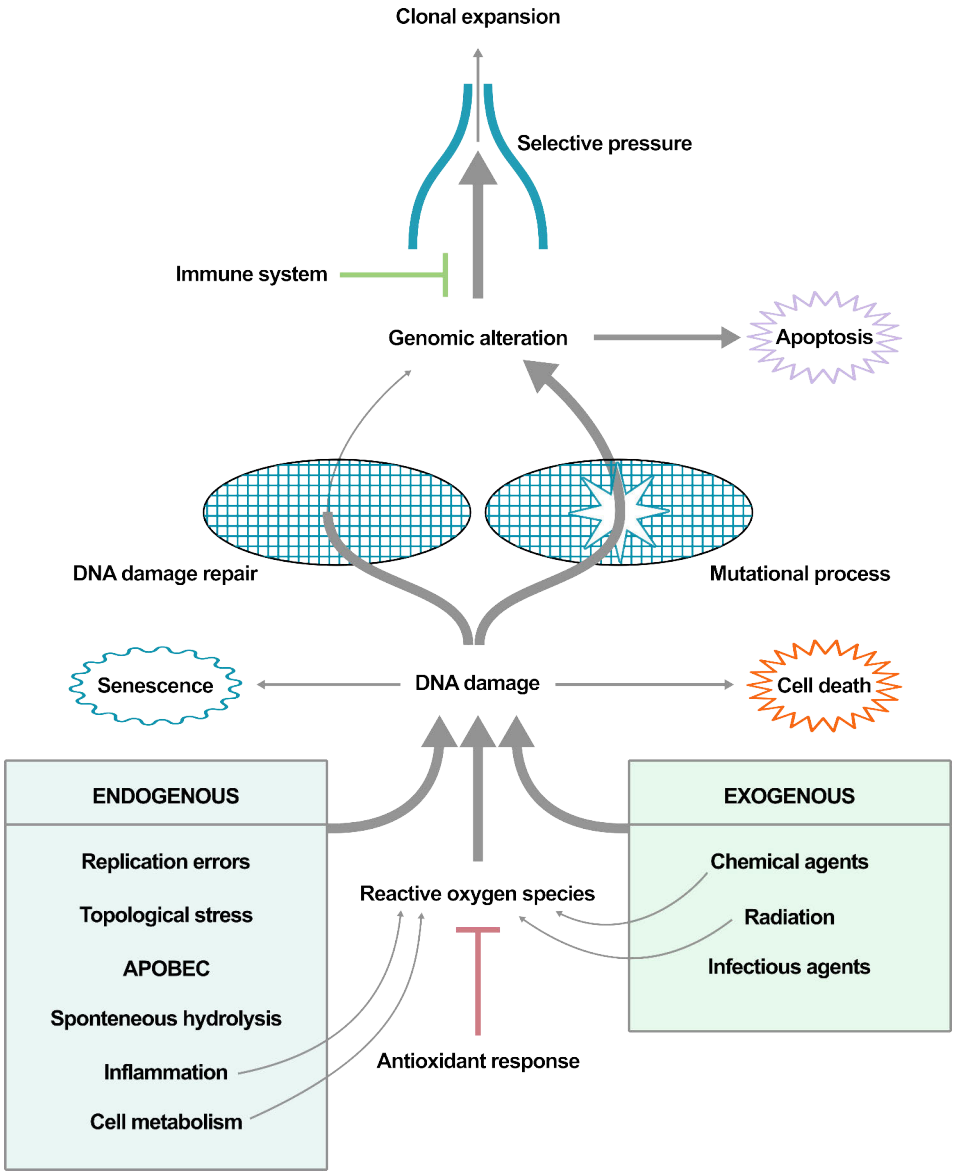

Figure 7. Schematic illustration of factors contributing to DNA damage and genomic alteration. Several endogenous and exogeneous mechanisms contribute to DNA damage in cell. Reactive oxygen species acts as an intermediate step for multiple factors, some of which cause damage both directly and via increased reactive oxygen species. DNA damage can trigger cell death or senescence as well as DNA damage repair/response. In most cases, damage is repaired, but repair can fail also in healthy cells, while a deficiency in a repair component function can cause recurrent error in DNA. Erronously repaired DNA should trigger rerepair or apoptosis in healthy cells, but this function can be deregulated in cancer. Additionally, immune cells identify and eliminate cells that express foreign molecules, thus preventing the survival of altered clones. However, in cancer, cells acquire genomic alterations and clonally expand when the acquired phenotype provides relative improved fitness.

2.5.1 DNA repair pathways

DNA can be damaged by chemical and physical insults, as well as by the dysfunction of interacting proteins, leading to structural instability (Figure 7). Specific DDR pathways are responsible for the repair of distinct types of damage. DDR operates through coordinated pathways involving sequential enzymatic activity (Figure 8). The double-helix structure of DNA allows the accurate repair of single-strand breaks (SSBs), as the intact complementary strand provides sequence information to guide repair. Unrepaired SSBs can lead to double-strand breaks (DSBs), particularly during replication (Groelly et al., 2023).

Some DNA repair pathways share key enzymes. For example, although PARP plays an essential role in DNA damage sensing of SSBs, it also serves minor regulatory roles in multiple pathways, including base excision repair (BER) and alternative end-joining (Alt-EJ; Caldecott, 2008). Certain repair pathways exhibit functional redundancy, meaning they can repair similar types of DNA damage depending on cellular conditions. Although this flexibility enables efficient genome maintenance across different cell types and conditions, it also creates an opportunity for cancer cells to bypass repair defects by engaging in alternative pathways (Dietlein et al., 2014; Helleday et al., 2008). This adaptability allows tumors to tolerate genomic instability, promotes survival, and facilitates the accumulation of mutations that drive cancer progression (R. Huang & Zhou, 2021).

While SSBs are simple to repair, with the appropriate pathways being guided by the available complementary strand, DSBs pose a greater challenge for DDR. Non-homologous end joining (NHEJ) is the most efficient and preferred pathway to repair DSBs. Under specific conditions, NHEJ is suppressed, as it can generate chromosomal rearrangements because it does not use a homologous chromatid as a template for repair. In these cases, HR, which usually uses the sister chromatid as a template, is preferred.

HR deficiency is often explained by the accumulation of DNA damage due to error-prone repair performed by NHEJ, but this is misleading because NHEJ is generally accurate (Blackford & Jackson, 2017). NHEJ is constantly used in healthy cells without inherently causing an accumulation of mutations. In fact, NHEJ is more common than HR (Mao et al., 2008). Moreover, NHEJ could more accurately be described as >99.9% error-free (Bétermier et al., 2014). Instead, when HR and NHEJ are unavailable for the repair of DSBs, cells may resort to alternative end joining or single-strand annealing pathways, which are highly mutagenic (Groelly et al., 2023).

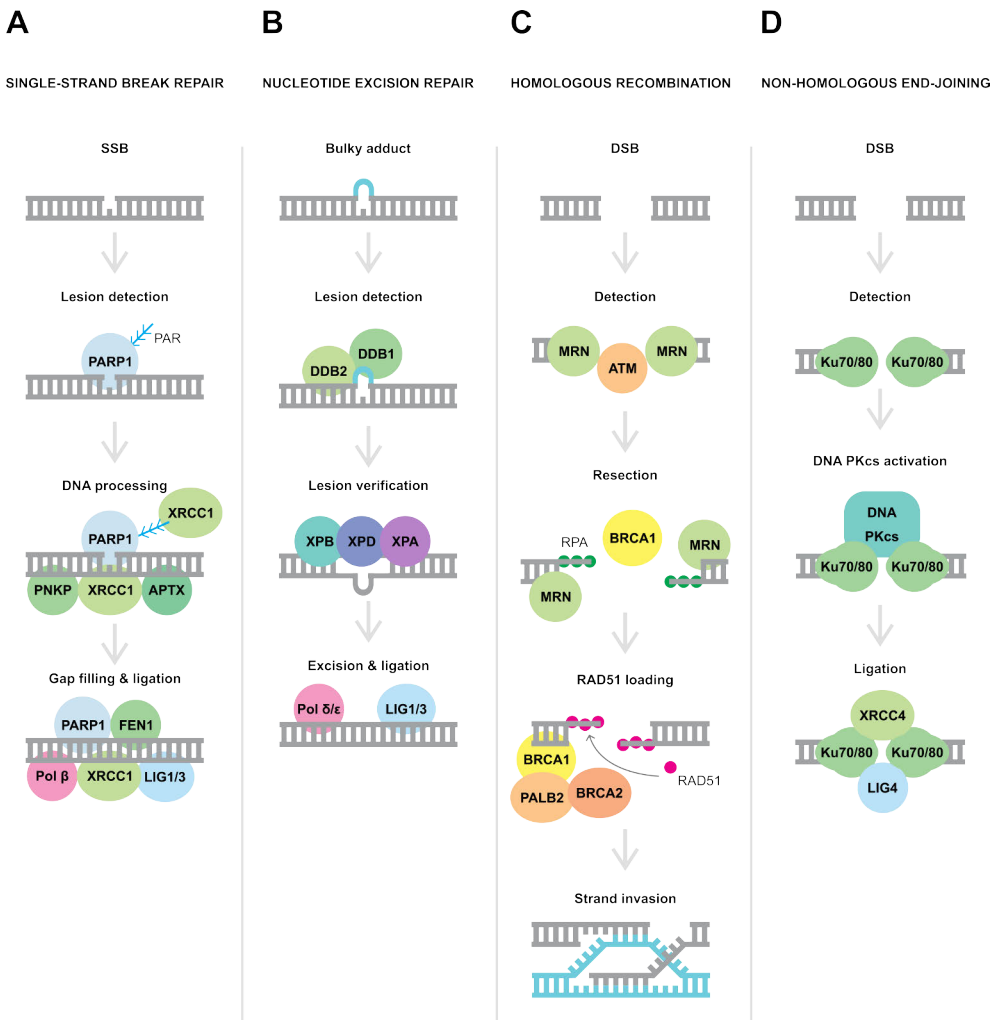

Figure 8. Simplified schematic depicting DNA repair pathways. The major DNA repair pathways are grouped according to lesion class and repair mechanism into single-strand break (SSB) repair, nucleotide excision repair, HR, and non-homologous end joining. (A) In SSB repair, PARP1 senses DNA SSBs and recruits X-ray repair cross-complementing protein 1 (XRCC1), which acts as a scaffold for end-processing enzymes including polynucleotide kinase 3′-phosphatase (PNKP) and aprataxin (APTX). Gap filling is primarily carried out by DNA polymerase β (Pol β), followed by ligation mediated by DNA ligase 1 and 3 (LIG1/3), with flap endonuclease 1 (FEN1) contributing in long-patch repair contexts. (B) In nucleotide excision repair, bulky DNA adducts are recognized by the DNA-damage-binding (DDB) protein complex DDB1–DDB2, followed by lesion verification mediated by xeroderma pigmentosum group B protein (XPB) and XPD in cooperation with XPA. Dual incision, repair synthesis by DNA polymerases δ/ε, and ligation by LIG1/3 restore DNA integrity. (C) In HR, DNA double-strand breaks are detected by the MRN complex, comprising of meiotic recombination 11 (MRE11), radiation sensitive 50 homolog (RAD50), and Nijmegen breakage syndrome protein 1 (NBS1), leading to ataxia-telangiectasia mutated (ATM) activation. End resection occurs in a BRCA1-licensed manner and is followed by the recruitment of breast cancer type 2

susceptibility protein (BRCA2) and partner and localizer of BRCA2 (PALB2). BRCA2 loads RAD51 onto the strand, which facilitates strand invasion and error-free repair using a homologous template. (D) In non-homologous end joining, DNA double-strand breaks are rapidly bound by the Ku70/80 heterodimer, which recruits and activates the DNA-dependent protein kinase catalytic subunit (DNA-PKcs). DNA ends are subsequently ligated by the XRCC4–LIG4 complex, restoring strand continuity without the need for a homologous template. HR = homologous recombination, PARP = poly(adenosine diphosphate-ribose) polymerase, BRCA1 = breast cancer type 1 susceptibility protein. Illustration adapted from Virtanen et al., Genes 2019.

Ataxia-telangiectasia mutated (ATM) and ataxia-telangiectasia and Rad3-related (ATR) are the main activating kinases involved in recognizing DSBs whereas PARP1 and PARP2 recognize SSBs (Caldecott, 2008; Shiloh, 2003). The meiotic recombination 11–radiation sensitive 50 homolog–Nijmegen breakage syndrome protein 1 (MRE11–RAD50–NBS1; MRN) complex senses DSBs and activates ATM (J.-H. Lee & Paull, 2005; Stracker & Petrini, 2011). DNA double-strand break foci are marked with the histone variant H2AX phosphorylated on Ser139 (γH2Ax) as one of the initial recruiting factors (Rogakou et al., 1998, 1999). This formation of γH2Ax foci occurring within a few minutes after DNA damage, is followed by a cascade of colocalization, first with BRCA1 colocalizing at the γH2Ax foci, followed by the colocalization of RAD50 and RAD51 at the foci (J.-H. Lee & Paull, 2005; M. Li & Yu, 2013).

2.5.2 BRCA1: genome maintenance, transcriptional control, and immune signaling

BRCA1 was named after the discovery of the hypothesized breast cancer susceptibility gene *BRCA1* in 1990 (Hall et al., 1990). *BRCA1* mutation carriers have a 70–80% and a 50% lifetime risks of developing breast and ovarian cancers, respectively (Roy et al., 2011). Estimated lifetime risk of developing PCa in *BRCA1* mutation carriers is 29%, corresponding to a relative risk increase of 2–4-fold (Nyberg et al., 2020). BRCA1 is a tumor suppressor that preserves genomic stability through its central role in DDR, particularly by mediating the repair of double-strand breaks via HR (Venkitaraman, 2002). The loss of *BRCA1* increases the likelihood of oncogenic alterations becoming fixed in the genome, thereby driving carcinogenesis and disease progression.

Beyond canonical DNA repair, BRCA1 is localized to centrosomes and spindle poles during mitosis (Hsu & White, 1998). In addition, BRCA1 has previously been suggested to broadly modulate transcription by interacting with a variety of key transcription factors (Savage & Harkin, 2015). However, more recent perspectives have proposed that these transcriptional observations may primarily arise as secondary consequences of HR deficiency, rather than direct transcriptional

regulation by BRCA1. Likewise, being highly regulated by the cell cycle is likely related to the role of BRCA1 in HR and mitosis. Even if secondary, these broad effects explain why complete BRCA1 knockout is embryonically lethal, why germline mutations are typically heterozygous, and why somatic loss is often accompanied by cooperative alterations such as TP53 mutations (Moser & Jonkers, 2025).

Structurally, BRCA1 is a large multi-domain protein consisting of an N-terminal RING domain, a coiled-coil domain, and a BRCA1 C-terminal (BRCT) domain. The RING domain is involved in the formation of RING–RING domain dimers, such as the BRCA1-BARD1 heterodimer, and is capable of E3 ubiquitin ligase activity (Brzovic et al., 2001). BRCA1 modulates the DNA repair mediated by breast cancer type 2 susceptibility protein (BRCA2) and RAD51 via its coiled-coil domain interacting with partner and localizer of BRCA2 (PALB2) which mediates the modulation of BRCA2-RAD51-mediated DNA repair by BRCA1 (Sy et al., 2009). The BRCT domain recognizes substrates phosphorylated by ATM and ATR, thereby functioning as a DNA damage–sensing structure (Manke et al., 2003). The large size of BRCA1, encompassing several functional parts that allow multiple combinations of interaction partners, including Abraxas, Broad complex–Tramtrack–Bric-à-brac and Cap ‘n’ Collar homology 1 (BACH1), and C-terminal–binding protein–interacting protein (CtIP), allows the formation of multiple distinct combinatory complexes with unique functions (Huen et al., 2010).

In the contexts of breast and ovarian cancers, *BRCA1* loss-of-function is tightly linked to chromosomal instability and therapeutic vulnerabilities to platinum-based agents and PARP inhibition (Stoppa-Lyonnet, 2016). Importantly, in 2005, two groups published the same finding that *BRCA1*/*2* mutant tumors are susceptible to PARP inhibitions, resulting in synthetic lethality due to a cascade of chromosomal instability, cell cycle arrest, and apoptosis (Bryant et al., 2005; Farmer et al., 2005). These findings established BRCA1 as a paradigmatic biomarker guiding precision oncology (Lord & Ashworth, 2016).

BRCA1 also contributes to antioxidant defense by stabilizing nuclear factor erythroid 2-related factor 2 (NRF2), a master regulator of oxidative stress responses, thereby protecting cells against oxidative DNA damage (Bae et al., 2004; Gorrini et al., 2013; Rojo de la Vega et al., 2018). This crosstalk integrates genome stability with cellular stress tolerance and illustrates how BRCA1 exerts tumor-suppressive functions across multiple pathways.

An additional emerging aspect of BRCA1 biology is its role in immune regulation. BRCA1 influences interferon signaling (Parkes et al., 2017)(Parkes et al. J Natl Cancer Inst 2017) and indirectly modulates immune checkpoint pathways via genomic instability (L. Ding et al., 2018). In *BRCA1*-deficient tumors, accumulation

of cytosolic DNA fragments activates cGAS–STING signaling, contributing to an immune-inflamed microenvironment (L. Ding et al., 2018; Pantelidou et al., 2019).

In PCa, alterations in DDR genes are detected in 20–30% of castration-resistant tumors, most often involving BRCA2, whereas BRCA1 mutations are rare, found in only 1–2% of cases (Abida et al., 2019; Armenia et al., 2018; Barbieri et al., 2012; Kumar et al., 2016; L. Nguyen et al., 2020; Robinson et al., 2015). The relatively low frequencies of BRCA1 mutations in pancreatic and PCa are in contrast to their high prevalence in breast and ovarian cancers (L. Nguyen et al., 2020). This tissue-specificity of BRCA1-mediated tumorigenesis has remained a key unresolved question in the three decades since the cloning of *BRCA1* (Moser & Jonkers, 2025).

2.5.3 DDR deficiencies and mutational processes in cancer

Deficiency in a DDR component causes a functional deficit in repair, leading to a mutational process, that creates an alternation imprint specific to the functional deficit (Figure 7; Martincorena & Campbell, 2015; Nik-Zainal et al., 2012). The actions of the process may depend on the context in which it functions, including other genomic aberrations and timing during cancer evolution. A tandem duplicator phenotype, characterized by genome-wide disruption of genes, loss of cell cycle control, DDR deficiency, and sensitivity to cisplatin chemotherapy, has been described in triple-negative breast, ovarian, and endometrial cancers (Menghi et al., 2016).

The tandem duplicator phenotype is associated with concurrent *TP53* and *BRCA1* mutations and increased DNA replication protein levels (Menghi et al., 2016). Interestingly, BRCA1-associated tandem duplications are not commonly observed in PCa. Instead, a distinct tandem duplicator phenotype associated with *CDK12* loss has been identified as a frequent and genomically defined subtype of CRPC, as discussed in chapter 2.4.6. Duplications in CRPC are prominent near *AR* and *MYC* (Viswanathan et al., 2018).

Different DDR alterations are associated with distinct structural variations in PCa. In addition to *CDK12* alterations associated with duplications, *BRCA2* alterations are associated with deletions and overall mutational burden, and *TP53* alterations are associated with inversions and chromotripsis (Quigley et al., 2018). *CDK12* alterations have been observed to be strongly enriched in cases of Gleason 8 or higher cases (Mateo et al., 2020).

Mismatch repair gene alterations that are associated with microsatellite instability and neoantigen expression due to systemic accumulation of mutations, are present in 12–22% of advanced PCa (Rodrigues et al., 2018). mCRPCs with mismatch repair deficiency have demonstrated an 81% disease control rate following dual immune checkpoint blockade, whereas rates were ≤25% in patients with high

mutational burden, *BRCA1/2* mutations or *CDK12* inactivation (van Wilpe et al., 2024).

Preclinical studies have suggested that AR signaling intersects with DDR; however, the findings are contradictory (Asim et al., 2017; Goodwin et al., 2013; Hasterok et al., 2023; L. Li et al., 2017; Polkinghorn et al., 2013). Activation of AR signaling increases the efficacy of DNA repair after IR, and inhibition of AR results in downregulation of NHEJ (Polkinghorn et al., 2013). DDR activation reciprocally supports AR activation mediated by DNA-dependent protein kinase catalytic subunit (Goodwin et al., 2013). Inhibitor of AR, enzalutamide, can downregulate the expression of the HR genes BRCA1 and Rad51C (Asim et al., 2017; L. Li et al., 2017).

Interestingly, luminal prostate cells express less γH2Ax than basal cells, which might be a consequence of their postmitotic state in the benign prostate, because these cells do not be anticipate DNA replication under benign conditions (Jäämaa et al., 2010). Thus, this lineage is inherently less competent in recognizing DNA lesions, which may make it more prone to acquire somatic alterations.

2.6 CaD as a structural regulator of cell contractility

CaD, named after calmodulin and the Greek *desmos* (binding), is a structural protein capable of binding actin, myosin, tropomyosin, and calmodulin, working as a part of the contractile apparatus in smooth muscle and non-muscle cells (Sobue et al., 1981; C. L. A. Wang, 2008). CaD inhibits myosin ATPase activity, which is required for myosin to move along the actin filaments, by binding to the two filaments. Notably, CaD binding interferes only with the force producing–stage and allows myosin to be fully primed for the next contraction (Z. Wang et al., 1997). This inhibitory effect can be modulated by Ca^{2+} via calmodulin and phosphorylation by kinases distinct from the actomyosin activators, positioning CaD as a regulatory interface for actomyosin contractility (Figure 9A; C. L. A. Wang, 2008).

Actin is the main microfilament and a fundamental component of the cytoskeleton and is involved in anything pertaining to movement and beyond in cells, including cell division, migration, exo- and endocytosis, apoptosis, inflammation, vesicle trafficking, and gene expression (C. L. A. Wang, 2008). While actin polymerizes spontaneously in vitro, actin organization in cells is highly regulated, from monomer binding to the formation of higher-order structures and networks comprising filaments (Pollard, 2016). The RhoA/Rho-associated coiled-coil containing kinase (ROCK) pathway is the key upstream initiator of stress fiber assembly and plays a broad role in diverse cellular processes. It promotes actomyosin contractility by activating myosin through phosphorylation of myosin light chain (MLC) and inhibition of myosin phosphatase (Ning et al., 2024). Actin organization

and remodeling are additionally modulated by a myriad of focal adhesion complex–associated adaptor and actin-binding proteins (C. L. A. Wang, 2008). At a fundamental level, actin-based cell motility involves protrusive structures driven by actin polymerization, and contractile structures mediated by interactions between actin and myosin (Svitkina, 2018).

Myosin, together with actin, forms the basic unit of the cellular contractile machinery, the actomyosin contractile apparatus. Although multiple myosin isoforms exist, each with distinct structural and functional properties, this thesis focuses specifically on class II myosins in the context of actomyosin-driven contractility. For simplicity, the term "myosin" is used throughout to refer to isoforms within this class. Nonetheless, it is important to note that non-muscle CaD and stress fibers are typically associated with non-muscle myosin II, which assembles into bipolar filaments that interact with oppositely oriented actin filaments. This arrangement enables myosin filaments to draw actin filaments toward each other, generating contractile force and cellular tension (Svitkina, 2018).

Tropomyosin functionally participates in the actomyosin contractile apparatus in the context of longer actin fibers as a regulator of myosin binding to actin in the presence of troponin and CaD (Pollard, 2016). Calmodulin is a Ca^{2+}-dependent activator of contraction in smooth muscle and non-muscle cells, promoting the activation of kinases phosphorylating actomyosin, and releasing the inhibition of actomyosin contractility by CaD and calponin. α-actinin functions as the main crosslinker of actin fibers in contractillity and ensures sufficient space between the actin fibers for myosin to interact with them (Svitkina, 2018).

While actomyosin contraction is ultimately executed by myosin motor activity on actin filaments, upstream regulation of this machinery is orchestrated by the Rho family GTPases. In particular, RhoA promotes stress fiber assembly and contractility through the activation of ROCK, which phosphorylates MLC and inhibits MLC phosphatase, thereby enhancing myosin II activity (Amano et al., 1996; Narumiya et al., 2009). This pathway is a major driver of actin–myosin contractility and focal adhesion maturation in migratory and mesenchymal-like cells. CaD does not oppose this process, but rather operates in parallel as a structural modulator that tunes the functional output of Rho–ROCK–MLC signaling. By crosslinking tropomyosin-rich actin filaments with myosin and inhibiting actomyosin ATPase activity in a calcium- and calmodulin-regulated manner, CaD shapes the spatial and temporal dynamics of contractile force generation (Kokate et al., 2022; C. L. Wang et al., 1991). Thus, CaD acts as a downstream scaffold and tension modulator within RhoA-driven cytoskeletal assemblies, maintaining the fiber architecture and controlling the magnitude and persistence of force transmission.

Stress fibers are associated with EMT and migratory and mesenchymal-like cells (Nurmagambetova et al., 2023). Moreover, they are involved in mechanosensing,

and stabile stress fibers are required for the maturation of focal adhesions, which are the primary points of interaction between the ECM and the cell (Figure 9B; Katsuta et al., 2024).

CALD1, located at 7q33, is translated into cell type–specific isoforms, with high-molecular-weight CaD (h-CaD) being expressed in smooth muscle cells and low-molecular-weight CaD (l-CaD) being expressed ubiquitiously in non-muscle cells. The structure of h-CaD differs from l-CaD only in the presence of a ~35 nm α-helical spacer that separates the myosin-binding N-terminal domain and the actin binding C-terminal domain (C. L. A. Wang, 2008). Although h-CaD plays a specific role in smooth muscle cells acting as a calcium-dependent regulator of actomyosin contraction, which is achieved with troponin in striated muscle cells, l-CaD exhibits a parallel role as a regulator of troponin-rich actomyosin contraction in non-muscle cells, whereas calponin regulates the contraction of troponin-poor fibers (Figure 9C).

2.6.1 Physiological and developmental roles of CaD

l-CaD has an elongated and extended shape, maintaining a regular structure in contractile stress fibers by ensuring a fixed spacing of myosin II filaments by binding and linking them to tropomyosin-actin fibers. Loss of l-CaD induces aberrant stress fiber organization, interfering with contractility and mechanosensing leading to problems with cell morphogenesis, migration, and invasion (Kokate et al., 2022).

In GEMM with an isoform-specific knockout of h-CaD, most pups developed omphaloceles, a severe abdominal wall defect that leads to perinatal death. However, surviving homozygotes exihibited no signs of herniation and showed compensatory upregulation of l-CaD in the bladder and vas deferens (H. Guo & Wang, 2005). A GEMM with a mutated CaD ATPase inhibitory site was homozygously lethal and exhibited an increased relative bladder size with hypertrophia in mice that were able to reproduce when heterozygous. Moreover, urinary bladder smooth muscle strips extracted from mice exhibit increased force in heterozygotes (Deng et al., 2013). *Cald1* knockout mice were also lethal and presented with omphaloceles, whereas heterozygous mice were viable with normal life spans. While the authors reported trends suggesting increased contractile force in heterozygotes and reduced force in homozygotes compared to the wild type, consistent with mechanistic expectations, these differences did not reach statistical significance in bladder or aortic preparations (Pütz et al., 2021). Moreover, a CaD knockout in the U2OS human osteosarcoma cell line diminished contractile forces, as measured using traction-force microscopy (Kokate et al., 2022). Stable expression of mutant CaD, which cannot be activated by calmodulin in Chinese hamster ovary cells, was shown to disrupt the assembly of focal adhesions and stress fibers while reducing cell motility of the cells (Y. Li et al., 2004).

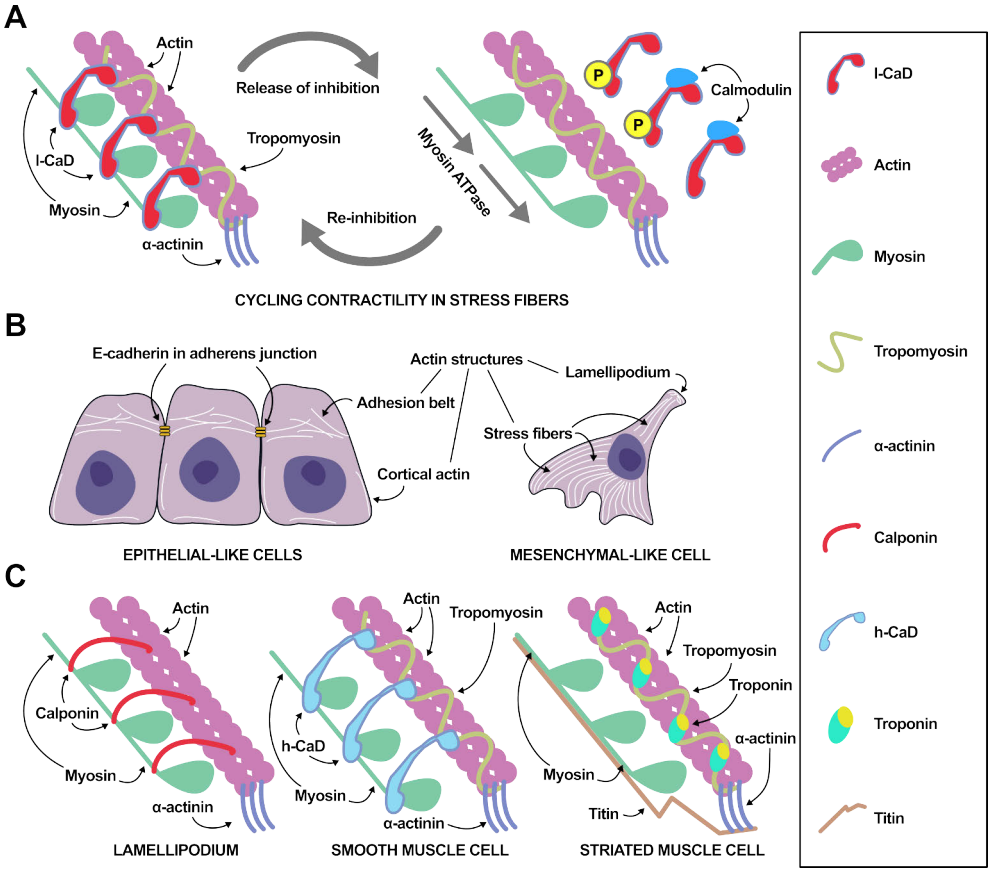

Figure 9. A schematic depicting the crude composition of the actomyosin contractile apparatus during the calcium-dependently inhibited state between smooth muscle cell, striated muscle cell/sarcomere, tropomyosin-rich actomyosin and tropomyosin-poor actomyosin using stress fiber as an example of a tropomyosin-rich actomyosin and lamellopodia as an example of tropomyosin poor actomyosin. (A) Tropomyosin associates with longer actin fibers. CaD binds tropomyosin-rich actin in non-striated muscle cells and there its other end binds to myosin. Actomyosin contractility is inhibited in this crosslinked state. (B) Particular cytoskeletal structures are enriched in different cell states. (C) Calponin plays a similar role in tropomyosin-poor fibers. CaD and calponin inhibition are relieved when they are either bound by calmodulin or phosphorylated (not shown). α-actinin is shown as an example of an actin crosslinker protein. In striated muscle cells/sarcomeres, troponin functions as the calcium-dependent inhibitor of actomyosin contraction. Instead of being activated by Ca^{2+}-sensing calmodulin, which is not expressed, troponin itself senses Ca^{2+}. Uniquely this inhibitory setup produces a truly relaxed state of actomyosin apparatus as unbound myosin is not mechanically restricted from moving relative to actin fibers, as it is when bound by CaD or calponin. This is in part allowed by titin and α-actinin together ensuring that distance between the fibers remains constant, even during movement. Whereas no free movement during inhibition can occur in non-striated muscle/sarcomere cells, the distance between actin fibers and myosin is however controlled by CaD/calponin binding. Notably, α-actinin is not involved in crosslinking actin to myosin alone or in concert with other proteins in cell types outside non-striated muscle cells/sarcomeres. CaD = caldesmon, l-CaD = low-molecular-weight CaD, h-CaD = high-molecular-weight CaD.

Reduced *cald1* expression via morpholino knockdown in *Xenopus laevis* leads to severe cartilage defects, resulting from impaired neural crest migration (Nie et al., 2011). In zebrafish, CaD is encoded by two genes: *cald1a*, encoding l-CaD- and h-CaD-like paralogs, and *cald1b*, which encodes only an l-CaD-like paralog (Abrams et al., 2012). In zebrafish, *cald1b* morpholino studies have reported profound defects in vasculogenesis, angiogenesis, and cardiac organogenesis during the first five days post-fertilization (P.-P. Zheng, Severijnen, van der Weiden, et al., 2009; P.-P. Zheng, Severijnen, Willemsen, et al., 2009). Another zebrafish morpholino study targeting h-CaD-like *cald1a* transcript while retaining l-CaD-like *cald1a* transcript expression, reported that intestinal propulsion was increased while the intestinal contractile rate did not change (Abrams et al., 2012). However, morpholino-induced phenotypes are often associated with off-target effects and can differ markedly from those of genetic mutants. Therefore, phenotypic validation using mutant lines is required (Stainier et al., 2017).

The functional divergence between CaD and calponin, two evolutionarily conserved actin-binding proteins expressed in a wide range of cell types, highlights the structural role of CaD in organizing the actomyosin architecture beyond mere inhibition of ATPase activity. Like CaD, calponin can bind to both actin and myosin, inhibit actomyosin ATPase, and is regulated by calcium-calmodulin binding and phosphorylation by ERK1/2 and protein kinase C (PKC; Hsieh & Jin, 2023). Despite this overlap, calponin lacks the ability to bind tropomyosin and is predominantly associated with cortical actin structures such as lamellipodia and membrane ruffles, which are typically low in tension and tropomyosin content. In contrast, CaD binds tropomyosin and is found in high-tension assemblies such as stress fibers, contractile rings, and focal adhesions, where actin–tropomyosin filaments are prominent (Kokate et al., 2022; C. L. Wang et al., 1991). Both proteins are not merely localized to these structures but appear to contribute to their formation. This is supported by experimental models in which disruption of either calponin or CaD leads to disorganization or loss of the corresponding cytoskeletal structures. These observations suggest that the central physiological role of CaD lies in its ability to stabilize and assemble tropomyosin-rich, tension-bearing actomyosin arrays, with ATPase inhibition arising as a secondary effect of this architectural role.

2.6.2 CaD in cancer

Published data regarding the role of l-CaD in cancer are conflicting. Several preclinical studies have reported anti-invasive or migration-suppressive effects, such as the inhibition of podosome/invadopodia formation or reduced contractility and focal adhesion formation (Helfman et al., 1999; Mayanagi et al., 2008; Yoshio et al., 2007). Conversely, other studies have shown pro-migratory and pro-invasive roles

across different lineages, including gastric cancer metastasis (Hou et al., 2013), breast cancer motility via cyclic guanosine monophosphate–protein kinase G type I beta–CaD (cGMP–PKGIβ–CaD) signaling (Schwappacher et al., 2013), ERK/CaD-driven EMT in hepatocellular carcinoma (J. Zhang et al., 2022), and TGF-β/zyxin-dependent stress fiber programs (Bianchi-Smiraglia et al., 2013).

Across patient cohorts, higher l-CaD/*CALD1* expression generally correlates with aggressive disease, including lymph-node metastasis, and poor prognosis in oral cavity squamous cell carcinoma (Chang et al., 2013), higher stages and reduced survival in gastric and colorectal cancers (K.-H. Kim et al., 2012; Y. Liu et al., 2021), higher grades and immune infiltration in glioblastoma and bladder cancer (Cheng et al., 2021; C. Li et al., 2021), and progression of non-muscle-invasive bladder cancer (M.-S. Lee et al., 2015). In bladder cancer, *CALD1* also promotes PD-L1 expression through JAK/STAT signaling, linking CaD to immune evasion (C. Li et al., 2021). Clinically, CaD has been associated with therapy resistance, including tamoxifen resistance in recurrent ER-positive breast cancer (De Marchi et al., 2016). In, colorectal cancer, l-CaD expression correlates with the primary tumor stage and lymph node stage and higher *CALD1* correlates with poor survival (Alnuaimi et al., 2023).

$\alpha_v\beta_3$, an integrin associated with bone metastases in PCa, has been shown to activate cdc2 (cdk1), which, together with l-CaD, localizes to membrane ruffles, where cdc2 phosphorylates l-CaD in motile LNCaP cells (Manes et al., 2003). Moreover, CaD is involved in the regulation of fascin in the bundling of actin (Ishikawa et al., 1998). Interestingly, fascin has been associated with metastasis and biochemical failure (Darnel et al., 2009). Moreover, *CALD1* is located on chromosome 7q33, a region frequently gained in PCa but lacking a well-characterized driver (Cancer Genome Atlas Research Network, 2015).

3 Aims

Even with the most recent multimodal combinatorial treatment regimens, high-risk diseases often progress to incurable CRPC. Metastases are the main cause of cancer-related mortality across cancers, yet no effective treatments currently exist that specifically target the process of metastasis.

Despite successful efforts to characterize the recurrent alterations in PCa, targeting AR signaling has remained the main approach to treating PCa, until the recent arrival of PARP inhibitors for specific DDR alteration carriers as the first precision oncology therapy in PCa.

This highlights the need to broaden the search for vulnerabilities in PCa biology beyond altered pathways to integrate the lessons learned in genomics with overlooked mechanisms to create a more accurate full view. The identification of such vulnerabilities requires that candidate targets intended for therapeutic intervention are supported by mechanistic evidence and exhibit context-specific roles that distinguish cancer-related functions from normal tissue requirements, allowing therapeutic intervention.

The tumor suppressor *BRCA1* is mutated in 1–2% of PCa. The functions and regulation of BRCA1 in PCa remain poorly understood. In parallel, new approaches are needed for CRPC, which eventually progresses to a lethal metastatic disease. The non-muscle contractility regulator l-CaD has been implicated in the metastasis of some cancer types but remains uncharacterized in the context of PCa.

The aims of this thesis were to:

1. Investigate the functional role and regulation of BRCA1 protein in PCa
2. Explore the role of l-CaD in PCa and assess its potential as a therapeutic target

4 Materials and Methods

4.1 Cell culture (I and II)

The cell lines PC-3, DU145, VCaP, PPC-1, RWPE-1, LNCaP, and 22Rv1 were obtained from the American Type Culture Collection (ATCC, Manassas, VA). PC-3, DU145, and VCaP cells were cultured in Dulbecco's modified Eagle's medium (DMEM; Gibco, Waltham, MA) supplemented with 10% fetal bovine serum (FBS; Gibco). Heat-inactivated FBS was used for PC-3 and DU145 cells, whereas VCaP cells were cultured in media containing non-inactivated FBS. PPC-1 cells were maintained in RPMI 1640 (Gibco) with 10% heat-inactivated FBS and 2 mM glutamine (Lonza, Quakertown, PA). RWPE-1 cells were cultured in Keratinocyte Serum-Free Medium (K-SFM; Gibco), supplemented with bovine pituitary extract and human recombinant epidermal growth factor (Gibco). LNCaP and 22Rv1 cells were cultured in RPMI 1640 supplemented with 10% heat-inactivated FBS, 2 mM glutamine (Lonza), 4500 mg/l D-glucose (Sigma-Aldrich, Burlington, MA), 10 mM HEPES (Lonza), and 1 mM sodium pyruvate (Gibco). All cell lines were maintained in the presence of 1% penicillin-streptomycin (Sigma-Aldrich) except during experimental treatments, routinely tested for mycoplasma contamination, and verified for cell line authenticity. A PC-3 cell line expressing mCherry was generated by lentiviral transduction using the pLV-mCherry vector (Addgene, Watertown, MA; #36084), followed by fluorescence-activated cell sorting to isolate fluorescent cells.

4.2 Zebrafish husbandry and genotyping (III)

Experiments were conducted under Finnish permits MMM/465/712–93, ESAVI/9339/04.10.07/2016, and ESAVI/31414/2020 in accordance with the Finnish Act on Animal Experimentation (62/2006) and the ARRIVE guidelines. The mutant lines *cald1a*^{sa16974} (*cald1a*−/−) and *cald1b*^{sa24667} (*cald1b*−/−) obtained from European Zebrafish Resource Centre (Karlsruhe, Germany) and provided by Dr. Derek Stemple (Wellcome Trust Sanger Institute, Genome Research Limited, Hinxton, United Kingdom) were used. Embryos were generated from heterozygote crosses to obtain homozygous mutants for the analyses and maintained in E3

medium supplemented with 1-phenyl-2-thiourea (PTU) at 28.5°C. For gene expression studies, DNA was extracted using the NucleoSpin TriPrep RNA/DNA/protein kits (Macherey-Nagel, Allentown, PA). For morphological and behavioral assays, embryos were lysed in 50 mM NaOH at 95°C for 10 min and neutralized with 1 M Tris-HCl (pH 8). Genotyping was performed using the Kompetitive Allele-specific PCR (KASP) assays (Biosearch Technologies, Hoddesdon, United Kingdom). The same protocol was used to genotype the adult carrier fish.

4.3 Antibodies (I and II)

Table 2. Antibodies used in this study. CaD = caldesmon, CST = Cell Signaling Technology, HRP = horse radish peroxidase, mAb = monoclonal antibody, SCB = Santa Cruz Biotechnology, Pa = patient samples, pAb = polyclonal antibody, Xe = xenograft samples

Antigen	Catalog no.	Type	WB	IF	IHC	Source	Study
Anti-rabbit IgG-HRP	A16104	Goat pAb	1:10,000	-	-	Invitrogen	I and II
Anti-mouse IgG-HRP	A16072	Goat pAb	1:10,000	-	-	Invitrogen	I and II
Alexa fluor 488 anti-rabbit	A-11034	Goat pAb	-	1:1,000	-	Invitrogen	I and II
Alexa fluor 555 anti-rabbit	A-21329	Goat pAb	-	1:1,000	-	Invitrogen	II
Alexa fluor 555 anti-mouse	A-21422	Goat pAb	-	1:1,000	-	Invitrogen	II
AKT	#4691	Rabbit mAb	1:1,000	-	-	CST	I
pAKT(Ser473)	#4060	Rabbit mAb	1:1,000	-			I
BRCA1	#9010	Rabbit mAb	1:1,000	-	-	CST	I
BRCA1	MS110	Mouse mAb	-	-	1:50	Millipore	I
pBRCA1 (Ser1524)	#9009	Rabbit mAb	1:1,000	-	-	CST	I
pBRCA1 (Ser1423)	ab47325	Rabbit pAb	-	-	1:500 (Xe), 1:150 (Pa)	Abcam	I
CaD	#12503	Rabbit mAb	1:1,000	1:200	-	CST	II
CaD	sc-25339	Mouse mAb	-	1:200	-	SCB	II
Cleaved caspase-3	#9664	Rabbit mAb	1:1,000	-	-	CST	I
E-cadherin	#3195	Rabbit mAb	-	1:1600	-	CST	II
FKBP5	#12210	Rabbit mAb	1:1,000	-	-	CST	I
FTH1	#4393	Rabbit mAb	1:1,000	-	-	CST	I

Antigen	Catalog no.	Type	WB	IF	IHC	Source	Study
GR	#12041	Rabbit mAb	1:1,000	1:200	-	CST	II
NRF2	ab62352	Rabbit mAb	1:1,000	-	-	Abcam	I
NQO1	#3187	Mouse mAb	1:1,000	-	-	CST	I
N-cadherin	#13116	Rabbit mAb	-	1:200	-	CST	II
PSA	#5365	Rabbit mAb	1:1,000	-	-	CST	I
Rad51	ab133534	Rabbit mAb	-	-	1:500	Abcam	I
Rad51	#8875	Rabbit mAb	1:1,000	-	-	CST	I
S6	#2317	Mouse mAb	1:500	-	-	CST	I
pS6 (Ser240/244)	#5364	Rabbit mAb	1:1,000	-	1:1,000	CST	I
Vinculin	sc-73614	Mouse mAb	1:1,000	-	-	SCB	I and II
ZEB1	#70512	Rabbit mAb	-	1:400	-	CST	II
β-actin	sc-1616	Goat pAb	1:1,000	-	-	SCB	II
β-actin	sc-47778	Mouse mAb	1:1,000	-	-	SCB	I
γH2Ax (Ser139)	#9718	Rabbit mAb	1:1,000	-	1:200	CST	I

4.4 Steroid hormones and inhibitors (I and II)

Androgen depletion (AD) treatments of VCaP cells was carried out 24 h after seeding or 48 h after transfection by washing two times and replacing the old media with media supplemented with 5% charcoal-stripped FBS (Gibco). 10 nM DHT (Sigma-Aldrich) or vehicle (methanol) was added after 48 h, and the cells were lysed after 24 h of DHT treatment.

PC-3 and DU145 cells were treated with 0.1, 1, or 10 μM dexamethasone (Abmole, Houston, TX or Selleckchem, Houston, TX) or vehicle (dimethyl sulfoxide; DMSO) 20 h after seeding and the cells were lysed after 24 or 48 h of treatment. DU145 cells were treated with 0.1, 1, or 10 μM prednisolone (Abmole) or vehicle (DMSO) 20 h after seeding and the cells were lysed after 48 h of treatment.

VCaP cells were treated with 10 μM enzalutamide (Abmole or Selleckchem) or vehicle (DMSO) (MP Biomedicals, Irvine, CA) 24 h after seeding. After five days of enzalutamide treatment, 0.1 μM dexamethasone or vehicle (DMSO) was added, and the cells were lysed after 24 h.

4.5 RNA interference (I and II)

Silencer® Select siRNAs (Ambion) targeting *CALD1*, *BRCA1*, and *NRF2* were used for the transfection (Table 3). For *CALD1* knockdown, PC-3 cells were transfected with 2.5 nM siRNA using 0.125% DharmaFECT 2 (Dharmacon); DU145 cells with

5 nM using DharmaFECT 1; and VCaP cells with 10 nM using DharmaFECT 3. For *BRCA1* knockdown, siRNA#457, #458, and #459 were used at 2.5 nM in PC-3 cells and 5 nM in LNCaP cells. *NRF2* knockdown was achieved using siRNA#9491 and #9492 at a concentration of 5 nM in LNCaP cells. Negative control siRNAs (siNeg1 and siNeg2) were used at matching concentrations. All siRNAs were diluted in Opti-MEM (Gibco), and transfection complexes were applied 24 h after seeding. Knockdown efficiency was verified by Western blotting 48 hours after transfection.

Table 3. siRNA oligonucleotides used in this study.

siRNA	Catalog no.	Target gene	Study
siNeg1	Neg CTRL#1	-	I and II
siNeg2	Neg CTRL#2	-	I and II
siBRCA1-1	siRNA#457	*BRCA1*	I
siBRCA1-2	siRNA#458	*BRCA1*	I
siBRCA1-3	siRNA#459	*BRCA1*	I
siCALD1-1	siRNA#2337	*CALD1*	II
siCALD1-2	siRNA#2339	*CALD1*	II
siNRF2-1	siRNA#9491	*NFE2L2*	I
siNRF2-2	siRNA#9492	*NFE2L2*	I

4.6 Cell lysis and Western blotting (I and II)

Cells were lysed using a buffer containing 1% Triton X-100, 20 mM Tris-HCl (pH 7.5), 1 mM EDTA, 150 mM NaCl, and 10 mM NaF. Immediately before use, the lysis buffer was supplemented with 2% cOmplete EDTA-free protease inhibitor cocktail (Roche, Penzberg, Germany), 10 mM Na4P2O7, and 1 mM Na3VO4. Cell lysates were incubated on ice and centrifuged to pellet the debris. Protein concentrations were determined, and 30–100 µg of total protein was resolved by SDS-PAGE using 4–15% gradient gels (Bio-Rad, Hercules, CA). Proteins were transferred onto nitrocellulose membranes (Santa Cruz Biotechnology, Dallas, TX), and nonspecific binding was blocked for 1 h in Tris-buffered saline with Tween-20 (TBST; 10 mM Tris-HCl, 150 mM NaCl, 0.05% Tween-20) containing 5% nonfat dry milk and 1% bovine serum albumin (BSA; Sigma-Aldrich). Membranes were incubated overnight at 4°C with primary antibodies diluted in TBST containing 5% BSA. The primary antibodies used were those against CaD, GR, BRCA1, NRF2, cleaved caspase-3, γH2Ax, and other targets (Table 2). After washing, membranes were incubated with horseradish peroxidase (HRP)-conjugated secondary antibodies

(goat anti-rabbit or goat anti-mouse IgG, 1:10,000; Invitrogen) for 1 h at room temperature. Bound antibody complexes were detected using the WesternBright Quantum chemiluminescence kit (Advansta, San Jose, CA) and imaged using either LAS-4000 (Fujifilm, Tokyo, Japan) or the ChemiDoc Touch Gel Imaging System (Bio-Rad, Hercules, CA).

4.7 RNA isolation, cDNA synthesis, and RT-qPCR (I and III)

Total RNA was extracted from cells using TRIsure (Meridian Bioscience) or TRIzol (Invitrogen), followed by purification using RNA Clean & Concentrator-25 kits (Zymo Research). The RNA quality and concentration were determined using a NanoDrop 2000 spectrophotometer (Thermo Fisher Scientific). RNA was isolated from zebrafish embryos using the NucleoSpin TriPrep kit (Macherey-Nagel). Complementary DNA (cDNA) was synthesized from 1 µg total RNA using either the SensiFAST cDNA Synthesis Kit (Meridian) or the High-Capacity cDNA Reverse Transcription Kit (Thermo Fisher Scientific). Quantitative PCR was performed using SYBR Green Master Mix (Applied Biosystems) with gene-specific primers or TaqMan Fast Advanced Master Mix (Thermo Fisher Scientific) with FAM-labeled probes. Amplification was carried out on a Bio-Rad CFX96 system under the following conditions: 50°C for 2 min (UNG activation), 95°C for 20 s, followed by 40 cycles of 95°C for 3 s and 60°C for 30 s. Relative gene expression was analyzed using the ΔΔCt method, normalized to ACTB (human) or Rpl13 (zebrafish) expression levels.

4.8 Tetrazolium-based viability assays (I and II)

Cell viability was assessed using the CellTiter 96® AQueous One Solution Cell Proliferation Assay (MTS; Promega, Madison, WI; G5430) according to the manufacturer's instructions. Cells were seeded in 96-well plates in triplicate and transfected with siRNA or treated as indicated. At the endpoint, MTS reagent was added directly to the culture medium, and plates were incubated at 37°C for the specified duration. The absorbance was measured at 490 nm using a Wallac Victor2 1420 Multilabel Counter (PerkinElmer, Waltham, MA). For PC-3 and VCaP cells, measurements were taken 48 h post-transfection, and for VCaP cells treated with AD medium and DHT, absorbance was measured 72 h after treatment.

4.9 Immunofluorescence (I and II)

For 2D immunofluorescence, monolayer-cultured cells were fixed with 4% paraformaldehyde for 10 min, washed with phosphate-buffered saline (PBS; 3 × 5 min), and permeabilized with 0.25% Triton X-100 for 10 min. After additional PBS washes, cells were blocked within 3% BSA in PBS for 1 h at room temperature. Cells were incubated overnight at 4°C with primary antibody against CaD (Cell Signaling; #12503, 1:200), washed, and then incubated for 1 h with Alexa Fluor 488-conjugated anti-rabbit IgG secondary antibody (Invitrogen; A-11034, 1:1000). Phalloidin 647 and DAPI were used for counterstaining. Imaging was performed using a Nikon Eclipse Ni microscope. Secondary-only controls were used to verify the specificity of each biological replicate.

For 3D spheroid staining, spheroids were fixed with 2% paraformaldehyde, transferred to tubes, and washed with 3D wash buffer (0.2% Triton X-100, 0.05% Tween-20, 0.1% BSA in PBS). Permeabilization was performed using 0.25% Triton X-100 for 10 minutes. After blocking in 2.5% BSA at room temperature, spheroids were incubated overnight at 4°C on a rotator with primary antibodies against N-cadherin (1:200), E-cadherin (1:1600), and ZEB1 (1:400) in wash buffer. The spheroids were then washed and incubated with Alexa Fluor 488- or 555-conjugated anti-rabbit IgG secondary antibodies (1:1000), followed by DAPI staining. Imaging was conducted using a 3i CSU-W1 spinning disk confocal microscope (Yokogawa, Tokyo, Japan), and intensity measurements were obtained in ImageJ using sum projections with background subtraction.

Immunofluorescence analysis of zebrafish embryos was performed as described by modifications from Inoue and Wittbrodt (Inoue and Wittbrodt Plos one 2011). Fixed embryos (4% paraformaldehyde overnight, 4°C) were permeabilized with 2% Triton X-100 for 1 hour and blocked overnight in PBSTx containing 5% FBS and 1% BSA. Embryos were stained with anti-N-cadherin (1:200) and anti-CaD (1:200), followed by staining with Alexa Fluor 488- and 555-conjugated secondary antibodies (1:1000) with DAPI. After four 1-hour washes, embryos were mounted on low-melting-point agarose and imaged using a 3i CSU-W1 spinning disk microscope.

4.10 Basement membrane matrix culture (I and II)

Cells were trypsinized 48 h after siRNA transfection, reconstituted in 25% basement membrane matrix (Corning, Corning, NY; Matrigel®, Growth Factor Reduced), and seeded in 96-well plates precoated with 50% basement membrane matrix (40 µl cell layer and 30 µl precoat /well) (Corning). 100 µl of culture media was added on top of the cell layer and the precoat after 1 h incubation at 37°C. The medium was replaced every 1–3 d. Dexamethasone (1 µM) or vehicle (DMSO) was added to the

treated wells on day 3. Duplicate wells were imaged on days 5 and 7 for a minimum of three 4x brightfield images per well using EVOS M5000 (Thermo Fisher Scientific, Waltham, MA). Spheroid size was measured in ImageJ with segmentation by manual thresholding and manual exclusion of spheroids merged owing to high initial proximity.

4.11 VCaP xenograft mice (I and II)

VCaP xenograft sections (I) were prepared according to a previously described protocol and permissions (Huhtaniemi et al. Am J Pathol 2018). Male mice bearing subcutaneous VCaP xenografts were surgically castrated four weeks after inoculation. Animals were sacrificed either two days (Cas 2D) or five days (Cas 5D) after castration, while intact controls were sacrificed at the same time as the Cas 5D animals. The tumors were collected, fixed in formalin, embedded in paraffin, and sectioned for immunohistochemical (IHC) analysis. Orthotopic (Knuuttila et al., 2014) and subcutaneous (Huhtaniemi et al., 2018, 2022) castration-resistant xenograft models (II) were generated previously.

4.12 Immunohistochemistry (I and II)

The sections were deparaffinized in xylene (3 × 7 min), rehydrated in an ethanol series, and rinsed in distilled water. Antigen retrieval was performed in citrate buffer (pH 6) using a microwave (7 min at 600 W, 7 min at 450 W) or a decloaking chamber for pBRCA1 and γH2AX staining. After cooling, endogenous peroxidase activity was quenched with 3% hydrogen peroxide, and nonspecific binding was blocked using antibody diluent. The sections were incubated for 1 h with primary antibodies (listed in Table 2), followed by incubation with secondary antibodies for 30 min. Signal detection was performed using DAB (Immunologic, WellMed BV, Duiven, the Netherlands), and nuclei were counterstained with Mayer's hematoxylin (Sigma-Aldrich). Slides were dehydrated using graded ethanol and xylene and mounted for imaging.

4.13 Digital pathology bioimage analysis using QuPath (I)

The slides were scanned using a Pannoramic P1000 slide scanner (3DHISTECH, Budapest, Hungary). Whole-tumor sections from xenografts were analyzed using QuPath version 0.4.4 (https://qupath.github.io/). Manual segmentation was first used to isolate the tumor tissue, and pixel classification algorithms were optimized for each antibody to detect regions with strong positive staining. Nonspecific

background staining and host tissues were excluded using custom classifiers and manual curation. Data extracted from the classified regions were exported for further analysis and visualization in R.

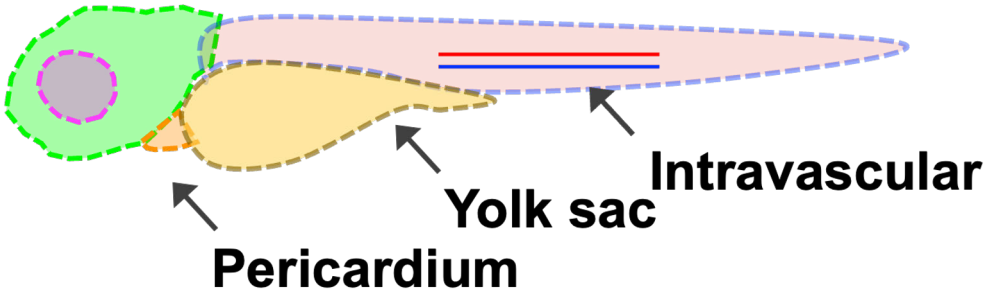

Figure 10. Schematic representation of zebrafish embryo morphology. Arrows indicate the injection sites used in the zebrafish metastasis assay. Dotted lines delineate anatomical regions quantified in Study II: eye (purple), head (green), pericardium (orange), yolk sac (yellow), and tail (blue).

4.14 Zebrafish xenograft metastasis assay (II)

Zebrafish embryos were generated in conditions described in chapter 4.2. Embryos were injected with mCherry-expressing PC3 cells or with DU145 and LNCaP cells, the latter two pre-labeled with CellTracker Green CFMDA (Invitrogen, Waltham, MA), using a Nanoject II microinjector (Drummond Scientific, Broomall, PA; Figure 10).

Following injection, embryos were transferred to E3 medium supplemented with PTU and PenStrep and incubated at 33°C. Imaging was performed under anesthesia one day post-injection (endpoint for the common cardinal vein assay) and 4 days post-injection using either a Zeiss AxioZoom V16 (Zeiss, Oberkochen, Germany) or Nikon Eclipse Ti2 (Nikon, Tokyo, Japan; Figure 11). Image data were processed using ImageJ, and all measurements were independently performed by two blinded investigators.

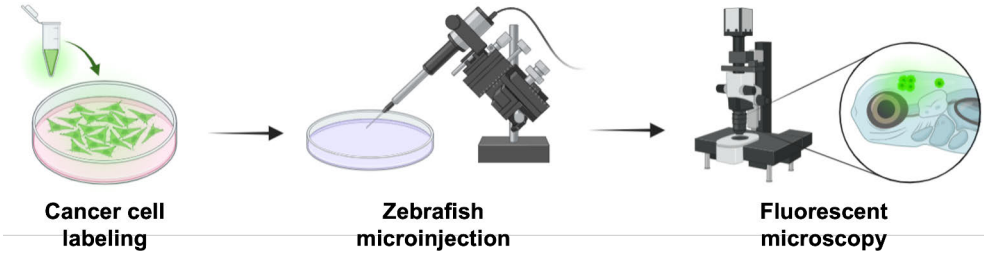

Figure 11. Schematic illustration depicting the zebrafish metastatic assay. Created with Biorender.com.

4.15 Zebrafish behavioral assays and morphological analysis (III)

DanioVision (Noldus IT; Wageningen, the Netherlands) instrument at 28.5°C was utilized for the behavioral assays. Four zebrafish embryos at 4 days post fertilization were placed in each well of square-bottom 96-well plates (Whatman Uniplate, Sigma-Aldrich) containing 300 µl of E3 medium. After a 30-minute adaptation period in darkness, the embryos were exposed to three consecutive cycles of 5 minutes of light and 5 minutes of darkness. Following the experiment, embryos were anesthetized in 200 mg/l tricaine, and DNA was extracted for genotyping.

Locomotor activity was recorded and analyzed using EthoVision XT software (Noldus IT) and GraphPad Prism 9 (GraphPad Software, San Diego, CA, USA). The first 20 minutes (adaptation phase) were excluded from the analysis. Baseline activity was calculated from the 20–30-minute time window and subtracted from subsequent values to correct for baseline variation. Statistical evaluation was performed using two-way ANOVA followed by Holm–Šidák post-hoc correction for multiple comparisons. To increase statistical power, genotypes were pooled as follows: wild type (wt = 52; wt + *cald1a*$^{+/-}$ + *cald1b*$^{+/-}$), cald1a (n = 24; *cald1a*$^{-/-}$ with *cald1b* +/+ or +/−), cald1b (n = 38; *cald1b*$^{-/-}$ with *cald1a* +/+ or +/−), and double mutant *cald1a*, *cald1b* (n = 13). In separate assays, embryos were exposed to 20 mM pentylenetetrazole (PTZ) and subjected to an identical adaptation and light–dark protocol. In these experiments, baseline subtraction and pooling were not applied.

For morphological analyses, anesthetized embryos were imaged using an Eclipse Ti2 microscope (Nikon). Morphometric parameters, including eye size, head size, body length, and pericardium size, were quantified using ImageJ software. Corresponding anatomical areas are highlighted in Figure 10. General morphology was visually inspected. All measurements were performed independently by investigators. Although no formal randomization or blinding was implemented,

genotyping was conducted after imaging, ensuring that phenotypic assessment was effectively blinded to genotype.

4.16 In silico dataset analyses (I, II, and III)

Publicly available datasets were used to investigate the regulation of gene expression, pathway enrichment, and patient survival. Expression data from LNCaP cells treated with R1881 were obtained from GSE50936 and downloaded via the R2: Genomics Analysis and Visualization Platform (http://r2.amc.nl). Differentially expressed genes were identified from RNA-seq data in GSE162225, comparing pooled samples of sh-BRCA1 (sh1 and sh2, n = 6) to sh-control (n = 3) using GEO2R (https://www.ncbi.nlm.nih.gov/geo/geo2r/). Significantly downregulated genes (adjusted p-value < 0.001, log2 fold-change > 1) were visualized as volcano plots using VolcaNoseR (https://huygens.science.uva.nl/VolcaNoseR/). Gene Ontology: Biological Process (GO:BP), Hallmark, and Oncogenic gene set enrichment analyses were performed using the Molecular Signatures Database (MSigDB v2024.1) (https://www.gsea-msigdb.org/). ReMap chromatin immunoprecipitation sequencing (ChIP-seq) tracks for AR and GR were acquired from the UCSC genome browser (https://genome.ucsc.edu/). Co-expression and survival analyses as well as mutation and expression profiling were performed using cBioPortal (https://www.cbioportal.org/) across multiple PCa cohorts, including patient-derived organoids.

4.17 Statistical analysis (I, II, and III)

All statistical analyses were performed using R Studio (https://www.posit.co/) and GraphPad Prism versions 8.4.2 or 10.1.2 (GraphPad Software). A two-tailed unpaired Student's t-tests or Mann–Whitney U tests were used to compare two independent groups. Analysis of variance (ANOVA) with appropriate post-hoc tests was used for multiple group comparisons. For zebrafish behavioral assays, 2-way ANOVA followed by Holm-Sidak post-hoc correction was applied where indicated. Correlation analyses were conducted using the Spearman's rank correlation coefficient. Categorical data were analyzed using Fisher's exact test or the chi-square test, where applicable. Data extracted from cBioPortal were based on version 4.1.9, and were analyzed using built-in tools or custom R scripts. For qPCR data, the ΔΔCt method was used to calculate fold changes, and all values were normalized to the reference genes (*ACTB* or *RPL13*). Statistical significance was set at p-value < 0.05, unless otherwise specified.

4.18 Ethical considerations (I, II, III)

The use of human tissue samples was approved by the Ethics Committee of the Hospital District of Helsinki and Uusimaa (decision number 84/13/03/00/2014), the Hospital District of Southwest Finland (T206/2014), and the National Supervisory Authority for Welfare and Health (VALVIRA, 8008/06.01.03/2014). All procedures were performed in accordance with the relevant guidelines and regulations. All zebrafish embryo experiments were conducted under licenses MMM/465/712–93, ESAVI/9339/04.10.07/2016, and ESAVI/31414/2020, granted by the appropriate Finnish regulatory authorities. Animal work was performed in compliance with the Finnish Act on Animal Experimentation (62/2006) and followed the ARRIVE guidelines.

5 Results

5.1 AR activation represses *BRCA1* in PCa

PCa is characterized by enhanced, aberrant, and evolving AR signaling. Despite recurrent somatic and germiline DDR alterations observed in PCa (Abida et al., 2019; Pritchard et al., 2016), *BRCA1* alterations are relatively rare in PCa compared with other DDR deficiency-associated cancer types (Abida et al., 2019; Stoppa-Lyonnet, 2016). Nevertheless, germline *BRCA1* mutations increase cumulative PCa risk (Nyberg et al., 2020), indicating a nuanced interplay between BRCA1 and AR signaling in PCa.

To investigate the regulation of BRCA1 by AR in PCa, we treated PCa cells with varying doses of DHT at different timepoints. Unexpectedly, we found that AR stimulated by its natural ligand DHT mediated the repression of BRCA1 expression at the doses and timepoints that induced PSA (I, Fig. 1). This was contrary to reports suggesting that DDR genes are upregulated in response to AR stimulation (Asim et al., 2017; Polkinghorn et al., 2013) and indicated that instead PSA and BRCA1 had inverse responses to AR stimulation. This finding was consistent between cell lines and was observed for both protein levels and in RNA expression. The repression at the protein level was more pronounced in the cell line with amplified *AR*, suggesting a dose dependent effect.

We did not assess whether repression occured in benign prostate cells or in cells of other tissue origins. Thus, the effect could be specific to PCa cells, as opposed to being universal for AR. This seems unlikely, however, as AR is enhanced and modulated by heterogeneous alterations in PCa, cell lines with varying alterations were used in our key experiments. If repression was limited to PCa, it would imply that these distinct alterations converge on a similarly modified AR function.

5.2 AR-mediated *BRCA1* repression controls NRF2-dependent ROS defense in PCa

To explore the functional effects of *BRCA1* repression in PCa, we analyzed genes downregulated during *BRCA1* silencing in LNCaP cells from a published dataset (Hoefer et al., 2014). As expected, gene sets related to the cell cycle, DNA

replication, and mitosis were downregulated. Notably, we also a observed significant downregulation of NRF2-regulated genes (I, Fig. 4A–C).

NRF2 is a master regulator of ROS defense and is known to be regulated by BRCA1, among other factors (Figure 12A; Bae et al., 2004; Gorrini et al., 2013; Rojo de la Vega et al., 2018). Several somatic events that occur already at the precursor lesion stage of PCa contribute to increased ROS (Costello & Franklin, 2006; Latonen et al., 2018; W. H. Lee et al., 1994; Pertega-Gomes et al., 2015), which may indicate that high ROS levels play a role in the initiation of PCa.

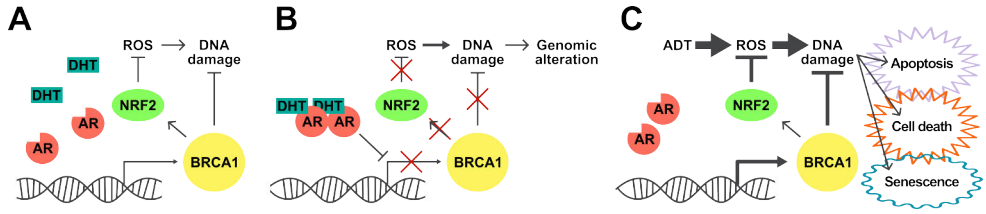

Figure 12. Schematic representation of AR-mediated regulation of *BRCA1* and activation of NRF2 by BRCA1 in PCa. (A) BRCA1 and NRF2 distinctly combat DNA damage and ROS, respectively, thus working in concert to prevent genomic alteration. BRCA1 supports NRF2 enabling its function in ROS defense. (B) Activated AR represses *BRCA1*, consequently disrupting DNA damage repair via BRCA1 and the NRF2 support by BRCA1, thus contributing to increased ROS. Increased ROS may escalate into increased DNA damage, which can eventually lead to genomic alteration. (C) ADT initially prevents AR activation, which reactivates BRCA1. ADT also induces massive ROS leading to high DNA damage, which can trigger senescence, apoptosis or cell death. BRCA1 and NRF2 collectively attenuate this effect. AR = androgen receptor, NRF2 = nuclear factor erythroid 2-related factor 2, BRCA1 = breast cancer type 1 susceptibility protein, ROS = reactive oxygen species, ADT = androgen deprivation therapy, DHT = dihydrotestosterone.

5.3 ADT sustains BRCA1 protein levels in PCa

ADT is the AR signal-disrupting cornerstone of therapies for high-risk PCa (Tilki et al., 2024), we studied the effects of ADT on *BRCA1* repression. In line with the repressive function of stimulated AR over *BRCA1* (Figure 12B), AD increased BRCA1 protein levels in cell lines that responded to AD with PSA decline (I, Fig. 2). Moreover, BRCA1 phosphorylation was induced in all cell lines in response to AD (I, Fig. 2).

Similar to BRCA1, NRF2 protein levels were upregulated in response to AD at longer timepoints (I, Fig. 4D). Furthermore, whereas silencing *BRCA1* did not downregulate NRF2 directly, NRF2 target protein product levels were downregulated (I, Fig. 5F). Moreover, silencing *NFE2L2* (gene encoding NRF2) inhibited BRCA1 upregulation under AD conditions (I, Fig. 4E; Figure 12C).

Similar results were observed in VCaP xenograft mice two days after castration, while results from later time points (day five) were inconclusive (I, Fig. 3A–D).

Importantly, pBRCA1 and PSA levels demonstrated a negative correlation also in vivo (I, Fig. 3E).

In paired patient samples obtained pre- and post-ADT, staining for BRCA1, pBRCA1, and γH2Ax was stronger in post-ADT specimens (I, Fig. 3F). This suggests that BRCA1 is upregulated in CRPC.

5.4 Sustained BRCA1 expression supports PCa growth in high ROS environment

As we had that tumors stained strongly for BRCA1 protein after ADT (I, Fig. 3F), we investigated whether BRCA1 expression contributed to resistance, thus aiming to provide an explanatory mechanism for selective pressure sustaining BRCA1.

Silencing *BRCA1* did not affect 2D viability, but restricted spheroid size in 3D culture. A similar reduction in spheroid growth was observed upon *NFE2L2* silencing (I, Fig. 5A–E). Furthermore, NRF2-regulated protein expression was significantly downregulated in the 3D culture of *BRCA1*-silenced LNCaP cells (I, Fig. 5F). This suggests that the NRF2-mediated antioxidant response was compromised following *BRCA1* silencing in a 3D setting. Because 3D culture has been associated with increased ROS (Q. Liu et al., 2018; Rybkowska et al., 2023), downregulation of antioxidant defenses likely contributed to reduced growth.

Finally, analysis of public patient datasets showed that *BRCA1* amplifications were present, although rare, in CRPC and that high *BRCA1* mRNA was associated with NEPC and poor prognosis in CRPC (I, Fig. 5G–K).

These findings imply that BRCA1 is an AR-depletion–responsive activator of NRF2, a known driver of therapy resistance in CRPC (P. Zhang et al., 2010). Moreover, our findings indicate that AR activity represses *BRCA1*, thereby simultaneously attenuating both NRF2-mediated ROS defense and BRCA1-mediated DNA repair.

5.5 AD downregulates l-CaD in PCa

We also found that steroid deprivation strongly downregulated l-CaD expression (II, Fig. 1D). l-CaD regulates of actomyosin contraction, particularly in stress fibers formed in non-muscle cells (C. L. A. Wang, 2008).

Stimulation with the AR ligand DHT rescued l-CaD expression after steroid deprivation (II, Fig. 1D), and stimulation with the GR ligand dexamethasone rescued l-CaD expression after enzalutamide treatment (II, Fig. 5A). Interestingly, neither ligand significantly increased l-CaD expression in highly AR-responsive VCaP cells when compared to the vehicle control (I, Fig. 1D and 5A), but dexamethasone and prednisolone upregulated l-CaD in AR-negative cells (II, Fig. 3D–F).

5.6 Nuclear receptor–associated *CALD1* RNA correlates with EMT- and migration-associated RNA in PCa

As l-CaD is not highly characterized in PCa, we explored its role by mapping its expression, alterations, co-expressed RNA and effects on viability in PCa.

We found that l-CaD was expressed in a panel of widely used commercial PCa cell lines, while no high-molecular weight isoform was observed (II, Fig. 1A). Moreover, *CALD1* amplifications were prevalent in a subset of patients across public datasets, with up to 5.9% present in the metastatic cohort (II, Fig. 1C).

We compared RNA expression data from seven patient datasets and found that patients with high *CALD1* mRNA also expressed higher levels of *NR3C1* (referred to as *GR* in I) mRNA and mRNA associated with EMT, migration, KRAS signaling, adipogenesis, the development of vasculature and cardiac ventricle, and expectedly, muscle cells (II, Fig. 1E–G).

Silencing *CALD1* did not affect viability in 2D culture but restricted spheroid size in 3D culture (II, Fig. 2A–C). These results suggest, that despite being highly steroid-regulated in PCa, l-CaD did not appear critical for 2D survival but was beneficial in 3D culture conditions.

5.7 l-CaD levels are induced by GR stimulation in PCa

Because GR overexpression is a well-defined resistance mechanism of bypassing AR signaling in PCa (Arora et al., 2013) and we found a high correlation between *CALD1* and *NR3C1* in PCa (II, Fig. 1E–G), we studied whether GR regulated *CALD1* in PCa. Additionally, *CALD1* has been shown to be regulated by GR in other cell types via the binding of DNA to glucocorticoid response elements located in the *CALD1* promoter (Mayanagi et al., 2008).

Dexamethasone also increased spheroid size in AR-negative cells, which was not observed in dexamethasone-treated cells with silenced *CALD1* (II, Fig. 3H). Moreover, in published ChIP-seq data, both AR and GR showed binding to the *CALD1* promoter region (II, Fig. 3A). This suggests that both the receptors, AR and GR receptors, likely participate in the regulation of *CALD1* transcription.

Using castrated subcutaneous VCaP xenografts subjected to antiandrogens (Huhtaniemi et al., 2022), we observed more positively stained cells for both CaD and GR (II, Fig. 5C and D). Using a similar model (Knuuttila et al., 2018), we observed that cells positively stained for CaD and GR were located in the same areas of the adjacent slides (II, Fig. 5E).

5.8 GR-driven resistance-associated l-CaD promotes EMT and metastasis in PCa

Since l-CaD is enriched in stress fibers that mediate migration particularly in mesenchymal-like non-muscle cells (Kokate et al., 2022; Nurmagambetova et al., 2023) and we found high correlation between *CALD1* and migration- as well as EMT-associated RNAs in PCa (II, Fig. 1E–G), we assayed the effect l-CaD in PCa metastasis using a zebrafish assay where human PCa cells were microinjected into zebrafish embryos.

Silencing *CALD1* reduced the rate of metastasis in AR-positive and AR-negative cell lines when injected into zebrafish embryos (II, Fig. 2D–M, Supplementary Fig. S4A–C). Primary tumors at the injection sites did not significantly differ in size between l-CaD-expressing and *CALD1*-silenced cells (II, Fig. 2G and K), suggesting that the reduced metastasis rate was not a secondary effect of altered primary tumor growth, but rather the result of l-CaD-dependent modulation of the metastatic cascade.

To study the mechanism by which l-CaD promoted metastasis, we focused on EMT, which is known to be involved in both metastasis and 3D growth, and was one of the highest-correlating gene sets in our co-expression analysis (II, Fig. 1E–G). Silencing *CALD1* resulted in the downregulation of the mesenchymal proteins ZEB1 and N-cadherin (II, Fig. 4A–G). Analysis of RNA-seq data from VCaP xenografts showed that epithelial *KRT8* expression was inversely correlated with *CALD1* expression (II, Fig. 5B and F).

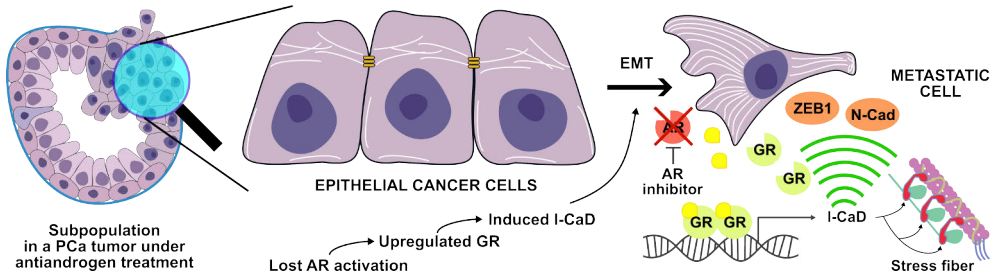

Figure 13. Schematic representing l-CaD as a novel regulator of PCa metastasis associated with therapy resistance. GR can become upregulated in response to AR inhibitor therapy in subpopulations of PCa cells. Activated GR allows cells to access transcriptome shared by AR and GR while bypassing AR signaling. GR activation via GR ligand (indicated in yellow) induces l-CaD, which localizes on stress fibers thus enabling efficient non-muscle contraction. In addition, l-CaD supports the expression of EMT regulator ZEB1 and the mesenchymal protein N-Cadherin. l-CaD = low-molecular-weight caldesmon, PCa = prostate cancer, GR = glucocorticoid receptor, AR = androgen receptor, EMT = epithelial-to-mesenchymal transition, N-Cad = N-Cadherin.

However, we found no difference in epithelial E-cadherin levels when *CALD1* was silenced, and no correlation between *CDH1* (referred to as *ECAD* in II) and *CALD1* was observed in VCaP xenografts (II, Fig. S5A, B, and S6A). This suggests that l-CaD protein levels correlated with a partial EMT shift, involving reciprocal changes in both epithelial and mesenchymal proteins, whereas the expression of some proteins, such as E-cadherin, appeared unrelated to l-CaD expression levels. However, in PCa, E-cadherin protein levels have been shown to be retained in EMT, even in the presence of ZEB1 downregulation (Putzke et al., 2011).

The implications of these results are summarized in Figure 13.

5.9 The loss of *cald1a*/*b* is tolerated in zebrafish embryos

Our findings suggest that l-CaD has oncogenic properties in PCa, promotes metastasis, and that its expression correlates with GR activation and EMT-like features in antiandrogen-resistant tumors. Therefore, we wanted to explore its potential as a therapeutic target.

Targeting a molecule systemically to effectively treat cancer requires reasonable tolerance for the inhibition of its function in healthy tissues. Ideally, such targeting would eliminate cancer cells without causing adverse effects on benign cells.

Previous studies have shown that homozygous loss of *Cald1* in mice is lethal, whereas heterozygotes exhibit diminished survival, often due to perinatal death caused by omphalocele (Deng et al., 2013; H. Guo et al., 2013; H. Guo & Wang, 2005; Pütz et al., 2021). However, surviving heterozygotes were able to reproduce and presented with mild changes related to the bladder (Deng et al., 2013).

In contrast, zebrafish morpholino studies targeting *cald1b*, which encodes an l-CaD-like transcript, reported severe defects in the vasculature and heart (P.-P. Zheng, Severijnen, van der Weiden, et al., 2009; P.-P. Zheng, Severijnen, Willemsen, et al., 2009). However, these results have not been confirmed using alternative approaches that avoid the potential off-target effects associated with morpholinos (Stainier et al., 2017).

To validate the zebrafish phenotype and investigate the potential of l-CaD as a therapeutic target, we studied the effects of CaD loss in healthy tissues using genetically engineered zebrafish.

We mapped the mRNA expression of *cald1a* and *cald1b* during early zebrafish development, focusing on tissue distribution and temporal expression patterns using publicly available datasets (III, Fig. 1). Our analysis indicated that *cald1a* was increasingly expressed throughout early development in a wide range of tissues, with the highest expression observed in the vasculature, heart, neural crest, retina, and basal cells. In contrast, *cald1b* showed a lower overall expression and was restricted

to a narrower set of tissues, including vascular smooth muscle cells and the neural crest.

Zebrafish lines carrying *cald1a*$^{-/-}$ and *cald1b*$^{-/-}$ mutant alleles were obtained. Heterozygous fish for both alleles were bred and subsequently incrossed into a dihybrid cross. The resulting offspring displayed allele frequencies consistent with Mendelian inheritance, suggesting that no genotype combination was lethal (III, Fig. 5).

The mRNA expression of both genes was analyzed in wild type, heterozygous mutants, and homozygous mutants for each gene, and no evidence of compensatory expression between the paralogs was observed (III, Fig. 3).

We measured and compared the gross morphology of single and double mutants between wild type as controls and observed no significant abnormalities (III, Fig. 2 and 4).

As a behavioral assay, we used light–dark illumination cycles to evoke visually induced swim responses and compared swim distances across genotypes. The double mutants exhibited altered responses to light stimuli (III, Fig. 6A). A similar but milder effect was observed in *cald1a* mutants, while *cald1b* mutants did not differ significantly from the wild type (III, Fig. 6B and C).

To assess whether this response resulted from increased general motility rather than altered sensory processing, we analyzed swimming behavior in response to the epileptogenic compound pentylenetetrazol, which induces robust locomotion independent of visual stimuli. Under pentylenetrazol stimulation, double mutants showed no significant differences compared to wild-type fish (III, Fig. 6D), suggesting that the altered response to light stimuli was due to neurological dysregulation rather than increased motor capacity.

These findings suggest that *cald1a*, and *cald1b* mutations are not lethal in zebrafish, and do not cause major developmental abnormalities during early embryogenesis. However, their loss was associated with a mild neural phenotype that likely reflected altered sensory processing, and additional physiological changes could possibly emerge later in development.

This supports the interpretation that CaD loss was relatively well tolerated in the early development of healthy zebrafish tissues, which suggests that despite its ubiquitous expression in non-muscle cells across a wide range of organisms, its critical functions were limited to specific developmental contexts rather than being universally required.

6 Discussion

6.1 New molecular mechanisms in CRPC

In this thesis, we describe mechanisms ranging temporally from factors potentially promoting acquisition of driver alterations at early disease to factors contributing to metastasis in late AR-independent disease. Owing to the evolving AR signaling in PCa, the mechanisms described span AR-mediated, AR-deprived, and AR-independent contexts.

A central insight is that the transforming AR signaling in PCa shapes selective pressures by dynamically adjusting the response to oxidative stress and DNA damage. DDR deficiencies are common in PCa (Abida et al., 2019; Pritchard et al., 2016) and other recurrent alterations are associated with increased DNA damage (Ruzanov et al., 2024; Watanabe et al., 2020). AR activity may cooperate with such alterations by attenuating NRF2-mediated oxidative stress response and DDR via *BRCA1* repression. Moreover, this regulation can also function as a buffer against ADT-induced oxidative stress (Blatt et al., 2023), as we demonstrated that ADT can reactivate this BRCA1-NRF2 regulatory axis, enabling PCa progression.

Selective pressures in PCa can also contribute to the emergence of AR-independent phenotypes such as the GR-driven bypass of the AR (Arora et al., 2013). Substitution of key transcriptional factors can enable phenotypic plasticity supported by altered cytoskeletal regulation. GR induces l-CaD, which enables stress fiber contraction and promotes EMT in PCa. This regulation bridges nuclear receptor signaling with therapy resistance and metastasis in PCa.

Taken together, these mechanisms highlight the multifaceted nature of PCa evolution. They integrate oxidative stress, compromised DDR, and triggered phenotypic plasticity. Detailing such molecular events in CRPC is essential for refining the integrative understanding of CRPC and identifying potential collective vulnerabilities within this heterogeneous disease.

6.2 Compromised ROS defense and transient DDR deficiency

Multiple highly common and early observed somatic events in PCa, such as *GSTP1* hypermethylation (W. H. Lee et al., 1994) and altered zinc levels, prompting a switch from the truncated TCA cycle to full (Costello & Franklin, 2006), collectively increase ROS. Moreover, the most common alterations in primary PCa, ETS fusion genes, and *SPOP* mutations, have been suggested to promote DNA damage (Ruzanov et al., 2024; Watanabe et al., 2020). As these features pertain to the majority of PCa cases, ROS and DNA damage are likely central, or even necessary, for PCa tumorigenesis.

AR stimulation strongly repressed *BRCA1* RNA expression and BRCA1 protein levels. This suggests that peaks in androgen availability or enhanced AR signaling create transient *BRCA1* deficiency states in PCa.

BRCA1 repression can lead to DDR deficiency via impaired HR. This functional, reversible DDR deficiency differs from classical loss-of-function mutations, and may lead to genomic instability under AR regulation. The functional significance of this deficiency is highly dependent on the concurrent presence or absence of DNA damage. As we also found that BRCA1 supports NRF2 function in 3D cultures of PCa, it may also be implied that ROS defense by NRF2 is compromised during *BRCA1* repression. Therefore, since PCa is almost universally affected by metabolic changes that increase oxidative stress (Costello & Franklin, 2006; W. H. Lee et al., 1994), AR-mediated *BRCA1* repression would be expected to exacerbate the effects of oxidative stress induced by these mechanisms.

Overall, early events in PCa collectively contribute to an increasingly dysregulated epithelium with increased oxidative stress and eventually DNA damage, synergizing with DDR defects or telomere dysfunction to allow the stochastic possibility of the emergence of aggressive disease drivers. Our results suggest a novel intrisic molecular mechanism with the potential to aggravate these pathogenic processes.

6.3 Tissue-specific tumorigenicity of BRCA1

BRCA1 mutations are rare in PCa despite *BRCA1* mutated tumors representing an aggressive phenotype with poor survival (Abida et al., 2019). Why *BRCA1* is highly mutated in some DDR deficiency–associated cancer types, whereas it is mutated relatively rarely in others, is a major unresolved question (Moser & Jonkers, 2025; B. Nguyen et al., 2022).

Our findings imply a novel rationale to answer this question in PCa: if AR signaling universally represses *BRCA1* in early PCa, there would be no selection for *BRCA1* mutations as all clones would be functionally *BRCA1* deficient. If this is the

case a similar tissue-specific *BRCA1*-repressive mechanism could also be present in pancreatic cancer.

An alternative explanation for the rarity of *BRCA1* mutation could be that BRCA1 protein is necessary for the survival of PCa cells. Notably, *AR* is not amplified unless subjected to AR signaling–targeting therapy, which may suggest a selective pressure against increased AR signal above the benign threshold. Reduced BRCA1 levels could be the mechanism for this selection if the BRCA1 protein is necessary for the survival of PCa cells. The promotion of NRF2 by BRCA1 could be one such rationale that may have the potential to create dependence.

Nevertheless, if peaks in AR activation occur in PCa, their expected consequence would be *BRCA1* repression and a simultaneous AR target hypertranscription. Oncogene-associated hypertranscription is associated with increased R-loop formation (Bowry et al., 2021). BRCA1 is required for the R-loop-driven DNA repair (Hatchi et al., 2015). Therefore, it is compelling to hypothesize that *BRCA1* repression by AR could contribute to AR transcription–driven DNA break events, such as ETS fusions.

Furthermore, ETS fusion–positive tumors exhibit chromoplexy at transcriptionally active loci, supporting a model in which transcription-associated DNA damage repeatedly results in complex rearrangements in susceptible tumors (Baca et al., 2013). This could be achieved by transcription-dependent *BRCA1* downregulation or a similar mutational process linked to transcriptional activity. Moreover, as ETS fusion proteins are associated with increased genotoxic stress (Ruzanov et al., 2024), they could speculatively synergistically exacerbate the *BRCA1* repression–phenotype. On the other hand, mCRPC with multiple concurrently hyperactive transcription factors may require BRCA1 activity to prevent massive R-loop-driven DNA damage.

In summary, our findings offer a plausible explanation for unresolved questions regarding the tissue-specific role of BRCA1 in PCa and expand hypotheses about the mechanistic origins of the ETS gene fusions, although further investigation is warranted.

6.4 ADT selects for ROS defense and activates BRCA1

AR-targeting therapies increase ROS thus creating a metabolic need to maintain antioxidant programs (Blatt et al., 2023). Our findings suggest that upon AD, BRCA1 is activated and may support NRF2 function in ROS defense. This would provide means for the tumors to balance ROS and DNA damage induced by the therapy.

An implication of this finding is that subclones carrying somatic *BRCA1* losses would have inferior fitness under selective pressure applied by ADT and would thus

be selected against. This is supported by our finding that silencing *BRCA1* results in poor 3D growth. This interpretation provides an additional rationale as to why *BRCA1* alterations are not enriched in CRPC compared with hormone-naïve PCa, similarly to other DDR alterations, such as *BRCA2* losses.

Speculatively, BRCA1 being sustained by ADT suggests enhanced HR efficiency, which may partially explain the limited effect reported for PARP inhibitors administered in combination with AR antagonists outside subgroups with HR mutations (Agarwal et al., 2023; Chi et al., 2023; Clarke et al., 2022; Fizazi et al., 2024; Saad et al., 2023), despite preclinical reports suggesting that AR antagonists may decrease BRCA1 levels thus creating a state of induced BRCAness (L. Li et al., 2017). Even if enzalutamide does decrease BRCA1, the functional significance could be thwarted by selective pressure favoring sustained BRCA1.

6.5 l-CaD is a novel regulator of PCa metastasis associated with therapy resistance

Using several injection sites and different PCa cell lines, we found that silencing *CALD1* decreased the rate of metastasis in PCa cells independently of AR status. l-CaD correlated with EMT, providing a putative mechanism for prometastatic function in addition to l-CaD, enabling enhanced motility.

In our study, E-cadherin levels remained stable, despite being a canonical epithelial marker, while N-cadherin and ZEB1 were correlated with l-CaD. This could be expected in PCa, as E-cadherin protein levels are high even in mCRPC and the protein might commonly remain expressed during the entire metastatic cascade in PCa (Putzke et al., 2011). This suggests that in PCa, epithelial cell–cell adhesions may remain intact during metastasis which could allow the migration of multiple cells together (Lambert et al., 2017).

Notably, the chromosomal region where *CALD1* is located is recurrently affected by arm-level amplification in PCa, but the relevance of this amplification remains poorly defined (Cancer Genome Atlas Research Network, 2015). Moreover, our data suggested a partial response to DHT stimulation after AD and moderate similarities between the AR and GR ChIP-seq profiles. Together, these findings support a possible broader relevance beyond GR-driven, AR bypass–associated resistance and warrant further investigation. One possible direction would be to examine the correlation between 7q amplifications and metastatic progression in more detail.

Our findings appear to have been partially reproduced in a recent analysis, as *CALD1* was positively selected for in lung metastases under CRISPR activation conditions in a genome-wide screening panel. Interestingly, in the same model, *BRCA1* was positively selected in bone metastases under both CRISPR activation and inhibition conditions, suggesting that both disrupted and activated *BRCA1* may

contribute to metastasis, which supports the rationale that the tumor suppressor also plays a secondary role by modulating the antioxidant response (Arriaga et al., 2024).

6.6 CaD is largely redundant in early zebrafish development

GEMMs have demonstrated that loss of homozygous CaD is lethal in mice. The apparent etiology for death suggested collectively by the models was omphalocele, with no other clear abnormalilities reported. In contrast, heterozygotes presented with increased bladder size and force (Deng et al., 2013; H. Guo & Wang, 2005; Pütz et al., 2021). Our findings in zebrafish suggest that mutant CaD causes mild neurological defects, with the absence of severe abnormalities during early development. Together, these findings suggest that CaD is irreplaceable only during specific developmental processes. Moreover, these specific processes might be specific to mammals and related to the closing of the umbilical cord, which may require higher cellular forces than those present in the development of oviparous animals. Instead, its absence appears to be largely compensable, likely by calponin and other cross-linkers of microfilaments.

Although morpholino knockdown of *cald1b* was previously reported to produce a severe vascular phenotype (P.-P. Zheng, Severijnen, van der Weiden, et al., 2009; P.-P. Zheng, Severijnen, Willemsen, et al., 2009), our genetic analysis revealed that zebrafish lacking both *cald1a* and *cald1b* were viable and exhibited no vascular defects, indicating that the earlier phenotype was not attributable to CaD loss. This supports the broader concern that morpholino-induced phenotypes may reflect off-target effects or stress responses rather than specific gene functions (Stainier et al., 2017).

This suggests that CaD is highly redundant outside of highly specific conditions pertaining to high forces and a high number of stress fibers. However, these implications would signify that CaD provides superior contractile strength. Such a capability would plausibly translate to efficient locomotion when acquired by cancer cells, as evidenced by our findings regarding GR-acquired l-CaD in PCa.

6.7 Reinterpreting l-CaD in stress fiber contraction

l-CaD is often cited as a regulator of contraction because of its ability to inhibit myosin binding to actin (Yao et al., 2021) or even an inhibitor of cell motility (Schwappacher et al., 2013). This contrasts with ours and others' reports of a prometastatic role for l-CaD (Chang et al., 2013; Hou et al., 2013; L. Zhang et al., 2014). Moreover, the concept of CaD as an inhibitor of contraction is inconsistent with evidence that its absence in mice causes lethal omphalocele (Deng et al., 2013;

H. Guo & Wang, 2005; Pütz et al., 2021). Importantly, omphaloceles also cause lethality in mice lacking ROCK (Y. Shimizu et al., 2005), which is considered the principal inducer of actomyosin contraction.

Taken together, these findings call for a more integrated description of the CaD function. The following paragraphs outline the reasoning behind the role of CaD as an enabler, rather than an inhibitor of contraction.

To understand the role of CaD, it may be useful to examine the only cell type which does not express it – the skeletal muscles. CaD is not expressed in striated muscle cells where actomyosin contractility is inhibited by troponin, which can completely prevent myosin from binding to actin. This inhibition additionally permits the relative free movement of filaments during relaxation in the presence of ATP (Gordon et al., 2000). Upon Ca^{2+}-induced activation, myosin readily binds to actin, aided by the precise filament alignment maintained by the sarcomeric cytoskeleton, primarily titin, α-actinin, and myomesin (Gautel, 2011; Gordon et al., 2000).

In contrast, CaD and calponin inhibit actomyosin contractility by physically bridging the actin and myosin filaments. This steric interaction not only suppresses ATPase activity, but also constrains filament spacing. As such, additional structural scaffolds may not be required to preserve alignment during relaxation, while it has to be noted that also other cross-linkers such as α-actinin (Sjöblom et al., 2008) are broadly expressed in non-muscle cells. Thus, CaD and calponin may simultaneously play dual roles analogous to those of sarcomeric structure proteins and troponin.

Importantly, CaD binding myosin does not interfere with myosin priming (Z. Wang et al., 1997). Therefore, CaD binding is likely to be immediately followed by actomyosin contraction when binding is relieved. This constrasts with inactivation of the RhoA/ROCK pathway, which prevents myosin ATPase activity. In this light, CaD binding is more accurately described as a delaying event rather than a preventing event. In some contexts, it may not interfere with contraction at all, but instead act to complement and coordinate actomyosin function.

Therefore, a more balanced interpretation would be to describe l-CaD as a key component in the contraction of stress fibers. This description makes it more intuitive to understand how l-CaD allows metastasis while being redundant to healthy cells.

6.8 Transient canonical mechanisms and vulnerabilities

Our suggested mechanism of AR-mediated *BRCA1* repression demonstrates that if, for example, an aggressive CRPC has one clear driver alteration but exhibits no other canonical genomic alterations in *PTEN*, *TP53*, *RB1*, *BRCA2*, or *CHD1*, it raises the question of whether the mere absence of mutation, deletion, or methylation is

sufficient to confirm an intact tumor-suppressive function. The lack of alteration in a canonical tumor suppressor in aggressive disease could easily be erroneously considered evidence of their continued protective function. However, this assumption does not consider the possibility that these proteins may adopt context-dependent roles in the altered regulatory environment of certain tumors. Functional suppression may be lost through transcriptional factor regulation, epigenetic silencing, post-translational inhibition, or pathway rewiring, all of which evade detection by genomic profiling.

As another example, SMAD4 is regularly cited as not being frequently altered in PCa. This is correct, but when low mRNA expression taken to account, over 50% of metastatic cases display reduced expression (Miller et al., 2024). Preclinical evidence suggests a strong potential for this protein to promote metastasis in PCa which is consistent with this finding. Therefore, it can be argued that there are common molecular factors outside the recurrent genetic factors that drive progression toward lethal PCa.

As identifying the genetic factors has not yet provided feasible therapies outside PARP inhibitors, better characterization of transient but canonical events should be a field of research expanded in the future for PCa. Notably, the most successful therapeutic strategy to target AR by ADT is not exploiting an alteration-based vulnerability. Therefore, it is not unexpected that more vulnerabilities could be exploited. Despite putative future mechanistical targets being non-altered per se, the genetic characterization of PCa will likely contribute to the discovery of such vulnerabilities.

6.9 Limitations

While multiple complementary approaches were applied across cellular, xenograft, and genetic models, in addition to patient data, to strengthen the conclusions, each system has inherent constraints that may affect how the observed phenomena translate to clinical settings. Recognizing these limitations is essential for defining the scope of the conclusions and interpreting their implications for guiding future studies.

Although most of our BRCA1-related findings were not derived from experiments utilizing *BRCA1* siRNA, the recent critique of setups involving strong overexpression or depletion is relevant to address. Experimental systems that induce strong RNA interference–mediated *BRCA1* depletion have been criticized, and the meaningful interpretation of BRCA1-specific effects has been questioned. This concern arises from the broad secondary effects caused by the loss of central functions, such as HR (Moser & Jonkers, 2025). To circumvent this, we used siRNA to induce partial loss instead of a complete loss. Additionally, these findings were

verified using an alternative approach, such as silencing *NFE2L2* in the case of the 3D growth effect. Thus, this experiment simultaneously tested the mechanical hypothesis and verified the suggested effect. Notably, silencing *BRCA1* during 2D growth did not affect viability, demonstrating that the suggested catastrophic effects of *BRCA1* loss via RNA interference were not evident under standard culture conditions. We interpreted the 3D effect to be, in part, due to increased ROS, which might imply that the lack of effect in 2D is due to the absence of DNA damage. There are other possible differences between 2D and 3D culture conditions that may cause the different findings.

The results regarding GR-driven phenotype, should not be interpreted simply as being glucocorticoid-driven. The regulation of glucocorticoid secretion is complex and the sensitivity to these hormones is additionally being regulated at tissue and cell-type level in a complex manner. Moreover, the clinically relevant source of GR activation in GR-driven PCa is not necessarily glucocorticoid-driven as the receptor can respond to multiple ligands. However, upregulation of GR expression in PCa cells is likely a more significant determinant of GR activity than the availability of ligands. Notably, glucocorticoids are effective and widely used in broad therapeutic attenuation of symptoms associated with PCa and other cancers.

The main general limitation of xenograft models is the heterologous TME and the lack of an immune response. The use of zebrafish embryo xenografts offers several practical advantages over costly and time-consuming murine xenografts. The main advantage of using mice over zebrafish xenografts is the higher similarity between the host and human tissues. The longer incubation times and the mammalian TME in mouse models are expected to contribute to a more sophisticated tumor structure with the presence of host fibroblasts and eventually vasculature within the tumors. Using mice as a host also enables the study of orthotopic xenografts.

On the other hand, the zebrafish xenograft model allows for a faster implementation of experimental settings with the possibility of inoculation of siRNA-transfected cells and broad compatibility with cell lines. Moreover, zebrafish require fewer inoculated cells, and their optical qualities allow non-invasive and live imaging, allowing large-scale experiments. Furthermore, our results with common PCa cell lines appeared to reproduce the metastatic patterns observed in similar mouse xenograft assays (X. Wu et al., 2013).

6.10 Future perspectives

As l-CaD is regulated by glucocorticosteroids, it poses the question of whether this regulation is utilized as a mechanism of metastasis by other types of cancers as well. Because AR signaling naturally inhibits GR signaling and, consequently, GR signaling is only significantly activated under treatment-specific conditions in PCa.

Therefore, the regulatory access for GR to l-CaD might be more readily available in other cancer types. Glucocorticoids are steadily produced by adrenals as part of physiological homeostasis. Moreover, tumor-adjacent tissues and the tumors themselves can contribute in extra-adrenal steroid synthesis. Additionally, glucocorticoids are broadly used to treat various cancer- and treatment-associated symptoms. As the responsiveness of l-CaD to GR stimulation has been demonstrated in lung cancer cells (Mayanagi et al., 2008), the regulation could potentially be present across multiple cancer types. The wide availability and presence of glucocorticoids in cancer and the lethality of metastases calls for further research on this topic.

Our results in early zebrafish embryos demonstrating non-lethality and a phenotype with no major defects apart from minor neurological impairment present l-CaD as a potential target molecule. Taken together with previous data in mouse models, where impaired abdominal wall closure led to some lethality and otherwise largely healthy tissues (Deng et al., 2013; H. Guo & Wang, 2005; Pütz et al., 2021), it appears that l-CaD is necessary only for specific developmental events. This difference between models could be explained by the mammal-specific requirement for l-CaD during development. This suggest that such high contractile forces could likely be redundant in fully developed animals after abdominal wall closure. For this to be logical, it would be necessary for calponin or similar proteins to overlap in function enough to make l-CaD redundant for survival. If this was the case, l-CaD would be an ideal target for inhibiting metastases, as it would suggest that benign motile cells can revert to calponin-mediated migration, whereas cancer cells could be expected to gain only one mechanism of contraction at a time. Therefore, in healthy cells, l-CaD inhibition might prevent one of the many mechanisms of migration, whereas the same inhibition in cancer cells could prevent the only mechanism available. This speculative rationale is based on the assumption that cancer cells gain adequate l-CaD expression from a completely non-contractile state. Thus, a natural continuation to further determine the potential of l-CaD as a target would be to study whether inhibiting l-CaD and calponin together would cease actomyosin-mediated migration.

Similarly, calponin could show similar potential as a target and should be explored in the context of cancer metastasis. One hurdle potentially preventing the utilization of these proteins as targets is the possibility of them being regulated by overlapping mechanisms. This would suggest that their functional redundancy may also be replicated in cancer. Therefore, mapping the cancer-specific regulation of both proteins would help clarify their potential as therapeutic targets.

Notably, targeting l-CaD, if further verified to be effective and tolerated, could provide a novel approach for cancer therapy, as instead of primarily killing tumor cells, it would more directly interfere with metastasis formation. Preventing

metastasis may already be sufficient to preserve life, as metastasis is a key event leading to cancer mortality. Ideally, such a therapy would have to be well tolerated in healthy tissues, as demonstrated by our findings in the case of l-CaD. Minimal adverse effects would be highly important in comparison to chemotherapy, as such therapy would only work if started before the tumor has disseminated and possibly continued over the course of the patient's life. This strategy of targeting events that lead to lethal disease instead of attempting to eradicate a highly adaptive tissue within a highly adaptive organism should also be explored outside l-CaD and calponin.

For example, if further studies suggest that *BRCA1* repression by AR contributes significantly to the early acquisition of driver alterations in PCa, this is another event towards lethal disease. Speculatively, early *BRCA1* repression could also be an opportunity for synthetic lethality via PARP inhibition. Importantly, the target cells would be single cells within a population with no drivers at this point. Therefore, the goal would not be the death of the majority of cells but to prevent an event leading toward lethality, in this case, particularly the acquisition of a driver alteration.

Overall, most cancers eventually develop resistance under continued cytotoxic pressure, whereas durable responses may be more likely in cancers with extremely high turnover rates, which render them particularly vulnerable to cytotoxic therapy. Unlike surgical ablation, which is typically pursued with the aim of complete tumor eradication, cytotoxic therapies are often evaluated by their ability to reduce tumor burden or delay progression rather than fully eliminate malignant cells. However, cytotoxicity permits further somatic evolution as long as there are surviving cells. Therefore, approaches directly targeting mechanisms underlying progression would complement tumor burden–reducing therapies with preventive rather than merely delaying effect, even if not all cancer cells can be eradicated.

In *BRCA*-mutated newly diagnosed ovarian cancer, PARP inhibitor maintenance therapy has shown lowered risk of disease progression or death by 70% at three years (Moore et al., 2018). This is an example of succesful therapy where susceptibility to synthetic lethality overlaps with the propensity to acquire driver alterations as both depend on DNA damage under BRCAness. The clinical benefit of PARP inhibition in pre-CRPC metastatic setting in PCa was recently shown, albeit in combination with AR signaling inhibition (Attard et al., 2025). Some of this benefit is likely purely cytotoxic but a part of it could be driven by the selective elimination of cells with the highest DNA damage, thus removing a proportion of cells with the highest potential for gaining new alterations. This benefit is potentially exploitable also in earlier disease settings as the rationale is not particularly limited to later disease.

Hypothetically, preventing driver mutations in PCa by turning selective pressure against *BRCA1* repression via PARP inhibition could prevent progression to lethal disease. Again, this would require an even earlier intervention that continues over

the course of the patient's life. In theory, a treatment aiming to prevent further clonal evolution would be more effective if administered as early as possible. Furthermore, our results suggest that this approach would be less effective after or during ADT as it activates BRCA1. This poses a challenge for patient selection, because high-risk patients are often the ones who benefit the most from interventions targeting AR signaling. Therefore, adverse effects would have to be well-tolerated, which would likely mean lower doses. However, particularly with PARP inhibitors, longer regimens raise concerns regarding the effects of sustained compromised DDR in other tissues.

7 Summary/Conclusions

This thesis aimed to expand the knowledge on the factors contributing to castration-resistance in PCa. This study broadened the defined role of the well-known tumor suppressor BRCA1 in PCa. This study revealed that AR signaling represses *BRCA1* to dynamically alter between NRF2-mediated ROS defense and attenuated DNA repair. This study also identified the stress fiber acto-myosin contractility–enabling protein l-CaD as a novel oncogene in GR-driven CRPC. This study found that l-CaD promotes PCa metastasis by supporting EMT. Additionally, we characterized the effects of *cald1a/b* mutations during early development in zebrafish embryos. These results imply that CaD inhibition is largely tolerated in healthy tissues, suggesting that the previously reported lethality may be exclusive to mammals and is particularly associated with the inability to close the abdominal wall.

The finding that BRCA1 retains a high AR regulatory influence during PCa progression underscores that the absence of deletion or mutation in a tumor suppressor does not necessarily indicate an intact tumor suppressive function. Our results on l-CaD highlight the strong invasive potential of this protein while demonstrating its redundancy in benign cell migration. Thus, l-CaD may be a potential target for inhibition of metastasis.

Together, these findings add to the knowledge on the broad non-genetic molecular mechanisms that drive aggressive lethal PCa.

Based on the results of this study, the following conclusions can be made:

1. AR signaling represses *BRCA1* in PCa
2. BRCA1 is activated upon AD and supports NRF2-mediated ROS defense to balance oxidative stress and DNA damage in CRPC
3. AR bypass by GR activates l-CaD, which promotes metastasis via EMT induction
4. CaD is largely redundant during early development in zebrafish embryos

Acknowledgements

This thesis research was carried out at the Department of Medical Biochemistry and Genetics, Cancer Research Unit, Institute of Biomedicine, and FICAN West Cancer Center Laboratory, Faculty of Medicine, University of Turku and Turku University Hospital, Finland. I thank the Head of Subject of Medical Biochemistry and Genetics and the Director of the Institute of Biomedicine, Professor Klaus Elenius, and the Director of FICAN West, Docent Pia Vihinen, for providing excellent facilities for conducting this research.

I want to express my gratitude to my supervisor, Docent Maria Sundvall, for building an environment that encouraged independence and creativity while always providing guidance and support when needed. Your example as a scientist has been deeply inspiring, and I have felt privileged to work alongside you. I am especially grateful for the way you led the research with a consistent commitment to high standards and intellectual honesty, so that the work always felt meaningful. Your support at important moments has meant a great deal to me, and the lessons I have learned while doing science under your supervision extend beyond research.

No amount of elbow grease alone can produce a thesis. For me, the process also involved becoming increasingly aware of the many conditions that made this work possible. It has deepened my gratitude not only for the research environment itself, but also for the education, experiences, and forms of support that preceded this work and made it conceivable in the first place, as well as for my teachers, friends, and family. Two pages offer too little space to mention everyone deserving of recognition, but this is my attempt to name a few who have mattered.

I thank my follow-up committee members, Professors Malin Åkerfelt and Matti Poutanen, for their time and careful engagement with my work. Their expert advice was invaluable to my research.

My co-authors, Drs. Ilkka Paatero, Kreetta Paunu, Riikka Huhtaniemi, Saiganesh Sriraman, Antti Kukkula, Mervi Toriseva, Saana Niva, Pekka Taimen, Sari Mäkelä, Ylva Junila, Terhi Jokilehto, Anni Lumiainen, and Gun West, contributed significantly to this work. Without them, this work would not have been possible.

I also want to thank the rest of the Sundvall lab members and visitors during the thesis work, Anniina Hyväkkä, Janita Sulonen, Veikko Pulkki, and Wilfried Mongie.

Additionally, I want to thank everyone on the fifth floor of Medisiina D for a pleasant working environment. In particular, I want to mention Drs. Olli Metsälä, Syeda Afshan, Nataliia Petruk, and Eleftheria Maranou.

I want to thank the skilled professionals at the University of Turku, particularly Sinikka Collanus, Minna Santanen, Dr. Jouko Sandholm, and Markus Peurla, for their technical assistance and expertise. I would also like to acknowledge the excellent Medical Bioinformatics Centre bioinformatics consultations and particularly thank Dr. Asta Laiho for her assistance.

I want to thank Suomen Kulttuurirahasto, TuDMM, Turun Yliopistosäätiö, Suomen Lääketieteen Säätiö, Emil Aaltosen säätiö, Paulon säätiö, Suomalais-Norjalainen Lääketieteen Säätiö, Lounais-Suomalaiset Syöpäjärjestöt, TYKS syöpäklinikka, TYKS-säätiö, and University of Turku PGE for making this thesis possible by funding my research. Additionally, I want to thank Emil Aaltosen säätiö and TuDMM for conference grants.

This thesis was significantly fueled by lunch and after-work discussions, particularly with Antti K. and Sai. Thank you for being passionate enough about our work to spend those "breaks" hypothesizing and brainstorming. Antti K., I trust your taste in research ideas as much as I trust your taste in cinema; thank you for lending your judgment. Sai, your creativity on a whiteboard is only matched by your enthusiasm for life in general; thank you for inspiring this work with your energy.

I also want to thank Turku Cancer Research Society for organizing inspirational events. My well-being during the thesis work was also supported by gatherings of the academic club of couplet appreciation, *Pistiäiset*, with Docent Antti, Drs. Perttu, Eero, and Samuel, as well as Konsta, Antti, Petteri, Antton, Henrik, Ilkka, and Juuso. I also want to thank Joonas K. for his friendship and for the pleasant format of peer support with a pint of beer and a game of chess. Attempting to put into words the significance of Docent Antti in my life would take another book and is thus outside the scope of this thesis.

I want to thank Salla for your patience, and particularly for the many occasions on which you lent an ear to sudden rough ideas on molecular specifics foreign to you. Thank you for listening kindly and with understanding in those moments. This thesis was completed during years that also included us becoming parents of Aisla and Auni, and I am deeply grateful for your support during that busy time. I also want to thank Pia and Esa for their hospitality. Some of my most significant scientific writing took shape while working on your sofa.

Finally, I want to thank my parents, Tarja Orvokki and Veli-Matti, for their love, support, and example. Iris, thank you for your friendship and for ensuring my hair was on fleek during this thesis work.

Seinäjoki, April 2026
Verneri Virtanen

References

Abida, W., Armenia, J., Gopalan, A., Brennan, R., Walsh, M., Barron, D., Danila, D., Rathkopf, D., Morris, M., Slovin, S., McLaughlin, B., Curtis, K., Hyman, D. M., Durack, J. C., Solomon, S. B., Arcila, M. E., Zehir, A., Syed, A., Gao, J., … Scher, H. I. (2017). Prospective Genomic Profiling of Prostate Cancer Across Disease States Reveals Germline and Somatic Alterations That May Affect Clinical Decision Making. *JCO Precision Oncology*, *2017*, PO.17.00029. https://doi.org/10.1200/PO.17.00029

Abida, W., Cyrta, J., Heller, G., Prandi, D., Armenia, J., Coleman, I., Cieslik, M., Benelli, M., Robinson, D., Van Allen, E. M., Sboner, A., Fedrizzi, T., Mosquera, J. M., Robinson, B. D., De Sarkar, N., Kunju, L. P., Tomlins, S., Wu, Y. M., Nava Rodrigues, D., … Sawyers, C. L. (2019). Genomic correlates of clinical outcome in advanced prostate cancer. *Proceedings of the National Academy of Sciences of the United States of America*, *116*(23), 11428–11436. https://doi.org/10.1073/pnas.1902651116

Abrams, J., Davuluri, G., Seiler, C., & Pack, M. (2012). Smooth muscle caldesmon modulates peristalsis in the wild type and non-innervated zebrafish intestine. *Neurogastroenterology & Motility*, *24*(3), 288–299. https://doi.org/10.1111/j.1365-2982.2011.01844.x

Agarwal, N., Azad, A. A., Carles, J., Fay, A. P., Matsubara, N., Heinrich, D., Szczylik, C., De Giorgi, U., Young Joung, J., Fong, P. C. C., Voog, E., Jones, R. J., Shore, N. D., Dunshee, C., Zschäbitz, S., Oldenburg, J., Lin, X., Healy, C. G., Di Santo, N., … Fizazi, K. (2023). Talazoparib plus enzalutamide in men with first-line metastatic castration-resistant prostate cancer (TALAPRO-2): A randomised, placebo-controlled, phase 3 trial. *Lancet (London, England)*, *402*(10398), 291–303. https://doi.org/10.1016/S0140-6736(23)01055-3

Aggarwal, R., Rydzewski, N. R., Zhang, L., Foye, A., Kim, W., Helzer, K. T., Bakhtiar, H., Chang, S. L., Perry, M. D., Gleave, M., Reiter, R. E., Huang, J., Evans, C. P., Alumkal, J. J., Lang, J. M., Yu, M., Quigley, D. A., Sjöström, M., Small, E. J., … Zhao, S. G. (2021). Prognosis Associated With Luminal and Basal Subtypes of Metastatic Prostate Cancer. *JAMA Oncology*, *7*(11), 1644–1652. https://doi.org/10.1001/jamaoncol.2021.3987

Agoulnik, I. U., Vaid, A., Bingman, W. E., III, Erdeme, H., Frolov, A., Smith, C. L., Ayala, G., Ittmann, M. M., & Weigel, N. L. (2005). Role of SRC-1 in the Promotion of Prostate Cancer Cell Growth and Tumor Progression. *Cancer Research*, *65*(17), 7959–7967. https://doi.org/10.1158/0008-5472.CAN-04-3541

Agoulnik, I. U., Vaid, A., Nakka, M., Alvarado, M., Bingman, W. E., Erdem, H., Frolov, A., Smith, C. L., Ayala, G. E., Ittmann, M. M., & Weigel, N. L. (2006). Androgens modulate expression of transcription intermediary factor 2, an androgen receptor coactivator whose expression level correlates with early biochemical recurrence in prostate cancer. *Cancer Research*, *66*(21), 10594–10602. https://doi.org/10.1158/0008-5472.CAN-06-1023

Alexandrov, L. B., Jones, P. H., Wedge, D. C., Sale, J. E., Campbell, P. J., Nik-Zainal, S., & Stratton, M. R. (2015). Clock-like mutational processes in human somatic cells. *Nature Genetics*, *47*(12), 1402–1407. https://doi.org/10.1038/ng.3441

Alnuaimi, A. R., Bottner, J., Nair, V. A., Ali, N., Alnakhli, R., Dreyer, E., Talaat, I. M., Busch, H., Perner, S., Kirfel, J., Hamoudi, R., & Abdel-Rahman, W. M. (2023). Immunohistochemical

Expression Analysis of Caldesmon Isoforms in Colorectal Carcinoma Reveals Interesting Correlations with Tumor Characteristics. *International Journal of Molecular Sciences*, *24*(3), 2275. https://doi.org/10.3390/ijms24032275

Amano, M., Mukai, H., Ono, Y., Chihara, K., Matsui, T., Hamajima, Y., Okawa, K., Iwamatsu, A., & Kaibuchi, K. (1996). Identification of a putative target for Rho as the serine-threonine kinase protein kinase N. *Science (New York, N.Y.)*, *271*(5249), 648–650. https://doi.org/10.1126/science.271.5249.648

Amin Al Olama, A., Dadaev, T., Hazelett, D. J., Li, Q., Leongamornlert, D., Saunders, E. J., Stephens, S., Cieza-Borrella, C., Whitmore, I., Benlloch Garcia, S., Giles, G. G., Southey, M. C., Fitzgerald, L., Gronberg, H., Wiklund, F., Aly, M., Henderson, B. E., Schumacher, F., Haiman, C. A., … Kote-Jarai, Z. (2015). Multiple novel prostate cancer susceptibility signals identified by fine-mapping of known risk loci among Europeans. *Human Molecular Genetics*, *24*(19), 5589–5602. https://doi.org/10.1093/hmg/ddv203

An, J., Wang, C., Deng, Y., Yu, L., & Huang, H. (2014). Destruction of full-length androgen receptor by wild-type SPOP, but not prostate-cancer-associated mutants. *Cell Reports*, *6*(4), 657–669. https://doi.org/10.1016/j.celrep.2014.01.013

Annala, M., Taavitsainen, S., Khalaf, D. J., Vandekerkhove, G., Beja, K., Sipola, J., Warner, E. W., Herberts, C., Wong, A., Fu, S., Finch, D. L., Oja, C. D., Vergidis, J., Zulfiqar, M., Eigl, B. J., Kollmansberger, C. K., Nykter, M., Gleave, M. E., Chi, K. N., & Wyatt, A. W. (2021). Evolution of Castration-Resistant Prostate Cancer in ctDNA during Sequential Androgen Receptor Pathway Inhibition. *Clinical Cancer Research: An Official Journal of the American Association for Cancer Research*, *27*(16), 4610–4623. https://doi.org/10.1158/1078-0432.CCR-21-1625

Antonarakis, E. S., Isaacsson Velho, P., Fu, W., Wang, H., Agarwal, N., Sacristan Santos, V., Maughan, B. L., Pili, R., Adra, N., Sternberg, C. N., Vlachostergios, P. J., Tagawa, S. T., Bryce, A. H., McNatty, A. L., Reichert, Z. R., Dreicer, R., Sartor, O., Lotan, T. L., & Hussain, M. (2020). CDK12-Altered Prostate Cancer: Clinical Features and Therapeutic Outcomes to Standard Systemic Therapies, Poly (ADP-Ribose) Polymerase Inhibitors, and PD-1 Inhibitors. *JCO Precision Oncology*, *4*, 370–381. https://doi.org/10.1200/po.19.00399

Antonarakis, E. S., Lu, C., Wang, H., Luber, B., Nakazawa, M., Roeser, J. C., Chen, Y., Mohammad, T. A., Chen, Y., Fedor, H. L., Lotan, T. L., Zheng, Q., De Marzo, A. M., Isaacs, J. T., Isaacs, W. B., Nadal, R., Paller, C. J., Denmeade, S. R., Carducci, M. A., … Luo, J. (2014). AR-V7 and resistance to enzalutamide and abiraterone in prostate cancer. *The New England Journal of Medicine*, *371*(11), 1028–1038. https://doi.org/10.1056/NEJMoa1315815

Armenia, J., Wankowicz, S. A. M., Liu, D., Gao, J., Kundra, R., Reznik, E., Chatila, W. K., Chakravarty, D., Han, G. C., Coleman, I., Montgomery, B., Pritchard, C., Morrissey, C., Barbieri, C. E., Beltran, H., Sboner, A., Zafeiriou, Z., Miranda, S., Bielski, C. M., … Van Allen, E. M. (2018). The long tail of oncogenic drivers in prostate cancer. *Nature Genetics*, *50*(5), 645–651. https://doi.org/10.1038/s41588-018-0078-z

Armstrong, A. J., Halabi, S., Luo, J., Nanus, D. M., Giannakakou, P., Szmulewitz, R. Z., Danila, D. C., Healy, P., Anand, M., Rothwell, C. J., Rasmussen, J., Thornburg, B., Berry, W. R., Wilder, R. S., Lu, C., Chen, Y., Silberstein, J. L., Kemeny, G., Galletti, G., … George, D. J. (2019). Prospective Multicenter Validation of Androgen Receptor Splice Variant 7 and Hormone Therapy Resistance in High-Risk Castration-Resistant Prostate Cancer: The PROPHECY Study. *Journal of Clinical Oncology: Official Journal of the American Society of Clinical Oncology*, *37*(13), 1120–1129. https://doi.org/10.1200/JCO.18.01731

Arora, V. K., Schenkein, E., Murali, R., Subudhi, S. K., Wongvipat, J., Balbas, M. D., Shah, N., Cai, L., Efstathiou, E., Logothetis, C., Zheng, D., & Sawyers, C. L. (2013). Glucocorticoid receptor confers resistance to antiandrogens by bypassing androgen receptor blockade. *Cell*, *155*(6), 1309–1322. https://doi.org/10.1016/j.cell.2013.11.012

Arriaga, J. M., Panja, S., Alshalalfa, M., Zhao, J., Zou, M., Giacobbe, A., Madubata, C. J., Kim, J. Y., Rodriguez, A., Coleman, I., Virk, R. K., Hibshoosh, H., Ertunc, O., Ozbek, B., Fountain, J., Jeffrey Karnes, R., Luo, J., Antonarakis, E. S., Nelson, P. S., … Abate-Shen, C. (2020). A MYC and RAS

co-activation signature in localized prostate cancer drives bone metastasis and castration resistance. *Nature Cancer*, *1*(11), 1082–1096. https://doi.org/10.1038/s43018-020-00125-0

Arriaga, J. M., Ronaldson-Bouchard, K., Picech, F., Nunes de Almeida, F., Afari, S., Chhouri, H., Vunjak-Novakovic, G., & Abate-Shen, C. (2024). In vivo genome-wide CRISPR screening identifies CITED2 as a driver of prostate cancer bone metastasis. *Oncogene*, *43*(17), 1303–1315. https://doi.org/10.1038/s41388-024-02995-5

Asim, M., Tarish, F., Zecchini, H. I., Sanjiv, K., Gelali, E., Massie, C. E., Baridi, A., Warren, A. Y., Zhao, W., Ogris, C., McDuffus, L.-A., Mascalchi, P., Shaw, G., Dev, H., Wadhwa, K., Wijnhoven, P., Forment, J. V., Lyons, S. R., Lynch, A. G., … Helleday, T. (2017). Synthetic lethality between androgen receptor signalling and the PARP pathway in prostate cancer. *Nature Communications*, *8*(1), 374. https://doi.org/10.1038/s41467-017-00393-y

Attard, G., Agarwal, N., Graff, J. N., Sandhu, S., Efstathiou, E., Özgüroğlu, M., Pereira de Santana Gomes, A. J., Vianna, K., Luo, H., Gotto, G. T., Cheng, H. H., Kim, W., Varela, C. R., Schaeffer, D., Kramer, K., Li, S., Baron, B., Shen, F., Mundle, S. D., … Rathkopf, D. E. (2025). Niraparib and abiraterone acetate plus prednisone for HRR-deficient metastatic castration-sensitive prostate cancer: A randomized phase 3 trial. *Nature Medicine*, 1–10. https://doi.org/10.1038/s41591-025-03961-8

Attard, G., Reid, A. H. M., A'Hern, R., Parker, C., Oommen, N. B., Folkerd, E., Messiou, C., Molife, L. R., Maier, G., Thompson, E., Olmos, D., Sinha, R., Lee, G., Dowsett, M., Kaye, S. B., Dearnaley, D., Kheoh, T., Molina, A., & de Bono, J. S. (2009). Selective inhibition of CYP17 with abiraterone acetate is highly active in the treatment of castration-resistant prostate cancer. *Journal of Clinical Oncology: Official Journal of the American Society of Clinical Oncology*, *27*(23), 3742–3748. https://doi.org/10.1200/JCO.2008.20.0642

Aytes, A., Mitrofanova, A., Lefebvre, C., Alvarez, M. J., Castillo-Martin, M., Zheng, T., Eastham, J. A., Gopalan, A., Pienta, K. J., Shen, M. M., Califano, A., & Abate-Shen, C. (2014). Cross-species regulatory network analysis identifies a synergistic interaction between FOXM1 and CENPF that drives prostate cancer malignancy. *Cancer Cell*, *25*(5), 638–651. https://doi.org/10.1016/j.ccr.2014.03.017

Azad, A. A., Volik, S. V., Wyatt, A. W., Haegert, A., Le Bihan, S., Bell, R. H., Anderson, S. A., McConeghy, B., Shukin, R., Bazov, J., Youngren, J., Paris, P., Thomas, G., Small, E. J., Wang, Y., Gleave, M. E., Collins, C. C., & Chi, K. N. (2015). Androgen Receptor Gene Aberrations in Circulating Cell-Free DNA: Biomarkers of Therapeutic Resistance in Castration-Resistant Prostate Cancer. *Clinical Cancer Research: An Official Journal of the American Association for Cancer Research*, *21*(10), 2315–2324. https://doi.org/10.1158/1078-0432.CCR-14-2666

Baca, S. C., Prandi, D., Lawrence, M. S., Mosquera, J. M., Romanel, A., Drier, Y., Park, K., Kitabayashi, N., MacDonald, T. Y., Ghandi, M., Van Allen, E., Kryukov, G. V., Sboner, A., Theurillat, J.-P., Soong, T. D., Nickerson, E., Auclair, D., Tewari, A., Beltran, H., … Garraway, L. A. (2013). Punctuated evolution of prostate cancer genomes. *Cell*, *153*(3), 666–677. https://doi.org/10.1016/j.cell.2013.03.021

Bae, I., Fan, S., Meng, Q., Rih, J. K., Kim, H. J., Kang, H. J., Xu, J., Goldberg, I. D., Jaiswal, A. K., & Rosen, E. M. (2004). BRCA1 induces antioxidant gene expression and resistance to oxidative stress. *Cancer Research*, *64*(21), 7893–7909. https://doi.org/10.1158/0008-5472.CAN-04-1119

Bakht, M. K., Yamada, Y., Ku, S.-Y., Venkadakrishnan, V. B., Korsen, J. A., Kalidindi, T. M., Mizuno, K., Ahn, S. H., Seo, J.-H., Garcia, M. M., Khani, F., Elemento, O., Long, H. W., Chaglassian, A., Pillarsetty, N., Lewis, J. S., Freedman, M., Belanger, A. P., Nguyen, Q.-D., & Beltran, H. (2023). Landscape of prostate-specific membrane antigen heterogeneity and regulation in AR-positive and AR-negative metastatic prostate cancer. *Nature Cancer*, *4*(5), 699–715. https://doi.org/10.1038/s43018-023-00539-6

Barbieri, C. E., Baca, S. C., Lawrence, M. S., Demichelis, F., Blattner, M., Theurillat, J.-P., White, T. A., Stojanov, P., Van Allen, E., Stransky, N., Nickerson, E., Chae, S.-S., Boysen, G., Auclair, D., Onofrio, R. C., Park, K., Kitabayashi, N., MacDonald, T. Y., Sheikh, K., … Garraway, L. A.

(2012). Exome sequencing identifies recurrent SPOP, FOXA1 and MED12 mutations in prostate cancer. *Nature Genetics*, *44*(6), 685–689. https://doi.org/10.1038/ng.2279

Barrie, S. E., Potter, G. A., Goddard, P. M., Haynes, B. P., Dowsett, M., & Jarman, M. (1994). Pharmacology of novel steroidal inhibitors of cytochrome P450(17) alpha (17 alpha-hydroxylase/C17-20 lyase). *The Journal of Steroid Biochemistry and Molecular Biology*, *50*(5–6), 267–273. https://doi.org/10.1016/0960-0760(94)90131-7

Barthel, S. R., Hays, D. L., Yazawa, E. M., Opperman, M., Walley, K. C., Nimrichter, L., Burdick, M. M., Gillard, B. M., Moser, M. T., Pantel, K., Foster, B. A., Pienta, K. J., & Dimitroff, C. J. (2013). Definition of Molecular Determinants of Prostate Cancer Cell Bone Extravasation. *Cancer Research*, *73*(2), 942–952. https://doi.org/10.1158/0008-5472.CAN-12-3264

Bell, K. J. L., Del Mar, C., Wright, G., Dickinson, J., & Glasziou, P. (2015). Prevalence of incidental prostate cancer: A systematic review of autopsy studies. *International Journal of Cancer*, *137*(7), 1749–1757. https://doi.org/10.1002/ijc.29538

Beltran, H., Hruszkewycz, A., Scher, H. I., Hildesheim, J., Isaacs, J., Yu, E. Y., Kelly, K., Lin, D., Dicker, A., Arnold, J., Hecht, T., Wicha, M., Sears, R., Rowley, D., White, R., Gulley, J. L., Lee, J., Diaz Meco, M., Small, E. J., … Nelson, P. S. (2019). The Role of Lineage Plasticity in Prostate Cancer Therapy Resistance. *Clinical Cancer Research: An Official Journal of the American Association for Cancer Research*, *25*(23), 6916–6924. https://doi.org/10.1158/1078-0432.CCR-19-1423

Beltran, H., Prandi, D., Mosquera, J. M., Benelli, M., Puca, L., Cyrta, J., Marotz, C., Giannopoulou, E., Chakravarthi, B. V. S. K., Varambally, S., Tomlins, S. A., Nanus, D. M., Tagawa, S. T., Van Allen, E. M., Elemento, O., Sboner, A., Garraway, L. A., Rubin, M. A., & Demichelis, F. (2016). Divergent clonal evolution of castration-resistant neuroendocrine prostate cancer. *Nature Medicine*, *22*(3), 298–305. https://doi.org/10.1038/nm.4045

Beltran, H., Rickman, D. S., Park, K., Chae, S. S., Sboner, A., MacDonald, T. Y., Wang, Y., Sheikh, K. L., Terry, S., Tagawa, S. T., Dhir, R., Nelson, J. B., de la Taille, A., Allory, Y., Gerstein, M. B., Perner, S., Pienta, K. J., Chinnaiyan, A. M., Wang, Y., … Rubin, M. A. (2011). Molecular characterization of neuroendocrine prostate cancer and identification of new drug targets. *Cancer Discovery*, *1*(6), 487–495. https://doi.org/10.1158/2159-8290.CD-11-0130

Berger, M. F., Lawrence, M. S., Demichelis, F., Drier, Y., Cibulskis, K., Sivachenko, A. Y., Sboner, A., Esgueva, R., Pflueger, D., Sougnez, C., Onofrio, R., Carter, S. L., Park, K., Habegger, L., Ambrogio, L., Fennell, T., Parkin, M., Saksena, G., Voet, D., … Garraway, L. A. (2011). The genomic complexity of primary human prostate cancer. *Nature*, *470*(7333), 214–220. https://doi.org/10.1038/nature09744

Bernasocchi, T., El Tekle, G., Bolis, M., Mutti, A., Vallerga, A., Brandt, L. P., Spriano, F., Svinkina, T., Zoma, M., Ceserani, V., Rinaldi, A., Janouskova, H., Bossi, D., Cavalli, M., Mosole, S., Geiger, R., Dong, Z., Yang, C.-G., Albino, D., … Theurillat, J.-P. P. (2021). Dual functions of SPOP and ERG dictate androgen therapy responses in prostate cancer. *Nature Communications*, *12*(1), 734. https://doi.org/10.1038/s41467-020-20820-x

Bétermier, M., Bertrand, P., & Lopez, B. S. (2014). Is Non-Homologous End-Joining Really an Inherently Error-Prone Process? *PLoS Genetics*, *10*(1), e1004086. https://doi.org/10.1371/journal.pgen.1004086

Bhandari, V., Hoey, C., Liu, L. Y., Lalonde, E., Ray, J., Livingstone, J., Lesurf, R., Shiah, Y.-J., Vujcic, T., Huang, X., Espiritu, S. M. G., Heisler, L. E., Yousif, F., Huang, V., Yamaguchi, T. N., Yao, C. Q., Sabelnykova, V. Y., Fraser, M., Chua, M. L. K., … Bristow, R. G. (2019). Molecular landmarks of tumor hypoxia across cancer types. *Nature Genetics*, *51*(2), 308–318. https://doi.org/10.1038/s41588-018-0318-2

Bianchi-Smiraglia, A., Kunnev, D., Limoge, M., Lee, A., Beckerle, M. C., & Bakin, A. V. (2013). Integrin-β5 and zyxin mediate formation of ventral stress fibers in response to transforming growth factor β. *Cell Cycle (Georgetown, Tex.)*, *12*(21), 3377–3389. https://doi.org/10.4161/cc.26388

Bishop, J. L., Thaper, D., Vahid, S., Davies, A., Ketola, K., Kuruma, H., Jama, R., Nip, K. M., Angeles, A., Johnson, F., Wyatt, A. W., Fazli, L., Gleave, M. E., Lin, D., Rubin, M. A., Collins, C. C., Wang, Y., Beltran, H., & Zoubeidi, A. (2017). The Master Neural Transcription Factor BRN2 Is an Androgen Receptor-Suppressed Driver of Neuroendocrine Differentiation in Prostate Cancer. *Cancer Discovery*, *7*(1), 54–71. https://doi.org/10.1158/2159-8290.CD-15-1263

Blackburn, J., Vecchiarelli, S., Heyer, E. E., Patrick, S. M., Lyons, R. J., Jaratlerdsiri, W., van Zyl, S., Bornman, M. S. R., Mercer, T. R., & Hayes, V. M. (2019). TMPRSS2-ERG fusions linked to prostate cancer racial health disparities: A focus on Africa. *The Prostate*, *79*(10), 1191–1196. https://doi.org/10.1002/pros.23823

Blackford, A. N., & Jackson, S. P. (2017). ATM, ATR, and DNA-PK: The Trinity at the Heart of the DNA Damage Response. *Molecular Cell*, *66*(6), 801–817. https://doi.org/10.1016/j.molcel.2017.05.015

Blatt, E. B., Parra, K., Neeb, A., Buroni, L., Bogdan, D., Yuan, W., Gao, Y., Gilbreath, C., Paschalis, A., Carreira, S., DeBerardinis, R. J., Mani, R. S., de Bono, J. S., & Raj, G. V. (2023). Critical role of antioxidant programs in enzalutamide-resistant prostate cancer. *Oncogene*, *42*(30), 2347–2359. https://doi.org/10.1038/s41388-023-02756-w

Blattner, M., Liu, D., Robinson, B. D., Huang, D., Poliakov, A., Gao, D., Nataraj, S., Deonarine, L. D., Augello, M. A., Sailer, V., Ponnala, L., Ittmann, M., Chinnaiyan, A. M., Sboner, A., Chen, Y., Rubin, M. A., & Barbieri, C. E. (2017). SPOP Mutation Drives Prostate Tumorigenesis In Vivo through Coordinate Regulation of PI3K/mTOR and AR Signaling. *Cancer Cell*, *31*(3), 436–451. https://doi.org/10.1016/j.ccell.2017.02.004

Bluemn, E. G., Coleman, I. M., Lucas, J. M., Coleman, R. T., Hernandez-Lopez, S., Tharakan, R., Bianchi-Frias, D., Dumpit, R. F., Kaipainen, A., Corella, A. N., Yang, Y. C., Nyquist, M. D., Mostaghel, E., Hsieh, A. C., Zhang, X., Corey, E., Brown, L. G., Nguyen, H. M., Pienta, K., … Nelson, P. S. (2017). Androgen Receptor Pathway-Independent Prostate Cancer Is Sustained through FGF Signaling. *Cancer Cell*, *32*(4), 474-489.e6. https://doi.org/10.1016/j.ccell.2017.09.003

Boire, A., Burke, K., Cox, T. R., Guise, T., Jamal-Hanjani, M., Janowitz, T., Kaplan, R., Lee, R., Swanton, C., Vander Heiden, M. G., & Sahai, E. (2024). Why do patients with cancer die? *Nature Reviews. Cancer*, *24*(8), 578–589. https://doi.org/10.1038/s41568-024-00708-4

Bonkhoff, H., & Remberger, K. (1996). Differentiation pathways and histogenetic aspects of normal and abnormal prostatic growth: A stem cell model. *The Prostate*, *28*(2), 98–106. https://doi.org/10.1002/(SICI)1097-0045(199602)28:2%253C98::AID-PROS4%253E3.0.CO;2-J

Bose, R., Karthaus, W. R., Armenia, J., Abida, W., Iaquinta, P. J., Zhang, Z., Wongvipat, J., Wasmuth, E. V., Shah, N., Sullivan, P. S., Doran, M. G., Wang, P., Patruno, A., Zhao, Y., International SU2C/PCF Prostate Cancer Dream Team, Zheng, D., Schultz, N., & Sawyers, C. L. (2017). ERF mutations reveal a balance of ETS factors controlling prostate oncogenesis. *Nature*, *546*(7660), 671–675. https://doi.org/10.1038/nature22820

Bova, G. S., Carter, B. S., Bussemakers, M. J., Emi, M., Fujiwara, Y., Kyprianou, N., Jacobs, S. C., Robinson, J. C., Epstein, J. I., & Walsh, P. C. (1993). Homozygous deletion and frequent allelic loss of chromosome 8p22 loci in human prostate cancer. *Cancer Research*, *53*(17), 3869–3873.

Bowen, C., Bubendorf, L., Voeller, H. J., Slack, R., Willi, N., Sauter, G., Gasser, T. C., Koivisto, P., Lack, E. E., Kononen, J., Kallioniemi, O. P., & Gelmann, E. P. (2000). Loss of NKX3.1 expression in human prostate cancers correlates with tumor progression. *Cancer Research*, *60*(21), 6111–6115.

Bowry, A., Kelly, R. D. W., & Petermann, E. (2021). Hypertranscription and replication stress in cancer. *Trends in Cancer*, *7*(9), 863–877. https://doi.org/10.1016/j.trecan.2021.04.006

Boysen, G., Rodrigues, D. N., Rescigno, P., Seed, G., Dolling, D., Riisnaes, R., Crespo, M., Zafeiriou, Z., Sumanasuriya, S., Bianchini, D., Hunt, J., Moloney, D., Perez-Lopez, R., Tunariu, N., Miranda, S., Figueiredo, I., Ferreira, A., Christova, R., Gil, V., … de Bono, J. S. (2018). SPOP-Mutated/CHD1-Deleted Lethal Prostate Cancer and Abiraterone Sensitivity. *Clinical Cancer*

Research: An Official Journal of the American Association for Cancer Research, *24*(22), 5585–5593. https://doi.org/10.1158/1078-0432.CCR-18-0937

Bryant, H. E., Schultz, N., Thomas, H. D., Parker, K. M., Flower, D., Lopez, E., Kyle, S., Meuth, M., Curtin, N. J., & Helleday, T. (2005). Specific killing of BRCA2-deficient tumours with inhibitors of poly(ADP-ribose) polymerase. *Nature*, *434*(7035), 913–917. https://doi.org/10.1038/nature03443

Brzovic, P. S., Rajagopal, P., Hoyt, D. W., King, M. C., & Klevit, R. E. (2001). Structure of a BRCA1-BARD1 heterodimeric RING-RING complex. *Nature Structural Biology*, *8*(10), 833–837. https://doi.org/10.1038/nsb1001-833

Burkhardt, L., Fuchs, S., Krohn, A., Masser, S., Mader, M., Kluth, M., Bachmann, F., Huland, H., Steuber, T., Graefen, M., Schlomm, T., Minner, S., Sauter, G., Sirma, H., & Simon, R. (2013). CHD1 is a 5q21 tumor suppressor required for ERG rearrangement in prostate cancer. *Cancer Research*, *73*(9), 2795–2805. https://doi.org/10.1158/0008-5472.CAN-12-1342

Cai, C., He, H. H., Chen, S., Coleman, I., Wang, H., Fang, Z., Chen, S., Nelson, P. S., Liu, X. S., Brown, M., & Balk, S. P. (2011). Androgen receptor gene expression in prostate cancer is directly suppressed by the androgen receptor through recruitment of lysine-specific demethylase 1. *Cancer Cell*, *20*(4), 457–471. https://doi.org/10.1016/j.ccr.2011.09.001

Calagua, C., Ficial, M., Jansen, C. S., Hirz, T., Del Balzo, L., Wilkinson, S., Lake, R., Ku, A. T., Voznesensky, O., Sykes, D. B., Saylor, P. J., Ye, H., Signoretti, S., Kissick, H., Sowalsky, A. G., Balk, S. P., & Einstein, D. J. (2021). A Subset of Localized Prostate Cancer Displays an Immunogenic Phenotype Associated with Losses of Key Tumor Suppressor Genes. *Clinical Cancer Research: An Official Journal of the American Association for Cancer Research*, *27*(17), 4836–4847. https://doi.org/10.1158/1078-0432.CCR-21-0121

Caldecott, K. W. (2008). Single-strand break repair and genetic disease. *Nature Reviews. Genetics*, *9*(8), 619–631. https://doi.org/10.1038/nrg2380

Cancer Genome Atlas Research Network. (2015). The Molecular Taxonomy of Primary Prostate Cancer. *Cell*, *163*(4), 1011–1025. https://doi.org/10.1016/j.cell.2015.10.025

Cantley, L. C., & Neel, B. G. (1999). New insights into tumor suppression: PTEN suppresses tumor formation by restraining the phosphoinositide 3-kinase/AKT pathway. *Proceedings of the National Academy of Sciences of the United States of America*, *96*(8), 4240–4245. https://doi.org/10.1073/pnas.96.8.4240

Cappell, K. M., & Kochenderfer, J. N. (2023). Long-term outcomes following CAR T cell therapy: What we know so far. *Nature Reviews. Clinical Oncology*, *20*(6), 359–371. https://doi.org/10.1038/s41571-023-00754-1

Carver, B. S., Chapinski, C., Wongvipat, J., Hieronymus, H., Chen, Y., Chandarlapaty, S., Arora, V. K., Le, C., Koutcher, J., Scher, H., Scardino, P. T., Rosen, N., & Sawyers, C. L. (2011). Reciprocal feedback regulation of PI3K and androgen receptor signaling in PTEN-deficient prostate cancer. *Cancer Cell*, *19*(5), 575–586. https://doi.org/10.1016/j.ccr.2011.04.008

Carver, B. S., Tran, J., Chen, Z., Carracedo-Perez, A., Alimonti, A., Nardella, C., Gopalan, A., Scardino, P. T., Cordon-Cardo, C., Gerald, W., & Pandolfi, P. P. (2009). ETS rearrangements and prostate cancer initiation. *Nature*, *457*(7231), E1; discussion E2-3. https://doi.org/10.1038/nature07738

Chang, K.-P., Wang, C.-L. A., Kao, H.-K., Liang, Y., Liu, S.-C., Huang, L.-L., Hseuh, C., Hsieh, Y.-J., Chien, K.-Y., Chang, Y.-S., Yu, J.-S., & Chi, L.-M. (2013). Overexpression of caldesmon is associated with lymph node metastasis and poorer prognosis in patients with oral cavity squamous cell carcinoma. *Cancer*, *119*(22), 4003–4011. https://doi.org/10.1002/cncr.28300

Chen, B., Yu, P., Chan, W. N., Xie, F., Zhang, Y., Liang, L., Leung, K. T., Lo, K. W., Yu, J., Tse, G. M. K., Kang, W., & To, K. F. (2024). Cellular zinc metabolism and zinc signaling: From biological functions to diseases and therapeutic targets. *Signal Transduction and Targeted Therapy*, *9*(1), 6. https://doi.org/10.1038/s41392-023-01679-y

Chen, L., Han, L., Mao, S., Xu, P., Xu, X., Zhao, R., Wu, Z., Zhong, K., Yu, G., & Wang, X. (2021). Discovery of A031 as effective proteolysis targeting chimera (PROTAC) androgen receptor (AR) degrader for the treatment of prostate cancer. *European Journal of Medicinal Chemistry*, *216*, 113307. https://doi.org/10.1016/j.ejmech.2021.113307

Chen, M., Wan, L., Zhang, J., Zhang, J., Mendez, L., Clohessy, J. G., Berry, K., Victor, J., Yin, Q., Zhu, Y., Wei, W., & Pandolfi, P. P. (2018). Deregulated PP1α phosphatase activity towards MAPK activation is antagonized by a tumor suppressive failsafe mechanism. *Nature Communications*, *9*(1), 159. https://doi.org/10.1038/s41467-017-02272-y

Chen, S., Zhu, G., Yang, Y., Wang, F., Xiao, Y.-T., Zhang, N., Bian, X., Zhu, Y., Yu, Y., Liu, F., Dong, K., Mariscal, J., Liu, Y., Soares, F., Loo Yau, H., Zhang, B., Chen, W., Wang, C., Chen, D., … Ren, S. (2021). Single-cell analysis reveals transcriptomic remodellings in distinct cell types that contribute to human prostate cancer progression. *Nature Cell Biology*, *23*(1), 87–98. https://doi.org/10.1038/s41556-020-00613-6

Cheng, Q., Tang, A., Wang, Z., Fang, N., Zhang, Z., Zhang, L., Li, C., & Zeng, Y. (2021). CALD1 Modulates Gliomas Progression via Facilitating Tumor Angiogenesis. *Cancers*, *13*(11), 2705. https://doi.org/10.3390/cancers13112705

Chi, K. N., Sandhu, S., Smith, M. R., Attard, G., Saad, M., Olmos, D., Castro, E., Roubaud, G., Pereira de Santana Gomes, A. J., Small, E. J., Rathkopf, D. E., Gurney, H., Jung, W., Mason, G. E., Dibaj, S., Wu, D., Diorio, B., Urtishak, K., Del Corral, A., … Efstathiou, E. (2023). Niraparib plus abiraterone acetate with prednisone in patients with metastatic castration-resistant prostate cancer and homologous recombination repair gene alterations: Second interim analysis of the randomized phase III MAGNITUDE trial. *Annals of Oncology: Official Journal of the European Society for Medical Oncology*, *34*(9), 772–782. https://doi.org/10.1016/j.annonc.2023.06.009

Chiarugi, P., Paoli, P., & Cirri, P. (2014). Tumor microenvironment and metabolism in prostate cancer. *Seminars in Oncology*, *41*(2), 267–280. https://doi.org/10.1053/j.seminoncol.2014.03.004

Chua, C. W., Shibata, M., Lei, M., Toivanen, R., Barlow, L. J., Bergren, S. K., Badani, K. K., McKiernan, J. M., Benson, M. C., Hibshoosh, H., & Shen, M. M. (2014). Single luminal epithelial progenitors can generate prostate organoids in culture. *Nature Cell Biology*, *16*(10), 951–961, 1–4. https://doi.org/10.1038/ncb3047

Ciriello, G., Miller, M. L., Aksoy, B. A., Senbabaoglu, Y., Schultz, N., & Sander, C. (2013). Emerging landscape of oncogenic signatures across human cancers. *Nature Genetics*, *45*(10), 1127–1133. https://doi.org/10.1038/ng.2762

Clarke, N. W., Armstrong, A. J., Thiery-Vuillemin, A., Oya, M., Shore, N., Loredo, E., Procopio, G., de Menezes, J., Girotto, G., Arslan, C., Mehra, N., Parnis, F., Brown, E., Schlürmann, F., Joung, J. Y., Sugimoto, M., Virizuela, J. A., Emmenegger, U., Navratil, J., … Saad, F. (2022). Abiraterone and Olaparib for Metastatic Castration-Resistant Prostate Cancer. *NEJM Evidence*, *1*(9), EVIDoa2200043. https://doi.org/10.1056/EVIDoa2200043

Clegg, N. J., Wongvipat, J., Joseph, J. D., Tran, C., Ouk, S., Dilhas, A., Chen, Y., Grillot, K., Bischoff, E. D., Cai, L., Aparicio, A., Dorow, S., Arora, V., Shao, G., Qian, J., Zhao, H., Yang, G., Cao, C., Sensintaffar, J., … Hager, J. H. (2012). ARN-509: A novel antiandrogen for prostate cancer treatment. *Cancer Research*, *72*(6), 1494–1503. https://doi.org/10.1158/0008-5472.CAN-11-3948

Coleman, R. E. (2001). Metastatic bone disease and the role of biochemical markers of bone metabolism in benign and malignant diseases. *Cancer Treatment Reviews*, *27*(3), 133–135. https://doi.org/10.1053/ctrv.2000.0206

Conteduca, V., Jayaram, A., Romero-Laorden, N., Wetterskog, D., Salvi, S., Gurioli, G., Scarpi, E., Castro, E., Marin-Aguilera, M., Lolli, C., Schepisi, G., Maugeri, A., Wingate, A., Farolfi, A., Casadio, V., Medina, A., Puente, J., Vidal, M. J. M., Morales-Barrera, R., … De Giorgi, U. (2019). Plasma Androgen Receptor and Docetaxel for Metastatic Castration-resistant Prostate Cancer. *European Urology*, *75*(3), 368–373. https://doi.org/10.1016/j.eururo.2018.09.049

Conteduca, V., Oromendia, C., Eng, K. W., Bareja, R., Sigouros, M., Molina, A., Faltas, B. M., Sboner, A., Mosquera, J. M., Elemento, O., Nanus, D. M., Tagawa, S. T., Ballman, K. V., & Beltran, H.

(2019). Clinical features of neuroendocrine prostate cancer. *European Journal of Cancer (Oxford, England: 1990)*, *121*, 7–18. https://doi.org/10.1016/j.ejca.2019.08.011

Cornford, P., Tilki, D., van den Bergh, R. C. N., Eberli, D., De Meerleer, G., De Santis, M., Gillessen, S., Henry, A. M., van Leenders, G. J. L. H., Oldenburg, J., Oprea-Lager, D. E., Matthew Roberts, Rouvière, O., Schoots, I. G., Stranne, J., & Wiegel, T. (2025). *EAU–EANM–ESTRO–ESUR–ISUP–SIOG Guidelines on Prostate Cancer: Limited Update March 2025* [Clinical practice guideline]. European Association of Urology. https://uroweb.org/

Cornford, P., van den Bergh, R. C. N., Briers, E., Van den Broeck, T., Brunckhorst, O., Darraugh, J., Eberli, D., De Meerleer, G., De Santis, M., Farolfi, A., Gandaglia, G., Gillessen, S., Grivas, N., Henry, A. M., Lardas, M., van Leenders, G. J. L. H., Liew, M., Linares Espinos, E., Oldenburg, J., … Tilki, D. (2024). EAU-EANM-ESTRO-ESUR-ISUP-SIOG Guidelines on Prostate Cancer-2024 Update. Part I: Screening, Diagnosis, and Local Treatment with Curative Intent. *European Urology*, *86*(2), 148–163. https://doi.org/10.1016/j.eururo.2024.03.027

Costello, L. C., & Franklin, R. B. (2006). The clinical relevance of the metabolism of prostate cancer; zinc and tumor suppression: Connecting the dots. *Molecular Cancer*, *5*, 17. https://doi.org/10.1186/1476-4598-5-17

Costello, L. C., & Franklin, R. B. (2016). A comprehensive review of the role of zinc in normal prostate function and metabolism; and its implications in prostate cancer. *Archives of Biochemistry and Biophysics*, *611*, 100–112. https://doi.org/10.1016/j.abb.2016.04.014

Crea, F., Sun, L., Mai, A., Chiang, Y. T., Farrar, W. L., Danesi, R., & Helgason, C. D. (2012). The emerging role of histone lysine demethylases in prostate cancer. *Molecular Cancer*, *11*(1), 52. https://doi.org/10.1186/1476-4598-11-52

Crumbaker, M., Khoja, L., & Joshua, A. M. (2017). AR Signaling and the PI3K Pathway in Prostate Cancer. *Cancers*, *9*(4), 34. https://doi.org/10.3390/cancers9040034

Culig, Z., Hoffmann, J., Erdel, M., Eder, I. E., Hobisch, A., Hittmair, A., Bartsch, G., Utermann, G., Schneider, M. R., Parczyk, K., & Klocker, H. (1999). Switch from antagonist to agonist of the androgen receptor bicalutamide is associated with prostate tumour progression in a new model system. *British Journal of Cancer*, *81*(2), 242–251. https://doi.org/10.1038/sj.bjc.6690684

Dardenne, E., Beltran, H., Benelli, M., Gayvert, K., Berger, A., Puca, L., Cyrta, J., Sboner, A., Noorzad, Z., MacDonald, T., Cheung, C., Yuen, K. S., Gao, D., Chen, Y., Eilers, M., Mosquera, J.-M., Robinson, B. D., Elemento, O., Rubin, M. A., … Rickman, D. S. (2016). N-Myc Induces an EZH2-Mediated Transcriptional Program Driving Neuroendocrine Prostate Cancer. *Cancer Cell*, *30*(4), 563–577. https://doi.org/10.1016/j.ccell.2016.09.005

Darnel, A. D., Behmoaram, E., Vollmer, R. T., Corcos, J., Bijian, K., Sircar, K., Su, J., Jiao, J., Alaoui-Jamali, M. A., & Bismar, T. A. (2009). Fascin regulates prostate cancer cell invasion and is associated with metastasis and biochemical failure in prostate cancer. *Clinical Cancer Research: An Official Journal of the American Association for Cancer Research*, *15*(4), 1376–1383. https://doi.org/10.1158/1078-0432.CCR-08-1789

de Bono, J. S., He, M., Shi, Z., Nowicka, M., Bracarda, S., Sternberg, C. N., Chi, K. N., Olmos, D., Sandhu, S., Massard, C., Matsubara, N., Chen, G., Bienz, N. S., Canter, D., Wongchenko, M., & Sweeney, C. (2025). Final Overall Survival and Molecular Data Associated with Clinical Outcomes in Patients Receiving Ipatasertib and Abiraterone in the Phase 3 IPATential150 Trial. *European Urology*, *87*(6), 672–682. https://doi.org/10.1016/j.eururo.2024.12.015

de Bono, J. S., Mateo, J., Fizazi, K., Saad, F., Shore, N., Sandhu, S., Chi, K. N., Sartor, O., Agarwal, N., Olmos, D., Thiery-Vuillemin, A., Twardowski, P., Mehra, N., Goessl, C., Kang, J., Burgents, J., Wu, W., Kohlmann, A., Adelman, C. A., & Hussain, M. (2020). Olaparib for Metastatic Castration-Resistant Prostate Cancer. *The New England Journal of Medicine*, *382*(22), 2091–2102. https://doi.org/10.1056/NEJMoa1911440

de Bono, J. S., Oudard, S., Ozguroglu, M., Hansen, S., Machiels, J.-P., Kocak, I., Gravis, G., Bodrogi, I., Mackenzie, M. J., Shen, L., Roessner, M., Gupta, S., Sartor, A. O., & TROPIC Investigators. (2010). Prednisone plus cabazitaxel or mitoxantrone for metastatic castration-resistant prostate

cancer progressing after docetaxel treatment: A randomised open-label trial. *Lancet (London, England)*, *376*(9747), 1147–1154. https://doi.org/10.1016/S0140-6736(10)61389-X

De Laere, B., Oeyen, S., Mayrhofer, M., Whitington, T., van Dam, P.-J., Van Oyen, P., Ghysel, C., Ampe, J., Ost, P., Demey, W., Hoekx, L., Schrijvers, D., Brouwers, B., Lybaert, W., Everaert, E. G., De Maeseneer, D., Strijbos, M., Bols, A., Fransis, K., … Dirix, L. Y. (2019). TP53 Outperforms Other Androgen Receptor Biomarkers to Predict Abiraterone or Enzalutamide Outcome in Metastatic Castration-Resistant Prostate Cancer. *Clinical Cancer Research: An Official Journal of the American Association for Cancer Research*, *25*(6), 1766–1773. https://doi.org/10.1158/1078-0432.CCR-18-1943

De Marchi, T., Timmermans, A. M., Smid, M., Look, M. P., Stingl, C., Opdam, M., Linn, S. C., Sweep, F. C. G. J., Span, P. N., Kliffen, M., van Deurzen, C. H. M., Luider, T. M., Foekens, J. A., Martens, J. W., & Umar, A. (2016). Annexin-A1 and caldesmon are associated with resistance to tamoxifen in estrogen receptor positive recurrent breast cancer. *Oncotarget*, *7*(3), 3098–3110. https://doi.org/10.18632/oncotarget.6521

De Marzo, A. M., Platz, E. A., Sutcliffe, S., Xu, J., Grönberg, H., Drake, C. G., Nakai, Y., Isaacs, W. B., & Nelson, W. G. (2007). Inflammation in prostate carcinogenesis. *Nature Reviews. Cancer*, *7*(4), 256–269. https://doi.org/10.1038/nrc2090

De, S., Chen, J., Narizhneva, N. V., Heston, W., Brainard, J., Sage, E. H., & Byzova, T. V. (2003). Molecular pathway for cancer metastasis to bone. *The Journal of Biological Chemistry*, *278*(40), 39044–39050. https://doi.org/10.1074/jbc.M304494200

de Wit, R., de Bono, J., Sternberg, C. N., Fizazi, K., Tombal, B., Wülfing, C., Kramer, G., Eymard, J.-C., Bamias, A., Carles, J., Iacovelli, R., Melichar, B., Sverrisdóttir, Á., Theodore, C., Feyerabend, S., Helissey, C., Ozatilgan, A., Geffriaud-Ricouard, C., Castellano, D., & CARD Investigators. (2019). Cabazitaxel versus Abiraterone or Enzalutamide in Metastatic Prostate Cancer. *The New England Journal of Medicine*, *381*(26), 2506–2518. https://doi.org/10.1056/NEJMoa1911206

Deng, M., Boopathi, E., Hypolite, J. A., Raabe, T., Chang, S., Zderic, S., Wein, A. J., & Chacko, S. (2013). Amino acid mutations in the caldesmon COOH-terminal functional domain increase force generation in bladder smooth muscle. *American Journal of Physiology. Renal Physiology*, *305*(10), F1455-1465. https://doi.org/10.1152/ajprenal.00174.2013

Deplus, R., Delliaux, C., Marchand, N., Flourens, A., Vanpouille, N., Leroy, X., de Launoit, Y., & Duterque-Coquillaud, M. (2016). TMPRSS2-ERG fusion promotes prostate cancer metastases in bone. *Oncotarget*, *8*(7), 11827–11840. https://doi.org/10.18632/oncotarget.14399

Dietlein, F., Thelen, L., & Reinhardt, H. C. (2014). Cancer-specific defects in DNA repair pathways as targets for personalized therapeutic approaches. *Trends in Genetics: TIG*, *30*(8), 326–339. https://doi.org/10.1016/j.tig.2014.06.003

Ding, L., Kim, H.-J., Wang, Q., Kearns, M., Jiang, T., Ohlson, C. E., Li, B. B., Xie, S., Liu, J. F., Stover, E. H., Howitt, B. E., Bronson, R. T., Lazo, S., Roberts, T. M., Freeman, G. J., Konstantinopoulos, P. A., Matulonis, U. A., & Zhao, J. J. (2018). PARP Inhibition Elicits STING-Dependent Antitumor Immunity in Brca1-Deficient Ovarian Cancer. *Cell Reports*, *25*(11), 2972-2980.e5. https://doi.org/10.1016/j.celrep.2018.11.054

Ding, L., Wang, R., Shen, D., Cheng, S., Wang, H., Lu, Z., Zheng, Q., Wang, L., Xia, L., & Li, G. (2021). Role of noncoding RNA in drug resistance of prostate cancer. *Cell Death & Disease*, *12*(6), 590. https://doi.org/10.1038/s41419-021-03854-x

Ding, Z., Wu, C.-J., Chu, G. C., Xiao, Y., Ho, D., Zhang, J., Perry, S. R., Labrot, E. S., Wu, X., Lis, R., Hoshida, Y., Hiller, D., Hu, B., Jiang, S., Zheng, H., Stegh, A. H., Scott, K. L., Signoretti, S., Bardeesy, N., … DePinho, R. A. (2011). SMAD4-dependent barrier constrains prostate cancer growth and metastatic progression. *Nature*, *470*(7333), 269–273. https://doi.org/10.1038/nature09677

Ding, Z., Wu, C.-J., Jaskelioff, M., Ivanova, E., Kost-Alimova, M., Protopopov, A., Chu, G. C., Wang, G., Lu, X., Labrot, E. S., Hu, J., Wang, W., Xiao, Y., Zhang, H., Zhang, J., Zhang, J., Gan, B., Perry, S. R., Jiang, S., … DePinho, R. A. (2012). Telomerase reactivation following telomere

dysfunction yields murine prostate tumors with bone metastases. *Cell*, *148*(5), 896–907. https://doi.org/10.1016/j.cell.2012.01.039

Domingo-Domenech, J., Vidal, S. J., Rodriguez-Bravo, V., Castillo-Martin, M., Quinn, S. A., Rodriguez-Barrueco, R., Bonal, D. M., Charytonowicz, E., Gladoun, N., de la Iglesia-Vicente, J., Petrylak, D. P., Benson, M. C., Silva, J. M., & Cordon-Cardo, C. (2012). Suppression of acquired docetaxel resistance in prostate cancer through depletion of notch- and hedgehog-dependent tumor-initiating cells. *Cancer Cell*, *22*(3), 373–388. https://doi.org/10.1016/j.ccr.2012.07.016

Donehower, L. A., Soussi, T., Korkut, A., Liu, Y., Schultz, A., Cardenas, M., Li, X., Babur, O., Hsu, T.-K., Lichtarge, O., Weinstein, J. N., Akbani, R., & Wheeler, D. A. (2019). Integrated Analysis of TP53 Gene and Pathway Alterations in The Cancer Genome Atlas. *Cell Reports*, *28*(5), 1370-1384.e5. https://doi.org/10.1016/j.celrep.2019.07.001

Dongre, A., & Weinberg, R. A. (2019). New insights into the mechanisms of epithelial-mesenchymal transition and implications for cancer. *Nature Reviews. Molecular Cell Biology*, *20*(2), 69–84. https://doi.org/10.1038/s41580-018-0080-4

Dutta, A., Rodriguez-Calero, A., Ronaldson-Bouchard, K., Offermann, A., Rahman, D., Vhatkar, T. B., Hasson, D., Alshalalfa, M., Davicioni, E., Karnes, R. J., Rubin, M. A., Vunjak-Novakovic, G., Abate-Shen, C., & Arriaga, J. M. (2025). ATAD2 Drives Prostate Cancer Progression to Metastasis. *Molecular Cancer Research: MCR*, *23*(5), 379–390. https://doi.org/10.1158/1541-7786.MCR-24-0544

Ellwood-Yen, K., Graeber, T. G., Wongvipat, J., Iruela-Arispe, M. L., Zhang, J., Matusik, R., Thomas, G. V., & Sawyers, C. L. (2003). Myc-driven murine prostate cancer shares molecular features with human prostate tumors. *Cancer Cell*, *4*(3), 223–238. https://doi.org/10.1016/s1535-6108(03)00197-1

Engholm, G., Ferlay, J., Christensen, N., Bray, F., Gjerstorff, M. L., Klint, A., Køtlum, J. E., Olafsdóttir, E., Pukkala, E., & Storm, H. H. (2010). NORDCAN--a Nordic tool for cancer information, planning, quality control and research. *Acta Oncologica (Stockholm, Sweden)*, *49*(5), 725–736. https://doi.org/10.3109/02841861003782017

Epstein, J. I., Egevad, L., Amin, M. B., Delahunt, B., Srigley, J. R., Humphrey, P. A., & Grading Committee. (2016). The 2014 International Society of Urological Pathology (ISUP) Consensus Conference on Gleason Grading of Prostatic Carcinoma: Definition of Grading Patterns and Proposal for a New Grading System. *The American Journal of Surgical Pathology*, *40*(2), 244–252. https://doi.org/10.1097/PAS.0000000000000530

Etzioni, R., Penson, D. F., Legler, J. M., di Tommaso, D., Boer, R., Gann, P. H., & Feuer, E. J. (2002). Overdiagnosis due to prostate-specific antigen screening: Lessons from U.S. prostate cancer incidence trends. *Journal of the National Cancer Institute*, *94*(13), 981–990. https://doi.org/10.1093/jnci/94.13.981

Ewing, C. M., Ray, A. M., Lange, E. M., Zuhlke, K. A., Robbins, C. M., Tembe, W. D., Wiley, K. E., Isaacs, S. D., Johng, D., Wang, Y., Bizon, C., Yan, G., Gielzak, M., Partin, A. W., Shanmugam, V., Izatt, T., Sinari, S., Craig, D. W., Zheng, S. L., … Cooney, K. A. (2012). Germline mutations in HOXB13 and prostate-cancer risk. *The New England Journal of Medicine*, *366*(2), 141–149. https://doi.org/10.1056/NEJMoa1110000

Eyunni, S., Mannan, R., Zhang, Y., Young, E., Zhang, Q., Luo, J., Pang, M., Mahapatra, S., Tien, J. C.-Y., George, J. M., Jaber, M., Hakkani, H., Carson, S. E., Todd, A. J., Hosseini, N., Gondal, M., Rebernick, R. J., Cao, X., Su, F., … Parolia, A. (2025). Divergent FOXA1 mutations drive prostate tumorigenesis and therapy-resistant cellular plasticity. *Science (New York, N.Y.)*, *389*(6764), eadv2367. https://doi.org/10.1126/science.adv2367

Farah, E., Li, C., Cheng, L., Kong, Y., Lanman, N. A., Pascuzzi, P., Lorenz, G. R., Zhang, Y., Ahmad, N., Li, L., Ratliff, T., & Liu, X. (2019). NOTCH signaling is activated in and contributes to resistance in enzalutamide-resistant prostate cancer cells. *Journal of Biological Chemistry*, *294*(21), 8543–8554. https://doi.org/10.1074/jbc.RA118.006983

Farmer, H., McCabe, N., Lord, C. J., Tutt, A. N. J., Johnson, D. A., Richardson, T. B., Santarosa, M., Dillon, K. J., Hickson, I., Knights, C., Martin, N. M. B., Jackson, S. P., Smith, G. C. M., & Ashworth, A. (2005). Targeting the DNA repair defect in BRCA mutant cells as a therapeutic strategy. *Nature*, *434*(7035), 917–921. https://doi.org/10.1038/nature03445

Ferrari, A. C., Alumkal, J. J., Stein, M. N., Taplin, M.-E., Babb, J., Barnett, E. S., Gomez-Pinillos, A., Liu, X., Moore, D., DiPaola, R., & Beer, T. M. (2019). Epigenetic Therapy with Panobinostat Combined with Bicalutamide Rechallenge in Castration-Resistant Prostate Cancer. *Clinical Cancer Research: An Official Journal of the American Association for Cancer Research*, *25*(1), 52–63. https://doi.org/10.1158/1078-0432.CCR-18-1589

Fizazi, K., Azad, A. A., Matsubara, N., Carles, J., Fay, A. P., De Giorgi, U., Joung, J. Y., Fong, P. C. C., Voog, E., Jones, R. J., Shore, N. D., Dunshee, C., Zschäbitz, S., Oldenburg, J., Ye, D., Lin, X., Healy, C. G., Di Santo, N., Laird, A. D., … Agarwal, N. (2024). First-line talazoparib with enzalutamide in HRR-deficient metastatic castration-resistant prostate cancer: The phase 3 TALAPRO-2 trial. *Nature Medicine*, *30*(1), 257–264. https://doi.org/10.1038/s41591-023-02704-x

Fizazi, K., Chi, K. N., de Bono, J. S., Gomella, L. G., Miller, K., Rathkopf, D. E., Ryan, C. J., Scher, H. I., Shore, N. D., De Porre, P., Londhe, A., McGowan, T., Pelhivanov, N., Charnas, R., Todd, M. B., & Montgomery, B. (2016). Low Incidence of Corticosteroid-associated Adverse Events on Long-term Exposure to Low-dose Prednisone Given with Abiraterone Acetate to Patients with Metastatic Castration-resistant Prostate Cancer. *European Urology*, *70*(3), 438–444. https://doi.org/10.1016/j.eururo.2016.02.035

Fizazi, K., Foulon, S., Carles, J., Roubaud, G., McDermott, R., Fléchon, A., Tombal, B., Supiot, S., Berthold, D., Ronchin, P., Kacso, G., Gravis, G., Calabro, F., Berdah, J.-F., Hasbini, A., Silva, M., Thiery-Vuillemin, A., Latorzeff, I., Mourey, L., … PEACE-1 investigators. (2022). Abiraterone plus prednisone added to androgen deprivation therapy and docetaxel in de novo metastatic castration-sensitive prostate cancer (PEACE-1): A multicentre, open-label, randomised, phase 3 study with a 2 × 2 factorial design. *Lancet (London, England)*, *399*(10336), 1695–1707. https://doi.org/10.1016/S0140-6736(22)00367-1

Fizazi, K., Piulats, J. M., Reaume, M. N., Ostler, P., McDermott, R., Gingerich, J. R., Pintus, E., Sridhar, S. S., Bambury, R. M., Emmenegger, U., Lindberg, H., Morris, D., Nolè, F., Staffurth, J., Redfern, C., Sáez, M. I., Abida, W., Daugaard, G., Heidenreich, A., … TRITON3 Investigators. (2023). Rucaparib or Physician's Choice in Metastatic Prostate Cancer. *The New England Journal of Medicine*, *388*(8), 719–732. https://doi.org/10.1056/NEJMoa2214676

Flynn, R. L., & Zou, L. (2011). ATR: A master conductor of cellular responses to DNA replication stress. *Trends in Biochemical Sciences*, *36*(3), 133–140. https://doi.org/10.1016/j.tibs.2010.09.005

Formaggio, N., Rubin, M. A., & Theurillat, J.-P. (2021). Loss and revival of androgen receptor signaling in advanced prostate cancer. *Oncogene*, *40*(7), 1205–1216. https://doi.org/10.1038/s41388-020-01598-0

Fraser, M., Sabelnykova, V. Y., Yamaguchi, T. N., Heisler, L. E., Livingstone, J., Huang, V., Shiah, Y.-J., Yousif, F., Lin, X., Masella, A. P., Fox, N. S., Xie, M., Prokopec, S. D., Berlin, A., Lalonde, E., Ahmed, M., Trudel, D., Luo, X., Beck, T. A., … Boutros, P. C. (2017). Genomic hallmarks of localized, non-indolent prostate cancer. *Nature*, *541*(7637), 359–364. https://doi.org/10.1038/nature20788

Freedland, S. J., de Almeida Luz, M., De Giorgi, U., Gleave, M., Gotto, G. T., Pieczonka, C. M., Haas, G. P., Kim, C.-S., Ramirez-Backhaus, M., Rannikko, A., Tarazi, J., Sridharan, S., Sugg, J., Tang, Y., Tutrone, R. F., Venugopal, B., Villers, A., Woo, H. H., Zohren, F., … EMBARK Study. (2023). Improved Outcomes with Enzalutamide in Biochemically Recurrent Prostate Cancer. *The New England Journal of Medicine*, *389*(16), 1453–1465. https://doi.org/10.1056/NEJMoa2303974

Freedland, S. J., Gleave, M., De Giorgi, U., Rannikko, A., Pieczonka, C. M., Tutrone, R. F., Venugopal, B., Woo, H. H., Ramirez-Backhaus, M., Supiot, S., Lantz, A., Ganguli, A., Ivanova, J., Kral, P., Huang, S.-P., Saad, F., & Shore, N. D. (2023). Enzalutamide and Quality of Life in Biochemically

Recurrent Prostate Cancer. *NEJM Evidence*, *2*(12), EVIDoa2300251. https://doi.org/10.1056/EVIDoa2300251

Gabbiani, G. (2003). The myofibroblast in wound healing and fibrocontractive diseases. *The Journal of Pathology*, *200*(4), 500–503. https://doi.org/10.1002/path.1427

Gan, W., Dai, X., Lunardi, A., Li, Z., Inuzuka, H., Liu, P., Varmeh, S., Zhang, J., Cheng, L., Sun, Y., Asara, J. M., Beck, A. H., Huang, J., Pandolfi, P. P., & Wei, W. (2015). SPOP Promotes Ubiquitination and Degradation of the ERG Oncoprotein to Suppress Prostate Cancer Progression. *Molecular Cell*, *59*(6), 917–930. https://doi.org/10.1016/j.molcel.2015.07.026

Gandaglia, G., Abdollah, F., Schiffmann, J., Trudeau, V., Shariat, S. F., Kim, S. P., Perrotte, P., Montorsi, F., Briganti, A., Trinh, Q.-D., Karakiewicz, P. I., & Sun, M. (2014). Distribution of metastatic sites in patients with prostate cancer: A population-based analysis. *The Prostate*, *74*(2), 210–216. https://doi.org/10.1002/pros.22742

Gao, H., Ouyang, X., Banach-Petrosky, W. A., Gerald, W. L., Shen, M. M., & Abate-Shen, C. (2006). Combinatorial activities of Akt and B-Raf/Erk signaling in a mouse model of androgen-independent prostate cancer. *Proceedings of the National Academy of Sciences of the United States of America*, *103*(39), 14477–14482. https://doi.org/10.1073/pnas.0606836103

Garabedian, E. M., Humphrey, P. A., & Gordon, J. I. (1998). A transgenic mouse model of metastatic prostate cancer originating from neuroendocrine cells. *Proceedings of the National Academy of Sciences of the United States of America*, *95*(26), 15382–15387. https://doi.org/10.1073/pnas.95.26.15382

Gautel, M. (2011). The sarcomeric cytoskeleton: Who picks up the strain? *Current Opinion in Cell Biology*, *23*(1), 39–46. https://doi.org/10.1016/j.ceb.2010.12.001

Gerhardt, J., Montani, M., Wild, P., Beer, M., Huber, F., Hermanns, T., Müntener, M., & Kristiansen, G. (2012). FOXA1 promotes tumor progression in prostate cancer and represents a novel hallmark of castration-resistant prostate cancer. *The American Journal of Pathology*, *180*(2), 848–861. https://doi.org/10.1016/j.ajpath.2011.10.021

Germain, L., Lafront, C., Paquette, V., Neveu, B., Paquette, J.-S., Pouliot, F., & Audet-Walsh, É. (2023). Preclinical models of prostate cancer—Modelling androgen dependency and castration resistance in vitro, ex vivo and in vivo. *Nature Reviews. Urology*, *20*(8), 480–493. https://doi.org/10.1038/s41585-023-00726-1

Gleason, D. F., & Mellinger, G. T. (1974). Prediction of prognosis for prostatic adenocarcinoma by combined histological grading and clinical staging. *The Journal of Urology*, *111*(1), 58–64. https://doi.org/10.1016/s0022-5347(17)59889-4

Glinsky, G. V., Berezovska, O., & Glinskii, A. B. (2005). Microarray analysis identifies a death-from-cancer signature predicting therapy failure in patients with multiple types of cancer. *The Journal of Clinical Investigation*, *115*(6), 1503–1521. https://doi.org/10.1172/JCI23412

Goodwin, J. F., Schiewer, M. J., Dean, J. L., Schrecengost, R. S., de Leeuw, R., Han, S., Ma, T., Den, R. B., Dicker, A. P., Feng, F. Y., & Knudsen, K. E. (2013). A hormone-DNA repair circuit governs the response to genotoxic insult. *Cancer Discovery*, *3*(11), 1254–1271. https://doi.org/10.1158/2159-8290.CD-13-0108

Gordon, A. M., Homsher, E., & Regnier, M. (2000). Regulation of contraction in striated muscle. *Physiological Reviews*, *80*(2), 853–924. https://doi.org/10.1152/physrev.2000.80.2.853

Gorrini, C., Baniasadi, P. S., Harris, I. S., Silvester, J., Inoue, S., Snow, B., Joshi, P. A., Wakeham, A., Molyneux, S. D., Martin, B., Bouwman, P., Cescon, D. W., Elia, A. J., Winterton-Perks, Z., Cruickshank, J., Brenner, D., Tseng, A., Musgrave, M., Berman, H. K., … Gauthier, M. L. (2013). BRCA1 interacts with Nrf2 to regulate antioxidant signaling and cell survival. *The Journal of Experimental Medicine*, *210*(8), 1529–1544. https://doi.org/10.1084/jem.20121337

Grasso, C. S., Wu, Y.-M., Robinson, D. R., Cao, X., Dhanasekaran, S. M., Khan, A. P., Quist, M. J., Jing, X., Lonigro, R. J., Brenner, J. C., Asangani, I. A., Ateeq, B., Chun, S. Y., Siddiqui, J., Sam, L., Anstett, M., Mehra, R., Prensner, J. R., Palanisamy, N., … Tomlins, S. A. (2012). The

mutational landscape of lethal castration-resistant prostate cancer. *Nature*, *487*(7406), 239–243. https://doi.org/10.1038/nature11125

Greaves, M., & Maley, C. C. (2012). Clonal evolution in cancer. *Nature*, *481*(7381), 306–313. https://doi.org/10.1038/nature10762

Groelly, F. J., Fawkes, M., Dagg, R. A., Blackford, A. N., & Tarsounas, M. (2023). Targeting DNA damage response pathways in cancer. *Nature Reviews Cancer*, *23*(2), 78–94. https://doi.org/10.1038/s41568-022-00535-5

Grossman, D. C., Curry, S. J., Owens, D. K., Bibbins-Domingo, K., Caughey, A. B., Davidson, K. W., Doubeni, C. A., Ebell, M., Epling, J. W., Kemper, A. R., Krist, A. H., Kubik, M., Landefeld, C. S., Mangione, C. M., Silverstein, M., Simon, M. A., Siu, A. L., & Tseng, C.-W. (2018). Screening for Prostate Cancer: US Preventive Services Task Force Recommendation Statement. *JAMA*, *319*(18), 1901–1913. https://doi.org/10.1001/jama.2018.3710

Gulati, R., Cheng, H. H., Lange, P. H., Nelson, P. S., & Etzioni, R. (2017). Screening Men at Increased Risk for Prostate Cancer Diagnosis: Model Estimates of Benefits and Harms. *Cancer Epidemiology, Biomarkers & Prevention: A Publication of the American Association for Cancer Research, Cosponsored by the American Society of Preventive Oncology*, *26*(2), 222–227. https://doi.org/10.1158/1055-9965.EPI-16-0434

Gundem, G., Van Loo, P., Kremeyer, B., Alexandrov, L. B., Tubio, J. M. C., Papaemmanuil, E., Brewer, D. S., Kallio, H. M. L., Högnäs, G., Annala, M., Kivinummi, K., Goody, V., Latimer, C., O'Meara, S., Dawson, K. J., Isaacs, W., Emmert-Buck, M. R., Nykter, M., Foster, C., … Bova, G. S. (2015). The evolutionary history of lethal metastatic prostate cancer. *Nature*, *520*(7547), 353–357. https://doi.org/10.1038/nature14347

Guo, C., Sharp, A., Gurel, B., Crespo, M., Figueiredo, I., Jain, S., Vogl, U., Rekowski, J., Rouhifard, M., Gallagher, L., Yuan, W., Carreira, S., Chandran, K., Paschalis, A., Colombo, I., Stathis, A., Bertan, C., Seed, G., Goodall, J., … de Bono, J. S. (2023). Targeting myeloid chemotaxis to reverse prostate cancer therapy resistance. *Nature*, *623*(7989), 1053–1061. https://doi.org/10.1038/s41586-023-06696-z

Guo, H., Huang, R., Semba, S., Kordowska, J., Huh, Y. H., Khalina-Stackpole, Y., Mabuchi, K., Kitazawa, T., & Wang, C.-L. A. (2013). Ablation of smooth muscle caldesmon affects the relaxation kinetics of arterial muscle. *Pflugers Archiv: European Journal of Physiology*, *465*(2), 283–294. https://doi.org/10.1007/s00424-012-1178-8

Guo, H., & Wang, C.-L. A. (2005). Specific disruption of smooth muscle caldesmon expression in mice. *Biochemical and Biophysical Research Communications*, *330*(4), 1132–1137. https://doi.org/10.1016/j.bbrc.2005.03.089

Gurel, B., Iwata, T., Koh, C. M., Jenkins, R. B., Lan, F., Van Dang, C., Hicks, J. L., Morgan, J., Cornish, T. C., Sutcliffe, S., Isaacs, W. B., Luo, J., & De Marzo, A. M. (2008). Nuclear MYC protein overexpression is an early alteration in human prostate carcinogenesis. *Modern Pathology: An Official Journal of the United States and Canadian Academy of Pathology, Inc*, *21*(9), 1156–1167. https://doi.org/10.1038/modpathol.2008.111

Haffner, M. C., Zwart, W., Roudier, M. P., True, L. D., Nelson, W. G., Epstein, J. I., De Marzo, A. M., Nelson, P. S., & Yegnasubramanian, S. (2021). Genomic and phenotypic heterogeneity in prostate cancer. *Nature Reviews. Urology*, *18*(2), 79–92. https://doi.org/10.1038/s41585-020-00400-w

Hall, J. M., Lee, M. K., Newman, B., Morrow, J. E., Anderson, L. A., Huey, B., & King, M. C. (1990). Linkage of early-onset familial breast cancer to chromosome 17q21. *Science (New York, N.Y.)*, *250*(4988), 1684–1689. https://doi.org/10.1126/science.2270482

Hamdy, F. C., Donovan, J. L., Lane, J. A., Metcalfe, C., Davis, M., Turner, E. L., Martin, R. M., Young, G. J., Walsh, E. I., Bryant, R. J., Bollina, P., Doble, A., Doherty, A., Gillatt, D., Gnanapragasam, V., Hughes, O., Kockelbergh, R., Kynaston, H., Paul, A., … ProtecT Study Group. (2023). Fifteen-Year Outcomes after Monitoring, Surgery, or Radiotherapy for Prostate Cancer. *The New England Journal of Medicine*, *388*(17), 1547–1558. https://doi.org/10.1056/NEJMoa2214122

Hamid, A. A., Gray, K. P., Shaw, G., MacConaill, L. E., Evan, C., Bernard, B., Loda, M., Corcoran, N. M., Van Allen, E. M., Choudhury, A. D., & Sweeney, C. J. (2019). Compound Genomic Alterations of TP53, PTEN, and RB1 Tumor Suppressors in Localized and Metastatic Prostate Cancer. *European Urology*, *76*(1), 89–97. https://doi.org/10.1016/j.eururo.2018.11.045

Hanahan, D. (2022). Hallmarks of Cancer: New Dimensions. *Cancer Discovery*, *12*(1), 31–46. https://doi.org/10.1158/2159-8290.CD-21-1059

Hanahan, D., & Weinberg, R. A. (2000). The hallmarks of cancer. *Cell*, *100*(1), 57–70. https://doi.org/10.1016/s0092-8674(00)81683-9

Hasan, A. M. M., Cremaschi, P., Wetterskog, D., Jayaram, A., Wong, S. Q., Williams, S., Pasam, A., Trigos, A., Trujillo, B., Grist, E., Friedrich, S., Vainauskas, O., Parry, M., Ismail, M., Devlies, W., Wingate, A., Linch, M., Naceur-Lombardelli, C., Swanton, C., … Attard, G. (2023). Copy number architectures define treatment-mediated selection of lethal prostate cancer clones. *Nature Communications*, *14*(1), 4823. https://doi.org/10.1038/s41467-023-40315-9

Hasterok, S., Scott, T. G., Roller, D. G., Spencer, A., Dutta, A. B., Sathyan, K. M., Frigo, D. E., Guertin, M. J., & Gioeli, D. (2023). The Androgen Receptor Does Not Directly Regulate the Transcription of DNA Damage Response Genes. *Molecular Cancer Research: MCR*, *21*(12), 1329–1341. https://doi.org/10.1158/1541-7786.MCR-23-0358

Hatchi, E., Skourti-Stathaki, K., Ventz, S., Pinello, L., Yen, A., Kamieniarz-Gdula, K., Dimitrov, S., Pathania, S., McKinney, K. M., Eaton, M. L., Kellis, M., Hill, S. J., Parmigiani, G., Proudfoot, N. J., & Livingston, D. M. (2015). BRCA1 recruitment to transcriptional pause sites is required for R-loop-driven DNA damage repair. *Molecular Cell*, *57*(4), 636–647. https://doi.org/10.1016/j.molcel.2015.01.011

He, B., Minges, J. T., Lee, L. W., & Wilson, E. M. (2002). The FXXLF motif mediates androgen receptor-specific interactions with coregulators. *The Journal of Biological Chemistry*, *277*(12), 10226–10235. https://doi.org/10.1074/jbc.M111975200

He, Y., Sun, M. M., Zhang, G. G., Yang, J., Chen, K. S., Xu, W. W., & Li, B. (2021). Targeting PI3K/Akt signal transduction for cancer therapy. *Signal Transduction and Targeted Therapy*, *6*(1), 425. https://doi.org/10.1038/s41392-021-00828-5

Helfman, D. M., Levy, E. T., Berthier, C., Shtutman, M., Riveline, D., Grosheva, I., Lachish-Zalait, A., Elbaum, M., & Bershadsky, A. D. (1999). Caldesmon Inhibits Nonmuscle Cell Contractility and Interferes with the Formation of Focal Adhesions. *Molecular Biology of the Cell*, *10*(10), 3097–3112. https://doi.org/10.1091/mbc.10.10.3097

Helleday, T., Petermann, E., Lundin, C., Hodgson, B., & Sharma, R. A. (2008). DNA repair pathways as targets for cancer therapy. *Nature Reviews. Cancer*, *8*(3), 193–204. https://doi.org/10.1038/nrc2342

Helminen, L., Huttunen, J., Tulonen, M., Aaltonen, N., Niskanen, E. A., Palvimo, J. J., & Paakinaho, V. (2024). Chromatin accessibility and pioneer factor FOXA1 restrict glucocorticoid receptor action in prostate cancer. *Nucleic Acids Research*, *52*(2), 625–642. https://doi.org/10.1093/nar/gkad1126

Hemminki, K. (2012). Familial risk and familial survival in prostate cancer. *World Journal of Urology*, *30*(2), 143–148. https://doi.org/10.1007/s00345-011-0801-1

Henry, G. H., Malewska, A., Joseph, D. B., Malladi, V. S., Lee, J., Torrealba, J., Mauck, R. J., Gahan, J. C., Raj, G. V., Roehrborn, C. G., Hon, G. C., MacConmara, M. P., Reese, J. C., Hutchinson, R. C., Vezina, C. M., & Strand, D. W. (2018). A Cellular Anatomy of the Normal Adult Human Prostate and Prostatic Urethra. *Cell Reports*, *25*(12), 3530-3542.e5. https://doi.org/10.1016/j.celrep.2018.11.086

Herberts, C., Annala, M., Sipola, J., Ng, S. W. S., Chen, X. E., Nurminen, A., Korhonen, O. V., Munzur, A. D., Beja, K., Schönlau, E., Bernales, C. Q., Ritch, E., Bacon, J. V. W., Lack, N. A., Nykter, M., Aggarwal, R., Small, E. J., Gleave, M. E., SU2C/PCF West Coast Prostate Cancer Dream Team, … Wyatt, A. W. (2022). Deep whole-genome ctDNA chronology of treatment-resistant prostate cancer. *Nature*, *608*(7921), 199–208. https://doi.org/10.1038/s41586-022-04975-9

Hernández-Muñoz, I., Lund, A. H., van der Stoop, P., Boutsma, E., Muijrers, I., Verhoeven, E., Nusinow, D. A., Panning, B., Marahrens, Y., & van Lohuizen, M. (2005). Stable X chromosome inactivation involves the PRC1 Polycomb complex and requires histone MACROH2A1 and the CULLIN3/SPOP ubiquitin E3 ligase. *Proceedings of the National Academy of Sciences*, *102*(21), 7635–7640. https://doi.org/10.1073/pnas.0408918102

Hieronymus, H., Murali, R., Tin, A., Yadav, K., Abida, W., Moller, H., Berney, D., Scher, H., Carver, B., Scardino, P., Schultz, N., Taylor, B., Vickers, A., Cuzick, J., & Sawyers, C. L. (2018). Tumor copy number alteration burden is a pan-cancer prognostic factor associated with recurrence and death. *eLife*, *7*, e37294. https://doi.org/10.7554/eLife.37294

Hieronymus, H., & Sawyers, C. L. (2012). Traversing the genomic landscape of prostate cancer from diagnosis to death. *Nature Genetics*, *44*(6), 613–614. https://doi.org/10.1038/ng.2301

Hiltunen, J., Helminen, L., & Paakinaho, V. (2024). Glucocorticoid receptor action in prostate cancer: The role of transcription factor crosstalk. *Frontiers in Endocrinology*, *15*. https://doi.org/10.3389/fendo.2024.1437179

Hoefer, J., Kern, J., Ofer, P., Eder, I. E., Schäfer, G., Dietrich, D., Kristiansen, G., Geley, S., Rainer, J., Gunsilius, E., Klocker, H., Culig, Z., & Puhr, M. (2014). SOCS2 correlates with malignancy and exerts growth-promoting effects in prostate cancer. *Endocrine-Related Cancer*, *21*(2), 175–187. https://doi.org/10.1530/ERC-13-0446

Hofman, M. S., Lawrentschuk, N., Francis, R. J., Tang, C., Vela, I., Thomas, P., Rutherford, N., Martin, J. M., Frydenberg, M., Shakher, R., Wong, L.-M., Taubman, K., Ting Lee, S., Hsiao, E., Roach, P., Nottage, M., Kirkwood, I., Hayne, D., Link, E., … proPSMA Study Group Collaborators. (2020). Prostate-specific membrane antigen PET-CT in patients with high-risk prostate cancer before curative-intent surgery or radiotherapy (proPSMA): A prospective, randomised, multicentre study. *Lancet (London, England)*, *395*(10231), 1208–1216. https://doi.org/10.1016/S0140-6736(20)30314-7

Hopkins, J. F., Sabelnykova, V. Y., Weischenfeldt, J., Simon, R., Aguiar, J. A., Alkallas, R., Heisler, L. E., Zhang, J., Watson, J. D., Chua, M. L. K., Fraser, M., Favero, F., Lawerenz, C., Plass, C., Sauter, G., McPherson, J. D., van der Kwast, T., Korbel, J., Schlomm, T., … Boutros, P. C. (2017). Mitochondrial mutations drive prostate cancer aggression. *Nature Communications*, *8*(1), 656. https://doi.org/10.1038/s41467-017-00377-y

Hoshino, A., Costa-Silva, B., Shen, T.-L., Rodrigues, G., Hashimoto, A., Tesic Mark, M., Molina, H., Kohsaka, S., Di Giannatale, A., Ceder, S., Singh, S., Williams, C., Soplop, N., Uryu, K., Pharmer, L., King, T., Bojmar, L., Davies, A. E., Ararso, Y., … Lyden, D. (2015). Tumour exosome integrins determine organotropic metastasis. *Nature*, *527*(7578), 329–335. https://doi.org/10.1038/nature15756

Hou, Q., Tan, H. T., Lim, K. H., Lim, T. K., Khoo, A., Tan, I. B. H., Yeoh, K. G., & Chung, M. C. M. (2013). Identification and functional validation of caldesmon as a potential gastric cancer metastasis-associated protein. *Journal of Proteome Research*, *12*(2), 980–990. https://doi.org/10.1021/pr3010259

Hsieh, T.-B., & Jin, J.-P. (2023). Evolution and function of calponin and transgelin. *Frontiers in Cell and Developmental Biology*, *11*, 1206147. https://doi.org/10.3389/fcell.2023.1206147

Hsu, L. C., & White, R. L. (1998). BRCA1 is associated with the centrosome during mitosis. *Proceedings of the National Academy of Sciences of the United States of America*, *95*(22), 12983–12988. https://doi.org/10.1073/pnas.95.22.12983

Huang, F. W., Mosquera, J. M., Garofalo, A., Oh, C., Baco, M., Amin-Mansour, A., Rabasha, B., Bahl, S., Mullane, S. A., Robinson, B. D., Aldubayan, S., Khani, F., Karir, B., Kim, E., Chimene-Weiss, J., Hofree, M., Romanel, A., Osborne, J. R., Kim, J. W., … Garraway, L. A. (2017). Exome Sequencing of African-American Prostate Cancer Reveals Loss-of-Function ERF Mutations. *Cancer Discovery*, *7*(9), 973–983. https://doi.org/10.1158/2159-8290.CD-16-0960

Huang, R., & Zhou, P.-K. (2021). DNA damage repair: Historical perspectives, mechanistic pathways and clinical translation for targeted cancer therapy. *Signal Transduction and Targeted Therapy*, *6*(1), 254. https://doi.org/10.1038/s41392-021-00648-7

Huen, M. S. Y., Sy, S. M. H., & Chen, J. (2010). BRCA1 and its toolbox for the maintenance of genome integrity. *Nature Reviews. Molecular Cell Biology*, *11*(2), 138–148. https://doi.org/10.1038/nrm2831

Huggins, C., & Hodgens, C. V. (1941). Studies on Prostatic Cancer. I. The Effect of Castration, of Estrogen and of Androgen Injection on Serum Phosphatases in Metastatic Carcinoma of the Prostate* | Cancer Research | American Association for Cancer Research. *Cancer Research*, *1*(4), 293–297.

Huhtaniemi, R., Oksala, R., Knuuttila, M., Mehmood, A., Aho, E., Laajala, T. D., Nicorici, D., Aittokallio, T., Laiho, A., Elo, L., Ohlsson, C., Kallio, P., Mäkelä, S., Mustonen, M. V. J., Sipilä, P., & Poutanen, M. (2018). Adrenals Contribute to Growth of Castration-Resistant VCaP Prostate Cancer Xenografts. *The American Journal of Pathology*, *188*(12), 2890–2901. https://doi.org/10.1016/j.ajpath.2018.07.029

Huhtaniemi, R., Sipilä, P., Junnila, A., Oksala, R., Knuuttila, M., Mehmood, A., Aho, E., Laajala, T. D., Aittokallio, T., Laiho, A., Elo, L., Ohlsson, C., Thulin, M. H., Kallio, P., Mäkelä, S., Mustonen, M. V. J., & Poutanen, M. (2022). High intratumoral dihydrotestosterone is associated with antiandrogen resistance in VCaP prostate cancer xenografts in castrated mice. *iScience*, *25*(5), 104287. https://doi.org/10.1016/j.isci.2022.104287

Hussain, M., Mateo, J., Fizazi, K., Saad, F., Shore, N., Sandhu, S., Chi, K. N., Sartor, O., Agarwal, N., Olmos, D., Thiery-Vuillemin, A., Twardowski, P., Roubaud, G., Özgüroğlu, M., Kang, J., Burgents, J., Gresty, C., Corcoran, C., Adelman, C. A., … PROfound Trial Investigators. (2020). Survival with Olaparib in Metastatic Castration-Resistant Prostate Cancer. *The New England Journal of Medicine*, *383*(24), 2345–2357. https://doi.org/10.1056/NEJMoa2022485

Hussain, M., Tombal, B., Saad, F., Fizazi, K., Sternberg, C. N., Crawford, E. D., Shore, N., Kopyltsov, E., Kalebasty, A. R., Bögemann, M., Ye, D., Cruz, F., Suzuki, H., Kapur, S., Srinivasan, S., Verholen, F., Kuss, I., Joensuu, H., & Smith, M. R. (2023). Darolutamide Plus Androgen-Deprivation Therapy and Docetaxel in Metastatic Hormone-Sensitive Prostate Cancer by Disease Volume and Risk Subgroups in the Phase III ARASENS Trial. *Journal of Clinical Oncology: Official Journal of the American Society of Clinical Oncology*, *41*(20), 3595–3607. https://doi.org/10.1200/JCO.23.00041

Hyväkkä, A., Virtanen, V., Kemppainen, J., Grönroos, T. J., Minn, H., & Sundvall, M. (2021). More Than Meets the Eye: Scientific Rationale behind Molecular Imaging and Therapeutic Targeting of Prostate-Specific Membrane Antigen (PSMA) in Metastatic Prostate Cancer and Beyond. *Cancers*, *13*(9), 2244. https://doi.org/10.3390/cancers13092244

Ishikawa, R., Yamashiro, S., Kohama, K., & Matsumura, F. (1998). Regulation of actin binding and actin bundling activities of fascin by caldesmon coupled with tropomyosin. *The Journal of Biological Chemistry*, *273*(41), 26991–26997. https://doi.org/10.1074/jbc.273.41.26991

Jäämaa, S., af Hällström, T. M., Sankila, A., Rantanen, V., Koistinen, H., Stenman, U.-H., Zhang, Z., Yang, Z., De Marzo, A. M., Taari, K., Ruutu, M., Andersson, L. C., & Laiho, M. (2010). DNA Damage Recognition via Activated ATM and p53 Pathway in Nonproliferating Human Prostate Tissue. *Cancer Research*, *70*(21), 8630–8641. https://doi.org/10.1158/0008-5472.CAN-10-0937

Jackson, S. P., & Bartek, J. (2009). The DNA-damage response in human biology and disease. *Nature*, *461*(7267), 1071–1078. https://doi.org/10.1038/nature08467

Jillson, L. K., Rider, L. C., Rodrigues, L. U., Romero, L., Karimpour-Fard, A., Nieto, C., Gillette, C., Torkko, K., Danis, E., Smith, E. E., Nolley, R., Peehl, D. M., Lucia, M. S., Costello, J. C., & Cramer, S. D. (2021). MAP3K7 Loss Drives Enhanced Androgen Signaling and Independently Confers Risk of Recurrence in Prostate Cancer with Joint Loss of CHD1. *Molecular Cancer Research: MCR*, *19*(7), 1123–1136. https://doi.org/10.1158/1541-7786.MCR-20-0913

Joseph, J. D., Lu, N., Qian, J., Sensintaffar, J., Shao, G., Brigham, D., Moon, M., Maneval, E. C., Chen, I., Darimont, B., & Hager, J. H. (2013). A Clinically Relevant Androgen Receptor Mutation Confers Resistance to Second-Generation Antiandrogens Enzalutamide and ARN-509. *Cancer Discovery*, *3*(9), 1020–1029. https://doi.org/10.1158/2159-8290.CD-13-0226

Jung, C., Kim, R.-S., Zhang, H.-J., Lee, S.-J., & Jeng, M.-H. (2004). HOXB13 induces growth suppression of prostate cancer cells as a repressor of hormone-activated androgen receptor signaling. *Cancer Research*, *64*(24), 9185–9192. https://doi.org/10.1158/0008-5472.CAN-04-1330

Jung, Y., Wang, J., Lee, E., McGee, S., Berry, J. E., Yumoto, K., Dai, J., Keller, E. T., Shiozawa, Y., & Taichman, R. S. (2015). Annexin 2-CXCL12 interactions regulate metastatic cell targeting and growth in the bone marrow. *Molecular Cancer Research: MCR*, *13*(1), 197–207. https://doi.org/10.1158/1541-7786.MCR-14-0118

Kang, J., La Manna, F., Bonollo, F., Sampson, N., Alberts, I. L., Mingels, C., Afshar-Oromieh, A., Thalmann, G. N., & Karkampouna, S. (2022). Tumor microenvironment mechanisms and bone metastatic disease progression of prostate cancer. *Cancer Letters*, *530*, 156–169. https://doi.org/10.1016/j.canlet.2022.01.015

Kang, Y., & Massagué, J. (2004). Epithelial-mesenchymal transitions: Twist in development and metastasis. *Cell*, *118*(3), 277–279. https://doi.org/10.1016/j.cell.2004.07.011

Kantoff, P. W., Higano, C. S., Shore, N. D., Berger, E. R., Small, E. J., Penson, D. F., Redfern, C. H., Ferrari, A. C., Dreicer, R., Sims, R. B., Xu, Y., Frohlich, M. W., Schellhammer, P. F., & IMPACT Study Investigators. (2010). Sipuleucel-T immunotherapy for castration-resistant prostate cancer. *The New England Journal of Medicine*, *363*(5), 411–422. https://doi.org/10.1056/NEJMoa1001294

Karlsson, R., Aly, M., Clements, M., Zheng, L., Adolfsson, J., Xu, J., Grönberg, H., & Wiklund, F. (2014). A population-based assessment of germline HOXB13 G84E mutation and prostate cancer risk. *European Urology*, *65*(1), 169–176. https://doi.org/10.1016/j.eururo.2012.07.027

Karthaus, W. R., Hofree, M., Choi, D., Linton, E. L., Turkekul, M., Bejnood, A., Carver, B., Gopalan, A., Abida, W., Laudone, V., Biton, M., Chaudhary, O., Xu, T., Masilionis, I., Manova, K., Mazutis, L., Pe'er, D., Regev, A., & Sawyers, C. L. (2020). Regenerative potential of prostate luminal cells revealed by single-cell analysis. *Science (New York, N.Y.)*, *368*(6490), 497–505. https://doi.org/10.1126/science.aay0267

Kassabov, S. R., Zhang, B., Persinger, J., & Bartholomew, B. (2003). SWI/SNF unwraps, slides, and rewraps the nucleosome. *Molecular Cell*, *11*(2), 391–403. https://doi.org/10.1016/s1097-2765(03)00039-x

Katsuta, H., Sokabe, M., & Hirata, H. (2024). From stress fiber to focal adhesion: A role of actin crosslinkers in force transmission. *Frontiers in Cell and Developmental Biology*, *12*. https://doi.org/10.3389/fcell.2024.1444827

Kelloff, G. J., Hoffman, J. M., Johnson, B., Scher, H. I., Siegel, B. A., Cheng, E. Y., Cheson, B. D., O'shaughnessy, J., Guyton, K. Z., Mankoff, D. A., Shankar, L., Larson, S. M., Sigman, C. C., Schilsky, R. L., & Sullivan, D. C. (2005). Progress and promise of FDG-PET imaging for cancer patient management and oncologic drug development. *Clinical Cancer Research: An Official Journal of the American Association for Cancer Research*, *11*(8), 2785–2808. https://doi.org/10.1158/1078-0432.CCR-04-2626

Kenfield, S. A., Batista, J. L., Jahn, J. L., Downer, M. K., Van Blarigan, E. L., Sesso, H. D., Giovannucci, E. L., Stampfer, M. J., & Chan, J. M. (2016). Development and Application of a Lifestyle Score for Prevention of Lethal Prostate Cancer. *Journal of the National Cancer Institute*, *108*(3), djv329. https://doi.org/10.1093/jnci/djv329

Kim, J., & Coetzee, G. A. (2004). Prostate specific antigen gene regulation by androgen receptor. *Journal of Cellular Biochemistry*, *93*(2), 233–241. https://doi.org/10.1002/jcb.20228

Kim, J., Jin, H., Zhao, J. C., Yang, Y. A., Li, Y., Yang, X., Dong, X., & Yu, J. (2017). FOXA1 inhibits prostate cancer neuroendocrine differentiation. *Oncogene*, *36*(28), 4072–4080. https://doi.org/10.1038/onc.2017.50

Kim, J., Kim, J., & Bae, J.-S. (2016). ROS homeostasis and metabolism: A critical liaison for cancer therapy. *Experimental & Molecular Medicine*, *48*(11), e269. https://doi.org/10.1038/emm.2016.119

Kim, K.-H., Yeo, S.-G., Kim, W. K., Kim, D. Y., Yeo, H. Y., Hong, J. P., Chang, H. J., Park, J. W., Kim, S. Y., Kim, B. C., & Yoo, B. C. (2012). Up-regulated expression of l-caldesmon associated with malignancy of colorectal cancer. *BMC Cancer*, *12*, 601. https://doi.org/10.1186/1471-2407-12-601

Kim, W. K., Buckley, A. J., Lee, D.-H., Hiroto, A., Nenninger, C. H., Olson, A. W., Wang, J., Li, Z., Vikram, R., Adzavon, Y. M., Yau, T., Bao, Y., Kahn, M., Geradts, J., Xiao, G.-Q., & Sun, Z. (2024). Androgen deprivation induces double-null prostate cancer via aberrant nuclear export and ribosomal biogenesis through HGF and Wnt activation. *Nature Communications*, *15*(1), 1231. https://doi.org/10.1038/s41467-024-45489-4

Kim, W. K., Olson, A. W., Mi, J., Wang, J., Lee, D.-H., Le, V., Hiroto, A., Aldahl, J., Nenninger, C. H., Buckley, A. J., Cardiff, R., You, S., & Sun, Z. (2022). Aberrant androgen action in prostatic progenitor cells induces oncogenesis and tumor development through IGF1 and Wnt axes. *Nature Communications*, *13*(1), 4364. https://doi.org/10.1038/s41467-022-32119-0

Kiviaho, A., Eerola, S. K., Kallio, H. M. L., Andersen, M. K., Hoikka, M., Tiihonen, A. M., Salonen, I., Spotbeen, X., Giesen, A., Parker, C. T. A., Taavitsainen, S., Hantula, O., Marttinen, M., Hermelo, I., Ismail, M., Midtbust, E., Wess, M., Devlies, W., Sharma, A., … Nykter, M. (2024). Single cell and spatial transcriptomics highlight the interaction of club-like cells with immunosuppressive myeloid cells in prostate cancer. *Nature Communications*, *15*(1), 9949. https://doi.org/10.1038/s41467-024-54364-1

Kluth, M., Hesse, J., Heinl, A., Krohn, A., Steurer, S., Sirma, H., Simon, R., Mayer, P.-S., Schumacher, U., Grupp, K., Izbicki, J. R., Pantel, K., Dikomey, E., Korbel, J. O., Plass, C., Sauter, G., Schlomm, T., & Minner, S. (2013). Genomic deletion of MAP3K7 at 6q12-22 is associated with early PSA recurrence in prostate cancer and absence of TMPRSS2:ERG fusions. *Modern Pathology: An Official Journal of the United States and Canadian Academy of Pathology, Inc*, *26*(7), 975–983. https://doi.org/10.1038/modpathol.2012.236

Knuuttila, M., Mehmood, A., Huhtaniemi, R., Yatkin, E., Häkkinen, M. R., Oksala, R., Laajala, T. D., Ryberg, H., Handelsman, D. J., Aittokallio, T., Auriola, S., Ohlsson, C., Laiho, A., Elo, L. L., Sipilä, P., Mäkelä, S. I., & Poutanen, M. (2018). Antiandrogens Reduce Intratumoral Androgen Concentrations and Induce Androgen Receptor Expression in Castration-Resistant Prostate Cancer Xenografts. *The American Journal of Pathology*, *188*(1), 216–228. https://doi.org/10.1016/j.ajpath.2017.08.036

Knuuttila, M., Yatkin, E., Kallio, J., Savolainen, S., Laajala, T. D., Aittokallio, T., Oksala, R., Häkkinen, M., Keski-Rahkonen, P., Auriola, S., Poutanen, M., & Mäkelä, S. (2014). Castration induces up-regulation of intratumoral androgen biosynthesis and androgen receptor expression in an orthotopic VCaP human prostate cancer xenograft model. *The American Journal of Pathology*, *184*(8), 2163–2173. https://doi.org/10.1016/j.ajpath.2014.04.010

Koistinen, H., Künnapuu, J., & Jeltsch, M. (2021). KLK3 in the Regulation of Angiogenesis-Tumorigenic or Not? *International Journal of Molecular Sciences*, *22*(24), 13545. https://doi.org/10.3390/ijms222413545

Koivisto, P., Kononen, J., Palmberg, C., Tammela, T., Hyytinen, E., Isola, J., Trapman, J., Cleutjens, K., Noordzij, A., Visakorpi, T., & Kallioniemi, O. P. (1997). Androgen receptor gene amplification: A possible molecular mechanism for androgen deprivation therapy failure in prostate cancer. *Cancer Research*, *57*(2), 314–319.

Kokate, S. B., Ciuba, K., Tran, V. D., Kumari, R., Tojkander, S., Engel, U., Kogan, K., Kumar, S., & Lappalainen, P. (2022). Caldesmon controls stress fiber force-balance through dynamic cross-linking of myosin II and actin-tropomyosin filaments. *Nature Communications*, *13*(1), 6032. https://doi.org/10.1038/s41467-022-33688-w

Korpal, M., Korn, J. M., Gao, X., Rakiec, D. P., Ruddy, D. A., Doshi, S., Yuan, J., Kovats, S. G., Kim, S., Cooke, V. G., Monahan, J. E., Stegmeier, F., Roberts, T. M., Sellers, W. R., Zhou, W., & Zhu, P. (2013). An F876L mutation in androgen receptor confers genetic and phenotypic resistance to MDV3100 (enzalutamide). *Cancer Discovery*, *3*(9), 1030–1043. https://doi.org/10.1158/2159-8290.CD-13-0142

Kote-Jarai, Z., Mikropoulos, C., Leongamornlert, D. A., Dadaev, T., Tymrakiewicz, M., Saunders, E. J., Jones, M., Jugurnauth-Little, S., Govindasami, K., Guy, M., Hamdy, F. C., Donovan, J. L., Neal, D. E., Lane, J. A., Dearnaley, D., Wilkinson, R. A., Sawyer, E. J., Morgan, A., Antoniou, A. C., … UK Genetic Prostate Cancer Study Collaborators, and the ProtecT Study Group. (2015). Prevalence of the HOXB13 G84E germline mutation in British men and correlation with prostate cancer risk, tumour characteristics and clinical outcomes. *Annals of Oncology: Official Journal of the European Society for Medical Oncology*, *26*(4), 756–761. https://doi.org/10.1093/annonc/mdv004

Kregel, S., Wang, C., Han, X., Xiao, L., Fernandez-Salas, E., Bawa, P., McCollum, B. L., Wilder-Romans, K., Apel, I. J., Cao, X., Speers, C., Wang, S., & Chinnaiyan, A. M. (2020). Androgen receptor degraders overcome common resistance mechanisms developed during prostate cancer treatment. *Neoplasia (New York, N.Y.)*, *22*(2), 111–119. https://doi.org/10.1016/j.neo.2019.12.003

Ku, S. Y., Rosario, S., Wang, Y., Mu, P., Seshadri, M., Goodrich, Z. W., Goodrich, M. M., Labbé, D. P., Gomez, E. C., Wang, J., Long, H. W., Xu, B., Brown, M., Loda, M., Sawyers, C. L., Ellis, L., & Goodrich, D. W. (2017). Rb1 and Trp53 cooperate to suppress prostate cancer lineage plasticity, metastasis, and antiandrogen resistance. *Science (New York, N.Y.)*, *355*(6320), 78–83. https://doi.org/10.1126/science.aah4199

Ku, S.-Y., Wang, Y., Garcia, M. M., Yamada, Y., Mizuno, K., Long, M. D., Rosario, S., Chinnam, M., Al Assaad, M., Puca, L., Kim, M. J., Bakht, M. K., Venkadakrishnan, V. B., Robinson, B. D., Acosta, A. M., Wadosky, K. M., Mosquera, J. M., Goodrich, D. W., & Beltran, H. (2024). Notch signaling suppresses neuroendocrine differentiation and alters the immune microenvironment in advanced prostate cancer. *The Journal of Clinical Investigation*, *134*(17), e175217. https://doi.org/10.1172/JCI175217

Kumar, A., Coleman, I., Morrissey, C., Zhang, X., True, L. D., Gulati, R., Etzioni, R., Bolouri, H., Montgomery, B., White, T., Lucas, J. M., Brown, L. G., Dumpit, R. F., DeSarkar, N., Higano, C., Yu, E. Y., Coleman, R., Schultz, N., Fang, M., … Nelson, P. S. (2016). Substantial interindividual and limited intraindividual genomic diversity among tumors from men with metastatic prostate cancer. *Nature Medicine*, *22*(4), 369–378. https://doi.org/10.1038/nm.4053

Kurita, T., Wang, Y. Z., Donjacour, A. A., Zhao, C., Lydon, J. P., O'Malley, B. W., Isaacs, J. T., Dahiya, R., & Cunha, G. R. (2001). Paracrine regulation of apoptosis by steroid hormones in the male and female reproductive system. *Cell Death & Differentiation*, *8*(2), 192–200. https://doi.org/10.1038/sj.cdd.4400797

Labelle, M., & Hynes, R. O. (2012). The Initial Hours of Metastasis: The Importance of Cooperative Host–Tumor Cell Interactions during Hematogenous Dissemination. *Cancer Discovery*, *2*(12), 1091–1099. https://doi.org/10.1158/2159-8290.CD-12-0329

Lallous, N., Volik, S. V., Awrey, S., Leblanc, E., Tse, R., Murillo, J., Singh, K., Azad, A. A., Wyatt, A. W., LeBihan, S., Chi, K. N., Gleave, M. E., Rennie, P. S., Collins, C. C., & Cherkasov, A. (2016). Functional analysis of androgen receptor mutations that confer anti-androgen resistance identified in circulating cell-free DNA from prostate cancer patients. *Genome Biology*, *17*(1), 10. https://doi.org/10.1186/s13059-015-0864-1

Lalonde, E., Ishkanian, A. S., Sykes, J., Fraser, M., Ross-Adams, H., Erho, N., Dunning, M. J., Halim, S., Lamb, A. D., Moon, N. C., Zafarana, G., Warren, A. Y., Meng, X., Thoms, J., Grzadkowski, M. R., Berlin, A., Have, C. L., Ramnarine, V. R., Yao, C. Q., … Bristow, R. G. (2014). Tumour genomic and microenvironmental heterogeneity for integrated prediction of 5-year biochemical recurrence of prostate cancer: A retrospective cohort study. *The Lancet. Oncology*, *15*(13), 1521–1532. https://doi.org/10.1016/S1470-2045(14)71021-6

Lambert, A. W., Pattabiraman, D. R., & Weinberg, R. A. (2017). Emerging Biological Principles of Metastasis. *Cell*, *168*(4), 670–691. https://doi.org/10.1016/j.cell.2016.11.037

Lamouille, S., Xu, J., & Derynck, R. (2014). Molecular mechanisms of epithelial-mesenchymal transition. *Nature Reviews. Molecular Cell Biology*, *15*(3), 178–196. https://doi.org/10.1038/nrm3758

Lane, J. A., Donovan, J. L., Davis, M., Walsh, E., Dedman, D., Down, L., Turner, E. L., Mason, M. D., Metcalfe, C., Peters, T. J., Martin, R. M., Neal, D. E., Hamdy, F. C., & ProtecT study group. (2014). Active monitoring, radical prostatectomy, or radiotherapy for localised prostate cancer: Study design and diagnostic and baseline results of the ProtecT randomised phase 3 trial. *The Lancet. Oncology*, *15*(10), 1109–1118. https://doi.org/10.1016/S1470-2045(14)70361-4

Latonen, L., Afyounian, E., Jylhä, A., Nättinen, J., Aapola, U., Annala, M., Kivinummi, K. K., Tammela, T. T. L., Beuerman, R. W., Uusitalo, H., Nykter, M., & Visakorpi, T. (2018). Integrative proteomics in prostate cancer uncovers robustness against genomic and transcriptomic aberrations during disease progression. *Nature Communications*, *9*(1), 1176. https://doi.org/10.1038/s41467-018-03573-6

Lázaro-Ibáñez, E., Sanz-Garcia, A., Visakorpi, T., Escobedo-Lucea, C., Siljander, P., Ayuso-Sacido, A., & Yliperttula, M. (2014). Different gDNA content in the subpopulations of prostate cancer extracellular vesicles: Apoptotic bodies, microvesicles, and exosomes. *The Prostate*, *74*(14), 1379–1390. https://doi.org/10.1002/pros.22853

Lee, G. Y., Shin, S.-H., Shin, H.-W., Chun, Y.-S., & Park, J.-W. (2018). NDRG3 lowers the metastatic potential in prostate cancer as a feedback controller of hypoxia-inducible factors. *Experimental & Molecular Medicine*, *50*(5), 1–13. https://doi.org/10.1038/s12276-018-0089-y

Lee, J.-H., & Paull, T. T. (2005). ATM activation by DNA double-strand breaks through the Mre11-Rad50-Nbs1 complex. *Science (New York, N.Y.)*, *308*(5721), 551–554. https://doi.org/10.1126/science.1108297

Lee, M.-S., Lee, J., Kim, J. H., Kim, W. T., Kim, W.-J., Ahn, H., & Park, J. (2015). Overexpression of caldesmon is associated with tumor progression in patients with primary non-muscle-invasive bladder cancer. *Oncotarget*, *6*(37), 40370–40384. https://doi.org/10.18632/oncotarget.5458

Lee, S., Kim, H., Woo, Y., Kim, J., Kim, H. W., Park, J. Y., Suh, B., Choi, Y., Ahn, J., Ryu, J. H., Roe, J., Song, J., & Lee, S. H. (2024). UBX-390: A Novel Androgen Receptor Degrader for Therapeutic Intervention in Prostate Cancer. *Advanced Science*, *11*(33), 2400398. https://doi.org/10.1002/advs.202400398

Lee, W. H., Morton, R. A., Epstein, J. I., Brooks, J. D., Campbell, P. A., Bova, G. S., Hsieh, W. S., Isaacs, W. B., & Nelson, W. G. (1994). Cytidine methylation of regulatory sequences near the pi-class glutathione S-transferase gene accompanies human prostatic carcinogenesis. *Proceedings of the National Academy of Sciences of the United States of America*, *91*(24), 11733–11737. https://doi.org/10.1073/pnas.91.24.11733

Leinonen, K. A., Saramäki, O. R., Furusato, B., Kimura, T., Takahashi, H., Egawa, S., Suzuki, H., Keiger, K., Ho Hahm, S., Isaacs, W. B., Tolonen, T. T., Stenman, U.-H., Tammela, T. L. J., Nykter, M., Bova, G. S., & Visakorpi, T. (2013). Loss of PTEN is associated with aggressive behavior in ERG-positive prostate cancer. *Cancer Epidemiology, Biomarkers & Prevention: A Publication of the American Association for Cancer Research, Cosponsored by the American Society of Preventive Oncology*, *22*(12), 2333–2344. https://doi.org/10.1158/1055-9965.EPI-13-0333-T

Levine, A. J., Momand, J., & Finlay, C. A. (1991). The p53 tumour suppressor gene. *Nature*, *351*(6326), 453–456. https://doi.org/10.1038/351453a0

Li, C., Yang, F., Wang, R., Li, W., Maskey, N., Zhang, W., Guo, Y., Liu, S., Wang, H., & Yao, X. (2021). CALD1 promotes the expression of PD-L1 in bladder cancer via the JAK/STAT signaling pathway. *Annals of Translational Medicine*, *9*(18), 1441. https://doi.org/10.21037/atm-21-4192

Li, J., Xu, C., Lee, H. J., Ren, S., Zi, X., Zhang, Z., Wang, H., Yu, Y., Yang, C., Gao, X., Hou, J., Wang, L., Yang, B., Yang, Q., Ye, H., Zhou, T., Lu, X., Wang, Y., Qu, M., … Sun, Y. (2020). A

genomic and epigenomic atlas of prostate cancer in Asian populations. *Nature*, *580*(7801), 93–99. https://doi.org/10.1038/s41586-020-2135-x

Li, J., Yen, C., Liaw, D., Podsypanina, K., Bose, S., Wang, S. I., Puc, J., Miliaresis, C., Rodgers, L., McCombie, R., Bigner, S. H., Giovanella, B. C., Ittmann, M., Tycko, B., Hibshoosh, H., Wigler, M. H., & Parsons, R. (1997). PTEN, a putative protein tyrosine phosphatase gene mutated in human brain, breast, and prostate cancer. *Science (New York, N.Y.)*, *275*(5308), 1943–1947. https://doi.org/10.1126/science.275.5308.1943

Li, L., Karanika, S., Yang, G., Wang, J., Park, S., Broom, B. M., Manyam, G. C., Wu, W., Luo, Y., Basourakos, S., Song, J. H., Gallick, G. E., Karantanos, T., Korentzelos, D., Azad, A. K., Kim, J., Corn, P. G., Aparicio, A. M., Logothetis, C. J., … Thompson, T. C. (2017). Androgen receptor inhibitor-induced "BRCAness" and PARP inhibition are synthetically lethal for castration-resistant prostate cancer. *Science Signaling*, *10*(480), eaam7479. https://doi.org/10.1126/scisignal.aam7479

Li, M., & Yu, X. (2013). Function of BRCA1 in the DNA damage response is mediated by ADP-ribosylation. *Cancer Cell*, *23*(5), 693–704. https://doi.org/10.1016/j.ccr.2013.03.025

Li, Y., Lin, J. L. C., Reiter, R. S., Daniels, K., Soll, D. R., & Lin, J. J. C. (2004). Caldesmon mutant defective in Ca(2+)-calmodulin binding interferes with assembly of stress fibers and affects cell morphology, growth and motility. *Journal of Cell Science*, *117*(Pt 16), 3593–3604. https://doi.org/10.1242/jcs.01216

Li, Z., Alyamani, M., Li, J., Rogacki, K., Abazeed, M., Upadhyay, S. K., Balk, S. P., Taplin, M.-E., Auchus, R. J., & Sharifi, N. (2016). Redirecting abiraterone metabolism to fine-tune prostate cancer anti-androgen therapy. *Nature*, *533*(7604), 547–551. https://doi.org/10.1038/nature17954

Lilja, H., Ulmert, D., & Vickers, A. J. (2008). Prostate-specific antigen and prostate cancer: Prediction, detection and monitoring. *Nature Reviews. Cancer*, *8*(4), 268–278. https://doi.org/10.1038/nrc2351

Lin, J., Wang, W., Hu, T., Zhu, G., Li, L., Zhang, C., Xu, Z., Yu, H., Wu, H., & Zhu, J. (2020). FOXM1 contributes to docetaxel resistance in castration-resistant prostate cancer by inducing AMPK/mTOR-mediated autophagy. *Cancer Letters*, *469*, 481–489. https://doi.org/10.1016/j.canlet.2019.11.014

Linn, D. E., Penney, K. L., Bronson, R. T., Mucci, L. A., & Li, Z. (2016). Deletion of Interstitial Genes between TMPRSS2 and ERG Promotes Prostate Cancer Progression. *Cancer Research*, *76*(7), 1869–1881. https://doi.org/10.1158/0008-5472.CAN-15-1911

Liu, Q., Wang, G., Li, Q., Jiang, W., Kim, J.-S., Wang, R., Zhu, S., Wang, X., Yan, L., Yi, Y., Zhang, L., Meng, Q., Li, C., Zhao, D., Qiao, Y., Li, Y., Gursel, D. B., Chinnaiyan, A. M., Chen, K., & Cao, Q. (2019). Polycomb group proteins EZH2 and EED directly regulate androgen receptor in advanced prostate cancer. *International Journal of Cancer*, *145*(2), 415–426. https://doi.org/10.1002/ijc.32118

Liu, Q., Zhang, Z., Liu, Y., Cui, Z., Zhang, T., Li, Z., & Ma, W. (2018). Cancer cells growing on perfused 3D collagen model produced higher reactive oxygen species level and were more resistant to cisplatin compared to the 2D model. *Journal of Applied Biomaterials & Functional Materials*, *16*(3), 144–150. https://doi.org/10.1177/2280800018764763

Liu, Y., Xie, S., Zhu, K., Guan, X., Guo, L., & Lu, R. (2021). CALD1 is a prognostic biomarker and correlated with immune infiltrates in gastric cancers. *Heliyon*, *7*(6), e07257. https://doi.org/10.1016/j.heliyon.2021.e07257

Ljungman, M., & Lane, D. P. (2004). Transcription—Guarding the genome by sensing DNA damage. *Nature Reviews. Cancer*, *4*(9), 727–737. https://doi.org/10.1038/nrc1435

Locke, J. A., Guns, E. S., Lubik, A. A., Adomat, H. H., Hendy, S. C., Wood, C. A., Ettinger, S. L., Gleave, M. E., & Nelson, C. C. (2008). Androgen levels increase by intratumoral de novo steroidogenesis during progression of castration-resistant prostate cancer. *Cancer Research*, *68*(15), 6407–6415. https://doi.org/10.1158/0008-5472.CAN-07-5997

Lord, C. J., & Ashworth, A. (2016). BRCAness revisited. *Nature Reviews Cancer*, *16*(2), 110–120. https://doi.org/10.1038/nrc.2015.21

Luzzi, K. J., MacDonald, I. C., Schmidt, E. E., Kerkvliet, N., Morris, V. L., Chambers, A. F., & Groom, A. C. (1998). Multistep nature of metastatic inefficiency: Dormancy of solitary cells after successful extravasation and limited survival of early micrometastases. *The American Journal of Pathology*, *153*(3), 865–873. https://doi.org/10.1016/S0002-9440(10)65628-3

Lynch, H. T., Kosoko-Lasaki, O., Leslie, S. W., Rendell, M., Shaw, T., Snyder, C., D'Amico, A. V., Buxbaum, S., Isaacs, W. B., Loeb, S., Moul, J. W., & Powell, I. (2016). Screening for familial and hereditary prostate cancer. *International Journal of Cancer*, *138*(11), 2579–2591. https://doi.org/10.1002/ijc.29949

Magi-Galluzzi, C., Tsusuki, T., Elson, P., Simmerman, K., LaFargue, C., Esgueva, R., Klein, E., Rubin, M. A., & Zhou, M. (2011). TMPRSS2-ERG gene fusion prevalence and class are significantly different in prostate cancer of Caucasian, African-American and Japanese patients. *The Prostate*, *71*(5), 489–497. https://doi.org/10.1002/pros.21265

Magnusson, C., Augustsson, P., Undvall Anand, E., Lenshof, A., Josefsson, A., Welén, K., Bjartell, A., Ceder, Y., Lilja, H., & Laurell, T. (2024). Acoustic Enrichment of Heterogeneous Circulating Tumor Cells and Clusters from Metastatic Prostate Cancer Patients. *Analytical Chemistry*, *96*(18), 6914–6921. https://doi.org/10.1021/acs.analchem.3c05371

Malik, R., Khan, A. P., Asangani, I. A., Cieślik, M., Prensner, J. R., Wang, X., Iyer, M. K., Jiang, X., Borkin, D., Escara-Wilke, J., Stender, R., Wu, Y.-M., Niknafs, Y. S., Jing, X., Qiao, Y., Palanisamy, N., Kunju, L. P., Krishnamurthy, P. M., Yocum, A. K., … Chinnaiyan, A. M. (2015). Targeting the MLL complex in castration-resistant prostate cancer. *Nature Medicine*, *21*(4), 344–352. https://doi.org/10.1038/nm.3830

Manes, T., Zheng, D.-Q., Tognin, S., Woodard, A. S., Marchisio, P. C., & Languino, L. R. (2003). Alpha(v)beta3 integrin expression up-regulates cdc2, which modulates cell migration. *The Journal of Cell Biology*, *161*(4), 817–826. https://doi.org/10.1083/jcb.200212172

Mani, R.-S., Tomlins, S. A., Callahan, K., Ghosh, A., Nyati, M. K., Varambally, S., Palanisamy, N., & Chinnaiyan, A. M. (2009). Induced Chromosomal Proximity and the Genesis of Gene Fusions in Prostate Cancer. *Science (New York, N.Y.)*, *326*(5957), 1230. https://doi.org/10.1126/science.1178124

Mani, S. A., Guo, W., Liao, M.-J., Eaton, E. N., Ayyanan, A., Zhou, A. Y., Brooks, M., Reinhard, F., Zhang, C. C., Shipitsin, M., Campbell, L. L., Polyak, K., Brisken, C., Yang, J., & Weinberg, R. A. (2008). The epithelial-mesenchymal transition generates cells with properties of stem cells. *Cell*, *133*(4), 704–715. https://doi.org/10.1016/j.cell.2008.03.027

Manke, I. A., Lowery, D. M., Nguyen, A., & Yaffe, M. B. (2003). BRCT repeats as phosphopeptide-binding modules involved in protein targeting. *Science (New York, N.Y.)*, *302*(5645), 636–639. https://doi.org/10.1126/science.1088877

Mantalaris, A., Panoskaltsis, N., Sakai, Y., Bourne, P., Chang, C., Messing, E. M., & David Wu, J. H. (2001). Localization of androgen receptor expression in human bone marrow. *The Journal of Pathology*, *193*(3), 361–366. https://doi.org/10.1002/1096-9896(0000)9999:9999%253C::AID-PATH803%253E3.0.CO;2-W

Mao, Z., Bozzella, M., Seluanov, A., & Gorbunova, V. (2008). DNA repair by nonhomologous end joining and homologous recombination during cell cycle in human cells. *Cell Cycle (Georgetown, Tex.)*, *7*(18), 2902–2906. https://doi.org/10.4161/cc.7.18.6679

Martincorena, I., & Campbell, P. J. (2015). Somatic mutation in cancer and normal cells. *Science (New York, N.Y.)*, *349*(6255), 1483–1489. https://doi.org/10.1126/science.aab4082

Martínez-Jiménez, F., Movasati, A., Brunner, S. R., Nguyen, L., Priestley, P., Cuppen, E., & Van Hoeck, A. (2023). Pan-cancer whole-genome comparison of primary and metastatic solid tumours. *Nature*, *618*(7964), 333–341. https://doi.org/10.1038/s41586-023-06054-z

Marx, F. J., & Karenberg, A. (2009). History of the term prostate. *The Prostate*, *69*(2), 208–213. https://doi.org/10.1002/pros.20871

Massie, C. E., Lynch, A., Ramos-Montoya, A., Boren, J., Stark, R., Fazli, L., Warren, A., Scott, H., Madhu, B., Sharma, N., Bon, H., Zecchini, V., Smith, D.-M., Denicola, G. M., Mathews, N.,

Osborne, M., Hadfield, J., Macarthur, S., Adryan, B., … Mills, I. G. (2011). The androgen receptor fuels prostate cancer by regulating central metabolism and biosynthesis. *The EMBO Journal*, *30*(13), 2719–2733. https://doi.org/10.1038/emboj.2011.158

Mateo, J., Seed, G., Bertan, C., Rescigno, P., Dolling, D., Figueiredo, I., Miranda, S., Nava Rodrigues, D., Gurel, B., Clarke, M., Atkin, M., Chandler, R., Messina, C., Sumanasuriya, S., Bianchini, D., Barrero, M., Petermolo, A., Zafeiriou, Z., Fontes, M., … de Bono, J. S. (2020). Genomics of lethal prostate cancer at diagnosis and castration resistance. *The Journal of Clinical Investigation*, *130*(4), 1743–1751. https://doi.org/10.1172/JCI132031

Mayanagi, T., Morita, T., Hayashi, K., Fukumoto, K., & Sobue, K. (2008). Glucocorticoid receptor-mediated expression of caldesmon regulates cell migration via the reorganization of the actin cytoskeleton. *The Journal of Biological Chemistry*, *283*(45), 31183–31196. https://doi.org/10.1074/jbc.M801606200

McCabe, N. P., De, S., Vasanji, A., Brainard, J., & Byzova, T. V. (2007). Prostate cancer specific integrin alphavbeta3 modulates bone metastatic growth and tissue remodeling. *Oncogene*, *26*(42), 6238–6243. https://doi.org/10.1038/sj.onc.1210429

McNeal, J. E. (1981). The zonal anatomy of the prostate. *The Prostate*, *2*(1), 35–49. https://doi.org/10.1002/pros.2990020105

Menghi, F., Barthel, F. P., Yadav, V., Tang, M., Ji, B., Tang, Z., Carter, G. W., Ruan, Y., Scully, R., Verhaak, R. G. W., Jonkers, J., & Liu, E. T. (2018). The Tandem Duplicator Phenotype Is a Prevalent Genome-Wide Cancer Configuration Driven by Distinct Gene Mutations. *Cancer Cell*, *34*(2), 197-210.e5. https://doi.org/10.1016/j.ccell.2018.06.008

Menghi, F., Inaki, K., Woo, X., Kumar, P. A., Grzeda, K. R., Malhotra, A., Yadav, V., Kim, H., Marquez, E. J., Ucar, D., Shreckengast, P. T., Wagner, J. P., MacIntyre, G., Murthy Karuturi, K. R., Scully, R., Keck, J., Chuang, J. H., & Liu, E. T. (2016). The tandem duplicator phenotype as a distinct genomic configuration in cancer. *Proceedings of the National Academy of Sciences*, *113*(17), E2373–E2382. https://doi.org/10.1073/pnas.1520010113

Mian, O. Y., Khattab, M. H., Hedayati, M., Coulter, J., Abubaker-Sharif, B., Schwaninger, J. M., Veeraswamy, R. K., Brooks, J. D., Hopkins, L., Shinohara, D. B., Cornblatt, B., Nelson, W. G., Yegnasubramanian, S., & DeWeese, T. L. (2016). GSTP1 Loss results in accumulation of oxidative DNA base damage and promotes prostate cancer cell survival following exposure to protracted oxidative stress. *The Prostate*, *76*(2), 199–206. https://doi.org/10.1002/pros.23111

Miller, K. A., Degan, S., Wang, Y., Cohen, J., Ku, S. Y., Goodrich, D. W., & Gelman, I. H. (2024). PTEN-regulated PI3K-p110 and AKT isoform plasticity controls metastatic prostate cancer progression. *Oncogene*, *43*(1), 22–34. https://doi.org/10.1038/s41388-023-02875-4

Min, J., Zaslavsky, A., Fedele, G., McLaughlin, S. K., Reczek, E. E., De Raedt, T., Guney, I., Strochlic, D. E., Macconaill, L. E., Beroukhim, R., Bronson, R. T., Ryeom, S., Hahn, W. C., Loda, M., & Cichowski, K. (2010). An oncogene-tumor suppressor cascade drives metastatic prostate cancer by coordinately activating Ras and nuclear factor-kappaB. *Nature Medicine*, *16*(3), 286–294. https://doi.org/10.1038/nm.2100

Mishra, R., Haldar, S., Placencio, V., Madhav, A., Rohena-Rivera, K., Agarwal, P., Duong, F., Angara, B., Tripathi, M., Liu, Z., Gottlieb, R. A., Wagner, S., Posadas, E. M., & Bhowmick, N. A. (2018). Stromal epigenetic alterations drive metabolic and neuroendocrine prostate cancer reprogramming. *The Journal of Clinical Investigation*, *128*(10), 4472–4484. https://doi.org/10.1172/JCI99397

Moilanen, A.-M., Riikonen, R., Oksala, R., Ravanti, L., Aho, E., Wohlfahrt, G., Nykänen, P. S., Törmäkangas, O. P., Palvimo, J. J., & Kallio, P. J. (2015). Discovery of ODM-201, a new-generation androgen receptor inhibitor targeting resistance mechanisms to androgen signaling-directed prostate cancer therapies. *Scientific Reports*, *5*, 12007. https://doi.org/10.1038/srep12007

Montironi, R., Mazzucchelli, R., & Scarpelli, M. (2002). Precancerous lesions and conditions of the prostate: From morphological and biological characterization to chemoprevention. *Annals of the New York Academy of Sciences*, *963*, 169–184. https://doi.org/10.1111/j.1749-6632.2002.tb04108.x

Moore, K., Colombo, N., Scambia, G., Kim, B.-G., Oaknin, A., Friedlander, M., Lisyanskaya, A., Floquet, A., Leary, A., Sonke, G. S., Gourley, C., Banerjee, S., Oza, A., González-Martín, A., Aghajanian, C., Bradley, W., Mathews, C., Liu, J., Lowe, E. S., … DiSilvestro, P. (2018). Maintenance Olaparib in Patients with Newly Diagnosed Advanced Ovarian Cancer. *The New England Journal of Medicine*, *379*(26), 2495–2505. https://doi.org/10.1056/NEJMoa1810858

Morel, A.-P., Lièvre, M., Thomas, C., Hinkal, G., Ansieau, S., & Puisieux, A. (2008). Generation of breast cancer stem cells through epithelial-mesenchymal transition. *PloS One*, *3*(8), e2888. https://doi.org/10.1371/journal.pone.0002888

Morris, M. J., Corey, E., Guise, T. A., Gulley, J. L., Kevin Kelly, W., Quinn, D. I., Scholz, A., & Sgouros, G. (2019). Radium-223 mechanism of action: Implications for use in treatment combinations. *Nature Reviews. Urology*, *16*(12), 745–756. https://doi.org/10.1038/s41585-019-0251-x

Moser, S. C., & Jonkers, J. (2025). Thirty Years of BRCA1: Mechanistic Insights and Their Impact on Mutation Carriers. *Cancer Discovery*, *15*(3), 461–480. https://doi.org/10.1158/2159-8290.CD-24-1326

Mosquera, J. M., Beltran, H., Park, K., MacDonald, T. Y., Robinson, B. D., Tagawa, S. T., Perner, S., Bismar, T. A., Erbersdobler, A., Dhir, R., Nelson, J. B., Nanus, D. M., & Rubin, M. A. (2013). Concurrent AURKA and MYCN gene amplifications are harbingers of lethal treatment-related neuroendocrine prostate cancer. *Neoplasia (New York, N.Y.)*, *15*(1), 1–10. https://doi.org/10.1593/neo.121550

Mottet, N., van den Bergh, R. C. N., Briers, E., Van den Broeck, T., Cumberbatch, M. G., De Santis, M., Fanti, S., Fossati, N., Gandaglia, G., Gillessen, S., Grivas, N., Grummet, J., Henry, A. M., van der Kwast, T. H., Lam, T. B., Lardas, M., Liew, M., Mason, M. D., Moris, L., … Cornford, P. (2021). EAU-EANM-ESTRO-ESUR-SIOG Guidelines on Prostate Cancer-2020 Update. Part 1: Screening, Diagnosis, and Local Treatment with Curative Intent. *European Urology*, *79*(2), 243–262. https://doi.org/10.1016/j.eururo.2020.09.042

Mu, P., Zhang, Z., Benelli, M., Karthaus, W. R., Hoover, E., Chen, C.-C., Wongvipat, J., Ku, S.-Y., Gao, D., Cao, Z., Shah, N., Adams, E. J., Abida, W., Watson, P. A., Prandi, D., Huang, C.-H., de Stanchina, E., Lowe, S. W., Ellis, L., … Sawyers, C. L. (2017). SOX2 promotes lineage plasticity and antiandrogen resistance in TP53- and RB1-deficient prostate cancer. *Science (New York, N.Y.)*, *355*(6320), 84–88. https://doi.org/10.1126/science.aah4307

Mucci, L. A., Hjelmborg, J. B., Harris, J. R., Czene, K., Havelick, D. J., Scheike, T., Graff, R. E., Holst, K., Möller, S., Unger, R. H., McIntosh, C., Nuttall, E., Brandt, I., Penney, K. L., Hartman, M., Kraft, P., Parmigiani, G., Christensen, K., Koskenvuo, M., … Nordic Twin Study of Cancer (NorTwinCan) Collaboration. (2016). Familial Risk and Heritability of Cancer Among Twins in Nordic Countries. *JAMA*, *315*(1), 68–76. https://doi.org/10.1001/jama.2015.17703

Mukherjee, D., Previs, R. A., Haines, C., Al Abo, M., Juras, P. K., Strickland, K. C., Chakraborty, B., Artham, S., Whitaker, R. S., Hebert, K., Fontenot, J., Patierno, S. R., Freedman, J. A., Lau, F. H., Burow, M. E., Chang, C.-Y., & McDonnell, D. P. (2023). Targeting CaMKK2 Inhibits Actin Cytoskeletal Assembly to Suppress Cancer Metastasis. *Cancer Research*, *83*(17), 2889–2907. https://doi.org/10.1158/0008-5472.CAN-22-1622

Mukherjee, R., Bartlett, J. M. S., Krishna, N. S., Underwood, M. A., & Edwards, J. (2005). Raf-1 expression may influence progression to androgen insensitive prostate cancer. *The Prostate*, *64*(1), 101–107. https://doi.org/10.1002/pros.20211

Mulholland, D. J., Tran, L. M., Li, Y., Cai, H., Morim, A., Wang, S., Plaisier, S., Garraway, I. P., Huang, J., Graeber, T. G., & Wu, H. (2011). Cell autonomous role of PTEN in regulating castration-resistant prostate cancer growth. *Cancer Cell*, *19*(6), 792–804. https://doi.org/10.1016/j.ccr.2011.05.006

Nacerddine, K., Beaudry, J.-B., Ginjala, V., Westerman, B., Mattiroli, F., Song, J.-Y., Poel, H. van der, Ponz, O. B., Pritchard, C., Cornelissen-Steijger, P., Zevenhoven, J., Tanger, E., Sixma, T. K., Ganesan, S., & Lohuizen, M. van. (2012). Akt-mediated phosphorylation of Bmi1 modulates its

oncogenic potential, E3 ligase activity, and DNA damage repair activity in mouse prostate cancer. *The Journal of Clinical Investigation*, *122*(5), 1920–1932. https://doi.org/10.1172/JCI57477

Narayan, V., Barber-Rotenberg, J. S., Jung, I.-Y., Lacey, S. F., Rech, A. J., Davis, M. M., Hwang, W.-T., Lal, P., Carpenter, E. L., Maude, S. L., Plesa, G., Vapiwala, N., Chew, A., Moniak, M., Sebro, R. A., Farwell, M. D., Marshall, A., Gilmore, J., Lledo, L., … Haas, N. B. (2022). PSMA-targeting TGFβ-insensitive armored CAR T cells in metastatic castration-resistant prostate cancer: A phase 1 trial. *Nature Medicine*, *28*(4), 724–734. https://doi.org/10.1038/s41591-022-01726-1

Narumiya, S., Tanji, M., & Ishizaki, T. (2009). Rho signaling, ROCK and mDia1, in transformation, metastasis and invasion. *Cancer Metastasis Reviews*, *28*(1–2), 65–76. https://doi.org/10.1007/s10555-008-9170-7

Naxerova, K. (2025). Evolutionary paths towards metastasis. *Nature Reviews. Cancer*, *25*(7), 545–560. https://doi.org/10.1038/s41568-025-00814-x

Neklesa, T., Snyder, L. B., Willard, R. R., Vitale, N., Pizzano, J., Gordon, D. A., Bookbinder, M., Macaluso, J., Dong, H., Ferraro, C., Wang, G., Wang, J., Crews, C. M., Houston, J., Crew, A. P., & Taylor, I. (2019). ARV-110: An oral androgen receptor PROTAC degrader for prostate cancer. *Journal of Clinical Oncology*, *37*(7_suppl), 259–259. https://doi.org/10.1200/JCO.2019.37.7_suppl.259

Nguyen, B., Fong, C., Luthra, A., Smith, S. A., DiNatale, R. G., Nandakumar, S., Walch, H., Chatila, W. K., Madupuri, R., Kundra, R., Bielski, C. M., Mastrogiacomo, B., Donoghue, M. T. A., Boire, A., Chandarlapaty, S., Ganesh, K., Harding, J. J., Iacobuzio-Donahue, C. A., Razavi, P., … Schultz, N. (2022). Genomic characterization of metastatic patterns from prospective clinical sequencing of 25,000 patients. *Cell*, *185*(3), 563-575.e11. https://doi.org/10.1016/j.cell.2022.01.003

Nguyen, C. B., Reimers, M. A., Perera, C., Abida, W., Chou, J., Feng, F. Y., Antonarakis, E. S., McKay, R. R., Pachynski, R. K., Zhang, J., Reichert, Z. R., Palmbos, P. L., Caram, M. E. V., Vaishampayan, U. N., Heath, E. I., Hopkins, A. C., Cieslik, M. P., Wu, Y.-M., Robinson, D. R., … Alva, A. S. (2024). Evaluating Immune Checkpoint Blockade in Metastatic Castration-Resistant Prostate Cancers with Deleterious CDK12 Alterations in the Phase 2 IMPACT Trial. *Clinical Cancer Research*, *30*(15), 3200–3210. https://doi.org/10.1158/1078-0432.CCR-24-0400

Nguyen, L. T., Tretiakova, M. S., Silvis, M. R., Lucas, J., Klezovitch, O., Coleman, I., Bolouri, H., Kutyavin, V. I., Morrissey, C., True, L. D., Nelson, P. S., & Vasioukhin, V. (2015). ERG Activates the YAP1 Transcriptional Program and Induces the Development of Age-Related Prostate Tumors. *Cancer Cell*, *27*(6), 797–808. https://doi.org/10.1016/j.ccell.2015.05.005

Nguyen, L., W. M. Martens, J., Van Hoeck, A., & Cuppen, E. (2020). Pan-cancer landscape of homologous recombination deficiency. *Nature Communications*, *11*(1), 5584. https://doi.org/10.1038/s41467-020-19406-4

Nickerson, M., Das, S., Im, K., Turan, S., Berndt, S., Li, H., Lou, H., Brodie, S., Billaud, J., Zhang, T., Bouk, A., Butcher, D., Wang, Z., Sun, L., Misner, K., Tan, W., Esnakula, A., Esposito, D., Huang, W., … Andresson, T. (2017). TET2 binds the androgen receptor and loss is associated with prostate cancer. *Oncogene*, *36*(15), 2172–2183. https://doi.org/10.1038/onc.2016.376

Nickols, N. G., Nazarian, R., Zhao, S. G., Tan, V., Uzunangelov, V., Xia, Z., Baertsch, R., Neeman, E., Gao, A. C., Thomas, G. V., Howard, L., De Hoedt, A. M., Stuart, J., Goldstein, T., Chi, K., Gleave, M. E., Graff, J. N., Beer, T. M., Drake, J. M., … Rettig, M. B. (2019). MEK-ERK signaling is a therapeutic target in metastatic castration resistant prostate cancer. *Prostate Cancer and Prostatic Diseases*, *22*(4), 531–538. https://doi.org/10.1038/s41391-019-0134-5

Nicolosi, P., Ledet, E., Yang, S., Michalski, S., Freschi, B., O'Leary, E., Esplin, E. D., Nussbaum, R. L., & Sartor, O. (2019). Prevalence of Germline Variants in Prostate Cancer and Implications for Current Genetic Testing Guidelines. *JAMA Oncology*, *5*(4), 523–528. https://doi.org/10.1001/jamaoncol.2018.6760

Nie, S., Kee, Y., & Bronner-Fraser, M. (2011). Caldesmon regulates actin dynamics to influence cranial neural crest migration in Xenopus. *Molecular Biology of the Cell*, *22*(18), 3355–3365. https://doi.org/10.1091/mbc.E11-02-0165

Nientiedt, C., Endris, V., Jenzer, M., Mansour, J., Sedehi, N. T. P., Pecqueux, C., Volckmar, A.-L., Leichsenring, J., Neumann, O., Kirchner, M., Hoveida, S., Lantwin, P., Kaltenecker, K., Dieffenbacher, S., Gasch, C., Hofer, L., Franke, D., Tosev, G., Görtz, M., … Duensing, S. (2020). High prevalence of DNA damage repair gene defects and TP53 alterations in men with treatment-naïve metastatic prostate cancer -Results from a prospective pilot study using a 37 gene panel. *Urologic Oncology*, *38*(7), 637.e17-637.e27. https://doi.org/10.1016/j.urolonc.2020.03.001

Nieto, M. A., Huang, R. Y.-J., Jackson, R. A., & Thiery, J. P. (2016). EMT: 2016. *Cell*, *166*(1), 21–45. https://doi.org/10.1016/j.cell.2016.06.028

Nik-Zainal, S., Alexandrov, L. B., Wedge, D. C., Van Loo, P., Greenman, C. D., Raine, K., Jones, D., Hinton, J., Marshall, J., Stebbings, L. A., Menzies, A., Martin, S., Leung, K., Chen, L., Leroy, C., Ramakrishna, M., Rance, R., Lau, K. W., Mudie, L. J., … Breast Cancer Working Group of the International Cancer Genome Consortium. (2012). Mutational processes molding the genomes of 21 breast cancers. *Cell*, *149*(5), 979–993. https://doi.org/10.1016/j.cell.2012.04.024

Ning, Y., Zheng, M., Zhang, Y., Jiao, Y., Wang, J., & Zhang, S. (2024). RhoA-ROCK2 signaling possesses complex pathophysiological functions in cancer progression and shows promising therapeutic potential. *Cancer Cell International*, *24*(1), 339. https://doi.org/10.1186/s12935-024-03519-7

Nishiyama, T., Hashimoto, Y., & Takahashi, K. (2004). The Influence of Androgen Deprivation Therapy on Dihydrotestosterone Levels in the Prostatic Tissue of Patients with Prostate Cancer. *Clinical Cancer Research*, *10*(21), 7121–7126. https://doi.org/10.1158/1078-0432.CCR-04-0913

Norris, J. D., Chang, C.-Y., Wittmann, B. M., Kunder, R. S., Cui, H., Fan, D., Joseph, J. D., & McDonnell, D. P. (2009). The homeodomain protein HOXB13 regulates the cellular response to androgens. *Molecular Cell*, *36*(3), 405–416. https://doi.org/10.1016/j.molcel.2009.10.020

Nowell, P. C. (1976). The clonal evolution of tumor cell populations. *Science (New York, N.Y.)*, *194*(4260), 23–28. https://doi.org/10.1126/science.959840

Nurmagambetova, A., Mustyatsa, V., Saidova, A., & Vorobjev, I. (2023). Morphological and cytoskeleton changes in cells after EMT. *Scientific Reports*, *13*(1), 22164. https://doi.org/10.1038/s41598-023-48279-y

Nyberg, T., Frost, D., Barrowdale, D., Evans, D. G., Bancroft, E., Adlard, J., Ahmed, M., Barwell, J., Brady, A. F., Brewer, C., Cook, J., Davidson, R., Donaldson, A., Eason, J., Gregory, H., Henderson, A., Izatt, L., Kennedy, M. J., Miller, C., … Antoniou, A. C. (2020). Prostate Cancer Risks for Male BRCA1 and BRCA2 Mutation Carriers: A Prospective Cohort Study. *European Urology*, *77*(1), 24–35. https://doi.org/10.1016/j.eururo.2019.08.025

Nyquist, M. D., Corella, A., Coleman, I., De Sarkar, N., Kaipainen, A., Ha, G., Gulati, R., Ang, L., Chatterjee, P., Lucas, J., Pritchard, C., Risbridger, G., Isaacs, J., Montgomery, B., Morrissey, C., Corey, E., & Nelson, P. S. (2020). Combined TP53 and RB1 Loss Promotes Prostate Cancer Resistance to a Spectrum of Therapeutics and Confers Vulnerability to Replication Stress. *Cell Reports*, *31*(8), 107669. https://doi.org/10.1016/j.celrep.2020.107669

Olson, A., Le, V., Aldahl, J., Yu, E.-J., Hooker, E., He, Y., Lee, D.-H., Kim, W. K., Cardiff, R. D., Geradts, J., & Sun, Z. (2019). The comprehensive role of E-cadherin in maintaining prostatic epithelial integrity during oncogenic transformation and tumor progression. *PLOS Genetics*, *15*(10), e1008451. https://doi.org/10.1371/journal.pgen.1008451

Pakula, H., Omar, M., Carelli, R., Pederzoli, F., Fanelli, G. N., Pannellini, T., Socciarelli, F., Van Emmenis, L., Rodrigues, S., Fidalgo-Ribeiro, C., Nuzzo, P. V., Brady, N. J., Dinalankara, W., Jere, M., Valencia, I., Saladino, C., Stone, J., Unkenholz, C., Garner, R., … Loda, M. (2024). Distinct mesenchymal cell states mediate prostate cancer progression. *Nature Communications*, *15*(1), 363. https://doi.org/10.1038/s41467-023-44210-1

Palanisamy, N., Ateeq, B., Kalyana-Sundaram, S., Pflueger, D., Ramnarayanan, K., Shankar, S., Han, B., Cao, Q., Cao, X., Suleman, K., Kumar-Sinha, C., Dhanasekaran, S. M., Chen, Y., Esgueva, R., Banerjee, S., LaFargue, C. J., Siddiqui, J., Demichelis, F., Moeller, P., … Chinnaiyan, A. M.

(2010). Rearrangements of the RAF kinase pathway in prostate cancer, gastric cancer and melanoma. *Nature Medicine*, *16*(7), 793–798. https://doi.org/10.1038/nm.2166

Pantelidou, C., Sonzogni, O., De Oliveria Taveira, M., Mehta, A. K., Kothari, A., Wang, D., Visal, T., Li, M. K., Pinto, J., Castrillon, J. A., Cheney, E. M., Bouwman, P., Jonkers, J., Rottenberg, S., Guerriero, J. L., Wulf, G. M., & Shapiro, G. I. (2019). PARP Inhibitor Efficacy Depends on CD8+ T-cell Recruitment via Intratumoral STING Pathway Activation in BRCA-Deficient Models of Triple-Negative Breast Cancer. *Cancer Discovery*, *9*(6), 722–737. https://doi.org/10.1158/2159-8290.CD-18-1218

Parker, C., Nilsson, S., Heinrich, D., Helle, S. I., O'Sullivan, J. M., Fosså, S. D., Chodacki, A., Wiechno, P., Logue, J., Seke, M., Widmark, A., Johannessen, D. C., Hoskin, P., Bottomley, D., James, N. D., Solberg, A., Syndikus, I., Kliment, J., Wedel, S., … ALSYMPCA Investigators. (2013). Alpha emitter radium-223 and survival in metastatic prostate cancer. *The New England Journal of Medicine*, *369*(3), 213–223. https://doi.org/10.1056/NEJMoa1213755

Parkes, E. E., Walker, S. M., Taggart, L. E., McCabe, N., Knight, L. A., Wilkinson, R., McCloskey, K. D., Buckley, N. E., Savage, K. I., Salto-Tellez, M., McQuaid, S., Harte, M. T., Mullan, P. B., Harkin, D. P., & Kennedy, R. D. (2017). Activation of STING-Dependent Innate Immune Signaling By S-Phase-Specific DNA Damage in Breast Cancer. *Journal of the National Cancer Institute*, *109*(1), djw199. https://doi.org/10.1093/jnci/djw199

Parolia, A., Eyunni, S., Verma, B. K., Young, E., Liu, Y., Liu, L., George, J., Aras, S., Das, C. K., Mannan, R., Ur Rasool, R., Mitchell-Velasquez, E., Mahapatra, S., Luo, J., Carson, S. E., Xiao, L., Gajjala, P. R., Venkatesh, S., Jaber, M., … Asangani, I. A. (2024). NSD2 is a requisite subunit of the AR/FOXA1 neo-enhanceosome in promoting prostate tumorigenesis. *Nature Genetics*, *56*(10), 2132–2143. https://doi.org/10.1038/s41588-024-01893-6

Penfold, L., Woods, A., Muckett, P., Nikitin, A. Y., Kent, T. R., Zhang, S., Graham, R., Pollard, A., & Carling, D. (2018). CAMKK2 Promotes Prostate Cancer Independently of AMPK via Increased Lipogenesis. *Cancer Research*, *78*(24), 6747–6761. https://doi.org/10.1158/0008-5472.CAN-18-0585

Pereira-Veiga, T., Schneegans, S., Pantel, K., & Wikman, H. (2022). Circulating tumor cell-blood cell crosstalk: Biology and clinical relevance. *Cell Reports*, *40*(9), 111298. https://doi.org/10.1016/j.celrep.2022.111298

Pertega-Gomes, N., Felisbino, S., Massie, C. E., Vizcaino, J. R., Coelho, R., Sandi, C., Simoes-Sousa, S., Jurmeister, S., Ramos-Montoya, A., Asim, M., Tran, M., Oliveira, E., Lobo da Cunha, A., Maximo, V., Baltazar, F., Neal, D. E., & Fryer, L. G. D. (2015). A glycolytic phenotype is associated with prostate cancer progression and aggressiveness: A role for monocarboxylate transporters as metabolic targets for therapy. *The Journal of Pathology*, *236*(4), 517–530. https://doi.org/10.1002/path.4547

Ploussard, G., Manceau, C., Beauval, J.-B., Lesourd, M., Almeras, C., Gautier, J.-R., Loison, G., Salin, A., Soulié, M., Tollon, C., Malavaud, B., & Roumiguié, M. (2020). Decreased accuracy of the prostate cancer EAU risk group classification in the era of imaging-guided diagnostic pathway: Proposal for a new classification based on MRI-targeted biopsies and early oncologic outcomes after surgery. *World Journal of Urology*, *38*(10), 2493–2500. https://doi.org/10.1007/s00345-019-03053-6

Plym, A., Zhang, Y., Stopsack, K. H., Ugalde-Morales, E., Seibert, T. M., Conti, D. V., Haiman, C. A., Baras, A., Stocks, T., Drake, I., Penney, K. L., Giovannucci, E., Kibel, A. S., Wiklund, F., & Mucci, L. A. (2024). Early Prostate Cancer Deaths Among Men With Higher vs Lower Genetic Risk. *JAMA Network Open*, *7*(7), e2420034. https://doi.org/10.1001/jamanetworkopen.2024.20034

Polkinghorn, W. R., Parker, J. S., Lee, M. X., Kass, E. M., Spratt, D. E., Iaquinta, P. J., Arora, V. K., Yen, W.-F., Cai, L., Zheng, D., Carver, B. S., Chen, Y., Watson, P. A., Shah, N. P., Fujisawa, S., Goglia, A. G., Gopalan, A., Hieronymus, H., Wongvipat, J., … Sawyers, C. L. (2013). Androgen receptor signaling regulates DNA repair in prostate cancers. *Cancer Discovery*, *3*(11), 1245–1253. https://doi.org/10.1158/2159-8290.CD-13-0172

Pollard, T. D. (2016). Actin and Actin-Binding Proteins. *Cold Spring Harbor Perspectives in Biology*, *8*(8), a018226. https://doi.org/10.1101/cshperspect.a018226

Pound, C. R., Partin, A. W., Eisenberger, M. A., Chan, D. W., Pearson, J. D., & Walsh, P. C. (1999). Natural history of progression after PSA elevation following radical prostatectomy. *JAMA*, *281*(17), 1591–1597. https://doi.org/10.1001/jama.281.17.1591

Pritchard, C. C., Mateo, J., Walsh, M. F., De Sarkar, N., Abida, W., Beltran, H., Garofalo, A., Gulati, R., Carreira, S., Eeles, R., Elemento, O., Rubin, M. A., Robinson, D., Lonigro, R., Hussain, M., Chinnaiyan, A., Vinson, J., Filipenko, J., Garraway, L., … Nelson, P. S. (2016). Inherited DNA-Repair Gene Mutations in Men with Metastatic Prostate Cancer. *The New England Journal of Medicine*, *375*(5), 443–453. https://doi.org/10.1056/NEJMoa1603144

Puhr, M., Hoefer, J., Eigentler, A., Ploner, C., Handle, F., Schaefer, G., Kroon, J., Leo, A., Heidegger, I., Eder, I., Culig, Z., Van der Pluijm, G., & Klocker, H. (2018). The Glucocorticoid Receptor Is a Key Player for Prostate Cancer Cell Survival and a Target for Improved Antiandrogen Therapy. *Clinical Cancer Research: An Official Journal of the American Association for Cancer Research*, *24*(4), 927–938. https://doi.org/10.1158/1078-0432.CCR-17-0989

Pujana-Vaquerizo, M., Bozal-Basterra, L., & Carracedo, A. (2024). Metabolic adaptations in prostate cancer. *British Journal of Cancer*, *131*(8), 1250–1262. https://doi.org/10.1038/s41416-024-02762-z

Pütz, S., Barthel, L. S., Frohn, M., Metzler, D., Barham, M., Pryymachuk, G., Trunschke, O., Lubomirov, L. T., Hescheler, J., Chalovich, J. M., Neiss, W. F., Koch, M., Schroeter, M. M., & Pfitzer, G. (2021). Caldesmon ablation in mice causes umbilical herniation and alters contractility of fetal urinary bladder smooth muscle. *The Journal of General Physiology*, *153*(7), e202012776. https://doi.org/10.1085/jgp.202012776

Putzke, A. P., Ventura, A. P., Bailey, A. M., Akture, C., Opoku-Ansah, J., Celiktaş, M., Hwang, M. S., Darling, D. S., Coleman, I. M., Nelson, P. S., Nguyen, H. M., Corey, E., Tewari, M., Morrissey, C., Vessella, R. L., & Knudsen, B. S. (2011). Metastatic progression of prostate cancer and e-cadherin regulation by zeb1 and SRC family kinases. *The American Journal of Pathology*, *179*(1), 400–410. https://doi.org/10.1016/j.ajpath.2011.03.028

Qiu, X., Boufaied, N., Hallal, T., Feit, A., de Polo, A., Luoma, A. M., Alahmadi, W., Larocque, J., Zadra, G., Xie, Y., Gu, S., Tang, Q., Zhang, Y., Syamala, S., Seo, J.-H., Bell, C., O'Connor, E., Liu, Y., Schaeffer, E. M., … Labbé, D. P. (2022). MYC drives aggressive prostate cancer by disrupting transcriptional pause release at androgen receptor targets. *Nature Communications*, *13*(1), 2559. https://doi.org/10.1038/s41467-022-30257-z

Quigley, D. A., Dang, H. X., Zhao, S. G., Lloyd, P., Aggarwal, R., Alumkal, J. J., Foye, A., Kothari, V., Perry, M. D., Bailey, A. M., Playdle, D., Barnard, T. J., Zhang, L., Zhang, J., Youngren, J. F., Cieslik, M. P., Parolia, A., Beer, T. M., Thomas, G., … Feng, F. Y. (2018). Genomic Hallmarks and Structural Variation in Metastatic Prostate Cancer. *Cell*, *174*(3), 758-769.e9. https://doi.org/10.1016/j.cell.2018.06.039

Randazzo, M., Müller, A., Carlsson, S., Eberli, D., Huber, A., Grobholz, R., Manka, L., Mortezavi, A., Sulser, T., Recker, F., & Kwiatkowski, M. (2016). A positive family history as a risk factor for prostate cancer in a population-based study with organised prostate-specific antigen screening: Results of the Swiss European Randomised Study of Screening for Prostate Cancer (ERSPC, Aarau). *BJU International*, *117*(4), 576–583. https://doi.org/10.1111/bju.13310

Räsänen, K., Itkonen, O., Koistinen, H., & Stenman, U.-H. (2016). Emerging Roles of SPINK1 in Cancer. *Clinical Chemistry*, *62*(3), 449–457. https://doi.org/10.1373/clinchem.2015.241513

Rasmussen-Torvik, L. J., Shay, C. M., Abramson, J. G., Friedrich, C. A., Nettleton, J. A., Prizment, A. E., & Folsom, A. R. (2013). Ideal cardiovascular health is inversely associated with incident cancer: The Atherosclerosis Risk In Communities study. *Circulation*, *127*(12), 1270–1275. https://doi.org/10.1161/CIRCULATIONAHA.112.001183

Rathkopf, D. E., Patel, M. R., Choudhury, A. D., Rasco, D., Lakhani, N., Hawley, J. E., Srinivas, S., Aparicio, A., Narayan, V., Runcie, K. D., Emamekhoo, H., Reichert, Z. R., Nguyen, M. H., Wells,

A. L., Kandimalla, R., Liu, C., Suryawanshi, S., Han, J., Wu, J., … Armstrong, A. J. (2025). Safety and clinical activity of BMS-986365 (CC-94676), a dual androgen receptor ligand-directed degrader and antagonist, in heavily pretreated patients with metastatic castration-resistant prostate cancer. *Annals of Oncology: Official Journal of the European Society for Medical Oncology*, *36*(1), 76–88. https://doi.org/10.1016/j.annonc.2024.09.005

Rebello, R. J., Oing, C., Gillessen, S., & Bristow, R. G. (2019). TP53 and Prognosis in mCRPC Survival: Biology or Coincidence? *Clinical Cancer Research: An Official Journal of the American Association for Cancer Research*, *25*(6), 1699–1701. https://doi.org/10.1158/1078-0432.CCR-18-3401

Rebello, R. J., Oing, C., Knudsen, K. E., Loeb, S., Johnson, D. C., Reiter, R. E., Gillessen, S., Van der Kwast, T., & Bristow, R. G. (2021). Prostate cancer. *Nature Reviews. Disease Primers*, *7*(1), 9. https://doi.org/10.1038/s41572-020-00243-0

Rescigno, P., Porta, N., Finneran, L., Riisnaes, R., Figueiredo, I., Carreira, S., Flohr, P., Miranda, S., Bertan, C., Ferreira, A., Crespo, M., Rodrigues, D. N., Gurel, B., Nobes, J., Crabb, S., Malik, Z., Ralph, C., McGovern, U., Hoskin, P., … de Bono, J. (2024). Capivasertib in combination with enzalutamide for metastatic castration resistant prostate cancer after docetaxel and abiraterone: Results from the randomized phase II RE-AKT trial. *European Journal of Cancer*, *205*, 114103. https://doi.org/10.1016/j.ejca.2024.114103

Ricciardelli, C., Choong, C. S., Buchanan, G., Vivekanandan, S., Neufing, P., Stahl, J., Marshall, V. R., Horsfall, D. J., & Tilley, W. D. (2005). Androgen receptor levels in prostate cancer epithelial and peritumoral stromal cells identify non-organ confined disease. *The Prostate*, *63*(1), 19–28. https://doi.org/10.1002/pros.20154

Riihimäki, M., Thomsen, H., Sundquist, K., Sundquist, J., & Hemminki, K. (2018). Clinical landscape of cancer metastases. *Cancer Medicine*, *7*(11), 5534–5542. https://doi.org/10.1002/cam4.1697

Robinson, D., Van Allen, E. M., Wu, Y.-M., Schultz, N., Lonigro, R. J., Mosquera, J.-M., Montgomery, B., Taplin, M.-E., Pritchard, C. C., Attard, G., Beltran, H., Abida, W., Bradley, R. K., Vinson, J., Cao, X., Vats, P., Kunju, L. P., Hussain, M., Feng, F. Y., … Chinnaiyan, A. M. (2015). Integrative clinical genomics of advanced prostate cancer. *Cell*, *161*(5), 1215–1228. https://doi.org/10.1016/j.cell.2015.05.001

Rodrigues, D. N., Rescigno, P., Liu, D., Yuan, W., Carreira, S., Lambros, M. B., Seed, G., Mateo, J., Riisnaes, R., Mullane, S., Margolis, C., Miao, D., Miranda, S., Dolling, D., Clarke, M., Bertan, C., Crespo, M., Boysen, G., Ferreira, A., … de Bono, J. S. (2018). Immunogenomic analyses associate immunological alterations with mismatch repair defects in prostate cancer. *The Journal of Clinical Investigation*, *128*(10), 4441–4453. https://doi.org/10.1172/JCI121924

Rogakou, E. P., Boon, C., Redon, C., & Bonner, W. M. (1999). Megabase chromatin domains involved in DNA double-strand breaks in vivo. *The Journal of Cell Biology*, *146*(5), 905–916. https://doi.org/10.1083/jcb.146.5.905

Rogakou, E. P., Pilch, D. R., Orr, A. H., Ivanova, V. S., & Bonner, W. M. (1998). DNA double-stranded breaks induce histone H2AX phosphorylation on serine 139. *The Journal of Biological Chemistry*, *273*(10), 5858–5868. https://doi.org/10.1074/jbc.273.10.5858

Rojo de la Vega, M., Chapman, E., & Zhang, D. D. (2018). NRF2 and the Hallmarks of Cancer. *Cancer Cell*, *34*(1), 21–43. https://doi.org/10.1016/j.ccell.2018.03.022

Romero, R., Chu, T., González Robles, T. J., Smith, P., Xie, Y., Kaur, H., Yoder, S., Zhao, H., Mao, C., Kang, W., Pulina, M. V., Lawrence, K. E., Gopalan, A., Zaidi, S., Yoo, K., Choi, J., Fan, N., Gerstner, O., Karthaus, W. R., … Sawyers, C. L. (2024). The neuroendocrine transition in prostate cancer is dynamic and dependent on ASCL1. *Nature Cancer*, *5*(11), 1641–1659. https://doi.org/10.1038/s43018-024-00838-6

Rotinen, M., You, S., Yang, J., Coetzee, S. G., Reis-Sobreiro, M., Huang, W.-C., Huang, F., Pan, X., Yáñez, A., Hazelett, D. J., Chu, C.-Y., Steadman, K., Morrissey, C. M., Nelson, P. S., Corey, E., Chung, L. W. K., Freedland, S. J., Di Vizio, D., Garraway, I. P., … Freeman, M. R. (2018).

ONECUT2 is a targetable master regulator of lethal prostate cancer that suppresses the androgen axis. *Nature Medicine*, *24*(12), 1887–1898. https://doi.org/10.1038/s41591-018-0241-1

Roy, R., Chun, J., & Powell, S. N. (2011). BRCA1 and BRCA2: Different roles in a common pathway of genome protection. *Nature Reviews. Cancer*, *12*(1), 68–78. https://doi.org/10.1038/nrc3181

Russo, G. I., Asmundo, M. G., Lo Giudice, A., Trefiletti, G., Cimino, S., Ferro, M., Lombardo, R., De Nunzio, C., Morgia, G., Piombino, E., Failla, M., Caltabiano, R., & Broggi, G. (2023). Is There a Role of Warburg Effect in Prostate Cancer Aggressiveness? Analysis of Expression of Enzymes of Lipidic Metabolism by Immunohistochemistry in Prostate Cancer Patients (DIAMOND Study). *Cancers*, *15*(3), 948. https://doi.org/10.3390/cancers15030948

Ruzanov, P., Evdokimova, V., Pachva, M. C., Minkovich, A., Zhang, Z., Langman, S., Gassmann, H., Thiel, U., Orlic-Milacic, M., Zaidi, S. H., Peltekova, V., Heisler, L. E., Sharma, M., Cox, M. E., McKee, T. D., Zaidi, M., Lapouble, E., McPherson, J. D., Delattre, O., … Sorensen, P. H. (2024). Oncogenic ETS fusions promote DNA damage and proinflammatory responses via pericentromeric RNAs in extracellular vesicles. *The Journal of Clinical Investigation*, *134*(9), e169470. https://doi.org/10.1172/JCI169470

Rybkowska, P., Radoszkiewicz, K., Kawalec, M., Dymkowska, D., Zabłocka, B., Zabłocki, K., & Sarnowska, A. (2023). The Metabolic Changes between Monolayer (2D) and Three-Dimensional (3D) Culture Conditions in Human Mesenchymal Stem/Stromal Cells Derived from Adipose Tissue. *Cells*, *12*(1), 178. https://doi.org/10.3390/cells12010178

Saad, F., Clarke, N. W., Oya, M., Shore, N., Procopio, G., Guedes, J. D., Arslan, C., Mehra, N., Parnis, F., Brown, E., Schlürmann, F., Joung, J. Y., Sugimoto, M., Sartor, O., Liu, Y.-Z., Poehlein, C., Barker, L., Del Rosario, P. M., & Armstrong, A. J. (2023). Olaparib plus abiraterone versus placebo plus abiraterone in metastatic castration-resistant prostate cancer (PROpel): Final prespecified overall survival results of a randomised, double-blind, phase 3 trial. *The Lancet. Oncology*, *24*(10), 1094–1108. https://doi.org/10.1016/S1470-2045(23)00382-0

Sahu, B., Laakso, M., Ovaska, K., Mirtti, T., Lundin, J., Rannikko, A., Sankila, A., Turunen, J.-P., Lundin, M., Konsti, J., Vesterinen, T., Nordling, S., Kallioniemi, O., Hautaniemi, S., & Jänne, O. A. (2011). Dual role of FoxA1 in androgen receptor binding to chromatin, androgen signalling and prostate cancer. *The EMBO Journal*, *30*(19), 3962–3976. https://doi.org/10.1038/emboj.2011.328

Savage, K. I., & Harkin, D. P. (2015). BRCA1, a "complex" protein involved in the maintenance of genomic stability. *The FEBS Journal*, *282*(4), 630–646. https://doi.org/10.1111/febs.13150

Schellhammer, P. F., el-Mahdi, A. M., Wright, G. L., Kolm, P., & Ragle, R. (1993). Prostate-specific antigen to determine progression-free survival after radiation therapy for localized carcinoma of prostate. *Urology*, *42*(1), 13–20. https://doi.org/10.1016/0090-4295(93)90325-5

Schröder, F. H., van der Maas, P., Beemsterboer, P., Kruger, A. B., Hoedemaeker, R., Rietbergen, J., & Kranse, R. (1998). Evaluation of the digital rectal examination as a screening test for prostate cancer. Rotterdam section of the European Randomized Study of Screening for Prostate Cancer. *Journal of the National Cancer Institute*, *90*(23), 1817–1823. https://doi.org/10.1093/jnci/90.23.1817

Schwappacher, R., Rangaswami, H., Su-Yuo, J., Hassad, A., Spitler, R., & Casteel, D. E. (2013). cGMP-dependent protein kinase Iβ regulates breast cancer cell migration and invasion via interaction with the actin/myosin-associated protein caldesmon. *Journal of Cell Science*, *126*(Pt 7), 1626–1636. https://doi.org/10.1242/jcs.118190

Sehrawat, A., Gao, L., Wang, Y., Bankhead, A., McWeeney, S. K., King, C. J., Schwartzman, J., Urrutia, J., Bisson, W. H., Coleman, D. J., Joshi, S. K., Kim, D.-H., Sampson, D. A., Weinmann, S., Kallakury, B. V. S., Berry, D. L., Haque, R., Van Den Eeden, S. K., Sharma, S., … Alumkal, J. J. (2018). LSD1 activates a lethal prostate cancer gene network independently of its demethylase function. *Proceedings of the National Academy of Sciences*, *115*(18), E4179–E4188. https://doi.org/10.1073/pnas.1719168115

Shah, N., Wang, P., Wongvipat, J., Karthaus, W. R., Abida, W., Armenia, J., Rockowitz, S., Drier, Y., Bernstein, B. E., Long, H. W., Freedman, M. L., Arora, V. K., Zheng, D., & Sawyers, C. L. (2017).

Regulation of the glucocorticoid receptor via a BET-dependent enhancer drives antiandrogen resistance in prostate cancer. *eLife*, *6*, e27861. https://doi.org/10.7554/eLife.27861

Sharifi, M. N., Sperger, J. M., Taylor, A. K., Tippins, K. E., Reese, S. R., Carreno, V., Kaufmann, K. R., Chang, A. H., Nunamaker, L. A., Linebarger, C., Mora-Rodriguez, L., Schehr, J. L., Krause, H. M., Helzer, K. T., Bootsma, M. L., Blitzer, G. C., Floberg, J. M., Kyriakopoulos, C. E., Emamekhoo, H., … Lang, J. M. (2025). High-purity CTC RNA sequencing identifies prostate cancer lineage phenotypes prognostic for clinical outcomes. *Cancer Discovery*, *15*(5), 969–987. https://doi.org/10.1158/2159-8290.CD-24-1509

Shen, M. M., & Abate-Shen, C. (2010). Molecular genetics of prostate cancer: New prospects for old challenges. *Genes & Development*, *24*(18), 1967–2000. https://doi.org/10.1101/gad.1965810

Shiloh, Y. (2003). ATM and related protein kinases: Safeguarding genome integrity. *Nature Reviews. Cancer*, *3*(3), 155–168. https://doi.org/10.1038/nrc1011

Shimizu, H., Ross, R. K., Bernstein, L., Yatani, R., Henderson, B. E., & Mack, T. M. (1991). Cancers of the prostate and breast among Japanese and white immigrants in Los Angeles County. *British Journal of Cancer*, *63*(6), 963–966. https://doi.org/10.1038/bjc.1991.210

Shimizu, Y., Thumkeo, D., Keel, J., Ishizaki, T., Oshima, H., Oshima, M., Noda, Y., Matsumura, F., Taketo, M. M., & Narumiya, S. (2005). ROCK-I regulates closure of the eyelids and ventral body wall by inducing assembly of actomyosin bundles. *The Journal of Cell Biology*, *168*(6), 941–953. https://doi.org/10.1083/jcb.200411179

Shiozawa, Y., Pedersen, E. A., Havens, A. M., Jung, Y., Mishra, A., Joseph, J., Kim, J. K., Patel, L. R., Ying, C., Ziegler, A. M., Pienta, M. J., Song, J., Wang, J., Loberg, R. D., Krebsbach, P. H., Pienta, K. J., & Taichman, R. S. (2011). Human prostate cancer metastases target the hematopoietic stem cell niche to establish footholds in mouse bone marrow. *The Journal of Clinical Investigation*, *121*(4), 1298–1312. https://doi.org/10.1172/JCI43414

Siegel, R. L., Kratzer, T. B., Giaquinto, A. N., Sung, H., & Jemal, A. (2025). Cancer statistics, 2025. *CA: A Cancer Journal for Clinicians*, *75*(1), 10–45. https://doi.org/10.3322/caac.21871

Sies, H., & Jones, D. P. (2020). Reactive oxygen species (ROS) as pleiotropic physiological signalling agents. *Nature Reviews. Molecular Cell Biology*, *21*(7), 363–383. https://doi.org/10.1038/s41580-020-0230-3

Signoretti, S., & Loda, M. (2006). Defining cell lineages in the prostate epithelium. *Cell Cycle (Georgetown, Tex.)*, *5*(2), 138–141. https://doi.org/10.4161/cc.5.2.2340

Singal, R., Ramachandran, K., Gordian, E., Quintero, C., Zhao, W., & Reis, I. M. (2015). Phase I/II study of azacitidine, docetaxel, and prednisone in patients with metastatic castration-resistant prostate cancer previously treated with docetaxel-based therapy. *Clinical Genitourinary Cancer*, *13*(1), 22–31. https://doi.org/10.1016/j.clgc.2014.07.008

Singh, M., Jha, R., Melamed, J., Shapiro, E., Hayward, S. W., & Lee, P. (2014). Stromal androgen receptor in prostate development and cancer. *The American Journal of Pathology*, *184*(10), 2598–2607. https://doi.org/10.1016/j.ajpath.2014.06.022

Sinha, A., Huang, V., Livingstone, J., Wang, J., Fox, N. S., Kurganovs, N., Ignatchenko, V., Fritsch, K., Donmez, N., Heisler, L. E., Shiah, Y.-J., Yao, C. Q., Alfaro, J. A., Volik, S., Lapuk, A., Fraser, M., Kron, K., Murison, A., Lupien, M., … Boutros, P. C. (2019). The Proteogenomic Landscape of Curable Prostate Cancer. *Cancer Cell*, *35*(3), 414-427.e6. https://doi.org/10.1016/j.ccell.2019.02.005

Sjöblom, B., Salmazo, A., & Djinović-Carugo, K. (2008). Alpha-actinin structure and regulation. *Cellular and Molecular Life Sciences: CMLS*, *65*(17), 2688–2701. https://doi.org/10.1007/s00018-008-8080-8

Smith, M. R., Hussain, M., Saad, F., Fizazi, K., Sternberg, C. N., Crawford, E. D., Kopyltsov, E., Park, C. H., Alekseev, B., Montesa-Pino, Á., Ye, D., Parnis, F., Cruz, F., Tammela, T. L. J., Suzuki, H., Utriainen, T., Fu, C., Uemura, M., Méndez-Vidal, M. J., … ARASENS Trial Investigators. (2022). Darolutamide and Survival in Metastatic, Hormone-Sensitive Prostate Cancer. *The New England Journal of Medicine*, *386*(12), 1132–1142. https://doi.org/10.1056/NEJMoa2119115

Sobue, K., Muramoto, Y., Fujita, M., & Kakiuchi, S. (1981). Purification of a calmodulin-binding protein from chicken gizzard that interacts with F-actin. *Proceedings of the National Academy of Sciences of the United States of America*, *78*(9), 5652–5655. https://doi.org/10.1073/pnas.78.9.5652

Sousa-Pimenta, M., Estevinho, L. M., Szopa, A., Basit, M., Khan, K., Armaghan, M., Ibrayeva, M., Sönmez Gürer, E., Calina, D., Hano, C., & Sharifi-Rad, J. (2023). Chemotherapeutic properties and side-effects associated with the clinical practice of terpene alkaloids: Paclitaxel, docetaxel, and cabazitaxel. *Frontiers in Pharmacology*, *14*, 1157306. https://doi.org/10.3389/fphar.2023.1157306

Stainier, D. Y. R., Raz, E., Lawson, N. D., Ekker, S. C., Burdine, R. D., Eisen, J. S., Ingham, P. W., Schulte-Merker, S., Yelon, D., Weinstein, B. M., Mullins, M. C., Wilson, S. W., Ramakrishnan, L., Amacher, S. L., Neuhauss, S. C. F., Meng, A., Mochizuki, N., Panula, P., & Moens, C. B. (2017). Guidelines for morpholino use in zebrafish. *PLOS Genetics*, *13*(10), e1007000. https://doi.org/10.1371/journal.pgen.1007000

Stanbrough, M., Bubley, G. J., Ross, K., Golub, T. R., Rubin, M. A., Penning, T. M., Febbo, P. G., & Balk, S. P. (2006). Increased expression of genes converting adrenal androgens to testosterone in androgen-independent prostate cancer. *Cancer Research*, *66*(5), 2815–2825. https://doi.org/10.1158/0008-5472.CAN-05-4000

Stankiewicz, E., Mao, X., Mangham, D. C., Xu, L., Yeste-Velasco, M., Fisher, G., North, B., Chaplin, T., Young, B., Wang, Y., Kaur Bansal, J., Kudahetti, S., Spencer, L., Foster, C. S., Møller, H., Scardino, P., Oliver, R. T., Shamash, J., Cuzick, J., … Lu, Y.-J. (2017). Identification of FBXL4 as a Metastasis Associated Gene in Prostate Cancer. *Scientific Reports*, *7*(1), 5124. https://doi.org/10.1038/s41598-017-05209-z

Stein, M. N., Vinceneux, A., Robbrecht, D., Doger, B., Autio, K. A., Schweizer, M. T., Calvo, E., Medina, L., Van Dongen, M., Deville, J.-L., Bernard-Tessier, A., Ghosh, D., Shotts, K., Shen, F., Jaiprasart, P., Chaudhary, R., Wu, S., Cartee, L., Schnepp, R., … Baldini, C. (2025). Pasritamig, a First-in-Class, Bispecific T-Cell Engager Targeting Human Kallikrein 2, in Metastatic Castration-Resistant Prostate Cancer: A Phase I Study. *Journal of Clinical Oncology: Official Journal of the American Society of Clinical Oncology*, *43*(22), 2515–2526. https://doi.org/10.1200/JCO-25-00678

Stoppa-Lyonnet, D. (2016). The biological effects and clinical implications of BRCA mutations: Where do we go from here? *European Journal of Human Genetics: EJHG*, *24 Suppl 1*(Suppl 1), S3-9. https://doi.org/10.1038/ejhg.2016.93

Stracker, T. H., & Petrini, J. H. J. (2011). The MRE11 complex: Starting from the ends. *Nature Reviews. Molecular Cell Biology*, *12*(2), 90–103. https://doi.org/10.1038/nrm3047

Stultz, J., & Fong, L. (2021). How to turn up the heat on the cold immune microenvironment of metastatic prostate cancer. *Prostate Cancer and Prostatic Diseases*, *24*(3), 697–717. https://doi.org/10.1038/s41391-021-00340-5

Su, B., Zheng, Q., Vaughan, M. M., Bu, Y., & Gelman, I. H. (2006). SSeCKS Metastasis-Suppressing Activity in MatLyLu Prostate Cancer Cells Correlates with Vascular Endothelial Growth Factor Inhibition. *Cancer Research*, *66*(11), 5599–5607. https://doi.org/10.1158/0008-5472.CAN-05-4123

Sugiura, M., Sato, H., Okabe, A., Fukuyo, M., Mano, Y., Shinohara, K.-I., Rahmutulla, B., Higuchi, K., Maimaiti, M., Kanesaka, M., Imamura, Y., Furihata, T., Sakamoto, S., Komiya, A., Anzai, N., Kanai, Y., Luo, J., Ichikawa, T., & Kaneda, A. (2021). Identification of AR-V7 downstream genes commonly targeted by AR/AR-V7 and specifically targeted by AR-V7 in castration resistant prostate cancer. *Translational Oncology*, *14*(1), 100915. https://doi.org/10.1016/j.tranon.2020.100915

Svitkina, T. (2018). The Actin Cytoskeleton and Actin-Based Motility. *Cold Spring Harbor Perspectives in Biology*, *10*(1), a018267. https://doi.org/10.1101/cshperspect.a018267

Swami, U., Isaacsson Velho, P., Nussenzveig, R., Chipman, J., Sacristan Santos, V., Erickson, S., Dharmaraj, D., Alva, A. S., Vaishampayan, U. N., Esther, J., Hahn, A. W., Maughan, B. L., Antonarakis, E. S., & Agarwal, N. (2020). Association of SPOP Mutations with Outcomes in Men with De Novo Metastatic Castration-sensitive Prostate Cancer. *European Urology*, *78*(5), 652–656. https://doi.org/10.1016/j.eururo.2020.06.033

Sweeney, C., Bracarda, S., Sternberg, C. N., Chi, K. N., Olmos, D., Sandhu, S., Massard, C., Matsubara, N., Alekseev, B., Parnis, F., Atduev, V., Buchschacher, G. L., Gafanov, R., Corrales, L., Borre, M., Stroyakovskiy, D., Alves, G. V., Bournakis, E., Puente, J., … de Bono, J. S. (2021). Ipatasertib plus abiraterone and prednisolone in metastatic castration-resistant prostate cancer (IPATential150): A multicentre, randomised, double-blind, phase 3 trial. *Lancet (London, England)*, *398*(10295), 131–142. https://doi.org/10.1016/S0140-6736(21)00580-8

Sy, S. M. H., Huen, M. S. Y., & Chen, J. (2009). PALB2 is an integral component of the BRCA complex required for homologous recombination repair. *Proceedings of the National Academy of Sciences of the United States of America*, *106*(17), 7155–7160. https://doi.org/10.1073/pnas.0811159106

Taichman, R. S., Cooper, C., Keller, E. T., Pienta, K. J., Taichman, N. S., & McCauley, L. K. (2002). Use of the stromal cell-derived factor-1/CXCR4 pathway in prostate cancer metastasis to bone. *Cancer Research*, *62*(6), 1832–1837.

Takayama, K., Misawa, A., Suzuki, T., Takagi, K., Hayashizaki, Y., Fujimura, T., Homma, Y., Takahashi, S., Urano, T., & Inoue, S. (2015). TET2 repression by androgen hormone regulates global hydroxymethylation status and prostate cancer progression. *Nature Communications*, *6*(1), 8219. https://doi.org/10.1038/ncomms9219

Takeda, D. Y., Spisák, S., Seo, J.-H., Bell, C., O'Connor, E., Korthauer, K., Ribli, D., Csabai, I., Solymosi, N., Szállási, Z., Stillman, D. R., Cejas, P., Qiu, X., Long, H. W., Tisza, V., Nuzzo, P. V., Rohanizadegan, M., Pomerantz, M. M., Hahn, W. C., & Freedman, M. L. (2018). A Somatically Acquired Enhancer of the Androgen Receptor Is a Noncoding Driver in Advanced Prostate Cancer. *Cell*, *174*(2), 422-432.e13. https://doi.org/10.1016/j.cell.2018.05.037

Tang, F., Xu, D., Wang, S., Wong, C. K., Martinez-Fundichely, A., Lee, C. J., Cohen, S., Park, J., Hill, C. E., Eng, K., Bareja, R., Han, T., Liu, E. M., Palladino, A., Di, W., Gao, D., Abida, W., Beg, S., Puca, L., … Khurana, E. (2022). Chromatin profiles classify castration-resistant prostate cancers suggesting therapeutic targets. *Science (New York, N.Y.)*, *376*(6596), eabe1505. https://doi.org/10.1126/science.abe1505

Taylor, B. S., Schultz, N., Hieronymus, H., Gopalan, A., Xiao, Y., Carver, B. S., Arora, V. K., Kaushik, P., Cerami, E., Reva, B., Antipin, Y., Mitsiades, N., Landers, T., Dolgalev, I., Major, J. E., Wilson, M., Socci, N. D., Lash, A. E., Heguy, A., … Gerald, W. L. (2010). Integrative genomic profiling of human prostate cancer. *Cancer Cell*, *18*(1), 11–22. https://doi.org/10.1016/j.ccr.2010.05.026

Tilki, D., van den Bergh, R. C. N., Briers, E., Van den Broeck, T., Brunckhorst, O., Darraugh, J., Eberli, D., De Meerleer, G., De Santis, M., Farolfi, A., Gandaglia, G., Gillessen, S., Grivas, N., Henry, A. M., Lardas, M., J L H van Leenders, G., Liew, M., Linares Espinos, E., Oldenburg, J., … Cornford, P. (2024). EAU-EANM-ESTRO-ESUR-ISUP-SIOG Guidelines on Prostate Cancer. Part II-2024 Update: Treatment of Relapsing and Metastatic Prostate Cancer. *European Urology*, *86*(2), 164–182. https://doi.org/10.1016/j.eururo.2024.04.010

Tomlins, S. A., Laxman, B., Varambally, S., Cao, X., Yu, J., Helgeson, B. E., Cao, Q., Prensner, J. R., Rubin, M. A., Shah, R. B., Mehra, R., & Chinnaiyan, A. M. (2008). Role of the TMPRSS2-ERG gene fusion in prostate cancer. *Neoplasia (New York, N.Y.)*, *10*(2), 177–188. https://doi.org/10.1593/neo.07822

Tomlins, S. A., Rhodes, D. R., Perner, S., Dhanasekaran, S. M., Mehra, R., Sun, X.-W., Varambally, S., Cao, X., Tchinda, J., Kuefer, R., Lee, C., Montie, J. E., Shah, R. B., Pienta, K. J., Rubin, M. A., & Chinnaiyan, A. M. (2005). Recurrent fusion of TMPRSS2 and ETS transcription factor genes in prostate cancer. *Science (New York, N.Y.)*, *310*(5748), 644–648. https://doi.org/10.1126/science.1117679

Tomlins, S. A., Rhodes, D. R., Yu, J., Varambally, S., Mehra, R., Perner, S., Demichelis, F., Helgeson, B. E., Laxman, B., Morris, D. S., Cao, Q., Cao, X., Andrén, O., Fall, K., Johnson, L., Wei, J. T., Shah, R. B., Al-Ahmadie, H., Eastham, J. A., … Chinnaiyan, A. M. (2008). The Role of SPINK1 in ETS Rearrangement Negative Prostate Cancers. *Cancer Cell*, *13*(6), 519–528. https://doi.org/10.1016/j.ccr.2008.04.016

Tran, C., Ouk, S., Clegg, N. J., Chen, Y., Watson, P. A., Arora, V., Wongvipat, J., Smith-Jones, P. M., Yoo, D., Kwon, A., Wasielewska, T., Welsbie, D., Chen, C. D., Higano, C. S., Beer, T. M., Hung, D. T., Scher, H. I., Jung, M. E., & Sawyers, C. L. (2009). Development of a second-generation antiandrogen for treatment of advanced prostate cancer. *Science (New York, N.Y.)*, *324*(5928), 787–790. https://doi.org/10.1126/science.1168175

Tuxhorn, J. A., Ayala, G. E., Smith, M. J., Smith, V. C., Dang, T. D., & Rowley, D. R. (2002). Reactive stroma in human prostate cancer: Induction of myofibroblast phenotype and extracellular matrix remodeling. *Clinical Cancer Research: An Official Journal of the American Association for Cancer Research*, *8*(9), 2912–2923.

Urabe, F., Matsuzaki, J., Yamamoto, Y., Kimura, T., Hara, T., Ichikawa, M., Takizawa, S., Aoki, Y., Niida, S., Sakamoto, H., Kato, K., Egawa, S., Fujimoto, H., & Ochiya, T. (2019). Large-scale Circulating microRNA Profiling for the Liquid Biopsy of Prostate Cancer. *Clinical Cancer Research: An Official Journal of the American Association for Cancer Research*, *25*(10), 3016–3025. https://doi.org/10.1158/1078-0432.CCR-18-2849

Valastyan, S., & Weinberg, R. A. (2011). Tumor metastasis: Molecular insights and evolving paradigms. *Cell*, *147*(2), 275–292. https://doi.org/10.1016/j.cell.2011.09.024

van Dessel, L. F., van Riet, J., Smits, M., Zhu, Y., Hamberg, P., van der Heijden, M. S., Bergman, A. M., van Oort, I. M., de Wit, R., Voest, E. E., Steeghs, N., Yamaguchi, T. N., Livingstone, J., Boutros, P. C., Martens, J. W. M., Sleijfer, S., Cuppen, E., Zwart, W., van de Werken, H. J. G., … Lolkema, M. P. (2019). The genomic landscape of metastatic castration-resistant prostate cancers reveals multiple distinct genotypes with potential clinical impact. *Nature Communications*, *10*(1), 5251. https://doi.org/10.1038/s41467-019-13084-7

Van Rompay, M. I., Solomon, K. R., Nickel, J. C., Ranganathan, G., Kantoff, P. W., & McKinlay, J. B. (2019). Prostate cancer incidence and mortality among men using statins and non-statin lipid-lowering medications. *European Journal of Cancer (Oxford, England: 1990)*, *112*, 118–126. https://doi.org/10.1016/j.ejca.2018.11.033

van Wilpe, S., Kloots, I. S. H., Slootbeek, P. H. J., den Brok, M., Westdorp, H., Franken, M. D., Coskunturk, M., Osinga, T., Bloemendal, H., Adema, G., Smeenk, R. J., Nagarajah, J., van Ipenburg, J., Kroeze, L. I., Ligtenberg, M. J. L., Schalken, J., Gerritsen, W. R., & Mehra, N. (2024). Ipilimumab with nivolumab in molecularly selected patients with castration-resistant prostate cancer: Primary analysis of the phase II INSPIRE trial. *Annals of Oncology: Official Journal of the European Society for Medical Oncology*, *35*(12), 1126–1137. https://doi.org/10.1016/j.annonc.2024.09.004

Varambally, S., Dhanasekaran, S. M., Zhou, M., Barrette, T. R., Kumar-Sinha, C., Sanda, M. G., Ghosh, D., Pienta, K. J., Sewalt, R. G. A. B., Otte, A. P., Rubin, M. A., & Chinnaiyan, A. M. (2002). The polycomb group protein EZH2 is involved in progression of prostate cancer. *Nature*, *419*(6907), 624–629. https://doi.org/10.1038/nature01075

Venkadakrishnan, V. B., Presser, A. G., Singh, R., Booker, M. A., Traphagen, N. A., Weng, K., Voss, N. C. E., Mahadevan, N. R., Mizuno, K., Puca, L., Idahor, O., Ku, S.-Y., Bakht, M. K., Borah, A. A., Herbert, Z. T., Tolstorukov, M. Y., Barbie, D. A., Rickman, D. S., Brown, M., & Beltran, H. (2024). Lineage-specific canonical and non-canonical activity of EZH2 in advanced prostate cancer subtypes. *Nature Communications*, *15*(1), 6779. https://doi.org/10.1038/s41467-024-51156-5

Venkitaraman, A. R. (2002). Cancer susceptibility and the functions of BRCA1 and BRCA2. *Cell*, *108*(2), 171–182. https://doi.org/10.1016/s0092-8674(02)00615-3

Virtanen, V., Paunu, K., Ahlskog, J. K., Varnai, R., Sipeky, C., & Sundvall, M. (2019). PARP Inhibitors in Prostate Cancer—The Preclinical Rationale and Current Clinical Development. *Genes*, *10*(8), 565. https://doi.org/10.3390/genes10080565

Virtanen, V., Rautiola, H., Poutanen, M., & Boström, P. J. (2020). Uusia työkaluja paikallisesti edenneen ja etäpesäkkeisen eturauhassyövän lääkehoitoon. *Duodecim*, *36*, 2013–2022.

Visakorpi, T., Hyytinen, E., Koivisto, P., Tanner, M., Keinänen, R., Palmberg, C., Palotie, A., Tammela, T., Isola, J., & Kallioniemi, O. P. (1995). In vivo amplification of the androgen receptor gene and progression of human prostate cancer. *Nature Genetics*, *9*(4), 401–406. https://doi.org/10.1038/ng0495-401

Viswanathan, S. R., Ha, G., Hoff, A. M., Wala, J. A., Carrot-Zhang, J., Whelan, C. W., Haradhvala, N. J., Freeman, S. S., Reed, S. C., Rhoades, J., Polak, P., Cipicchio, M., Wankowicz, S. A., Wong, A., Kamath, T., Zhang, Z., Gydush, G. J., Rotem, D., PCF/SU2C International Prostate Cancer Dream Team, … Meyerson, M. (2018). Structural Alterations Driving Castration-Resistant Prostate Cancer Revealed by Linked-Read Genome Sequencing. *Cell*, *174*(2), 433-447.e19. https://doi.org/10.1016/j.cell.2018.05.036

Voeller, H. J., Wilding, G., & Gelmann, E. P. (1991). V-rasH Expression Confers Hormone-Independent in Vitro Growth to LNCaP Prostate Carcinoma Cells. *Molecular Endocrinology*, *5*(2), 209–216. https://doi.org/10.1210/mend-5-2-209

Wang, C. L. A. (2008). Caldesmon and the regulation of cytoskeletal functions. *Advances in Experimental Medicine and Biology*, *644*, 250–272. https://doi.org/10.1007/978-0-387-85766-4_19

Wang, C. L., Wang, L. W., Xu, S. A., Lu, R. C., Saavedra-Alanis, V., & Bryan, J. (1991). Localization of the calmodulin- and the actin-binding sites of caldesmon. *The Journal of Biological Chemistry*, *266*(14), 9166–9172.

Wang, G., Lu, X., Dey, P., Deng, P., Wu, C. C., Jiang, S., Fang, Z., Zhao, K., Konaparthi, R., Hua, S., Zhang, J., Li-Ning-Tapia, E. M., Kapoor, A., Wu, C.-J., Patel, N. B., Guo, Z., Ramamoorthy, V., Tieu, T. N., Heffernan, T., … DePinho, R. A. (2016). Targeting YAP-dependent MDSC infiltration impairs tumor progression. *Cancer Discovery*, *6*(1), 80–95. https://doi.org/10.1158/2159-8290.CD-15-0224

Wang, G., Zhao, D., Spring, D. J., & DePinho, R. A. (2018). Genetics and biology of prostate cancer. *Genes & Development*, *32*(17–18), 1105–1140. https://doi.org/10.1101/gad.315739.118

Wang, L., Xiong, H., Wu, F., Zhang, Y., Wang, J., Zhao, L., Guo, X., Chang, L.-J., Zhang, Y., You, M. J., Koochekpour, S., Saleem, M., Huang, H., Lu, J., & Deng, Y. (2014). Hexokinase 2-mediated Warburg effect is required for PTEN- and p53-deficiency-driven prostate cancer growth. *Cell Reports*, *8*(5), 1461–1474. https://doi.org/10.1016/j.celrep.2014.07.053

Wang, S., Gao, J., Lei, Q., Rozengurt, N., Pritchard, C., Jiao, J., Thomas, G. V., Li, G., Roy-Burman, P., Nelson, P. S., Liu, X., & Wu, H. (2003). Prostate-specific deletion of the murine Pten tumor suppressor gene leads to metastatic prostate cancer. *Cancer Cell*, *4*(3), 209–221. https://doi.org/10.1016/s1535-6108(03)00215-0

Wang, X., Kruithof-de Julio, M., Economides, K. D., Walker, D., Yu, H., Halili, M. V., Hu, Y.-P., Price, S. M., Abate-Shen, C., & Shen, M. M. (2009). A luminal epithelial stem cell that is a cell of origin for prostate cancer. *Nature*, *461*(7263), 495–500. https://doi.org/10.1038/nature08361

Wang, Z. A., Toivanen, R., Bergren, S. K., Chambon, P., & Shen, M. M. (2014). Luminal cells are favored as the cell of origin for prostate cancer. *Cell Reports*, *8*(5), 1339–1346. https://doi.org/10.1016/j.celrep.2014.08.002

Wang, Z., Jiang, H., Yang, Z.-Q., & Chacko, S. (1997). Both N-terminal myosin-binding and C-terminal actin-binding sites on smooth muscle caldesmon are required for caldesmon-mediated inhibition of actin filament velocity. *Proceedings of the National Academy of Sciences*, *94*(22), 11899–11904. https://doi.org/10.1073/pnas.94.22.11899

Warburg, O., Wind, F., & Negelein, E. (1927). THE METABOLISM OF TUMORS IN THE BODY. *The Journal of General Physiology*, *8*(6), 519–530. https://doi.org/10.1085/jgp.8.6.519

Watanabe, R., Maekawa, M., Hieda, M., Taguchi, T., Miura, N., Kikugawa, T., Saika, T., & Higashiyama, S. (2020). SPOP is essential for DNA-protein cross-link repair in prostate cancer cells: SPOP-dependent removal of topoisomerase 2A from the topoisomerase 2A-DNA cleavage complex. *Molecular Biology of the Cell*, *31*(6), 478–490. https://doi.org/10.1091/mbc.E19-08-0456

Watson, P. A., Arora, V. K., & Sawyers, C. L. (2015). Emerging mechanisms of resistance to androgen receptor inhibitors in prostate cancer. *Nature Reviews. Cancer*, *15*(12), 701–711. https://doi.org/10.1038/nrc4016

Webber, J. P., Spary, L. K., Sanders, A. J., Chowdhury, R., Jiang, W. G., Steadman, R., Wymant, J., Jones, A. T., Kynaston, H., Mason, M. D., Tabi, Z., & Clayton, A. (2015). Differentiation of tumour-promoting stromal myofibroblasts by cancer exosomes. *Oncogene*, *34*(3), 290–302. https://doi.org/10.1038/onc.2013.560

Webber, J., Steadman, R., Mason, M. D., Tabi, Z., & Clayton, A. (2010). Cancer exosomes trigger fibroblast to myofibroblast differentiation. *Cancer Research*, *70*(23), 9621–9630. https://doi.org/10.1158/0008-5472.CAN-10-1722

Welti, J., Sharp, A., Brooks, N., Yuan, W., McNair, C., Chand, S. N., Pal, A., Figueiredo, I., Riisnaes, R., Gurel, B., Rekowski, J., Bogdan, D., West, W., Young, B., Raja, M., Prosser, A., Lane, J., Thomson, S., Worthington, J., … de Bono, J. S. (2021). Targeting the p300/CBP Axis in Lethal Prostate Cancer. *Cancer Discovery*, *11*(5), 1118–1137. https://doi.org/10.1158/2159-8290.CD-20-0751

Wen, S., Chang, H.-C., Tian, J., Shang, Z., Niu, Y., & Chang, C. (2015). Stromal androgen receptor roles in the development of normal prostate, benign prostate hyperplasia, and prostate cancer. *The American Journal of Pathology*, *185*(2), 293–301. https://doi.org/10.1016/j.ajpath.2014.10.012

Weng, C.-C., Ding, P.-Y., Liu, Y.-H., Hawse, J. R., Subramaniam, M., Wu, C.-C., Lin, Y.-C., Chen, C.-Y., Hung, W.-C., & Cheng, K.-H. (2019). Mutant Kras-induced upregulation of CD24 enhances prostate cancer stemness and bone metastasis. *Oncogene*, *38*(12), 2005–2019. https://doi.org/10.1038/s41388-018-0575-7

West, C. D., Hollander, V. P., Whitmore, W. F., Randall, H. T., & Pearson, O. H. (1952). The effect of bilateral adrenalectomy upon neoplastic disease in man. *Cancer*, *5*(5), 1009–1018. https://doi.org/10.1002/1097-0142(195209)5:5%253C1009::aid-cncr2820050516%253E3.0.co;2-m

Whang, Y. E., Wu, X., Suzuki, H., Reiter, R. E., Tran, C., Vessella, R. L., Said, J. W., Isaacs, W. B., & Sawyers, C. L. (1998). Inactivation of the tumor suppressor PTEN/MMAC1 in advanced human prostate cancer through loss of expression. *Proceedings of the National Academy of Sciences*, *95*(9), 5246–5250. https://doi.org/10.1073/pnas.95.9.5246

Wikström, P., Marusic, J., Stattin, P., & Bergh, A. (2009). Low stroma androgen receptor level in normal and tumor prostate tissue is related to poor outcome in prostate cancer patients. *The Prostate*, *69*(8), 799–809. https://doi.org/10.1002/pros.20927

Wilt, T. J., & Ahmed, H. U. (2013). Prostate cancer screening and the management of clinically localized disease. *BMJ (Clinical Research Ed.)*, *346*, f325. https://doi.org/10.1136/bmj.f325

Wu, X., Gong, S., Roy-Burman, P., Lee, P., & Culig, Z. (2013). Current mouse and cell models in prostate cancer research. *Endocrine-Related Cancer*, *20*(4), R155-170. https://doi.org/10.1530/ERC-12-0285

Wu, Y.-M., Cieślik, M., Lonigro, R. J., Vats, P., Reimers, M. A., Cao, X., Ning, Y., Wang, L., Kunju, L. P., de Sarkar, N., Heath, E. I., Chou, J., Feng, F. Y., Nelson, P. S., de Bono, J. S., Zou, W., Montgomery, B., Alva, A., PCF/SU2C International Prostate Cancer Dream Team, … Chinnaiyan, A. M. (2018). Inactivation of CDK12 Delineates a Distinct Immunogenic Class of Advanced Prostate Cancer. *Cell*, *173*(7), 1770-1782.e14. https://doi.org/10.1016/j.cell.2018.04.034

Xia, R., Xu, M., Yang, J., & Ma, X. (2022). The role of Hedgehog and Notch signaling pathway in cancer. *Molecular Biomedicine*, *3*, 44. https://doi.org/10.1186/s43556-022-00099-8

Xian, Z.-Y., Liu, J.-M., Chen, Q.-K., Chen, H.-Z., Ye, C.-J., Xue, J., Yang, H.-Q., Li, J.-L., Liu, X.-F., & Kuang, S.-J. (2015). Inhibition of LDHA suppresses tumor progression in prostate cancer. *Tumour Biology: The Journal of the International Society for Oncodevelopmental Biology and Medicine*, *36*(10), 8093–8100. https://doi.org/10.1007/s13277-015-3540-x

Xiao, L., Parolia, A., Qiao, Y., Bawa, P., Eyunni, S., Mannan, R., Carson, S. E., Chang, Y., Wang, X., Zhang, Y., Vo, J. N., Kregel, S., Simko, S. A., Delekta, A. D., Jaber, M., Zheng, H., Apel, I. J., McMurry, L., Su, F., … Chinnaiyan, A. M. (2022). Targeting SWI/SNF ATPases in enhancer-addicted prostate cancer. *Nature*, *601*(7893), 434–439. https://doi.org/10.1038/s41586-021-04246-z

Xie, Q., Liu, Y., Cai, T., Horton, C., Stefanson, J., & Wang, Z. A. (2017). Dissecting cell-type-specific roles of androgen receptor in prostate homeostasis and regeneration through lineage tracing. *Nature Communications*, *8*, 14284. https://doi.org/10.1038/ncomms14284

Yamada, K. M., & Sixt, M. (2019). Mechanisms of 3D cell migration. *Nature Reviews Molecular Cell Biology*, *20*(12), 738–752. https://doi.org/10.1038/s41580-019-0172-9

Yamada, Y., Venkadakrishnan, V. B., Mizuno, K., Bakht, M., Ku, S.-Y., Garcia, M. M., & Beltran, H. (2023). Targeting DNA methylation and B7-H3 in RB1-deficient and neuroendocrine prostate cancer. *Science Translational Medicine*, *15*(722), eadf6732. https://doi.org/10.1126/scitranslmed.adf6732

Yáñez-Mó, M., Siljander, P. R.-M., Andreu, Z., Zavec, A. B., Borràs, F. E., Buzas, E. I., Buzas, K., Casal, E., Cappello, F., Carvalho, J., Colás, E., Cordeiro-da Silva, A., Fais, S., Falcon-Perez, J. M., Ghobrial, I. M., Giebel, B., Gimona, M., Graner, M., Gursel, I., … De Wever, O. (2015). Biological properties of extracellular vesicles and their physiological functions. *Journal of Extracellular Vesicles*, *4*, 27066. https://doi.org/10.3402/jev.v4.27066

Yao, Y.-B., Xiao, C.-F., Lu, J.-G., & Wang, C. (2021). Caldesmon: Biochemical and Clinical Implications in Cancer. *Frontiers in Cell and Developmental Biology*, *9*, 634759. https://doi.org/10.3389/fcell.2021.634759

Yoshio, T., Morita, T., Kimura, Y., Tsujii, M., Hayashi, N., & Sobue, K. (2007). Caldesmon suppresses cancer cell invasion by regulating podosome/invadopodium formation. *FEBS Letters*, *581*(20), 3777–3782. https://doi.org/10.1016/j.febslet.2007.06.073

Yu, S., Yeh, C.-R., Niu, Y., Chang, H.-C., Tsai, Y.-C., Moses, H. L., Shyr, C.-R., Chang, C., & Yeh, S. (2012). Altered prostate epithelial development in mice lacking the androgen receptor in stromal fibroblasts. *The Prostate*, *72*(4), 437–449. https://doi.org/10.1002/pros.21445

Zagars, G. K., & Pollack, A. (1997). Kinetics of serum prostate-specific antigen after external beam radiation for clinically localized prostate cancer. *Radiotherapy and Oncology: Journal of the European Society for Therapeutic Radiology and Oncology*, *44*(3), 213–221. https://doi.org/10.1016/s0167-8140(97)00123-0

Zhang, C., Wang, L., Wu, D., Chen, H., Chen, Z., Thomas-Ahner, J. M., Zynger, D. L., Eeckhoute, J., Yu, J., Luo, J., Brown, M., Clinton, S. K., Nephew, K. P., Huang, T. H.-M., Li, W., & Wang, Q. (2011). Definition of a FoxA1 Cistrome that is crucial for G1 to S-phase cell-cycle transit in castration-resistant prostate cancer. *Cancer Research*, *71*(21), 6738–6748. https://doi.org/10.1158/0008-5472.CAN-11-1882

Zhang, H., Pan, Y., Zheng, L., Choe, C., Lindgren, B., Jensen, E. D., Westendorf, J. J., Cheng, L., & Huang, H. (2011). FOXO1 inhibits Runx2 transcriptional activity and prostate cancer cell migration and invasion. *Cancer Research*, *71*(9), 3257–3267. https://doi.org/10.1158/0008-5472.CAN-10-2603

Zhang, J., Ren, Z., Zheng, D., Song, Z., Lin, J., Luo, Y., Zou, X., Pan, Y., Qi, N., Li, A., & Liu, X. (2022). AHSA1 Promotes Proliferation and EMT by Regulating ERK/CALD1 Axis in Hepatocellular Carcinoma. *Cancers*, *14*(19), 4600. https://doi.org/10.3390/cancers14194600

Zhang, L., Sun, J., Liu, Z., Dai, Y., Luo, Z., Jiang, X., Li, Z., Li, Y., Cao, P., Zhou, Y., Zeng, Z., Tang, A., Li, X., Li, X., Xiang, J., & Li, G. (2014). Mesenchymal stem cells regulate cytoskeletal

dynamics and promote cancer cell invasion through low dose nitric oxide. *Current Molecular Medicine*, *14*(6), 749–761. https://doi.org/10.2174/1566524014666140724102301

Zhang, L., Yu, X., Zheng, L., Zhang, Y., Li, Y., Fang, Q., Gao, R., Kang, B., Zhang, Q., Huang, J. Y., Konno, H., Guo, X., Ye, Y., Gao, S., Wang, S., Hu, X., Ren, X., Shen, Z., Ouyang, W., & Zhang, Z. (2018). Lineage tracking reveals dynamic relationships of T cells in colorectal cancer. *Nature*, *564*(7735), 268–272. https://doi.org/10.1038/s41586-018-0694-x

Zhang, P., Singh, A., Yegnasubramanian, S., Esopi, D., Kombairaju, P., Bodas, M., Wu, H., Bova, S. G., & Biswal, S. (2010). Loss of Kelch-like ECH-associated protein 1 function in prostate cancer cells causes chemoresistance and radioresistance and promotes tumor growth. *Molecular Cancer Therapeutics*, *9*(2), 336–346. https://doi.org/10.1158/1535-7163.MCT-09-0589

Zhang, W., Fan, Y., Zhang, Y., Feng, Y., Luo, Y., Zhou, X., Chen, Z., Wang, C., Lu, T., Tang, F., Chen, Y., Li, H., & Jiao, Y. (2024). Discovery of novel biphenyl derivatives as androgen receptor degraders for the treatment of enzalutamide-resistant prostate cancer. *Bioorganic Chemistry*, *148*, 107433. https://doi.org/10.1016/j.bioorg.2024.107433

Zhang, W., Liu, B., Wu, W., Li, L., Broom, B. M., Basourakos, S. P., Korentzelos, D., Luan, Y., Wang, J., Yang, G., Park, S., Azad, A. K., Cao, X., Kim, J., Corn, P. G., Logothetis, C. J., Aparicio, A. M., Chinnaiyan, A. M., Navone, N., … Thompson, T. C. (2018). Targeting the MYCN–PARP–DNA Damage Response Pathway in Neuroendocrine Prostate Cancer. *Clinical Cancer Research*, *24*(3), 696–707. https://doi.org/10.1158/1078-0432.CCR-17-1872

Zhang, X.-Q., Kondrikov, D., Yuan, T.-C., Lin, F.-F., Hansen, J., & Lin, M.-F. (2003). Receptor protein tyrosine phosphatase alpha signaling is involved in androgen depletion-induced neuroendocrine differentiation of androgen-sensitive LNCaP human prostate cancer cells. *Oncogene*, *22*(43), 6704–6716. https://doi.org/10.1038/sj.onc.1206764

Zhang, Y., Donaher, J. L., Das, S., Li, X., Reinhardt, F., Krall, J. A., Lambert, A. W., Thiru, P., Keys, H. R., Khan, M., Hofree, M., Wilson, M. M., Yedier-Bayram, O., Lack, N. A., Onder, T. T., Bagci-Onder, T., Tyler, M., Tirosh, I., Regev, A., … Weinberg, R. A. (2022). Genome-wide CRISPR screen identifies PRC2 and KMT2D-COMPASS as regulators of distinct EMT trajectories that contribute differentially to metastasis. *Nature Cell Biology*, *24*(4), 554–564. https://doi.org/10.1038/s41556-022-00877-0

Zhang, Z., Zhou, C., Li, X., Barnes, S. D., Deng, S., Hoover, E., Chen, C.-C., Lee, Y. S., Zhang, Y., Wang, C., Metang, L. A., Wu, C., Tirado, C. R., Johnson, N. A., Wongvipat, J., Navrazhina, K., Cao, Z., Choi, D., Huang, C.-H., … Mu, P. (2020). Loss of CHD1 Promotes Heterogeneous Mechanisms of Resistance to AR-Targeted Therapy via Chromatin Dysregulation. *Cancer Cell*, *37*(4), 584-598.e11. https://doi.org/10.1016/j.ccell.2020.03.001

Zhao, D., Lu, X., Wang, G., Lan, Z., Liao, W., Li, J., Liang, X., Chen, J. R., Shah, S., Shang, X., Tang, M., Deng, P., Dey, P., Chakravarti, D., Chen, P., Spring, D. J., Navone, N. M., Troncoso, P., Zhang, J., … DePinho, R. A. (2017). Synthetic essentiality of chromatin remodelling factor CHD1 in PTEN-deficient cancer. *Nature*, *542*(7642), 484–488. https://doi.org/10.1038/nature21357

Zhao, S. G., Chen, W. S., Li, H., Foye, A., Zhang, M., Sjöström, M., Aggarwal, R., Playdle, D., Liao, A., Alumkal, J. J., Das, R., Chou, J., Hua, J. T., Barnard, T. J., Bailey, A. M., Chow, E., Perry, M., Dang, H. X., Yang, R., … Feng, F. Y. (2020). DNA methylation landscapes in advanced prostate cancer. *Nature Genetics*, *52*(8), 778–789. https://doi.org/10.1038/s41588-020-0648-8

Zheng, J., Lu, J., Qi, J., Yang, Q., Zhao, H., Liu, H., Chen, Z., Huang, L., Ye, Y., Xu, M., Xu, Y., Wang, T., Li, M., Zhao, Z., Zheng, R., Wang, S., Lin, H., Hu, C., Ling Chui, C. S., … Bi, Y. (2024). The effect of SGLT2 inhibition on prostate cancer: Mendelian randomization and observational analysis using electronic healthcare and cohort data. *Cell Reports. Medicine*, *5*(8), 101688. https://doi.org/10.1016/j.xcrm.2024.101688

Zheng, P.-P., Severijnen, L.-A., van der Weiden, M., Willemsen, R., & Kros, J. M. (2009). A crucial role of caldesmon in vascular development in vivo. *Cardiovascular Research*, *81*(2), 362–369. https://doi.org/10.1093/cvr/cvn294

Zheng, P.-P., Severijnen, L.-A., Willemsen, R., & Kros, J. M. (2009). Caldesmon is essential for cardiac morphogenesis and function: In vivo study using a zebrafish model. *Biochemical and Biophysical Research Communications*, *378*(1), 37–40. https://doi.org/10.1016/j.bbrc.2008.10.165

Zhu, S., Zhao, D., Yan, L., Jiang, W., Kim, J.-S., Gu, B., Liu, Q., Wang, R., Xia, B., Zhao, J. C., Song, G., Mi, W., Wang, R.-F., Shi, X., Lam, H.-M., Dong, X., Yu, J., Chen, K., & Cao, Q. (2018). BMI1 regulates androgen receptor in prostate cancer independently of the polycomb repressive complex 1. *Nature Communications*, *9*(1), 500. https://doi.org/10.1038/s41467-018-02863-3

Zhuang, M., Calabrese, M. F., Liu, J., Waddell, M. B., Nourse, A., Hammel, M., Miller, D. J., Walden, H., Duda, D. M., Seyedin, S. N., Hoggard, T., Harper, J. W., White, K. P., & Schulman, B. A. (2009). Structures of SPOP-substrate complexes: Insights into molecular architectures of BTB-Cul3 ubiquitin ligases. *Molecular Cell*, *36*(1), 39–50. https://doi.org/10.1016/j.molcel.2009.09.022

Zivanovic, A., Miller, J. T., Munro, S. A., Knutson, T. P., Li, Y., Passow, C. N., Simonaitis, P., Lynch, M., Oseth, L., Zhao, S. G., Feng, F. Y., Wikström, P., Corey, E., Morrissey, C., Henzler, C., Raphael, B. J., & Dehm, S. M. (2023). Co-evolution of AR gene copy number and structural complexity in endocrine therapy resistant prostate cancer. *NAR Cancer*, *5*(3), zcad045. https://doi.org/10.1093/narcan/zcad045

Original Publications

Sriraman S, Virtanen V, Kukkula A, Toriseva M, Lumiainen A, West G, Poutanen M, Taimen P, Sundvall M. (2025)
Androgen receptor-mediated regulation of BRCA1 modulates the antioxidant defense in prostate cancer.
The Journal of Pathology

I

Journal of Pathology
J Pathol 2025
Published online 3 October 2025 in Wiley Online Library (wileyonlinelibrary.com) DOI: 10.1002/path.6468

ORIGINAL ARTICLE

Androgen receptor–mediated regulation of BRCA1 modulates the antioxidant defense in prostate cancer

Saiganesh Sriraman[1†], Verneri Virtanen[1†], Antti Kukkula[1], Mervi Toriseva[1], Anni Lumiainen[1], Gun West[1,2], Matti Poutanen[3,4], Pekka Taimen[1,2,5] and Maria Sundvall[1,6*]

[1] *Cancer Research Unit, Institute of Biomedicine, and FICAN West Cancer Center Laboratory, University of Turku and Turku University Hospital, Turku, Finland*
[2] *InFLAMES Research Flagship Center, University of Turku and Åbo Akademi University, Turku, Finland*
[3] *Research Centre for Integrative Physiology and Pharmacology, Institute of Biomedicine, and FICAN West Cancer Center, University of Turku, Turku, Finland*
[4] *Institute of Medicine, Sahlgrenska Academy at University of Gothenburg, Gothenburg, Sweden*
[5] *Department of Pathology, Tyks Laboratories, Turku University Hospital, Turku, Finland*
[6] *Department of Oncology, Turku University Hospital, Turku, Finland*

**Correspondence to: M Sundvall, Cancer Research Unit, Institute of Biomedicine, FICAN West Cancer Center Laboratory, University of Turku and Turku University Hospital, Kiinamyllynkatu 10, 20520, Turku, Finland. E-mail: mahesu@utu.fi*

[†]These authors contributed equally to this work.

Abstract

Lethal prostate cancer (PCa) is a genetically heterogeneous disease characterized by evolving androgen receptor (AR) signaling, eventually culminating in castration resistance. The tumor suppressor gene *BRCA1* has multiple functions that include secondary processes cooperating with its main function as a caretaker of genomic integrity. *BRCA1* is often mutated in breast and ovarian cancer, but *BRCA1* mutations are also associated with PCa, although they are less frequently observed. Most PCa patients do not, however, carry *BRCA1* mutations, and interestingly, it has been shown that *BRCA1* expression is enriched in castration-resistant PCa. In this study we elucidated the prostate tissue-specific role of the BRCA1 protein. Although the regulation of DNA damage response genes has been studied in PCa, comprehensive analyses of *BRCA1* regulation in the context of androgen signaling are lacking. Our results indicate that *BRCA1* is dynamically regulated by AR signaling and that activation of AR via its natural ligand, dihydrotestosterone, represses BRCA1 expression. Our analyses both *in vitro* and of patient samples and mouse xenografts showed that BRCA1 expression was induced and sustained after androgen deprivation. Moreover, we observed that oxidative stress–related pathways were regulated by BRCA1 in PCa cells and that androgen deprivation therapy–induced activation of BRCA1 supported the function of NRF2, the master regulator of antioxidant defense, and a known interactor of BRCA1. Impaired NRF2 activity, in the absence of BRCA1, decreased growth in a 3D environment. Our findings shed light on the functional role of BRCA1 protein in PCa and suggest that *BRCA1* is regulated by the evolving AR signaling state during PCa progression. Thus, AR-mediated suppression of *BRCA1* accumulates oncogenic alterations in the early phases of PCa tumor progression and safeguards from excessive reactive oxygen species (ROS) when upregulated during androgen deprivation therapy.

Keywords: castration-resistant prostate cancer; androgen deprivation therapy; androgen receptor; BRCA1; DNA damage; oxidative stress; NRF2

Received 13 March 2025; Revised 14 June 2025; Accepted 7 August 2025

No conflicts of interest were declared.

Introduction

BRCA1 is a tumor suppressor that supports genomic integrity via its central role in DNA damage response (DDR), where it is specifically involved in the repair of double-strand DNA breaks by homologous recombination (HR) [1]. Therefore, when BRCA1 function is lost, somatic oncogenic alterations are more likely to become incorporated in the DNA, consequently inducing carcinogenesis or cancer progression [1]. In addition, BRCA1 functions as a transcriptional factor and part of a ubiquitin ligase complex and has pleiotropic roles in cells pertaining to the cell cycle, centrosome function, and the immune system [1,2]. In keeping with the connection to various essential functions, as well as the role in maintaining genomic integrity, *BRCA1* knockout is

embryonically lethal, *BRCA1* germline mutations are heterozygous, and *BRCA1* somatic mutations require the presence of an accompanying mutation such as p53 [1,2]. BRCA1 also prevents the degradation of the master regulator for antioxidant response, nuclear factor erythroid 2-related factor 2 (NRF2) [3–5]. This secondary effect cooperates with the tumor suppressor gene function by protecting cells against reactive oxygen species (ROS), thereby supporting genomic integrity [5].

DDR genes are frequently mutated in prostate cancer (PCa), with alterations observed in up to 20–30% of castration-resistant PCa (CRPC) cases [6–8]. Most mutations target *BRCA2* and *BRCA1* mutations and are only found in 1%–2% of patients [6,7,9–11]. Previous preclinical studies have demonstrated an interplay between androgen receptor (AR) signaling and DDR in PCa [12–16]. However, the results are contradictory, and the interpretation of these findings remains complex. For instance, while influential work in the field has suggested that AR activation promotes DDR, data from major PCa patient datasets appear to paradoxically indicate that *BRCA1* expression is enriched in CRPC [13,17,18]. Adding to this complexity, the antiandrogen enzalutamide decreases BRCA1 expression in preclinical models [13]. Importantly, the regulation of BRCA1 protein by AR by its natural ligands or by androgen deprivation (AD) has not been reported. Most studies have instead relied on a limited number of synthetic androgens, AR inhibitors, or small RNAs instead of systematic physiological approaches, or they have reported effects on DDR genes but excluded *BRCA1* [12–16].

Here, we characterized the regulation of BRCA1 by AR signaling using a panel of cell lines, patient samples, and a mouse xenograft model of AD therapy (ADT) and studied the implications of this regulation by exploring the tissue-specific role of BRCA1 protein in PCa. We discovered that AR activation is a repressor of *BRCA1* transcription, and conversely, BRCA1 expression is sustained in response to AD. Furthermore, we showed that PCa hijacks a BRCA1-NRF2 regulatory axis to implement an antioxidant response against ROS generated by AD, enabling PCa progression.

Materials and methods

Ethics approval

The use of patient tissue material was approved by the Ethics Committee of the Hospital District of Helsinki and Uusimaa (84/13/03/00/2014; §3 30.01.2015), the Hospital District of Southwest Finland (number T206/2014), and the National Supervisory Authority for Welfare and Health (VALVIRA, 8008/06.01.03/2014).

Cell culture and treatments

PC-3, VCaP, LNCaP, and 22Rv1 cells (ATCC, Manassas, VA, USA) were cultured in the presence of 1% penicillin–streptomycin solution (Sigma-Aldrich, St. Louis, MO, USA), except during the experiments, routinely tested to be mycoplasma-free and checked for authenticity, as previously described [19].

AD was performed using phenol-red free media containing 5% charcoal-stripped FBS (Gibco, Waltham, MA, USA; AD media [ADM]). Normal culture conditions were used as controls for deprivation experiments and are referred to as control media (CM). Dihydrotestosterone (DHT; Sigma-Aldrich) and R1881 (Sigma-Aldrich) were used to stimulate AR after incubation in ADM for 48 h by incubating for 24 h prior to lysis unless specified otherwise. Cell proliferation (confluence) in a 2D culture was monitored in real time for up to 72 h using IncuCyte S3 (Sartorius, Göttingen, Germany) 24 h after transfection. MTS cell viability assay was done as previously described [19].

RNA interference and transfection

Transfection was performed using *Silencer*® Select siRNA oligonucleotides (Ambion, Austin, TX, USA), which are listed, together with the percentage and type of Dharmafect reagent (Horizon Discovery, Waterbeach, UK), in the supplementary material, Table S1 as previously described [19].

Organotypic 3D growth assays

PC-3 and LNCaP cells were grown in 3D as previously described [19]. The multispheroid average area was measured using 10 wells from each condition using the IncuCyte S3 multispheroid analysis software (Sartorius). Cell recovery solution (Corning® Cell Recovery Solution, Sigma-Aldrich) was added following the manufacturer's protocol to extract the organoids from the basement membrane matrix prior to lysis.

Cell lysis and immunoblotting

Cells were lysed and western blotting was performed as previously described [19]. Equal amounts of 30–100 μg of total protein from the lysate supernatants were analyzed. The antibodies used are listed in the supplementary material, Table S2.

RT-qPCR

The isolated RNA was concentrated, and its purity and concentration were assessed before cDNA synthesis, following the manufacturer's protocol. RT-qPCR was then performed using TaqMan™ Fast Advanced Master Mix (Thermo Fisher Scientific, Waltham, Massachusetts, USA). The TaqMan™ Gene Expression Assay (FAM) probes used in the assay are listed in the supplementary material, Table S3. Additional details are provided in the Supplementary Materials and Methods.

Murine VCaP xenografts of early ADT response

VCaP xenograft sections were generated according to a previously described protocol and permissions [20]. Subcutaneous tumors were grown for 4 weeks, and surgical castration was performed. The mice were

sacrificed either 2 days (Cas 2D) or 5 days (Cas 5D) after castration. The Intact group, serving as the noncastrated control, was sacrificed 5 days after the surgery in the treatment groups. Tumors generated under these conditions were collected and fixed in formalin, followed by sectioning and sample preparation.

Immunohistochemistry (IHC) and digital image analyses

Tissue sections from patient samples in a tissue microarray and from tumor xenografts were deparaffinized with xylene (3 × 7 min) and rehydrated in absolute ethanol (2 × 2 min) and 96% ethanol (2 × 2 min), followed by three washes with distilled water. Antigen retrieval was performed in citrate buffer (pH 6) using a microwave for 7 min at 600 W, 7 min at 450 W, and the sections were left to cool down for 20 min. For pBRCA1 and γH2Ax staining, antigen retrieval was performed using a decloaking chamber (Biocare Medical NxGen, Pacheco, CA, USA) for 20 min. After three washes with distilled water, sections were blocked with 3% hydrogen peroxide for 10 min at room temperature (RT), washed with Tris–HCl buffer, followed by pre-protein blocking in antibody diluent for 10 min at RT, and incubated using antibodies and concentrations specified in the supplementary material, Table S2 for 60 min at RT. After washing with Tris–HCl buffer, the sections were incubated with secondary antibody for 30 min at RT and washed again with Tris–HCl buffer. DAB (Immunologic, WellMed BV, Duiven, the Netherlands) incubation was washed with distilled water after 10 min at RT, and the sections were counterstained with Mayer's hematoxylin (Sigma-Aldrich) for 1 min at RT, followed by washing with distilled water, dehydration twice in 96% ethanol, twice in absolute ethanol, and three times in xylene.

Slides were scanned using a Pannoramic P1000 slide scanner (3DHISTECH, Budapest, Hungary). Xenograft whole-tumor sections were measured for total tumor area in QuPath v0.4.4 (open-source software available from https://qupath.github.io/) using a pixel classifier after refining the area analyzed using manual segmentation. Areas with strong staining were detected using a QuPath pixel classifier. For patient samples, two researchers independently performed manual scoring.

In silico analyses

The effects of R1881 on *BRCA1* and *KLK3* (which encodes prostate-specific antigen [PSA]) mRNA expression in LNCaP cells were analyzed using the GSE50936 dataset [21]. Expression data (log2) were downloaded from the R2: Genomics Analysis and Visualization Platform (http://r2.amc.nl).

Differentially expressed genes were analyzed from the GSE162225 [22] dataset containing RNA-seq data of sh-control and sh-BRCA1 samples of LNCaP cells. Sh1-BRCA1 ($n = 3$) and sh2-BRCA1 (n = 3) samples were pooled and compared to sh-control ($n = 3$) samples, and the data were downloaded from the GEO2R platform at https://www.ncbi.nlm.nih.gov/geo/geo2r/. Volcano plots of differentially expressed genes were generated with VolcaNoseR [23] at https://huygens.science.uva.nl/VolcaNoseR/ using an FDR/adjusted p-value <0.001 (Benjamini–Hochberg) and log2 fold change >1 as the threshold for statistical significance. The lists of the top 500 downregulated genes (supplementary material, Table S4) were compared to the Molecular Signatures Database (MsigDB) (v2024.1) Gene Ontology: Biological Processes (GO:BP), Hallmark and Oncogenic gene set collections at https://www.gsea-msigdb.org/gsea/msigdb to identify significant overlaps with gene sets ($p < 0.05$, FDR < 0.05).

Data of genetic alterations of *BRCA1*, association of expression with clinical features, coexpression analyses of PCa patient and patient-derived organoid datasets, and survival analyses of patients were extracted from cBioPortal at https://www.cbioportal.org/.

Statistical analysis

Statistical analyses were performed using R Studio (open-source software available from https://www.posit.co/) and GraphPad Prism 10.1.2 (GraphPad Software, San Diego, CA, USA). Data extracted from cBioPortal v4.1.9 were generated using the default methods. Spearman's rank correlation coefficient was used to analyze correlations. Two-tailed unpaired Student's t-test or Mann–Whitney U test were used for comparisons between two groups. Analysis of variance (ANOVA) test was used to analyze the differences between the means of more than two groups.

Results

AR activation by DHT and R1881 represses *BRCA1* transcription

In this study we used the PCa cell lines VCaP (*AR*-amplified, *TP53*-mutated, *TMPRSS2-ERG* fusion), LNCaP (*AR*-mutated, *CHEK2*-SNV, *PTEN* loss), 22Rv1 (*AR* splice variant, *BRCA2*-mutated, *ATM*-SNV, *TP53*-mutated, *TMPRSS2–ERG* fusion), and PC-3 (AR-negative, *PTEN* loss) [24]. Thus, three AR-positive cell lines with different AR signaling statuses were used.

To study BRCA1 protein levels in response to AR activation, we first pretreated the highly AR-responsive VCaP cell line with AD mimicking conditions for 96 h. During the last 24, 48, and 72 h of this period, we further stimulated the cells with different DHT concentrations (0.05–10 nM), and all cells were lysed at the 96-h timepoint. DHT treatment increased the levels of AR transcriptional target proteins PSA and FKBP5 at concentrations between 0.5–10 nM (Figure 1A,B). In contrast, BRCA1 protein was downregulated in a dose-dependent manner. As a readout of DNA damage, γH2Ax was downregulated, particularly at later timepoints. Another essential HR protein, Rad51, was also downregulated. These results suggested that unlike the

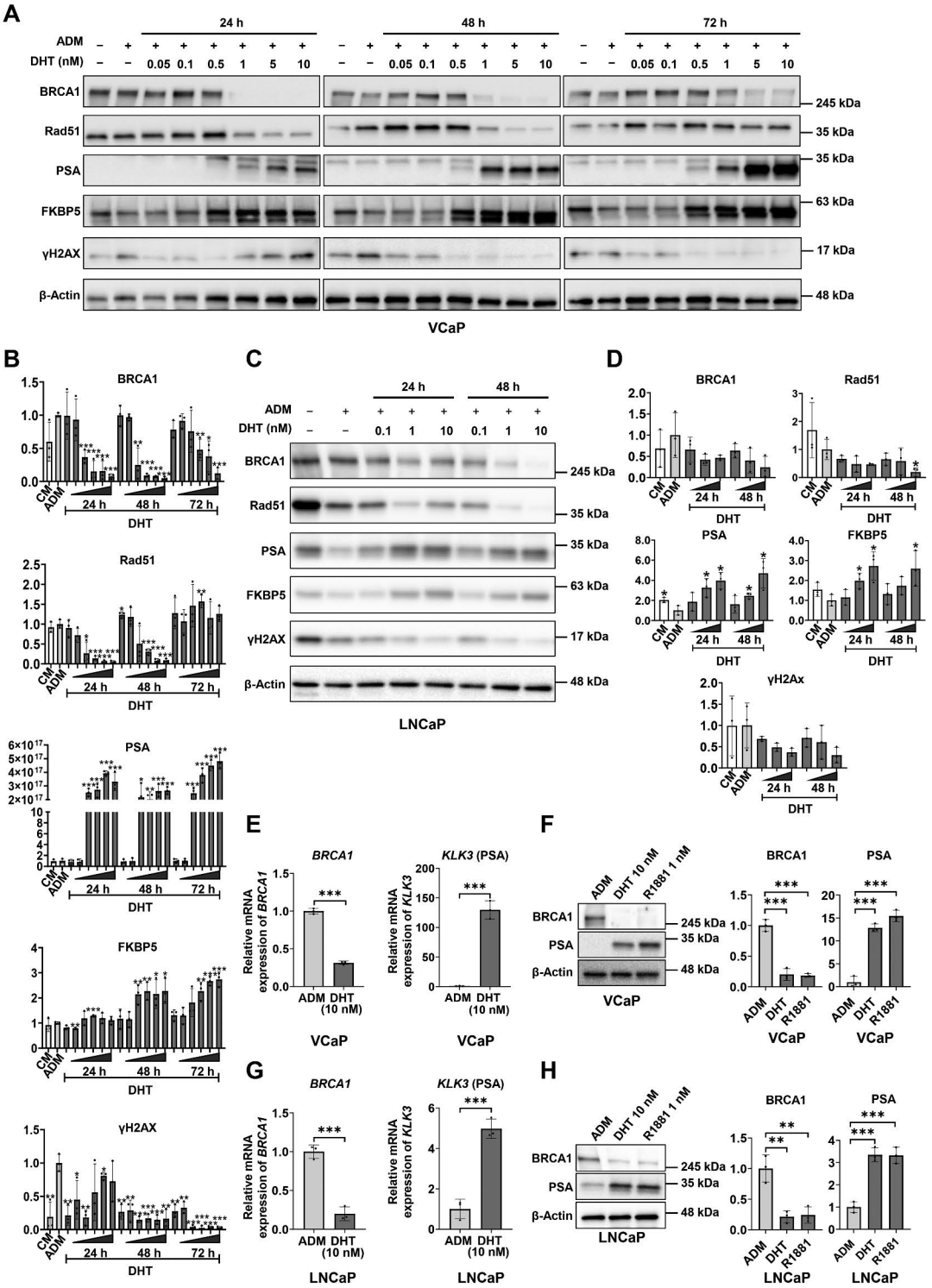

Figure 1 Legend on next page.

protein products of AR target genes KLK3 and FKBP5, BRCA1 and Rad51 expression levels were downregulated in contrast to previous reports of AR activation inducing DDR gene expression.

Stimulation of AR signaling was performed similarly in LNCaP cells (Figure 1C,D). As expected for a cell line with a lower degree of AR amplification, PSA and FKBP5 responses were less extreme, yet highly dose-dependent, while the trends matched the results with VCaP cells for all readouts, and only Rad51 reached significance. These results imply that, unlike known target genes, the HR proteins BRCA1 and Rad51 were not upregulated after stimulating the AR with a natural ligand.

We also examined the correlation between *BRCA1* and AR transcriptional target mRNAs in PCa patient, patient-derived organoid, and patient-derived xenograft datasets [6,9,18,25–27] (supplementary material, Figure S1A,B). The datasets showed a trend of negative correlation, further supporting a possible repressive function of AR activation over *BRCA1*.

Next, we wanted to determine how AR activation mediated BRCA1 downregulation. BRCA1 seemed to be oppositely regulated at similar doses and timepoints as the upregulated AR targets, suggesting that *BRCA1* was regulated by AR activation at the transcriptional level. To test this, we performed RT-qPCR in VCaP cells subjected to 10 nM DHT or vehicle after AD and observed downregulated *BRCA1* mRNA levels in response to AR stimulation (Figure 1E). Synthetic androgen R1881 (1 nM) also downregulated BRCA1 in VCaP cells in a comparable manner to DHT (Figure 1F). Similarly, significant reductions were observed in LNCaP cells (Figure 1G,H). A response in *BRCA1* mRNA to R1881 was also observed by analyzing a published RNA dataset [21] (supplementary material, Figure S1C). This suggested that AR activation repressed *BRCA1* by suppressing its transcription.

AD induces DNA damage and activates BRCA1 in PCa cells

We used media supplemented with a steroid-free serum to deprive AR of its ligand in order to mimic ADT. As expected, VCaP and LNCaP cells showed downregulation of PSA, while 22Rv1, with high AR-V7 expression, retained PSA expression (Figure 2A–D).

We observed upregulation of total BRCA1 in VCaP and LNCaP cells under AD conditions, suggesting that AR-mediated repression of *BRCA1* was abolished upon AD (Figure 2A–C; supplementary material, Figure S2A,B). In contrast, this effect appeared transient in the LNCaP cells, but sustained in VCaP cells. In 22Rv1 cells with no clear PSA response to AD, BRCA1 levels were constant, suggesting that *BRCA1* remained repressed by constitutive AR-V7 activation (Figure 2A,D; supplementary material, Figure S2C). This supported the conclusion that BRCA1 protein levels are linked to AR activity. We observed upregulated γH2Ax and cleaved caspase-3 levels in all cell lines, notably also in the 22Rv1 cell line (Figure 2A–D). We also observed increased levels of phosphorylated BRCA1 (pBRCA1) [28] in all cell lines, indicative of its activation. This suggested that the regulation of BRCA1 activation was separate from the regulation of its expression and might have been induced by AD-related DNA-damaging processes in PCa.

Rad51 was observed to have a trend of downregulation in all cell lines, reaching significance in VCaP and 22Rv1 cells (Figure 2A–D). This suggested that Rad51, unlike BRCA1, did not have a simple inverse correlation with AR activation.

S6 and Akt, as readouts of the PI3K-Akt/mTOR signaling pathway involved in the regulation of cell growth, survival, and protein synthesis, showed an initial surge of phosphorylation in response to AD, but were strongly dephosphorylated at later timepoints in VCaP and 22Rv1 cells (Figure 2A–D; supplementary material, Figure S2A–C). Not surprisingly, this pattern was not present for Akt and barely detectable for phosphorylated S6 (pS6) in LNCaP cells, where constitutive Akt activation due to PTEN loss likely limits further phosphorylation.

Taken together, our results demonstrated that BRCA1 levels were induced in conditions that showed PSA decrease, further supporting the idea that AR activation mediates the repression of BRCA1 levels. Also, γH2Ax, cleaved caspase-3, and pBRCA1 were induced by AD in all cell lines independently of PSA response. This suggested that AR regulates *BRCA1* expression, while BRCA1 phosphorylation appeared to be initiated

Figure 1. BRCA1 and Rad51 expression is repressed by AR activation. (A) Representative western blotting of BRCA1, Rad51, PSA, FKBP5, γH2Ax, and β-actin (loading control) expression in VCaP cells treated with DHT (0.05–10 nM) for 24, 48, and 72 h after preincubation in ADM for 96 h before lysis. Vehicle (methanol) and ADM (96 h) were used as controls. (B) Bar graphs depicting pooled western blotting densitometry results of three independent biological repeats in VCaP cells. Statistical comparisons were performed relative to ADM. (C) Representative western blotting of LNCaP cells treated with DHT (0.1–10 nM) for 24 h, and 48 h after preincubation in ADM for 96 h before lysis with vehicle (methanol) and ADM (96 h) as controls. (D) Bar graphs depicting pooled western blotting densitometry results of three independent biological repeats in LNCaP cells. (E) Bar graphs depicting relative expression of *BRCA1* and *KLK3* (gene encoding PSA) mRNA by RT-qPCR in VCaP cells subjected to ADM for 72 h or DHT (10 nM) for 24 h after 48 h of ADM. (F) Representative western blotting and bar graphs of BRCA1, PSA, and loading control expression in VCaP cells subjected to 72 h of ADM, 24 h of DHT (10 nM), and 24 h R1881 (1 nM) treatments after 48 h of ADM. Vehicle (methanol and/or ethanol) were added to wells not containing DHT and/or R1881, respectively. (G) Bar graphs depicting relative expression of *BRCA1* and *KLK3* mRNA by RT-qPCR in LNCaP cells subjected to ADM for 72 h or DHT (10 nM) for 24 h after 48 h of ADM. (H) Representative western blotting and bar graphs of BRCA1, PSA, and loading control expression in LNCaP cells subjected to 72 h of ADM, 24 h of DHT (10 nM), and 24 h R1881 (1 nM) treatments following 48 h of ADM. Control wells that did not receive DHT or R1881 were treated with the corresponding vehicle (methanol for DHT and ethanol for R1881). The mean and SD from three experiments are represented as bar graphs (*$p < 0.05$, **$p < 0.01$, and ***$p < 0.001$ as determined by Student's *t*-test).

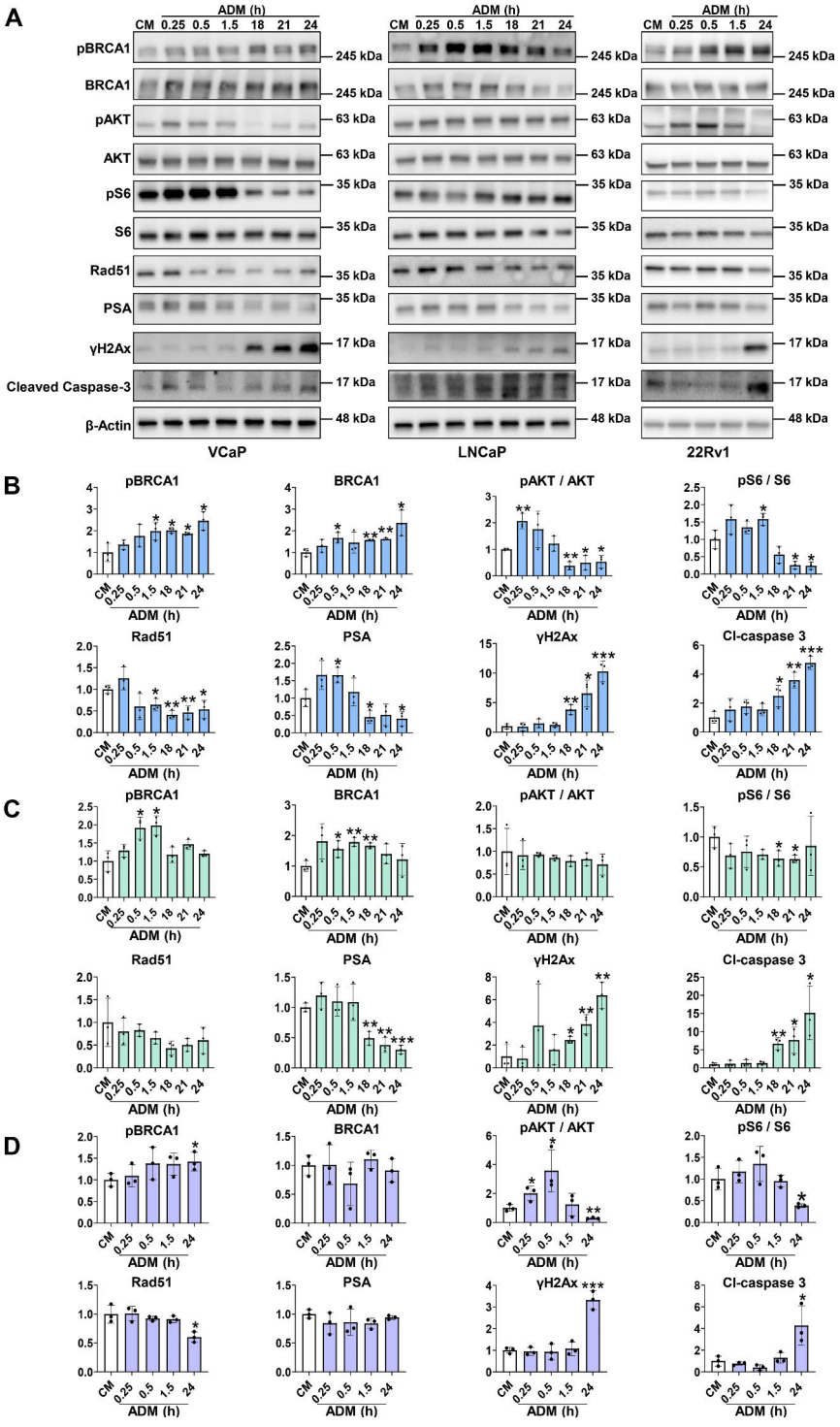

Figure 2 Legend on next page.

primarily by DNA-damaging processes, independent of AR.

ADT induces DNA damage and BRCA1 phosphorylation in murine VCaP xenografts

To assess the reproducibility of our findings *in vivo*, we used a murine VCaP xenograft model of ADT (Figure 3A). Tumor volume and PSA were measured weekly, and after sacrifice, tumor weight as well as tumor tissue section area were measured. As expected, trends suggesting tumor regression and concurrent PSA decline were observed in response to ADT (supplementary material, Figure S3A,B), suggesting that reduced AR may lead to cell death in xenograft tumors (supplementary material, Figure S3C,D).

Next, we performed IHC on xenograft tumors using γH2Ax, pBRCA1, Rad51, and pS6 antibodies and measured relative areas of strong positive staining (Figure 3B). We observed induced γH2Ax, increased pBRCA1, decreased Rad51, and decreased pS6 based on the staining of the VCaP xenografts from day 2, matching our earlier VCaP cell results (Figure 2A,B), indicating that these proteins were indeed regulated *in vivo* (Figure 3C,D; supplementary material, Figures S3E and S4A). Samples from day 5 showed similar trends, albeit with greater variability, which may have resulted from the most severely affected cells perishing by this later timepoint. A massive sudden DNA damage event, if inadequately resolved, would likely have resulted in cell death. Consequently, the surviving cells at later timepoints may have become enriched for unaffected cells, potentially contributing to the observed variability. Importantly, pBRCA1 staining negatively correlated with PSA, further evidencing that AR activity is inversely associated with BRCA1 (Figure 3E). Interestingly, the correlation was also evident when analyzing the intact group separately, suggesting that BRCA1 regulation by AR activity was significant already without intervention (supplementary material, Figure S4B). Taken together, these data supported our finding that AD induced DNA damage and increased BRCA1 activation.

ADT induces expression and phosphorylation of BRCA1 and increases DNA damage in clinical PCa specimens

We further investigated whether the protein expression of BRCA1, pBRCA1, and γH2Ax is altered in clinical PCa tumors upon ADT, similar to our *in vitro* and *in vivo* models. Paired samples from 11 PCa patients before (all primary tumors) and after ADT (64% from metastases, 64% CRPC, Table 1) were analyzed by IHC using the antibodies against BRCA1, pBRCA1, and γH2Ax (Figure 3F; supplementary material, Figure S5). Based on scoring of IHC staining, BRCA1, pBRCA1, and γH2Ax were upregulated post-ADT in all cases except one, suggesting that DNA damage and active phospho-BRCA1 became enriched post-ADT and may have contributed to the development of resistance to ADT.

AD induces BRCA1 together with the antioxidant transcription factor NRF2

We investigated previously published transcriptomic data from *BRCA1*-silenced PCa cells [22]. To assess which processes were potentially lost during BRCA1 repression and promoted during BRCA1 activation, we focused on genes downregulated in *BRCA1*-silenced cells (Figure 4A–C). We observed that the differentially expressed genes showed the highest association with gene sets relating to biological processes and hallmarks that already had an established association with *BRCA1*. Notably, the number one oncogenic gene set associated with changes seen in this PCa cell line was a set of NRF2-regulated genes [29,30] (Figure 4C). AD has been suggested to increase the expression of antioxidant markers and ROS in PCa cells, which is linked to castration resistance [31,32]. We hypothesized that ROS could, in part, be linked to the observed BRCA1 phosphorylation as a universal response to AD because the BRCA1 phosphorylation site activator ATM is also directly activated by ROS [33]. NRF2 is a well-attributed master transcription factor for antioxidant synthesis [5,34]. BRCA1 was previously reported to regulate NRF2-dependent antioxidant signaling by physically interacting with NRF2 and promoting its stability and activation [3–5]. Here, we observed that 5 days of ADM upregulated both BRCA1 and NRF2 expression (Figure 4D). Furthermore, ADM-induced BRCA1 expression was blocked upon *NFE2L2* (NRF2) knockdown (Figure 4E). These data suggested that NRF2 was indeed involved in BRCA1 regulation in response to AD.

The BRCA1-NRF2 regulatory axis regulates PCa cell spheroidal growth

Next, we examined the effects of modified *BRCA1* expression in PCa cells. We chose to use siRNA for gene silencing, given its ability to partially retain protein expression, thereby protecting cell viability from the complete loss of essential functions of BRCA1. After silencing *BRCA1*, no difference was observed in the viability of LNCaP cells in 2D culture (Figure 5A); however, a 54.5% smaller size was observed for LNCaP cell spheroids (Figure 5B–D). In AR-negative

Figure 2. AD induces DNA damage and cell death in PCa. (A) Representative western blotting depicting expression of key HR components, AR targets, and markers of PI3K-Akt/mTOR signaling, DNA damage, and apoptosis with loading control expression in VCaP, LNCaP, and 22Rv1 cells subjected to ADM (0.25–24 h) along with control (normal culture media, CM). (B–D) Bar graphs depicting pooled western blot densitometry results of three biological repeats. The mean and SD from three experiments are represented as a bar graph (*$p < 0.05$, **$p < 0.01$, and ***$p < 0.001$ as determined by Student's *t*-test).

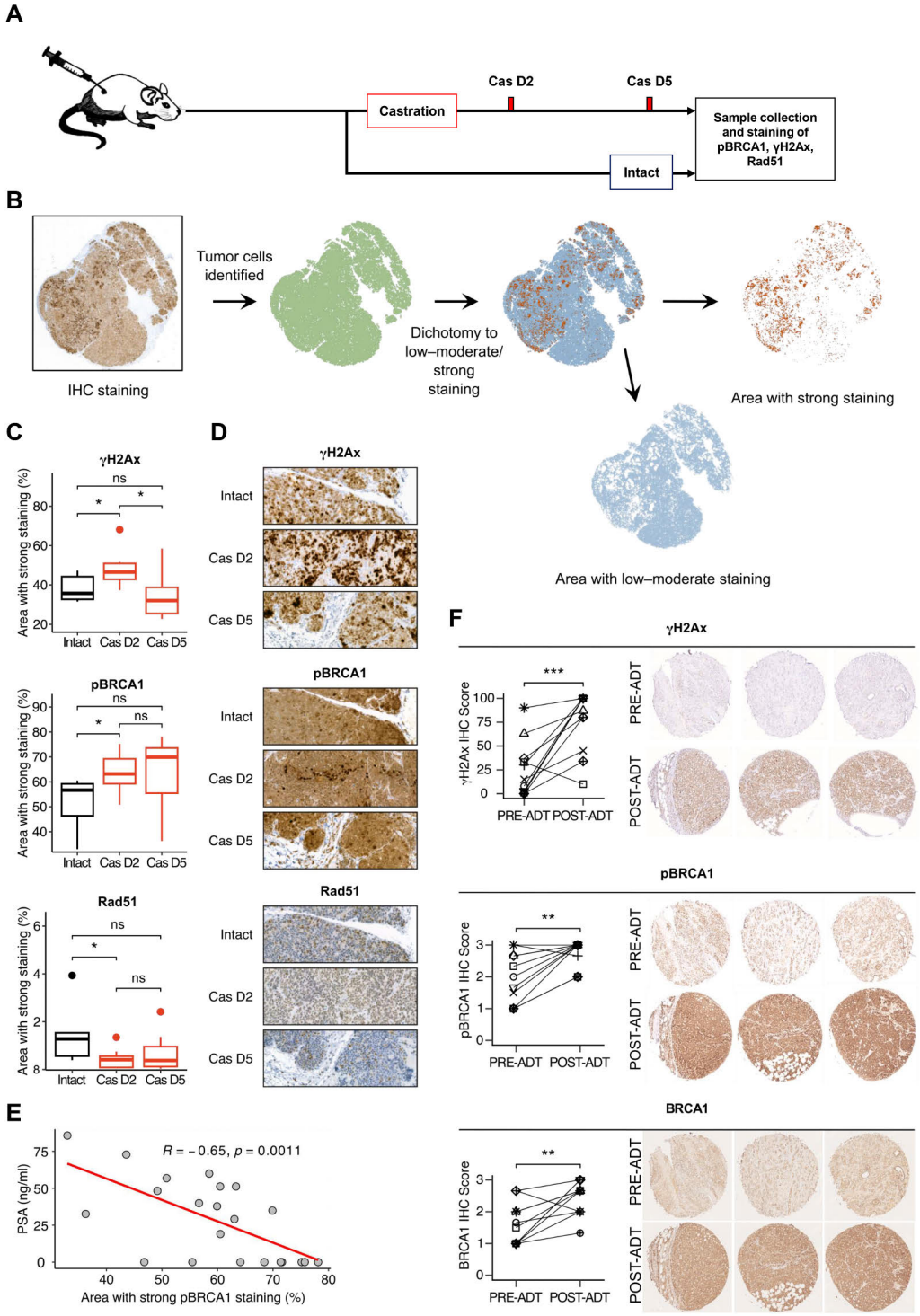

Figure 3 Legend on next page.

Table 1. Baseline characteristics of the patients.

Age (years) at initial diagnosis of prostate cancer	
Median (range)	58 (54–79)
Gleason score at initial diagnosis of prostate cancer (*n*, %)	
7	4 (36)
8	3 (27)
9	4 (36)
PSA (μg/l) level at primary diagnosis	
Median (range)	13 (3.9–57)
Initial treatment (*n*, %)	
ADT + RT	3 (27)
Surgery + ADT	6 (54)
ADT only	2 (18)
Time since start of ADT to post-ADT sample (months)	
Median (range)	66 (18–107)
Other hormonal treatments after ADT (*n*, %)	
AR inhibitors	11 (100)
Abiraterone	1 (9)
Origin of post-ADT sample (*n*, %)	
Prostate (TURP)	4 (36)
Metastasis	7 (64)
Clinical castration resistance at post-ADT sample (*n*, %)	
CRPC	7 (64)
No[a]	4 (36)
Metastases[b] (*n*, %)	
None	1 (9)
Bone only	2 (18)
Lymph node only	1 (9)
Bone + lymph node or visceral only	6 (54)
Visceral	5 (45)

Abbreviation: ADT, androgen deprivation therapy; CRPC, castration-resistant prostate cancer; PSA, prostate-specific antigen; RT, radiotherapy; TURP, transurethral resection of the prostate.
[a]Relapse after ADT but no CRPC at the time of post-ADT sample.
[b]At the time of post-ADT sample.

PC-3 cells, *BRCA1* knockdown had no significant effect on confluence of cells in 2D culture, but the spheroids in 3D were 84.5% smaller (supplementary material, Figure S6A–E), similar to LNCaP cells. Taken together, this suggested that the function of BRCA1 was more important for PCa cells in the 3D culture context, enriched with ROS [35,36].

Interestingly, silencing *NFE2L2* reduced spheroid size in the LNCaP cells, similar to silencing *BRCA1* (Figure 5E). Moreover, silencing of *BRCA1* in LNCaP cells downregulated the protein products of NRF2 target genes, NQO1 and FTH1, in 3D culture (Figure 5F). In PC-3 cells, silencing of *BRCA1* equally led to downregulation of NRF2 targets, as well as NRF2 itself (supplementary material, Figure S6F). These results suggested a bidirectional regulatory axis for BRCA1 and NRF2 in PCa cells.

Whereas *BRCA1* is well known to be mutated in PCa and is among the PCa predisposing DDR genes, we found that amplified *BRCA1* was also observed at similar rates compared to mutations across published cohorts [6,7,9,11,37,38] (Figure 5G). Furthermore, we found that neuroendocrine PCa (NEPC) features were more common in patients with high *BRCA1* expression levels in metastatic CRPC [6] (Figure 5H). This and the fact that BRCA1 was expressed in all widely used PCa cell lines suggested that BRCA1 expression is still prevalent in non-BRCA1 mutated PCa.

We examined *BRCA1* expression in public patient datasets and found that high *BRCA1* expression was correlated with shorter progression- and disease-free survival in TCGA and MSK cohorts, respectively, whereas the effect on overall survival was not significant in TCGA [18] (Figure 5I,J). Furthermore, we found that high expression of *BRCA1* and several known NRF2-regulated genes are associated with worse overall survival in metastatic CRPC patients in the SU2C dataset [6] (Figure 5K; supplementary material, Table S5) [6]. Taken together, these data suggest that high *BRCA1* expression is prevalent in progressing PCa. The frequencies of *BRCA1* mutations were low in the analyzed cohorts, and consequently, the low *BRCA1* groups do not represent the aggressive phenotype of genomic *BRCA1* loss. Therefore, it is plausible that the observed survival correlations were a consequence of AR activation-mediated modulation of the BRCA1-NRF2 regulatory axis. Thus, we conclude that the tumor suppressor gene *BRCA1* is expressed and activated by ADT for its antioxidant properties and repressed during hyperactive AR signaling, putatively exacerbating progression via the loss of its tumor suppressive function (Figure 6).

Discussion

Preclinical studies in PCa have suggested that AR signaling regulates DDR [12–16]. However, findings from these studies are in part contradictory, and the regulation of *BRCA1* by natural ligands of AR or ADT has not been reported [12–16]. Moreover, the low frequency of *BRCA1* mutations observed in PCa compared to the high frequency observed in other HR-prone cancers, such as breast and ovarian cancer, remains unexplained [10]. Therefore, we sought to systematically characterize the regulation of

Figure 3. BRCA1 expression is retained and phosphorylated in response to ADT. (A) A schematic figure representing the sample generation process of Intact, Cas D2, and Cas D5 VCaP mice xenograft tumors. (B) A schematic figure representing the analysis pipeline in QuPath for scoring the IHC staining. (C) Boxplots depicting the percentages of strong IHC staining of pBRCA1, Rad51, and γH2Ax in VCaP xenograft tumors (ns = not significant and $*p < 0.05$ as determined by Mann–Whitney *U*-test). (D) Representative images of IHC staining in VCaP xenograft tumor. High-resolution versions of the images shown are provided in the supplementary material, Figure S4A. (E) Scatterplots depicting Pearson correlation between PSA concentration (ng/ml) and the percentage of strong IHC staining of BRCA1 in VCaP xenograft tumors. (F) Representative IHC staining and scoring of γH2Ax, pBRCA1, and BRCA1 from PCa samples obtained from the same patients before and after starting ADT (representative images shown, total $n = 11$ patients, $*p < 0.05$ and $**p < 0.01$ as determined by Student's *t*-test). High-resolution versions of the images shown are provided in the supplementary material, Figure S5.

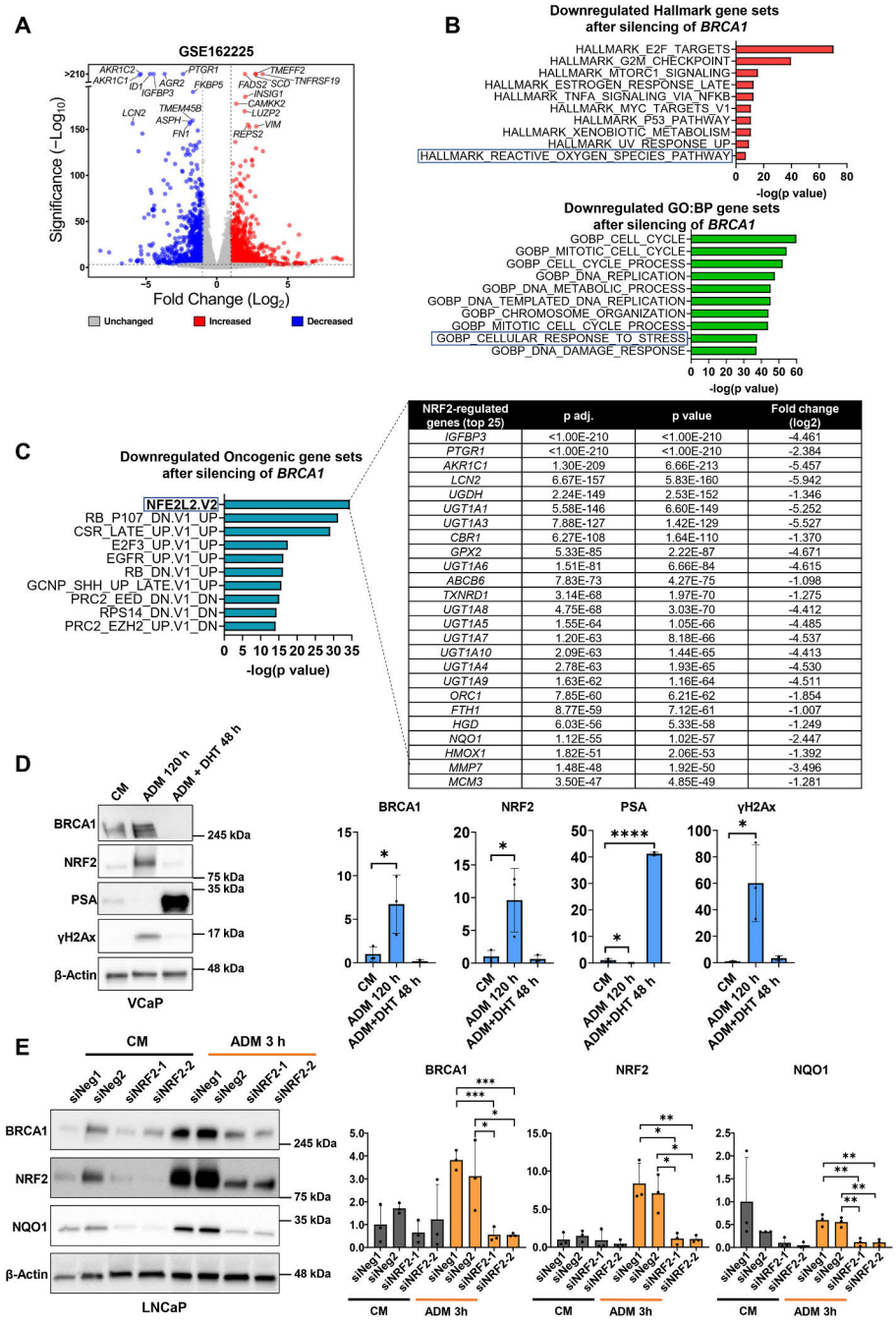

NRF2-regulated genes (top 25)	p adj.	p value	Fold change (log2)
IGFBP3	<1.00E-210	<1.00E-210	-4.461
PTGR1	<1.00E-210	<1.00E-210	-2.384
AKR1C1	1.30E-209	6.66E-213	-5.457
LCN2	6.67E-157	5.83E-160	-5.942
UGDH	2.24E-149	2.53E-152	-1.346
UGT1A1	5.58E-146	6.60E-149	-5.252
UGT1A3	7.88E-127	1.42E-129	-5.527
CBR1	6.27E-108	1.64E-110	-1.370
GPX2	5.33E-85	2.22E-87	-4.671
UGT1A6	1.51E-81	6.66E-84	-4.615
ABCB6	7.83E-73	4.27E-75	-1.098
TXNRD1	3.14E-68	1.97E-70	-1.275
UGT1A8	4.75E-68	3.03E-70	-4.412
UGT1A5	1.55E-64	1.05E-66	-4.485
UGT1A7	1.20E-63	8.18E-66	-4.537
UGT1A10	2.09E-63	1.44E-65	-4.413
UGT1A4	2.78E-63	1.93E-65	-4.530
UGT1A9	1.63E-62	1.16E-64	-4.511
ORC1	7.85E-60	6.21E-62	-1.854
FTH1	8.77E-59	7.12E-61	-1.007
HGD	6.03E-56	5.33E-58	-1.249
NQO1	1.12E-55	1.02E-57	-2.447
HMOX1	1.82E-51	2.06E-53	-1.392
MMP7	1.48E-48	1.92E-50	-3.496
MCM3	3.50E-47	4.85E-49	-1.281

Figure 4. BRCA1 associates with NRF2-mediated antioxidant signaling during AD-induced oxidative stress in PCa. (A) Volcano plot depicting differentially regulated genes in LNCaP cells after silencing *BRCA1*. (B) Plots of significantly downregulated Hallmark gene sets and GO:BP gene sets from MSigDB after silencing *BRCA1* in LNCaP cells (C) Significantly downregulated Oncogenic gene sets from MSigDB after silencing *BRCA1* in LNCaP cells. The Table highlights the top 25 downregulated genes after silencing *BRCA1*, in the gene set NFE2L2.V2, based on genes downregulated after silencing *NFE2L2*. (D) Western blotting and bar graphs of pooled western blotting densitometry depicting BRCA1, NRF2, PSA, γH2Ax, and loading control expression in VCaP cells subjected to vehicle (methanol), 5 days of ADM, and 48 h of DHT (10 nM) after 3 days of ADM treatment. (E) Western blotting and bar graphs of pooled western blotting densitometry depicting BRCA1, NRF2, NQO1, and loading control expression after transfection with siNeg1, siNeg2, siNRF2-1, and siNRF2-2 with or without ADM (3 h) in LNCaP cells. The mean and SD from three experiments are represented as bar graph, unless otherwise indicated (ns = not significant, $*p < 0.05$, and $**p < 0.01$ as determined by Student's *t*-test).

BRCA1 by AR and explore the functions of BRCA1 in PCa.

Our results demonstrate that AR activation by ligand mediates the repression of *BRCA1* transcription. The inverse correlation between AR activation and BRCA1 expression was further reinforced by our mouse xenograft data and *in silico* analyses. *BRCA1* has been suggested to be repressed by Id4, the E2F family of

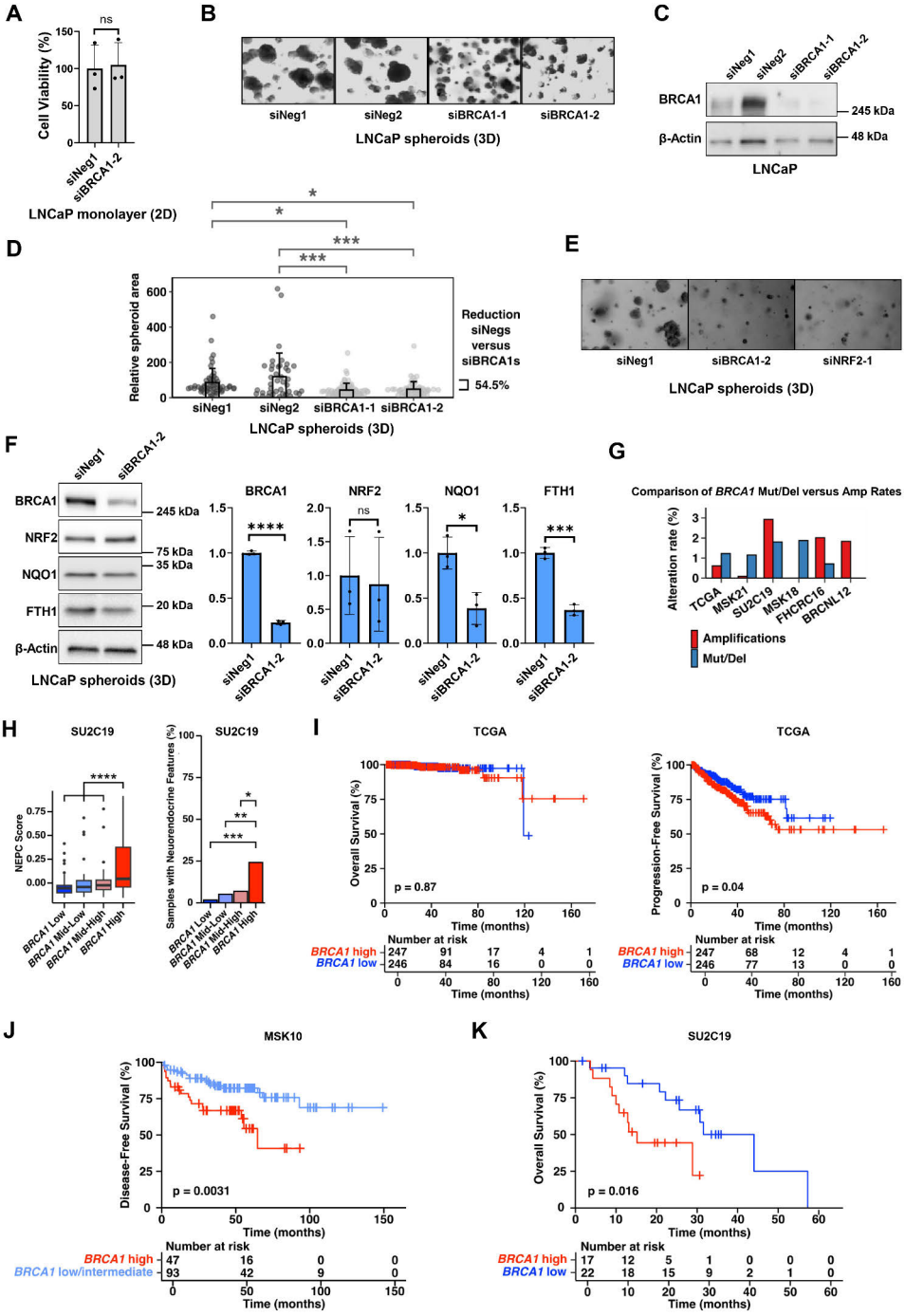

Figure 5 Legend on next page.

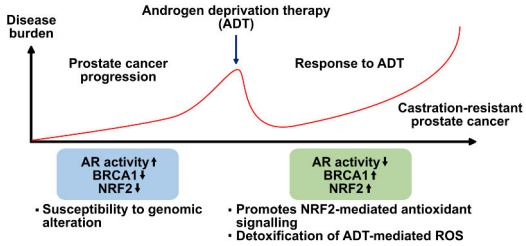

Figure 6. PCa uses AR to repress the BRCA1 tumor suppressor function and to hijack the BRCA1-NRF2 regulatory axis in ROS defense. A schematic diagram depicting how the alternating states of AR activation, dynamically regulated by PCa progression and response to ADT, result in reduced caretaker activity of BRCA1 or improved ROS defense via the modulation of BRCA1-NRF2 regulatory axis in PCa.

transcription factors, Slug, and microRNAs [39–42]. This suggests that the AR may regulate or interact with these or other yet-unidentified repressors or that it directly represses *BRCA1*. The frequency of *BRCA1* mutations found in breast and ovarian cancer is high compared to other cancer types. This has been hypothesized to result from other tissues not surviving without BRCA1 expression [43]. Our finding demonstrating that *BRCA1* is repressed under AR activation provides a rationale for the hypothesis that the AR-driven PCa repression may transiently impair the tumor suppressor function of BRCA1, thus supporting the accumulation of oncogenic alterations. Therefore, the already impaired tumor suppressor gene function would provide no selective pressure toward somatic *BRCA1* mutations. On the other hand, we found that ADT activates *BRCA1* to defend against ROS, which may, in turn, select against somatic *BRCA1* mutations.

Interestingly, ADM induced DNA damage and apoptosis, while simultaneously increasing BRCA1 expression or phosphorylation independently of AR activation. This suggested that BRCA1 phosphorylation might be more sensitive towards other AD-induced processes, such as ROS. Alternatively, the putative dephosphorylation or inhibition of BRCA1 phosphorylation may require the nuclear localization of domains that are absent in non-full-length AR-V7 present in 22Rv1, as full-length AR remains cytoplasmic during AD. Furthermore, we demonstrated that AD similarly induced both BRCA1 and NRF2, and silencing *BRCA1* or *NFE2L2* resulted in a reciprocal downregulation in specific conditions such as AD, organoid culture, or AR-negative cells, which suggests the involvement of ROS. AD induces ROS-mediated oxidative stress, and BRCA1 regulates and interacts with NRF2 [3–5,33,34]. Our data revealed that the BRCA1-NRF2 regulatory axis is active in PCa and potentially hijacked by CRPC to defend against toxic ROS.

Patient data suggested that high *BRCA1* expression was linked to a poor prognosis of PCa patients. High *BRCA1* levels were also found to be associated with neuroendocrine PCa features. Interestingly, a recent patient-derived organoid study showed increased DDR gene expression in neuroendocrine PCa samples, which suggests that AR independence is linked to the increased function of some DDR genes [26]. This complements our finding that, while *BRCA1* appears to be suppressed in association with AR activation in AR-driven PCa, its expression remains unaffected in less AR-dependent PCa.

In conclusion, our study sheds light on the role of the tumor suppressor BRCA1 in PCa. Inherited *BRCA1* mutations are associated with a predisposition for aggressive PCa, but most PCa patients still carry intact *BRCA1*. We demonstrate that AR mediates *BRCA1* repression and that ADT activates, rather than suppresses, BRCA1 expression in PCa. Thus, we propose that BRCA1 plays two distinct roles in PCa when not mutated: first, as a repressed tumor suppressor, thus putatively promoting tumorigenesis and progression and, in the later stage, through ADT-mediated activation, to protect tumor cells against ROS by inducing NRF2 and its targets.

Acknowledgments

We thank Sinikka Collanus and the Histology core facility of the Institute of Biomedicine, University of Turku, for their assistance with IHC. We thank Minna Santanen, Jukka Karhu, and Barbara Ramos Artigot for their

Figure 5. BRCA1 supports organotypic 3D spheroid growth of PCa cells. (A) Plots representing cell viability (%) of LNCaP cells with or without *BRCA1* knockdown. (B) Representative brightfield images from day 7 in 3D culture of LNCaP cells treated with siNeg1, siNeg2, siBRCA1-1, or siBRCA1-2. (C) Western blotting depicting BRCA1 and loading control expression 48 h after transfection for 3D culture in LNCaP cells. (D) Plots depicting relative 3D spheroid area in brightfield images for LNCaP cells on day 7 of 3D culture. (E) Representative brightfield images from day 5 in a 3D culture of LNCaP cells treated with siNeg1, siBRCA1-2, or siNRF2-1. (F) Western blotting and bar graphs depicting the expression of NRF2 and its targets NQO1 and FTH1 along with BRCA1 and loading control expression after 5 days of 3D culture in LNCaP cells with or without *BRCA1* knockdown. (G) Plots representing *BRCA1* alterations in PCa patient datasets TCGA [37], MSK21 [38], SUC19 [6], MSK18 [7], FHCRC16 [9], and BRCNL12 [11]. (H) Plots representing the presence of histological NEPC features and transcript-based NEPC score in PCa patients stratified by *BRCA1* mRNA expression quartiles analyzed from the SU2C cohort. (I) Kaplan–Meier plot depicting overall survival and progression-free survival of PCa patients stratified by *BRCA1* mRNA medians analyzed from the TCGA PanCancer Atlas cohort. (J) Kaplan–Meier plot depicting disease-free survival of PCa patients stratified by *BRCA1* mRNA expression tertiles, comparing the highest tertile to the combined lower tertiles analyzed from the MSK Cancer Cell 2010 cohort. (K) Kaplan–Meier plot depicting overall survival of PCa patients stratified by *BRCA1* mRNA quartiles, comparing the highest quartile to the lowest quartile analyzed from the SU2C cohort. Statistical significance of the Kaplan–Meier survival curves was determined using the log-rank test. The mean and SD from three experiments are represented as bar graphs (*$p < 0.05$, **$p < 0.01$, and ***$p < 0.001$ as determined by Student's *t*-test).

excellent technical assistance. We also thank the Turku Center for Disease Modeling (TCDM), Guillermo Martinez Nieto, and Petra Sipilä for providing their expertise in generating mouse xenograft models. We thank Syeda Afshan for providing us with synthetic androgen R1881 for the studies. The results here are partly based upon data generated by the TCGA Research Network: https://www.cancer.gov/tcga. This study was supported by grants from the Academy of Finland, Finnish Medical Foundation, Cancer Foundation Finland, Cancer Society of Southwest Finland, Turku University Foundation, Hospital District of Southwest Finland, Sigrid Jusélius Foundation, Paulo Foundation, Instrumentarium Foundation, Finnish National Agency for Education (EDUFI) and Turku Doctoral Programme of Molecular Medicine. Open access publishing facilitated by Turun yliopisto, as part of the Wiley - FinELib agreement.

Author contributions statement

SS, VV, AK and MS designed the study, conceived the experiments, and analyzed the data. SS, VV and AK prepared the figures. SS, VV, AK, AL and MT carried out experiments. SS, VV, AK and MS designed the *in silico* analyses. MP designed the xenograft experiment. PT designed the human IHC analyses and provided the samples. GW analyzed the human IHC samples. SS, VV and MS wrote the article and all authors commented on and approved the final version. MS acquired the funding and supervised the study.

Data availability statement

Raw data generated in this study are available upon reasonable request to the corresponding author.

References

1. Venkitaraman AR. Cancer susceptibility and the functions of BRCA1 and BRCA2. *Cell* 2002; **108**: 171–182.
2. van Vugt MA, Parkes EE. When breaks get hot: inflammatory signaling in BRCA1/2-mutant cancers. *Trends Cancer* 2022; **8**: 174–189.
3. Bae I, Fan S, Meng Q, *et al*. BRCA1 induces antioxidant gene expression and resistance to oxidative stress. *Cancer Res* 2004; **64**: 7893–7909.
4. Gorrini C, Baniasadi PS, Harris IS, *et al*. BRCA1 interacts with Nrf2 to regulate antioxidant signaling and cell survival. *J Exp Med* 2013; **210**: 1529–1544.
5. de la Vega MR, Chapman E, Zhang DD. NRF2 and the hallmarks of cancer. *Cancer Cell* 2018; **34**: 21–43.
6. Abida W, Cyrta J, Heller G, *et al*. Genomic correlates of clinical outcome in advanced prostate cancer. *Proc Natl Acad Sci U S A* 2019; **116**: 11428–11436.
7. Armenia J, Wankowicz SA, Liu D, *et al*. The long tail of oncogenic drivers in prostate cancer. *Nat Genet* 2018; **50**: 645–651.
8. Robinson D, Van Allen EM, Wu Y-M, *et al*. Integrative clinical genomics of advanced prostate cancer. *Cell* 2015; **161**: 1215–1228.
9. Kumar A, Coleman I, Morrissey C, *et al*. Substantial interindividual and limited intraindividual genomic diversity among tumors from men with metastatic prostate cancer. *Nat Med* 2016; **22**: 369–378.
10. Nguyen L, Martens WM, Van Hoeck A, *et al*. Pan-cancer landscape of homologous recombination deficiency. *Nat Commun* 2020; **11**: 5584.
11. Barbieri CE, Baca SC, Lawrence MS, *et al*. Exome sequencing identifies recurrent SPOP, FOXA1 and MED12 mutations in prostate cancer. *Nat Genet* 2012; **44**: 685–689.
12. Goodwin JF, Schiewer MJ, Dean JL, *et al*. A hormone–DNA repair circuit governs the response to genotoxic insult. *Cancer Discov* 2013; **3**: 1254–1271.
13. Li L, Karanika S, Yang G, *et al*. Androgen receptor inhibitor–induced "BRCAness" and PARP inhibition are synthetically lethal for castration-resistant prostate cancer. *Sci Signal* 2017; **10**: eaam7479.
14. Asim M, Tarish F, Zecchini HI, *et al*. Synthetic lethality between androgen receptor signalling and the PARP pathway in prostate cancer. *Nat Commun* 2017; **8**: 374.
15. Polkinghorn WR, Parker JS, Lee MX, *et al*. Androgen receptor signaling regulates DNA repair in prostate cancers. *Cancer Discov* 2013; **3**: 1245–1253.
16. Hasterok S, Scott TG, Roller DG, *et al*. The androgen receptor does not directly regulate the transcription of DNA damage response genes. *Mol Cancer Res* 2023; **21**: 1329–1341.
17. Grasso CS, Wu Y-M, Robinson DR, *et al*. The mutational landscape of lethal castration-resistant prostate cancer. *Nature* 2012; **487**: 239–243.
18. Taylor BS, Schultz N, Hieronymus H, *et al*. Integrative genomic profiling of human prostate cancer. *Cancer Cell* 2010; **18**: 11–22.
19. Virtanen V, Paunu K, Kukkula A, *et al*. Glucocorticoid receptor-induced non-muscle caldesmon regulates metastasis in castration-resistant prostate cancer. *Oncogene* 2023; **12**: 42.
20. Huhtaniemi R, Oksala R, Knuuttila M, *et al*. Adrenals contribute to growth of castration-resistant VCaP prostate cancer xenografts. *Am J Pathol* 2018; **188**: 2890–2901.
21. Hoefer J, Kern J, Ofer P, *et al*. SOCS2 correlates with malignancy and exerts growth-promoting effects in prostate cancer. *Endocr Relat Cancer* 2013; **21**: 175.
22. Han H, Wang Y, Curto J, *et al*. Mesenchymal and stem-like prostate cancer linked to therapy-induced lineage plasticity and metastasis. *Cell Rep* 2022; **39**: 110595.
23. Goedhart J, Luijsterburg MS. VolcaNoseR is a web app for creating, exploring, labeling and sharing volcano plots. *Sci Rep* 2020; **10**: 20560.
24. Tsherniak A, Vazquez F, Montgomery PG, *et al*. Defining a cancer dependency map. *Cell* 2017; **170**: e516.
25. Gao D, Vela I, Sboner A, *et al*. Organoid cultures derived from patients with advanced prostate cancer. *Cell* 2014; **159**: 176–187.
26. Anselmino N, Labanca E, Shepherd PD, *et al*. Integrative molecular analyses of the MD Anderson prostate cancer patient-derived xenograft (MDA PCa PDX) series. *Clin Cancer Res* 2024; **30**: 2272–2285.
27. Gerhauser C, Favero F, Risch T, *et al*. Molecular evolution of early-onset prostate cancer identifies molecular risk markers and clinical trajectories. *Cancer Cell* 2018; **34**: 996–1011.e8.
28. Cortez D, Wang Y, Qin J, *et al*. Requirement of ATM-dependent phosphorylation of brca1 in the DNA damage response to double-strand breaks. *Science* 1999; **286**: 1162–1166.
29. Malhotra D, Portales-Casamar E, Singh A, *et al*. Global mapping of binding sites for Nrf2 identifies novel targets in cell survival response through ChIP-seq profiling and network analysis. *Nucleic Acids Res* 2010; **38**: 5718–5734.
30. Kim JW, Botvinnik OB, Abudayyeh O, *et al*. Characterizing genomic alterations in cancer by complementary functional associations. *Nat Biotechnol* 2016; **34**: 539–546.
31. Shiota M, Song Y, Takeuchi A, *et al*. Antioxidant therapy alleviates oxidative stress by androgen deprivation and prevents conversion

from androgen dependent to castration resistant prostate cancer. *J Urol* 2012; **187**: 707–714.
32. Ferrari N, Granata I, Capaia M, *et al*. Adaptive phenotype drives resistance to androgen deprivation therapy in prostate cancer. *Cell Commun Signal* 2017; **15**: 1–14.
33. Guo Z, Kozlov S, Lavin MF, *et al*. ATM activation by oxidative stress. *Science* 2010; **330**: 517–521.
34. Sies H, Jones DP. Reactive oxygen species (ROS) as pleiotropic physiological signalling agents. *Nat Rev Mol Cell Biol* 2020; **21**: 363–383.
35. Rybkowska P, Radoszkiewicz K, Kawalec M, *et al*. The metabolic changes between monolayer (2D) and three-dimensional (3D) culture conditions in human mesenchymal stem/stromal cells derived from adipose tissue. *Cells* 2023; **12**: 178.
36. Liu Q, Zhang Z, Liu Y, *et al*. Cancer cells growing on perfused 3D collagen model produced higher reactive oxygen species level and were more resistant to cisplatin compared to the 2D model. *J Appl Biomater Funct Mater* 2018; **16**: 144–150.
37. ICGC/TCGA Pan-Cancer Analysis of Whole Genomes Consortium. Pan-cancer analysis of whole genomes. *Nature* 2020; **578**: 82–93.
38. Nguyen B, Fong C, Luthra A, *et al*. Genomic characterization of metastatic patterns from prospective clinical sequencing of 25,000 patients. *Cell* 2022; **185**: 563–575.e11.
39. Beger C, Pierce LN, Krüger M, *et al*. Identification of Id4 as a regulator of BRCA1 expression by using a ribozyme-library-based inverse genomics approach. *Proc Natl Acad Sci U S A* 2001; **98**: 130–135.
40. Bindra RS, Gibson SL, Meng A, *et al*. Hypoxia-induced down-regulation of BRCA1 expression by E2Fs. *Cancer Res* 2005; **65**: 11597–11604.
41. Wu Z-Q, Li X-Y, Hu CY, *et al*. Canonical Wnt signaling regulates slug activity and links epithelial–mesenchymal transition with epigenetic breast cancer 1, early onset (BRCA1) repression. *Proc Natl Acad Sci U S A* 2012; **109**: 16654–16659.
42. Chang S, Sharan SK. BRCA1 and microRNAs: emerging networks and potential therapeutic targets. *Mol Cells* 2012; **34**: 425–432.
43. Elledge SJ, Amon A. The BRCA1 suppressor hypothesis: an explanation for the tissue-specific tumor development in BRCA1 patients. *Cancer Cell* 2002; **1**: 129–132.

SUPPLEMENTARY MATERIAL ONLINE

Supplementary materials and methods

Figure S1. Association between AR and BRCA1 in androgen-dependent PCa

Figure S2. Analysis of additional DDR markers in AD conditions and influence of mTOR signaling pathway in HR repair pathway in PCa

Figure S3. Representation of key attributes of Intact, Cas D2, and Cas D5 tumors obtained from VCaP mice xenografts

Figure S4. VCaP xenograft high-resolution IHC images and correlation between PSA levels and BRCA1 staining intensity

Figure S5. PCa patient sample high-resolution IHC images

Figure S6. Association of BRCA1 with organotypic growth and antioxidant signaling pathway in PCa

Table S1. List of siRNAs used in this study

Table S2. List of antibodies used in this study

Table S3. List of TaqMan probes used in this study

Table S4. List of the top 500 downregulated genes in *BRCA1*-silenced LNCaP cells

Table S5. Association of BRCA1 and NRF2 signaling pathway in PCa

Virtanen V, Paunu K, Kukkula A, Niva S, Junila Y, Toriseva M, Jokilehto T, Mäkelä S, Huhtaniemi R, Poutanen M, Paatero I, Sundvall M. (2023)
Glucocorticoid receptor-induced non-muscle caldesmon regulates metastasis in castration-resistant prostate cancer.
Oncogenesis

II

ARTICLE OPEN

Glucocorticoid receptor-induced non-muscle caldesmon regulates metastasis in castration-resistant prostate cancer

Verneri Virtanen[1], Kreetta Paunu[1], Antti Kukkula[1], Saana Niva[1], Ylva Junila[1], Mervi Toriseva[1], Terhi Jokilehto[1], Sari Mäkelä[2], Riikka Huhtaniemi[2], Matti Poutanen[2], Ilkka Paatero[3] and Maria Sundvall[1,4]✉

Lethal prostate cancer (PCa) is characterized by the presence of metastases and development of resistance to therapies. Metastases form in a multi-step process enabled by dynamic cytoskeleton remodeling. An actin cytoskeleton regulating gene, *CALD1*, encodes a protein caldesmon (CaD). Its isoform, low-molecular-weight CaD (l-CaD), operates in non-muscle cells, supporting the function of filaments involved in force production and mechanosensing. Several factors, including glucocorticoid receptor (GR), have been identified as regulators of l-CaD in different cell types, but the regulation of l-CaD in PCa has not been defined. PCa develops resistance in response to therapeutic inhibition of androgen signaling by multiple strategies. Known strategies include androgen receptor (AR) alterations, modified steroid synthesis, and bypassing AR signaling, for example, by GR upregulation. Here, we report that in vitro downregulation of l-CaD promotes epithelial phenotype and reduces spheroid growth in 3D, which is reflected in vivo in reduced formation of metastases in zebrafish PCa xenografts. In accordance, *CALD1* mRNA expression correlates with epithelial-to-mesenchymal transition (EMT) transcripts in PCa patients. We also show that *CALD1* is highly co-expressed with *GR* in multiple PCa data sets, and GR activation upregulates l-CaD in vitro. Moreover, GR upregulation associates with increased l-CaD expression after the development of resistance to antiandrogen therapy in PCa xenograft mouse models. In summary, GR-regulated l-CaD plays a role in forming PCa metastases, being clinically relevant when antiandrogen resistance is attained by the means of bypassing AR signaling by GR upregulation.

Oncogenesis (2023)12:42 ; https://doi.org/10.1038/s41389-023-00485-z

INTRODUCTION

PCa is globally the second most common cancer in men [1]. While a substantial part of local PCa tumors are indolent, a subset of them are aggressive and cannot be curatively treated. Some patients are also diagnosed primarily with metastatic disease. In metastatic PCa, androgen deprivation therapy (ADT) and anti-androgens are used to inhibit the single most important driver of PCa progression—AR signaling. Although most of the patients respond initially, the cancer cells eventually adapt and develop resistance to therapies targeting AR signaling. Resistance to antiandrogens in PCa is currently understood to be attainable by mechanisms leading to restored AR signaling, such as AR amplifications, and other AR-targeting mutations or changes in the adrenal and intratumoral steroid synthesis; AR bypass signaling, such as GR upregulation; and complete AR independence [2]. Further knowledge of these mechanisms is of clinical importance and may uncover potential targets to address antiandrogen resistance in PCa.

Regulation of actin cytoskeleton has a central role in the formation of metastases [3]. *CALD1*-gene encodes two major molecular weight isoforms that regulate actin cytoskeleton by direct actin-binding: high-molecular-weight CaD (h-CaD, 120–150 kDa) and l-CaD (70–80 kDa) [4, 5]. Both isoforms produced by alternative splicing share the currently known functional regions, including regions for binding actin, tropomyosin, calmodulin, myosin, and phospholipids [6, 7]. h-CaD, also known as smooth muscle CaD, is a contractility regulator highly expressed in smooth muscle cells [8]. h-CaD is also expressed in the prostatic stroma, including vascular endothelial cells [9]. l-CaD, on the other hand, is a ubiquitously expressed protein localized in membrane ruffles and lamellipodial extensions of migrating cells and associates with the regulation of microfilaments by actomyosin cross-linking and actin polymerization [5, 10–13]. The effect of l-CaD on contractility and migration, however, seems to be two-fold, as both the loss of and increased levels of l-CaD are reported to result in dysfunctional migration or reduced contractile function [14–16]. In vivo CaD knockout and mutant mouse homozygotes die perinatally, whereas a homozygous loss restricted to h-CaD is not lethal [15, 17–19]. Further, a xenopus morpholino l-CaD knockdown model shows reduced neural crest migration [20]. Additionally, vascular and heart developmental defects are present in a zebrafish morpholino CaD knockdown model; however, similar defects are not reported in other known in vivo models [15, 17–22].

[1]Cancer Research Unit, Institute of Biomedicine, and FICAN West Cancer Center Laboratory, University of Turku, and Turku University Hospital, Kiinamyllynkatu 10, 20520 Turku, Finland. [2]Research Centre for Integrative Physiology and Pharmacology, Institute of Biomedicine, and FICAN West Cancer Center, University of Turku, Kiinamyllynkatu 10, 20520 Turku, Finland. [3]Turku Bioscience Centre, University of Turku and Åbo Akademi University, Tykistökatu 6, 20520 Turku, Finland. [4]Department of Oncology, Turku University Hospital, PL52, 20521 Turku, Finland. ✉email: mahesu@utu.fi

Received: 22 December 2022 Revised: 18 July 2023 Accepted: 25 July 2023
Published online: 12 August 2023

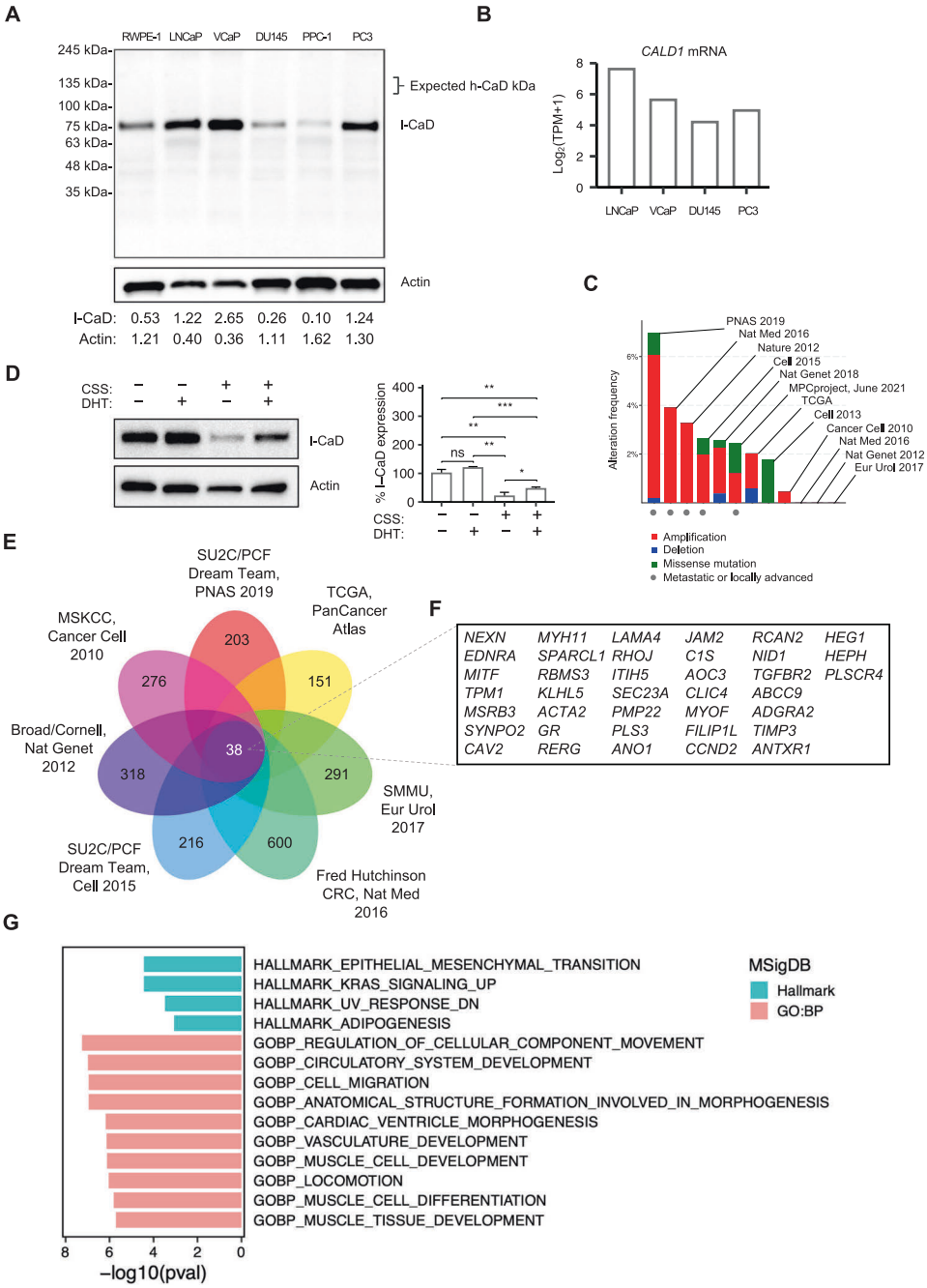

Fig. 1 l-CaD is expressed in PCa cell lines, and *CALD1* co-expresses with positive regulators of EMT in PCa patient data sets. A Western blot depicting l-CaD protein expression in commercial PCa cell lines. **B** Barplots representing *CALD1* mRNA expression data in PCa cell lines acquired from Cancer Cell Line Encyclopedia. **C** Frequency of *CALD1* alterations in publicly available PCa patient data sets containing *CALD1* mutation and copy number alteration data [67–78]. **D** Representative Western blot depicting l-CaD expression and barplot depicting pooled densitometry of Western blot bands from three biological repeats after 72 h of 5% CSS culture and 24 h DHT treatment. **E** Venn diagram showing the concordance of top 1000 mRNAs co-expressed with *CALD1* between PCa patient data sets available on cBioPortal. **F** List of concordant hits of mRNA co-expression with *CALD1*. **G** MSigDB (version 7.5) hallmark gene sets that significantly overlap and ten MSigDB GO:BP gene sets with the highest percentage of overlap with the list of mRNA concordantly co-expressed with *CALD1*.

Published data on the role of l-CaD in cancer are, in part, conflicting and suggest that *CALD1* acts both as a tumor suppressor or as an oncogene. Some preclinical studies suggest that l-CaD suppresses cancer cell migration in vitro [23–28]. However, conversely, in vitro data from both older and more recent studies also suggest that l-CaD promotes migration and invasion of cancer cells [29–33]. Studies based on patient samples suggest that higher l-CaD expression associates with worse prognosis (oral squamous cell carcinoma, gastric cancer, and bladder cancer), higher histopathological grade (glioblastoma and bladder cancer), increased immune infiltrates (gastric cancer and bladder cancer), and metastases (oral squamous cell carcinoma)

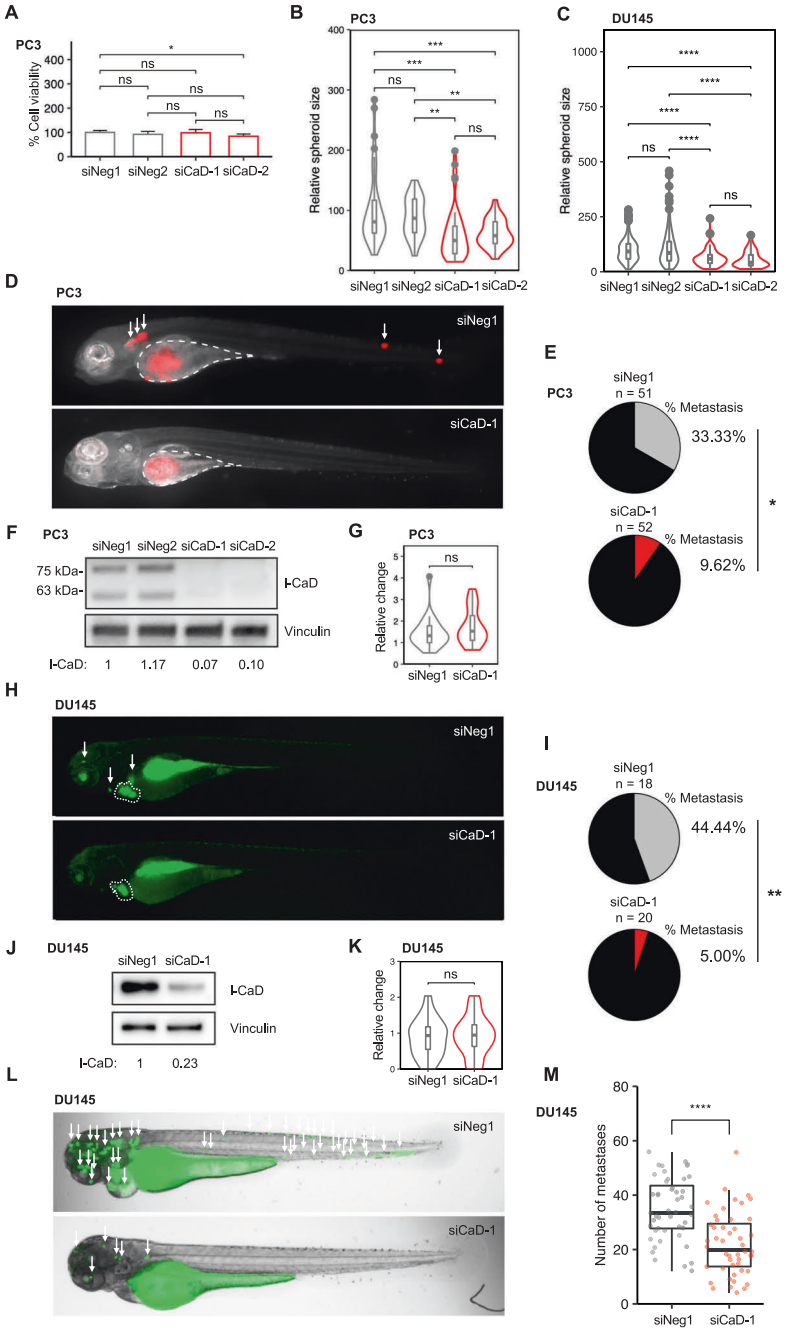

Fig. 2 Loss of l-CaD impairs metastasis and invasion of PCa cells. A Barplot representing viability in PC3 cells transfected with siNeg1, siNeg2, siCaD-1, or siCaD-2. The mean and standard deviation (SD) of three experiments are shown (ns = not significant and $*p < 0.05$ as determined by the Mann–Whitney–Wilcoxon two-sided test). **B** Violin plot of relative spheroid size in PC3 cells ($n = 160$) transfected with siNeg1, siNeg2, siCaD-1, or siCaD-2 and grown in 3D basement membrane matrix culture. Boxplot indicates median and whiskers indicate 1.5 times interquartile range pooled from three experiments (ns = not significant, $**p < 0.01$, and $***p < 0.001$ as determined by *t*-test). **C** Violin plot of relative spheroid size in DU145 cells ($n = 527$) transfected with siNeg1, siNeg2, siCaD-1, or siCaD-2 and grown in 3D basement membrane matrix culture. Boxplot indicates median and whiskers indicate 1.5 times interquartile range pooled from three experiments (ns = not significant, $**p < 0.01$, and $***p < 0.001$ as determined by *t*-test). **D** Representative fluorescent merge images of zebrafish embryos 4 days after yolk sac microinjection of mCherry PC3 cells transfected with siNeg1 or siCaD-1. The injection site is highlighted in white. Metastases are indicated with arrows. **E** Pie chart showing the percentage of zebrafish embryos with visible metastases 4 days after injection pooled from three experiments ($*p < 0.05$ as analyzed by Fisher's exact test). **F** Western blot depicting expression levels of l-CaD in mCherry PC3 cells transfected with siNeg1, siNeg2, siCaD-1, or siCaD-2 48 h after transfection. **G** Representative violin plots of relative change in primary tumor size (size 4 days after injection / size 1 day after injection). The tumor area was measured from fluorescent images of zebrafish. Boxplot indicates median, and whiskers indicate 1.5 times interquartile range (ns = not significant as determined by *t*-test). **H** Representative fluorescent images of zebrafish embryos 4 days after pericardial microinjection of CellTracker Green labeled DU145 cells transfected with siNeg1 or siCaD-1. The primary tumor is highlighted in white. Metastases are indicated with arrows. **I** Pie chart showing the percentage of zebrafish embryos with visible metastases 4 days after injection to the pericardial cavity ($**p < 0.01$ as analyzed by Fisher's exact test). **J** Western blot depicting expression levels of l-CaD in DU145 cells transfected with siNeg1 or siCaD-1 48 h after transfection. **K** Violin plots of relative change in primary tumor size (size 4 days after injection/size 1 day after injection). The tumor area was measured from fluorescent images of zebrafish. Boxplot indicates median, and whiskers indicate 1.5 times interquartile range (ns = not significant as determined by *t*-test). **L** Representative brightfield and fluorescent merge images of zebrafish embryos 1 day after microinjection of CellTracker Green labeled DU145 cells transfected with siNeg1 or siCaD-1 to the common cardinal vein. Metastases are indicated with arrows. **M** Box and jitter plots depicting the number of metastases in zebrafish embryos ($n = 96$). Boxplot indicates median, and whiskers indicate 1.5 times interquartile range ($****p < 0.0001$ as determined by *t*-test).

[31, 32, 34–36]. Additionally, upregulated l-CaD expression associates with therapy resistance to the estrogen receptor modulator tamoxifen in breast cancer and with resistance to chemoradiotherapy in rectal cancer [37, 38]. The regulation of l-CaD expression in cancer is likely yet to be fully uncovered, but several factors, including p53, GR, and Cdk5, are implicated to have a role in specific contexts [24, 30, 39–46].

Here, we have characterized the role of l-CaD in PCa by analyzing co-expression data from the largest PCa patient data sets and experimentally by using monolayer- and 3D-cultured PCa cells, zebrafish PCa xenograft models, and castration-resistant VCaP xenograft mouse models. We show that l-CaD associates with EMT, GR-mediated antiandrogen resistance, and the formation of metastases in PCa. We conclude that l-CaD is critical in forming metastases in PCa and is upregulated in PCa cells that acquire therapy resistance by GR upregulation.

RESULTS

l-CaD is expressed in PCa cell lines and is strongly downregulated during steroid hormone deprivation

To examine which CaD isoforms were expressed in PCa, we performed a Western blot to analyze the protein expression from a variety of commercial PCa cell lines cultured in recommended growth conditions (Fig. 1A). All the tested cell lines solely expressed the non-muscle isoform l-CaD (70–80 kDa). No bands were detected in the 120–150 kDa range where the smooth muscle-associated isoform h-CaD migrates. The protein expression levels detected were in line with mRNA data from the Cancer Cell Line Encyclopedia (Fig. 1B). Notably, no differences in expression between androgen-sensitive and androgen-independent cell lines were observed.

Next, we examined published PCa patient data sets with both mutation and copy number alteration data available to study the frequency of alterations in the *CALD1* gene (Fig. 1C). Overall, *CALD1* alterations in tumors were not particularly common, but interestingly, amplifications were the most common alteration observed, and deletion was the least frequent type of alteration. The data sets with the highest frequency of amplifications were data sets of metastatic or locally advanced tumors. Comparing survival between altered and unaltered patients in the metastatic data sets, we observed a significantly decreased overall survival in a data set of 48 cases of metastatic and high-grade localized PCa, while differences in other data sets were not significant (Supplementary Fig. S1A, B).

To study whether l-CaD was regulated by AR signaling—the major driver of PCa progression—we looked at l-CaD expression in androgen-sensitive VCaP cells in conditions altering the AR activation status. We observed a substantial reduction of l-CaD expression in VCaP cells cultured in charcoal-stripped serum (CSS) media, while the expression levels were increased upon the addition of dihydrotestosterone (DHT) to the cells (Fig. 1D). Next, we wanted to study whether l-CaD associated with AR expression in PCa but found no correlation between *AR* and *CALD1* mRNA expression by examining the published PCa patient data sets, including TCGA (Supplementary Fig. S1C). Taken together, these data suggested that l-CaD expressed in PCa cells strongly responded to steroid hormone deprivation in androgen-sensitive cell lines, but the expression was also retained even in AR-negative cells, and *CALD1* did not correlate with *AR* expression in PCa.

CALD1 expression in PCa is associated with the expression of positive regulators of EMT and known markers of the mesenchymal phenotype

To assess in an unbiased manner which transcripts were associated with *CALD1* in PCa, we performed an integrative analysis of co-expression data from seven PCa data sets (Fig. 1E). We found 38 transcripts that were among the top 1000 positively co-expressed mRNAs in all data sets (Fig. 1F). To this list of 38 transcripts, we performed Molecular Signatures Database (MSigDB) analysis comparing the list with hallmark gene sets and gene ontology gene sets of biological processes (Fig. 1G). Interestingly, the identified list shared transcripts with EMT, cell migration, and locomotion gene sets. The identified EMT-associated transcripts were either involved in the positive regulation of EMT or commonly expressed in the mesenchymal phenotype. Other interrelated gene sets were circulatory system development and vasculature development, suggesting *CALD1* may also be involved in angiogenesis. Identified transcripts were also associated with three muscle-related gene sets.

We further explored *CALD1* co-expression with regulators of cancer hallmarks, actin-related processes, and relevant signaling pathways based on curated sets of positive and negative regulators separately (Gene Ontology: Biological Processes) on mRNA level in the largest single PCa patient data set (PCa subset of the PanCancer TCGA data set) by producing *CALD1* co-expression heatmaps. The percentages of positively and negatively co-expressed (determined in our analysis by cutoff at

Spearman's rank correlation coefficient ≥0.3 and ≤−0.3, respectively) regulators were evaluated (Supplementary Table 1). Positively co-expressed regulators were most common within the gene set of positive regulators of EMT (52.1% of regulators in the gene set) (Supplementary Fig. S2C and Supplementary Table 1). Other evaluated positive regulators of cancer hallmarks that showed high co-expression were regulators of angiogenesis (38.1%) and proliferation (32.6%) (Supplementary Fig. S2A, S2B, and Supplementary Table 1). Co-expression appeared to be, to some extent, present in both negative and positive regulators in analyzed processes, with the exception of anoikis, which was interestingly observed to have an almost exclusively negative

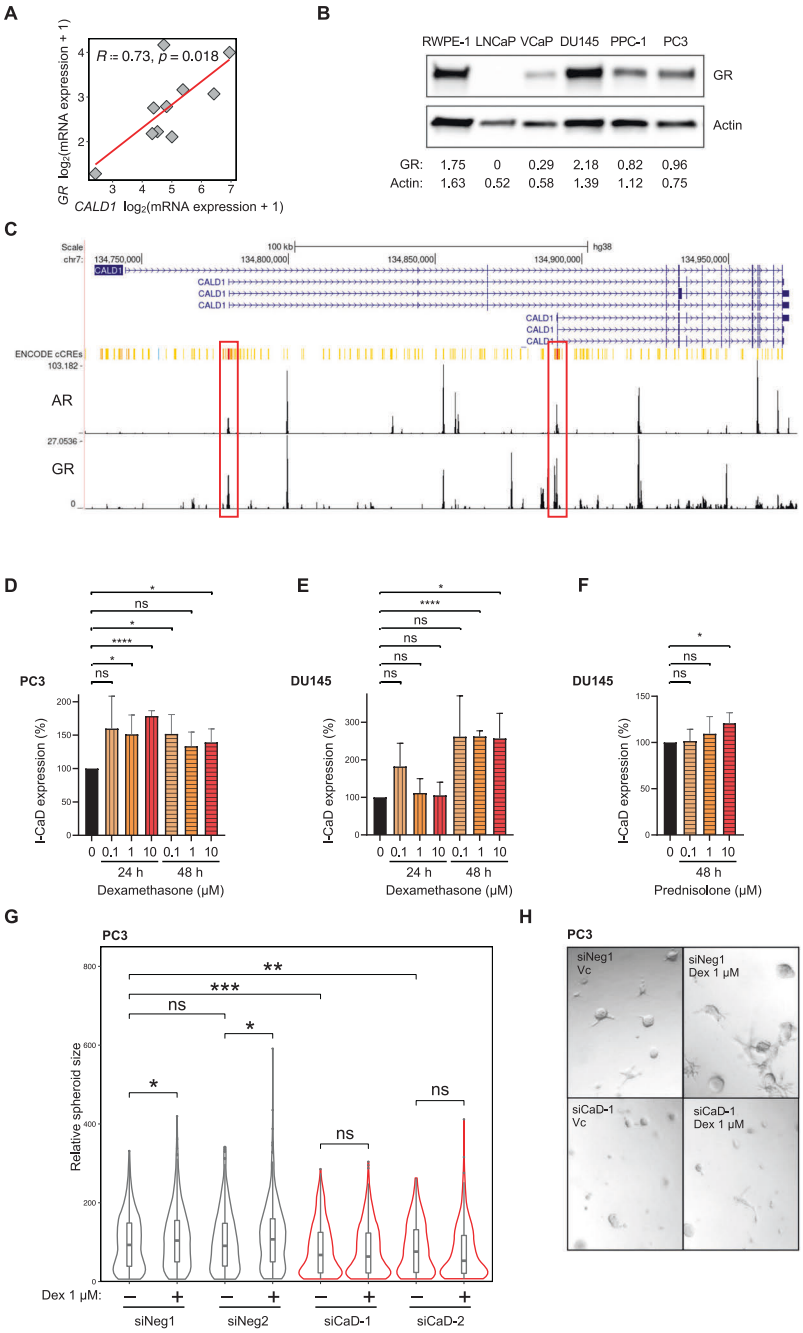

Fig. 3 l-CaD expression is upregulated by GR activation promoting growth in organotypic cell culture. A Correlation between *GR* and *CALD1* mRNA in patient-derived organoids (cBioPortal) [79]. **B** Western blot depicting GR expression in commercial PCa cell lines. **C** UCSC genome browser visualization of ReMap ChIP-seq tracks for AR and GR in *CALD1* with ENCODE candidate promoter-like signatures highlighted in red and enhancer-like signatures highlighted in yellow and orange. **D** Barplots depicting l-CaD protein expression in PC3 cells treated with Dex (0.1 μM, 1 μM, or 10 μM) after 24 or 48 hours. The mean and SD of three experiments are shown (ns = not significant, $*p < 0.05$, and $****p < 0.0001$ as determined by *t*-test). **E** Barplots depicting l-CaD protein expression in DU145 cells treated with Dex (0.1 μM, 1 μM, or 10 μM) after 24 or 48 hours. The mean and SD of three experiments are shown (ns = not significant, $*p < 0.05$, and $****p < 0.0001$ as determined by *t*-test). **F** Barplots depicting l-CaD protein expression in DU145 cells treated with prednisolone (0.1 μM, 1 μM, or 10 μM) after 48 hours. The mean and SD of three experiments are shown (ns = not significant and $*p < 0.05$ as determined by *t*-test). **G** Violin plots of relative spheroid size in PC3 cells transfected with siNeg1 or siCaD-1 and grown in the presence or absence of 1 μM Dex in basement membrane matrix. Boxplot indicates median and whiskers indicate 1.5 times interquartile range pooled form three experiments (ns = not significant, $*p < 0.05$, and $**p < 0.01$ as determined by *t*-test). **H** Representative brightfield image of day 5 organotypic culture of PC3 cells treated with siNeg-1 or siCaD-1 and exposed to 1 μM Dex or vehicle (DMSO) on day 3 of culture in basement membrane matrix.

association with *CALD1* (Supplementary Fig. S2F and Supplementary Table 1). To further investigate the association between *CALD1* and EMT using co-expression data in an alternative approach, we generated a custom gene set of epithelial and mesenchymal markers in which we observed predominantly positive co-expression between *CALD1* and the mesenchymal markers (Supplementary Fig. S2D).

l-CaD enhances growth in organotypic culture while knockdown of l-CaD does not change proliferation in 2D culture

Next, we experimentally investigated in vitro whether l-CaD played a role in regulating viability corresponding to our in silico analysis suggesting a positive correlation with proliferation. We did not observe any significant change in PC3 cell viability after l-CaD knockdown with siRNAs as measured by an MTS assay (Fig. 2A). In accordance, no significant effect on viability was found either after l-CaD knockdown in androgen-sensitive VCaP cells (Supplementary Fig. S3A). We then continued to study the role of l-CaD in the regulation of PCa growth using an organotypic basement membrane matrix culture, and the results showed that the knockdown of l-CaD reduced growth in 3D cultures (Fig. 2B, C, and Supplementary Fig. S3B). These data suggested that l-CaD was beneficial for the PCa cells in organotypic growth in 3D, although downregulation did not significantly affect viability in monolayer culture.

Knockdown of l-CaD impairs the formation of metastases in PCa xenograft zebrafish

Our co-expression analysis (Fig. 1G–I) suggested that *CALD1* was co-expressed with transcripts involved in the regulation of EMT and associated with cell migration and locomotion. To study the role of l-CaD in cancer cell migration and invasion in vivo, we injected mCherry PC3 cells transfected with siRNAs targeting l-CaD or non-targeting siRNAs into zebrafish larvae yolk sacs and assessed the formation of metastases after four days (Fig. 2D, E). The zebrafish assays were performed in parallel with viability assessments by monolayer culture MTS and with organotypic 3D culture growth area analysis, as well as with the knockdown verification at protein level by Western blotting (Fig. 2F). We observed that the rate of metastases in the xenografted zebrafish was reduced to less than one-third upon siRNA knockdown of *CALD1* (Fig. 2E). The size of the primary tumor was not changed after l-CaD knockdown, suggesting a specific effect pertaining to the metastasis process (Fig. 2G). As with non-mCherry PC3 cells, viability was not affected by l-CaD knockdown in mCherry PC3 cells (Supplementary Fig. S3C). While remaining viable, and producing spheroids in basement membrane matrix, the mCherry PC3 cells exhibited reduced growth after l-CaD knockdown similar to non-mCherry PC3 cells (Supplementary Fig. S3D, E). Similar results were observed in two DU145 cell xenograft models, wherein l-CaD knockdown led to a lower rate of metastasis and a reduced number of metastases after the cells were microinjected into pericardial cavity or common cardinal vein (Fig. 2H–M). These data suggested that when l-CaD expression was downregulated, aggressive PCa cells exhibited decreased capability to metastasize while remaining otherwise viable, indicating that l-CaD was specifically involved in metastasis and invasion.

l-CaD is upregulated upon GR activation in PCa in vitro

After establishing the anti-tumorigenic effect of l-CaD knockdown, we extended our analysis of patient samples to investigate possible regulators of l-CaD in PCa. Among the concordant hits of co-expression with *CALD1* between seven patient data sets (Fig. 1F), there were two transcription factors, GR (*NR3C1*) and melanocyte inducing transcription factor (*MITF*), that could directly regulate l-CaD expression. Due to the known connection of GR to PCa, we focused further on characterizing the GR–CaD interplay in PCa. To confirm that the significant co-expression was not caused by stromal h-CaD mRNA in the patient samples, we analyzed a published data set of patient-derived organoids lacking stroma and found a strong correlation between *CALD1* and *GR* expression (Fig. 3A).

We observed that GR was expressed in commercial PCa cell lines except for LNCaP cells which also have a CaD mutation (Fig. 3B). We performed zebrafish xenograft assay also with LNCaP cells microinjecting them into common cardinal vein and found that l-CaD knockdown reduced the number of metastases despite LNCaP cells being AR-positive and lacking GR expression (Supplementary Fig. S4A–C). To further understand the role of AR and GR in the regulation of l-CaD, we examined ReMap ChIP-seq tracks for AR and GR in the UCSC genome browser, and found that both receptors displayed peaks in the putative promoter and enhancer sites at *CALD1* (Fig. 3C). Next, we investigated the effect of GR activation on the expression of l-CaD in PCa cells. We observed that GR-expressing PC3 cells responded to a GR activator dexamethasone (Dex) with l-CaD upregulation at 24 or 48 hours (Fig. 3B, D). Similarly, in DU145 cells, treatment with Dex and prednisolone resulted in the upregulation of l-CaD expression after 48 hours of treatment (Fig. 3E, F). Dex stimulation improved spheroid growth of PC3 cells in basement membrane matrix cultures unless the l-CaD expression was knocked down using siRNA prior to the Dex treatment (Fig. 3G, H). These data suggested that l-CaD was upregulated by GR activation in AR-negative PCa.

Knockdown of l-CaD shifts the phenotype away from the mesenchymal cell state in PCa in organotypic culture

After associating *CALD1* with the expression of positive EMT regulators and mesenchymal markers in the patient data (Fig. 1), we wanted to see if these same markers could be observed in the models used to demonstrate that l-CaD silencing leads to diminished invasiveness. l-CaD colocalized with actin in PC3 cell filopodia (Fig. 4A). Staining PC3 cell spheroids cultured in basement membrane matrix showed downregulated expression of the mesenchymal cell state-associated N-cadherin after l-CaD knockdown (Fig. 4B, C), whereas no difference in the expression of E-cadherin was observed upon l-CaD knockdown

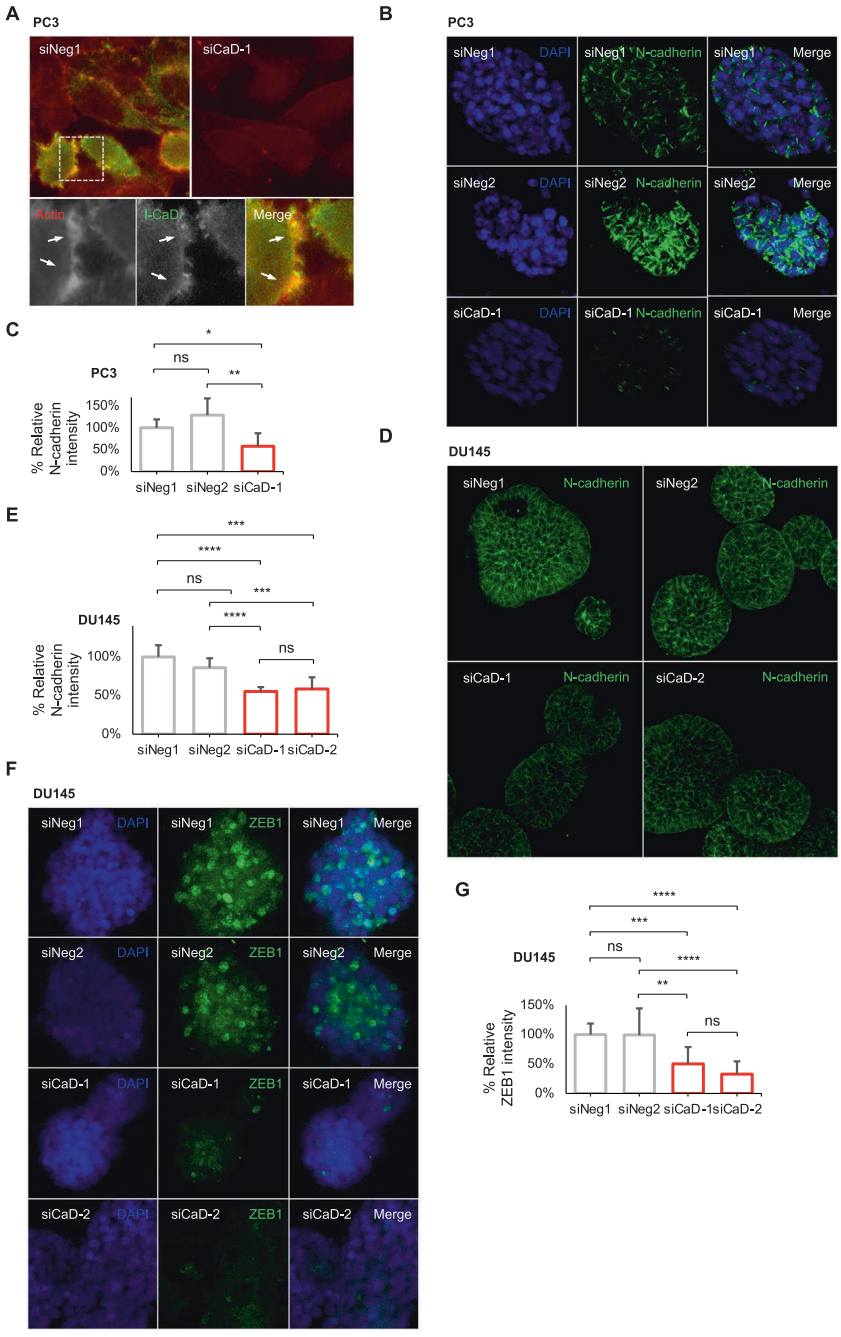

(Supplementary Fig. S5A, B). Furthermore, DU145 cell spheroids were similarly observed having downregulated N-cadherin and ZEB1 expression after l-CaD knockdown (Fig. 4D–G). By staining the zebrafish used in the in vivo xenograft model studying metastases, we confirmed the lack of l-CaD and reduced N-cadherin expression in the PC3 mCherry cells after l-CaD knockdown with siRNA (Supplementary Fig. S5C). These data taken together with the patient co-expression analyses, provided evidence supporting the role of l-CaD in promoting EMT in PCa.

Fig. 4 l-CaD colocalizes with actin in filopodia, and the knockdown of l-CaD downregulates N-cadherin. A Representative fluorescent merge images of PC3 cells transfected with siNeg1 or siCaD-1 and stained with antibodies recognizing actin and l-CaD. The lower row shows separate images of actin, l-CaD, and merge in a close-up of the upper siNeg1 image. **B** Representative fluorescent images of PC3 spheroids transfected with siNeg1, siNeg2, or siCaD-1, stained with N-cadherin, and counterstained with DAPI. **C** Barplots depicting N-cadherin protein intensity in spheroids formed by transfected PC3 cells shown in **B**. Average was calculated from multiple individual spheroids ($N = 22$) measured for mean intensity. The mean and SD are shown (ns = not significant, $*p < 0.05$, and $**p < 0.01$ as determined by *t*-test). **D** Representative fluorescent images of DU145 spheroids transfected with siNeg1, siNeg2, siCaD-1, or siCaD-2 stained against N-cadherin. **E** Barplots depicting N-cadherin protein intensity in spheroids formed by transfected DU145 cells shown in **D**. Average was calculated from multiple individual spheroids ($N = 30$) measured for mean intensity. The mean and SD shown (ns = not significant, $***p < 0.001$, and $****p < 0.0001$ as determined by *t*-test). **F** Representative fluorescent images of DU145 spheroids transfected with siNeg1, siNeg2, siCaD-1, or siCaD-2 stained against ZEB1. **G** Barplots depicting ZEB1 protein intensity in spheroids formed by transfected DU145 cells shown in **F**. Average was calculated from multiple individual spheroids ($N = 58$) measured for mean intensity. The mean and SD shown (ns = not significant, $**p < 0.001$, $***p < 0.001$, and $****p < 0.0001$ as determined by *t*-test).

GR upregulation in enzalutamide resistance leads to upregulated l-CaD expression in vivo

To study l-CaD during the development of resistance to AR-targeting therapies, we used androgen-sensitive PCa cells. To overcome interference to GR signaling by AR activation, we used a lead-in treatment with an antiandrogen (enzalutamide) in VCaP cells and observed that l-CaD expression was upregulated by Dex, while also slightly increasing in response to Dex in the absence of prior antiandrogen (Fig. 5A). As an in vivo model of castration resistance, we re-analyzed subcutaneous VCaP xenograft tumors grown in nude mice [47, 48]. Mice with castration-resistant tumors were treated with an antiandrogen (enzalutamide) and sacrificed either when tumors were still responding to antiandrogen or after the eventual appearance of resistance to antiandrogen. We re-analyzed RNA-Seq data of the subcutaneous tumors and observed *GR* having a positive correlation with *CALD1* (Fig. 5B). To examine l-CaD and GR at protein levels and to distinguish between stromal and tumor CaD, we performed IHC on the xenograft tumors. We observed the appearance of islands of cells with upregulated l-CaD expression by IHC in resistant tumors when compared with tumors from mice sacrificed during antiandrogen response (Fig. 5C). Notably, one mouse in the response group with exceptionally high PSA (9.462 ng ml^{-1} vs. an average of 2.037 ng ml^{-1} in the rest of the response group), which likely reflects incomplete response, was observed to have areas of l-CaD expression similar to that of the resistant group. Staining of the samples with an antibody recognizing GR showed a similar pattern of spotted upregulation in the resistant samples, whereas a lower baseline expression was observed in the response group (Fig. 5D). We also stained adjacent slides of an orthotopic VCaP xenograft mouse model [49] and observed similar islands of l-CaD upregulation in tumors treated with the antiandrogen (apalutamide) within the same regions that presented GR upregulation (Fig. 5E). Moreover, we re-analyzed previously generated RNA-seq data of reported orthotopic xenografts and found similar positive correlation between *GR* and *CALD1* in the resistant tumors (Fig. 5F). Western blot analysis of tumor homogenates from the orthotopic VCaP xenografts also showed a trend of increase in both GR and l-CaD expression in the tumors treated with the antiandrogen (apalutamide), although the expressions were heterogeneous as expected based on our IHC analyses (Fig. 5G). Thus, l-CaD upregulation was associated in vivo with areas of GR upregulation after resistance to antiandrogens.

GR expression correlates with *CALD1* expression, while *KRT8* expression is negatively correlated with *CALD1* in vivo

After establishing the connection between GR and l-CaD in the VCaP xenograft mouse models, we used RNA-Seq analysis to study the association with EMT-related transcripts. We observed *CALD1* having a negative correlation with *KRT8* in both the subcutaneous and the orthotopic xenografts (Fig. 5B, F). In line with our in silico analyses from patient data (Fig. 1) and our analysis of immunofluorescence in PC3 cell spheroids (Supplementary Fig. S5A, B), *CALD1* and *CDH1* (encodes E-cadherin) expressions were non-correlating in the subcutaneous xenografts (Supplementary Fig. S6A). Fitting the VCaP model being non-metastatic, markers for mesenchymal phenotype were commonly undetectable or lowly expressed in VCaP xenografts (Supplementary Table 2). None of the correlation analyses with *CALD1* and mesenchymal markers reached statistical significance in the subcutaneous xenografts, which again is likely due to the VCaP model being non-metastatic (Supplementary Fig. S6A). However, some positive EMT-related correlations in the orthotopic model were significant (*SNAI1* in the apalutamide resistance and *TWIST2* in the enzalutamide resistance), despite the VCaP model being non-metastatic (Supplementary Fig. S6B). Using IHC staining of vimentin in the subcutaneous tumors we observed no expression in the samples of the resistant group (Supplementary Fig. S6C). In conclusion, using the VCaP xenograft mouse models, we were able to verify our initial observations from PCa patient data sets showing the association between *CALD1* and *KRT8* and *GR*.

DISCUSSION

Despite the initial response to the therapeutic targeting of AR signaling, aggressive PCa eventually develops castration resistance and progresses to lethal metastatic PCa. Here, we have characterized one critical mechanism involved in antiandrogen therapy-resistant PCa. We report that l-CaD is expressed in PCa cell lines and that *CALD1* amplifications are more common in metastatic or locally advanced than primary tumor PCa patient data sets. In a co-expression analysis of the largest PCa patient data sets, we find *CALD1* to correlate with EMT markers and *GR*. The knockdown of l-CaD in vitro limits organotypic growth and downregulates EMT marker expression but has no effect on monolayer growth. Finally, we experimentally show in vivo that l-CaD induces EMT, promotes metastasis, and is upregulated in antiandrogen-resistant PCa together with GR.

Several previous studies have described an upregulation of GR as one important mechanism in antiandrogen-resistant PCa [50–55]. We show that l-CaD is upregulated by GR activation in AR-negative PCa cell lines and after AR inhibition in AR-positive cells. Moreover, *CALD1* expression correlates with *GR* expression in PCa patient samples and patient-derived organoids, and by IHC, we show that l-CaD and GR are upregulated in antiandrogen-resistant VCaP xenograft mouse models. The detailed mechanism for GR-induced upregulation in PCa is not known, but interestingly previous work shows that activated GR binds to *CALD1* promoter in lung cancer cells, providing a mechanism for l-CaD upregulation by GR [24]. In accordance, our analysis of the published ChIP-seq data available on the UCSC genome browser also support that GR may directly contribute to l-CaD expression regulation. With a myriad of identified regulators for CaD, modulators other than GR could also play a part in pushing l-CaD expression in PCa [30, 39–46]. Additionally, calmodulin binding and the regulation of

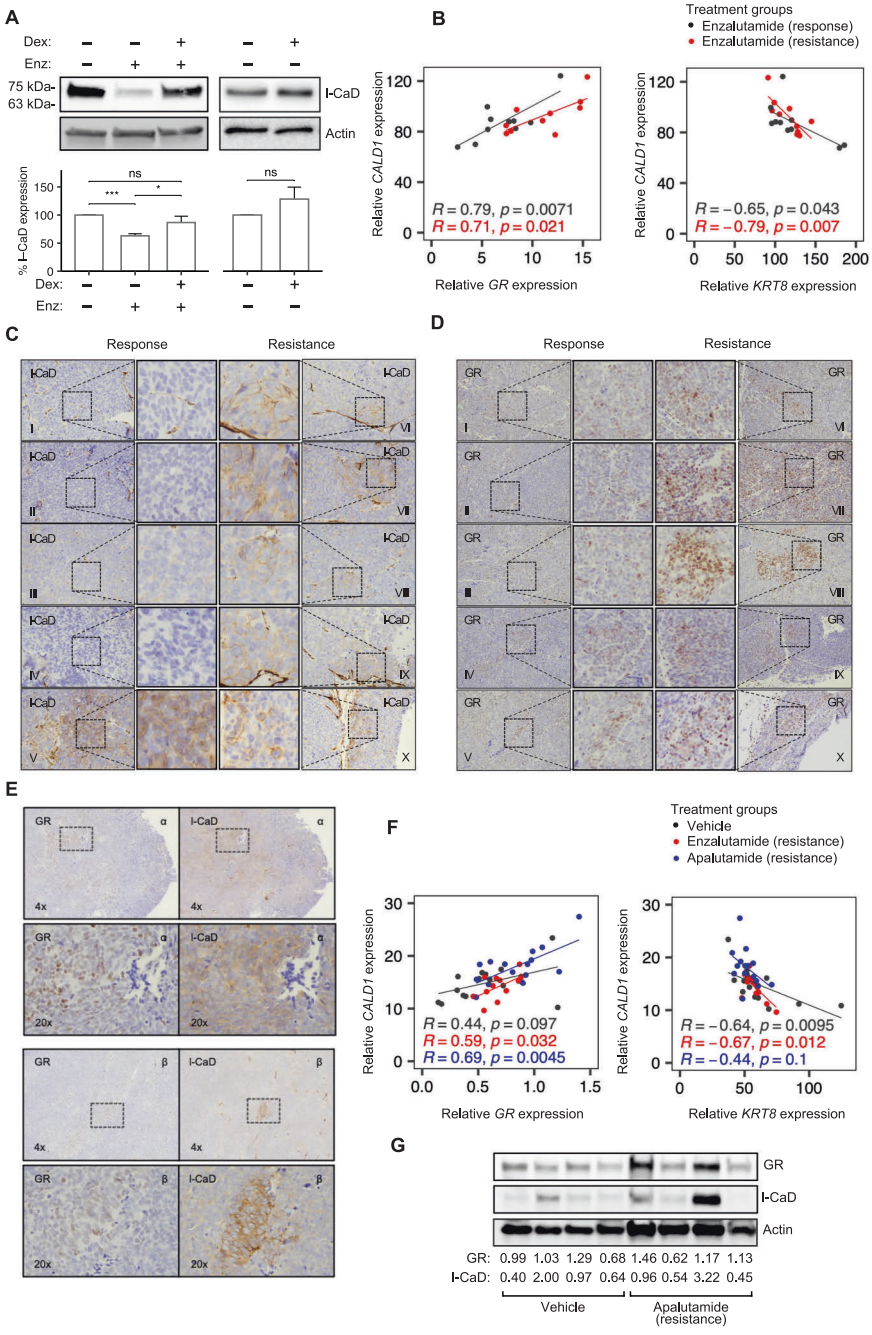

I-CaD phosphorylation by CDK1, Erk, p38 MAPK, isoforms of s100, and p21-activated kinases (PAK) 1 and 2 may further enhance I-CaD effects in PCa [29, 40, 56–59].

In our analyses, I-CaD shows no association with the common PCa driver AR, but, interestingly, a few *CALD1* amplifications were already present in primary tumor patients, adding to the possibility of I-CaD having a role in PCa progression outside antiandrogen-resistance via AR bypassing by GR upregulation. GR signaling in PCa is also a complex entity as glucocorticoids act as partial antiandrogens in the presence of androgens, lower steroid

Fig. 5 l-CaD expression is upregulated during enzalutamide resistance in vivo. A Representative Western blot depicting l-CaD expression and barplot depicting pooled densitometry of Western blot bands from three biological repeats after treatment with enzalutamide (5 days, 10 μM) and Dex (24 h, 0.1 μM). **B** Scatterplots depicting Pearson correlation between *CALD1* and *GR* or *KRT8* mRNA from enzalutamide-treated VCaP xenograft mice. **C** IHC of l-CaD in castration-resistant VCaP xenografts during enzalutamide response (left) and after attained enzalutamide resistance (right). Individual mice are denoted using Roman numerals. **D** IHC of GR in castration-resistant VCaP xenografts during enzalutamide response (left) and after attained enzalutamide resistance (right). Individual mice are denoted using Roman numerals. **E** IHC of l-CaD and GR from adjacent slices of VCaP xenograft tumors in mice during apalutamide resistance. The lower row shows a higher magnification image of the area highlighted on the upper row. Individual mice are denoted using Greek letters. **F** Scatterplots depicting Pearson correlation between *CALD1* and *GR* or *KRT8* mRNA from vehicle-, enzalutamide-, and apalutamide-treated VCaP xenograft mice. **G** Western blot of vehicle- and apalutamide-treated castration-resistant VCaP xenografts. Quantification of the GR and l-CaD signal relative to actin loading control signal and the average vehicle-treated signal is shown below.

levels by inducing balancing feedback in the pituitary, and effectively alleviate the side effects of utilized therapies. The presence of AR seems to complicate the acute response to GR ligands which may, in part, be explained by AR signaling regulating GR negatively [53]. Our experiments with VCaP cells show that l-CaD is upregulated by GR activation when stimulation is preceded by antiandrogen treatment. Thus, the GR-dependent upregulation of l-CaD in AR-expressing cells seems to be enhanced by AR inhibition. Our analysis of the published ChIP-seq data suggest that, in addition to GR, also AR may contribute to l-CaD regulation. Furhermore, it is probable that the regulation is also modulated variously during different phases of PCa progression and if direct, it is likely further influenced by co-factor binding. Taken together, our results display the complexity of the interconnected AR and GR signaling in therapy resistant PCa and suggest that GR activation upregulates l-CaD in the absence of active AR signaling in PCa.

Using PCa cells injected into zebrafish larvae as a model, we now show that l-CaD expression is critical for PCa metastasis in vivo. Silencing l-CaD reduces the rate of metastases in the PC3 xenograft zebrafish by two-thirds and leads to an even more pronounced reduction in the rate of metastasis in the DU145 xenograft zebrafish. Importantly, viability is unaffected by the silencing of l-CaD, supporting a specific role in metastasis. Notably, our results in the zebrafish metastasis assay with AR-positive and GR-negative LNCaP cells, suggest a more general role for l-CaD in promoting metastasis in PCa cells independently of AR or GR status. Interestingly, the silencing of l-CaD also reduces spheroid size when cells are grown in basement membrane matrix. The discrepancy between the results observed in plastic 2D and 3D basement membrane matrix gel is possibly attributable to the latter model not only measuring proliferation capacity but more closely resembling in vivo environment and also characteristics involved in metastasis. Moreover, 3D culture may also represent the microenvironment more accurately when compared to the traditional invasion and migration assays. Previous preclinical studies in vitro show an increase in migration and invasion after l-CaD knockdown in lung cancer, gastric cancer, breast cancer, hepatocellular carcinoma, and PCa cells in contrast to our results [24–28]. However, supporting our findings, a positive correlation of l-CaD expression with in vitro migration and invasion is reported in myoblasts, HeLa, bladder cancer, and osteosarcoma cells [29–31, 33]. Similarly, previous reports on the role of GR in migration and invasion in vitro are contrasting [60, 61]. Previous work on the role of GR signaling in radial migration of neurons interestingly suggests that an appropriate l-CaD level is critical for optimal migration in vivo [14]. In conclusion, by providing for the first time in vivo data of metastatic zebrafish xenografts, our results add to the evidence supporting that l-CaD promotes invasion and migration and, further, the formation of metastases.

Cancer cell plasticity is a requirement for the formation of metastases, which cells can obtain to different extents by undergoing EMT [62]. VCaP xenograft mouse models we use are not metastatic, which is reflected in the low expression of mesenchymal markers in the tumor data. However, we show that epithelial marker expression is negatively correlated with *CALD1* in the xenografts, and two mesenchymal marker-expressing PCa cell lines have reduced N-cadherin expression after silencing l-CaD in 3D culture. Additionally, we show high co-expression with several EMT regulators and mesenchymal markers and *CALD1* in PCa TCGA and combined analysis of six other PCa patient data sets. Notably, the common epithelial marker E-cadherin does not correlate with l-CaD in the patient data sets and does not show differential expression upon silencing l-CaD in 3D culture. Retained E-cadherin expression may suggest that l-CaD induces partial EMT, which is interestingly associated with calmodulin, a known interactor of l-CaD [62, 63].

It is important to acknowledge limitations associated with specific cell lines used to study PCa. While PC3 and DU145 cells are among the most widely utilized PCa cell lines alongside LNCaP cells, they do not express significant levels of AR protein in contrast to LNCaP and VCaP cells [64]. Given that the majority of PCa express AR, it is important to avoid generalizing the findings obtained with AR-negative cell lines. Instead, PC3 and DU145 cells may be considered representative of AR low or negative PCa subtypes, which, including neuroendocrine PCa, may make up one-fifth of castration-resistant PCa cases [65, 66].

Our results describe a new mechanism that promotes EMT and metastasis in GR-upregulated antiandrogen-resistant PCa. In summary, our data suggest that antiandrogen resistance may give rise to colonies of GR-upregulated PCa cells within the tumor where l-CaD expression is induced in response to GR activation in the absence of AR signaling. The induction of l-CaD promotes EMT in the PCa cells and may eventually stimulate the dissemination of the colony. In conclusion, our study demonstrates that l-CaD is involved in facilitating metastasis in PCa. Herein described, l-CaD upregulation is potentially one specific target to prevent metastases in therapy resistant PCa.

MATERIALS AND METHODS

Available in Supplementary information.

DATA AVAILABILITY

Data are available upon reasonable request.

REFERENCES

1. Sung H, Ferlay J, Siegel RL, Laversanne M, Soerjomataram I, Jemal A, et al. Global Cancer Statistics 2020: GLOBOCAN Estimates of Incidence and Mortality Worldwide for 36 Cancers in 185 Countries. CA Cancer J Clin. 2021;71:209–49.
2. Watson PA, Arora VK, Sawyers CL. Emerging mechanisms of resistance to androgen receptor inhibitors in prostate cancer. Nat Rev Cancer. 2015;15:701–11.
3. Yamaguchi H, Condeelis J. Regulation of the actin cytoskeleton in cancer cell migration and invasion. Biochim Biophys Acta. 2007;1773:642–52.
4. Sobue K, Muramoto Y, Fujita M, Kakiuchi S. Purification of a calmodulin-binding protein from chicken gizzard that interacts with F-actin. Proc Natl Acad Sci USA. 1981;78:5652–5.

5. Sobue K, Tanaka T, Kanda K, Ashino N, Kakiuchi S. Purification and characterization of caldesmon77: a calmodulin-binding protein that interacts with actin filaments from bovine adrenal medulla. Proc Natl Acad Sci USA. 1985;82:5025–9.
6. Hayashi K, Yano H, Hashida T, Takeuchi R, Takeda O, Asada K, et al. Genomic structure of the human caldesmon gene. Proc Natl Acad Sci USA. 1992;89:12122–6.
7. Payne AM, Yue P, Pritchard K, Marston SB. Caldesmon mRNA splicing and isoform expression in mammalian smooth-muscle and non-muscle tissues. Biochem J. 1995;305:445–50.
8. Watanabe K, Kusakabe T, Hoshi N, Saito A, Suzuki T. h-Caldesmon in leiomyosarcoma and tumors with smooth muscle cell-like differentiation: its specific expression in the smooth muscle cell tumor. Hum Pathol. 1999;30:392–6.
9. Walther S, Strittmatter F, Roosen A, Heinzer F, Rutz B, Stief CG, et al. Expression and alpha1-adrenoceptor regulation of caldesmon in human prostate smooth muscle. Urology. 2012;79:745.e5–12.
10. Hemric ME, Chalovich JM. Effect of caldesmon on the ATPase activity and the binding of smooth and skeletal myosin subfragments to actin. J Biol Chem. 1988;263:1878–85.
11. Marston SB, Redwood CS. Inhibition of actin-tropomyosin activation of myosin MgATPase activity by the smooth muscle regulatory protein caldesmon. J Biol Chem. 1992;267:16796–800.
12. Goncharova EA, Shirinsky VP, Shevelev AY, Marston SB, Vorotnikov AV. Actomyosin cross-linking by caldesmon in non-muscle cells. FEBS Lett. 2001;497:113–7.
13. Makuch R, Kulikova N, Graziewicz MA, Nowak E, Dabrowska R. Polymerization of actin induced by actin-binding fragments of caldesmon. Biochim Biophys Acta. 1994;1206:49–54.
14. Fukumoto K, Morita T, Mayanagi T, Tanokashira D, Yoshida T, Sakai A, et al. Detrimental effects of glucocorticoids on neuronal migration during brain development. Mol Psychiatry. 2009;14:1119–31.
15. Pütz S, Barthel LS, Frohn M, Metzler D, Barham M, Pryymachuk G, et al. Caldesmon ablation in mice causes umbilical herniation and alters contractility of fetal urinary bladder smooth muscle. J Gen Physiol. 2021;153:e202012776.
16. Helfman DM, Levy ET, Berthier C, Shtutman M, Riveline D, Grosheva I, et al. Caldesmon inhibits nonmuscle cell contractility and interferes with the formation of focal adhesions. Mol Biol Cell. 1999;10:3097–112.
17. Guo H, Wang CL. Specific disruption of smooth muscle caldesmon expression in mice. Biochem Biophys Res Commun. 2005;330:1132–7.
18. Guo H, Huang R, Semba S, Kordowska J, Huh YH, Khalina-Stackpole Y, et al. Ablation of smooth muscle caldesmon affects the relaxation kinetics of arterial muscle. Pflug Arch. 2013;465:283–94.
19. Deng M, Boopathi E, Hypolite JA, Raabe T, Chang S, Zderic S, et al. Amino acid mutations in the caldesmon COOH-terminal functional domain increase force generation in bladder smooth muscle. Am J Physiol Ren Physiol. 2013;305:F1455–65.
20. Nie S, Kee Y, Bronner-Fraser M. Caldesmon regulates actin dynamics to influence cranial neural crest migration in Xenopus. Mol Biol Cell. 2011;22:3355–65.
21. Zheng PP, Severijnen LA, van der Weiden M, Willemsen R, Kros JM. A crucial role of caldesmon in vascular development in vivo. Cardiovasc Res. 2009;81:362–9.
22. Zheng PP, Severijnen LA, Willemsen R, Kros JM. Caldesmon is essential for cardiac morphogenesis and function: in vivo study using a zebrafish model. Biochem Biophys Res Commun. 2009;378:37–40.
23. Yoshio T, Morita T, Kimura Y, Tsujii M, Hayashi N, Sobue K. Caldesmon suppresses cancer cell invasion by regulating podosome/invadopodium formation. FEBS Lett. 2007;581:3777–82.
24. Mayanagi T, Morita T, Hayashi K, Fukumoto K, Sobue K. Glucocorticoid receptor-mediated expression of caldesmon regulates cell migration via the reorganization of the actin cytoskeleton. J Biol Chem. 2008;283:31183–96.
25. Hou Q, Tan HT, Lim KH, Lim TK, Khoo A, Tan IB, et al. Identification and functional validation of caldesmon as a potential gastric cancer metastasis-associated protein. J Proteome Res. 2013;12:980–90.
26. Schwappacher R, Rangaswami H, Su-Yuo J, Hassad A, Spitler R, Casteel DE. cGMP-dependent protein kinase Iβ regulates breast cancer cell migration and invasion via interaction with the actin/myosin-associated protein caldesmon. J Cell Sci. 2013;126:1626–36.
27. Dierks S, von Hardenberg S, Schmidt T, Bremmer F, Burfeind P, Kaulfuß S. Leupaxin stimulates adhesion and migration of prostate cancer cells through modulation of the phosphorylation status of the actin-binding protein caldesmon. Oncotarget. 2015;6:13591–606.
28. Zhang J, Ren Z, Zheng D, Song Z, Lin J, Luo Y, et al. AHSA1 Promotes Proliferation and EMT by Regulating ERK/CALD1 Axis in Hepatocellular Carcinoma. Cancers. 2022;14:4600.
29. Manes T, Zheng DQ, Tognin S, Woodard AS, Marchisio PC, Languino LR. Alpha(v) beta3 integrin expression up-regulates cdc2, which modulates cell migration. J Cell Biol. 2003;161:817–26.
30. Jang SM, Kim JW, Kim D, Kim CH, An JH, Choi KH, et al. Sox4-mediated caldesmon expression facilitates differentiation of skeletal myoblasts. J Cell Sci. 2013;126:5178–88.
31. Lee MS, Lee J, Kim JH, Kim WT, Kim WJ, Ahn H, et al. Overexpression of caldesmon is associated with tumor progression in patients with primary non-muscle-invasive bladder cancer. Oncotarget 2015;6:40370–84.
32. Li C, Yang F, Wang R, Li W, Maskey N, Zhang W, et al. CALD1 promotes the expression of PD-L1 in bladder cancer via the JAK/STAT signaling pathway. Ann Transl Med. 2021;9:1441.
33. Kokate SB, Ciuba K, Tran VD, Kumari R, Tojkander S, Engel U, et al. Caldesmon controls stress fiber force-balance through dynamic cross-linking of myosin II and actin-tropomyosin filaments. Nat Commun. 2022;13:6032.
34. Chang KP, Wang CL, Kao HK, Liang Y, Liu SC, Huang LL, et al. Overexpression of caldesmon is associated with lymph node metastasis and poorer prognosis in patients with oral cavity squamous cell carcinoma. Cancer 2013;119:4003–11.
35. Cheng Q, Tang A, Wang Z, Fang N, Zhang Z, Zhang L, et al. CALD1 Modulates Gliomas Progression via Facilitating Tumor Angiogenesis. Cancers. 2021;13:2705.
36. Liu Y, Xie S, Zhu K, Guan X, Guo L, Lu R. CALD1 is a prognostic biomarker and correlated with immune infiltrates in gastric cancers. Heliyon. 2021;7:e07257.
37. Kim KH, Yeo SG, Kim WK, Kim DY, Yeo HY, Hong JP, et al. Up-regulated expression of l-caldesmon associated with malignancy of colorectal cancer. BMC Cancer. 2012;12:601.
38. De Marchi T, Timmermans AM, Smid M, Look MP, Stingl C, Opdam M, et al. Annexin-A1 and caldesmon are associated with resistance to tamoxifen in estrogen receptor positive recurrent breast cancer. Oncotarget. 2016;7:3098–110.
39. Nishida W, Nakamura M, Mori S, Takahashi M, Ohkawa Y, Tadokoro S, et al. A triad of serum response factor and the GATA and NK families governs the transcription of smooth and cardiac muscle genes. J Biol Chem. 2002;277:7308–17.
40. Morita T, Mayanagi T, Yoshio T, Sobue K. Changes in the balance between caldesmon regulated by p21-activated kinases and the Arp2/3 complex govern podosome formation. J Biol Chem. 2007;282:8454–63.
41. Mukhopadhyay UK, Eves R, Jia L, Mooney P, Mak AS. p53 suppresses Src-induced podosome and rosette formation and cellular invasiveness through the upregulation of caldesmon. Mol Cell Biol. 2009;29:3088–98.
42. Quintavalle M, Elia L, Price JH, Heynen-Genel S, Courtneidge SA. A cell-based high-content screening assay reveals activators and inhibitors of cancer cell invasion. Sci Signal. 2011;4:ra49.
43. Bianchi-Smiraglia A, Kunnev D, Limoge M, Lee A, Beckerle MC, Bakin AV. Integrin-β5 and zyxin mediate formation of ventral stress fibers in response to transforming growth factor β. Cell Cycle. 2013;12:3377–89.
44. Zhang L, Liu J, Wang X, Li Z, Zhang X, Cao P, et al. Upregulation of cytoskeleton protein and extracellular matrix protein induced by stromal-derived nitric oxide promotes lung cancer invasion and metastasis. Curr Mol Med. 2014;14:762–71.
45. Bisht S, Nolting J, Schütte U, Haarmann J, Jain P, Shah D, et al. Cyclin-Dependent Kinase 5 (CDK5) Controls Melanoma Cell Motility, Invasiveness, and Metastatic Spread-Identification of a Promising Novel therapeutic target. Transl Oncol. 2015;8:295–307.
46. Zhang S, Wang Q, Li W, Chen J. MIR100HG Regulates CALD1 Gene Expression by Targeting miR-142-5p to Affect the Progression of Bladder Cancer Cells in vitro, as Revealed by Transcriptome Sequencing. Front Mol Biosci. 2022;8:793493.
47. Huhtaniemi R, Oksala R, Knuuttila M, Mehmood A, Aho E, Laajala TD, et al. Adrenals Contribute to Growth of Castration-Resistant VCaP Prostate Cancer Xenografts. Am J Pathol. 2018;188:2890–901.
48. Huhtaniemi R, Sipilä P, Junnila A, Oksala R, Knuuttila M, Mehmood A, et al. High intratumoral dihydrotestosterone is associated with antiandrogen resistance in VCaP prostate cancer xenografts in castrated mice. iScience. 2022;25:104287.
49. Knuuttila M, Yatkin E, Kallio J, Savolainen S, Laajala TD, Aittokallio T, et al. Castration induces up-regulation of intratumoral androgen biosynthesis and androgen receptor expression in an orthotopic VCaP human prostate cancer xenograft model. Am J Pathol. 2014;184:2163–73.
50. Sahu B, Laakso M, Pihlajamaa P, Ovaska K, Sinielnikov I, Hautaniemi S, et al. FoxA1 specifies unique androgen and glucocorticoid receptor binding events in prostate cancer cells. Cancer Res. 2013;73:1570–80.
51. Arora VK, Schenkein E, Murali R, Subudhi SK, Wongvipat J, Balbas MD, et al. Glucocorticoid receptor confers resistance to antiandrogens by bypassing androgen receptor blockade. Cell 2013;155:1309–22.
52. Isikbay M, Otto K, Kregel S, Kach J, Cai Y, Vander Griend DJ, et al. Glucocorticoid receptor activity contributes to resistance to androgen-targeted therapy in prostate cancer. Horm Cancer. 2014;5:72–89.
53. Xie N, Cheng H, Lin D, Liu L, Yang O, Jia L, et al. The expression of glucocorticoid receptor is negatively regulated by active androgen receptor signaling in prostate tumors. Int J Cancer. 2015;136:E27–38.

54. Lam HM, McMullin R, Nguyen HM, Coleman I, Gormley M, Gulati R, et al. Characterization of an Abiraterone Ultraresponsive Phenotype in Castration-Resistant Prostate Cancer Patient-Derived Xenografts. Clin Cancer Res. 2017;23:2301–12.
55. Puhr M, Hoefer J, Eigentler A, Ploner C, Handle F, Schaefer G, et al. The Glucocorticoid Receptor Is a Key Player for Prostate Cancer Cell Survival and a Target for Improved Antiandrogen Therapy. Clin Cancer Res. 2018;24:927–38.
56. Polyakov AA, Huber PA, Marston SB, Gusev NB. Interaction of isoforms of S100 protein with smooth muscle caldesmon. FEBS Lett. 1998;422:235–9.
57. D'Angelo G, Graceffa P, Wang CA, Wrangle J, Adam LP. Mammal-specific, ERK-dependent, caldesmon phosphorylation in smooth muscle. Quantitation using novel anti-phosphopeptide antibodies. J Biol Chem. 1999;274:30115–21.
58. Yamashiro S, Chern H, Yamakita Y, Matsumura F. Mutant Caldesmon lacking cdc2 phosphorylation sites delays M-phase entry and inhibits cytokinesis. Mol Biol Cell. 2001;12:239–50.
59. Chrétien A, Dierick JF, Delaive E, Larsen MR, Dieu M, Raes M, et al. Role of TGF-beta1-independent changes in protein neosynthesis, p38alphaMAPK, and cdc42 in hydrogen peroxide-induced senescence-like morphogenesis. Free Radic Biol Med. 2008;44:1732–51.
60. Xiao D, Singh SV. z-Guggulsterone, a constituent of Ayurvedic medicinal plant Commiphora mukul, inhibits angiogenesis in vitro and in vivo. Mol Cancer Ther. 2008;7:171–80.
61. Guo J, Ma K, Xia HM, Chen QK, Li L, Deng J, et al. Androgen receptor reverts dexamethasone-induced inhibition of prostate cancer cell proliferation and migration. Mol Med Rep. 2018;17:5887–93.
62. Bakir B, Chiarella AM, Pitarresi JR, Rustgi AK. EMT, MET, Plasticity, and Tumor Metastasis. Trends Cell Biol. 2020;30:764–76.
63. Norgard RJ, Pitarresi JR, Maddipati R, Aiello-Couzo NM, Balli D, Li J, et al. Calcium signaling induces a partial EMT. EMBO Rep. 2021;22:e51872.
64. Sobel RE, Sadar MD. Cell lines used in prostate cancer research: a compendium of old and new lines–part 1. J Urol. 2005;173:342–59.
65. Bluemn EG, Coleman IM, Lucas JM, Coleman RT, Hernandez-Lopez S, Tharakan R, et al. Androgen Receptor Pathway-Independent Prostate Cancer Is Sustained through FGF Signaling. Cancer Cell. 2017;32:474–489.e6.
66. Vellky JE, Ricke WA. Development and prevalence of castration-resistant prostate cancer subtypes. Neoplasia. 2020;22:566–75.
67. Abida W, Cyrta J, Heller G, Prandi D, Armenia J, Coleman I, et al. Genomic correlates of clinical outcome in advanced prostate cancer. Proc Natl Acad Sci USA. 2019;116:11428–36.
68. Kumar A, Coleman I, Morrissey C, Zhang X, True LD, Gulati R, et al. Substantial interindividual and limited intraindividual genomic diversity among tumors from men with metastatic prostate cancer. Nat Med. 2016;22:369–78.
69. Grasso CS, Wu YM, Robinson DR, Cao X, Dhanasekaran SM, Khan AP, et al. The mutational landscape of lethal castration-resistant prostate cancer. Nature. 2012;487:239–43.
70. Robinson D, Van Allen EM, Wu YM, Schultz N, Lonigro RJ, Mosquera JM, et al. Integrative clinical genomics of advanced prostate cancer. Cell. 2015;161:1215–28.
71. Taylor BS, Schultz N, Hieronymus H, Gopalan A, Xiao Y, Carver BS, et al. Integrative genomic profiling of human prostate cancer. Cancer Cell. 2010;18:11–22.
72. Armenia J, Wankowicz SAM, Liu D, Gao J, Kundra R, Reznik E, et al. The long tail of oncogenic drivers in prostate cancer. Nat Genet. 2018;50:645–51.
73. Crowdis J, Balch S, Sterlin L, Thomas BS, Camp SY, Dunphy M, et al. A patient-driven clinicogenomic partnership for metastatic prostate cancer. Cell Genom. 2022;2:100169.
74. The ICGC/TCGA Pan-Cancer Analysis of Whole Genomes Consortium. Pan-cancer analysis of whole genomes. Nature. 2020;578:82–93.
75. Baca SC, Prandi D, Lawrence MS, Mosquera JM, Romanel A, Drier Y, et al. Punctuated evolution of prostate cancer genomes. Cell 2013;153:666–77.
76. Beltran H, Prandi D, Mosquera JM, Benelli M, Puca L, Cyrta J, et al. Divergent clonal evolution of castration-resistant neuroendocrine prostate cancer. Nat Med. 2016;22:298–305.
77. Barbieri CE, Baca SC, Lawrence MS, Demichelis F, Blattner M, Theurillat JP, et al. Exome sequencing identifies recurrent SPOP, FOXA1 and MED12 mutations in prostate cancer. Nat Genet. 2012;44:685–9.
78. Ren S, Wei GH, Liu D, Wang L, Hou Y, Zhu S, et al. Whole-genome and Transcriptome Sequencing of Prostate Cancer Identify New Genetic Alterations Driving Disease Progression. Eur Urol. 2018;73:322–39.
79. Gao D, Vela I, Sboner A, Iaquinta PJ, Karthaus WR, Gopalan A, et al. Organoid cultures derived from patients with advanced prostate cancer. Cell. 2014;159:176–87.

ACKNOWLEDGEMENTS

We thank Zebrafish Core, Cell Imaging Core, Finnish Functional Genomics Centre, and Medical Bioinformatics Centre (all in Turku Bioscience Centre and supported by Biocenter Finland) for services, instrumentation, and consultations. We thank Sinikka Collanus and the Histology core facility of the Institute of Biomedicine, University of Turku, for their help with IHC. We thank Minna Santanen for excellent technical assistance. We thank Petra Sipilä for her help with ChIP-Seq analysis. The results included here include the use of data from The Metastatic Prostate Cancer Project (https://mpcproject.org/), a project of Count Me In (https://joincountmein.org/). The results published here are in part based upon data generated by the TCGA Research Network: https://www.cancer.gov/tcga.

AUTHOR CONTRIBUTIONS

VV, KP, AK, IP, and MS designed the experiments; SM, RH, and MP designed and provided the two VCaP xenograft models; VV, AK, and MS designed the in silico analyses; KP and IP carried out the zebrafish experiments; VV, KP, SN, and IP extracted measurements from the zebrafish; VV, KP, AK, and IP prepared the figures; SN, YJ, MT and TJ contributed with experimental support; VV, KP, and MS prepared the original draft; VV, KP, AK, IP, SM, MP, and MS reviewed and edited the article; MS supervised the study; MS acquired funding; All authors have read and agreed to the published version of the manuscript.

FUNDING

This work was supported by grants from Academy of Finland, Finnish Medical Foundation, Finnish Cancer Foundations, Turku University Foundation, Turku University Hospital, TYKS Foundation, Finnish Cultural Foundation, and Turku Doctoral Programme of Molecular Medicine (TuDMM).

COMPETING INTERESTS

VV has received support to participate in educational events and conferences from Janssen. MS has received support to participate in educational events and conferences from Astellas, Amgen, Bayer, Novartis, BMS, Pierre Fabre, Lilly, and Roche; and received consultant fees from MSD, BMS, Roche, and Ipsen. KP, AK, SN, YJ, MT, TJ, and IP declare no competing financial interests.

ADDITIONAL INFORMATION

Supplementary information The online version contains supplementary material available at https://doi.org/10.1038/s41389-023-00485-z.

Correspondence and requests for materials should be addressed to Maria Sundvall.

Reprints and permission information is available at http://www.nature.com/reprints

Publisher's note Springer Nature remains neutral with regard to jurisdictional claims in published maps and institutional affiliations.

Virtanen V, Paunu K, Niva S, Sundvall M*, Paatero I* (2023)
Effect of caldesmon mutations in the development of zebrafish embryos.
Biochemical and Biophysical Research Communications

III

Biochemical and Biophysical Research Communications 669 (2023) 10–18

Contents lists available at ScienceDirect

Biochemical and Biophysical Research Communications

journal homepage: www.elsevier.com/locate/ybbrc

Effect of caldesmon mutations in the development of zebrafish embryos

Verneri Virtanen [a], Kreetta Paunu [a], Saana Niva [a], Maria Sundvall [a, b, **], Ilkka Paatero [c, *]

[a] Cancer Research Unit, Institute of Biomedicine, FICAN West Cancer Center Laboratory, University of Turku, Turku University Hospital, Kiinamyllynkatu 10, 20520, Turku, Finland
[b] Department of Oncology, Turku University Hospital, PL52, 20521, Turku, Finland
[c] Turku Bioscience Centre, University of Turku and Åbo Akademi University, Tykistökatu 6, 20520, Turku, Finland

ARTICLE INFO

Article history:
Received 3 May 2023
Accepted 20 May 2023
Available online 22 May 2023

Keywords:
Caldesmon
Zebrafish
Mutation
Developmental biology

ABSTRACT

Cancer is a profound medical concern and better treatments are needed for cancer patients. Therefore, new cancer targets are constantly being studied. These targets need not only be relevant for cancer progression, but their modulation needs to be tolerated reasonably well by the host. Caldesmon is one of these proposed novel targets for cancer therapy. Therefore, we analyzed effects of caldesmon mutations in normal development using genetically modified zebrafish embryos. We analyzed mutations in both zebrafish caldesmon genes, *cald1a* and *cald1b* and analyzed effects of either mutation alone or as in combination in double homozygous embryos using molecular, morphological and functional analyses. The effects of caldesmon mutations were mild and the gross development of zebrafish embryos was normal. The caldesmon mutant embryos had, however, alterations in response to light-stimulus in behavioural assays. Taken together, the effects of caldesmon mutations in the development of zebrafish embryos were reasonably well tolerated and did not indicate significant concerns for caldesmon being a potential target for cancer therapy.

1. Introduction

Cancer is a one of the leading causes of death and the need for new therapeutics and therapeutic targets is evident. Many factors related to actomyosin contractions have been implicated as integral regulators of cell migration. In the directionally migrating non-muscle cells, actomyosin contractions produce motility via stress fibers, which can both rupture and strengthen focal adhesions by contraction [1]. Thus, factors interacting with the actomyosin bundles contribute to generating forces that migrating cells exert towards the extracellular matrix. The ability to migrate can be attained by cancer cells that undergo epithelial to mesenchymal transition (EMT), which entails the loss of polarity and cell-to-cell adhesions [2]. The multistage metastatic process set in motion by cancer cells invading into the adjacent tissues is thus initiated by factors promoting cell motility and EMT [3].

One of the factors in actomyosin pathway is caldesmon, which is encoded by the *CALD1* gene in humans [4]. The human *CALD1* produces two major isoforms by alternative splicing, h-caldesmon and l-caldesmon, which both share common actin-, myosin-, tropomyosin- and calmodulin-binding domains, but are exclusively expressed in muscle cells and in non-muscle cells, respectively [5,6]. Observations from of the role of *CALD1* in tumor invasion and metastasis [7–10], indicated the potential of *CALD1* as a therapeutic target for anti-cancer treatments.

In an optimal case, a potential therapeutic target has significant adverse effects only in tumor but not in healthy tissues. Finding and developing novel chemical compounds for new target molecules is slow and costly process [11] and many novel therapeutics fail due to safety concerns [12]. These failures may be related to toxic side effects or target-related toxicities. Already in the early stages of target validation, the potential of target-related toxicities can be evaluated by using gene-modified animal models [13]. Zebrafish are an affordable model, large number of mutant alleles are available, and the development of embryo and larvae can be easily analyzed [14]. Here, we chose to utilize mutant zebrafish models to characterize potential side effects of targeting *cald1*. We generated single-mutant zebrafish for both *cald1a* and *cald1b* genes as well as

* Corresponding author.
** Corresponding author. Department of Oncology, Turku University Hospital, PL52, 20521, Turku, Finland.
E-mail addresses: mahesu@utu.fi (M. Sundvall), ilanpa@utu.fi (I. Paatero).

https://doi.org/10.1016/j.bbrc.2023.05.079

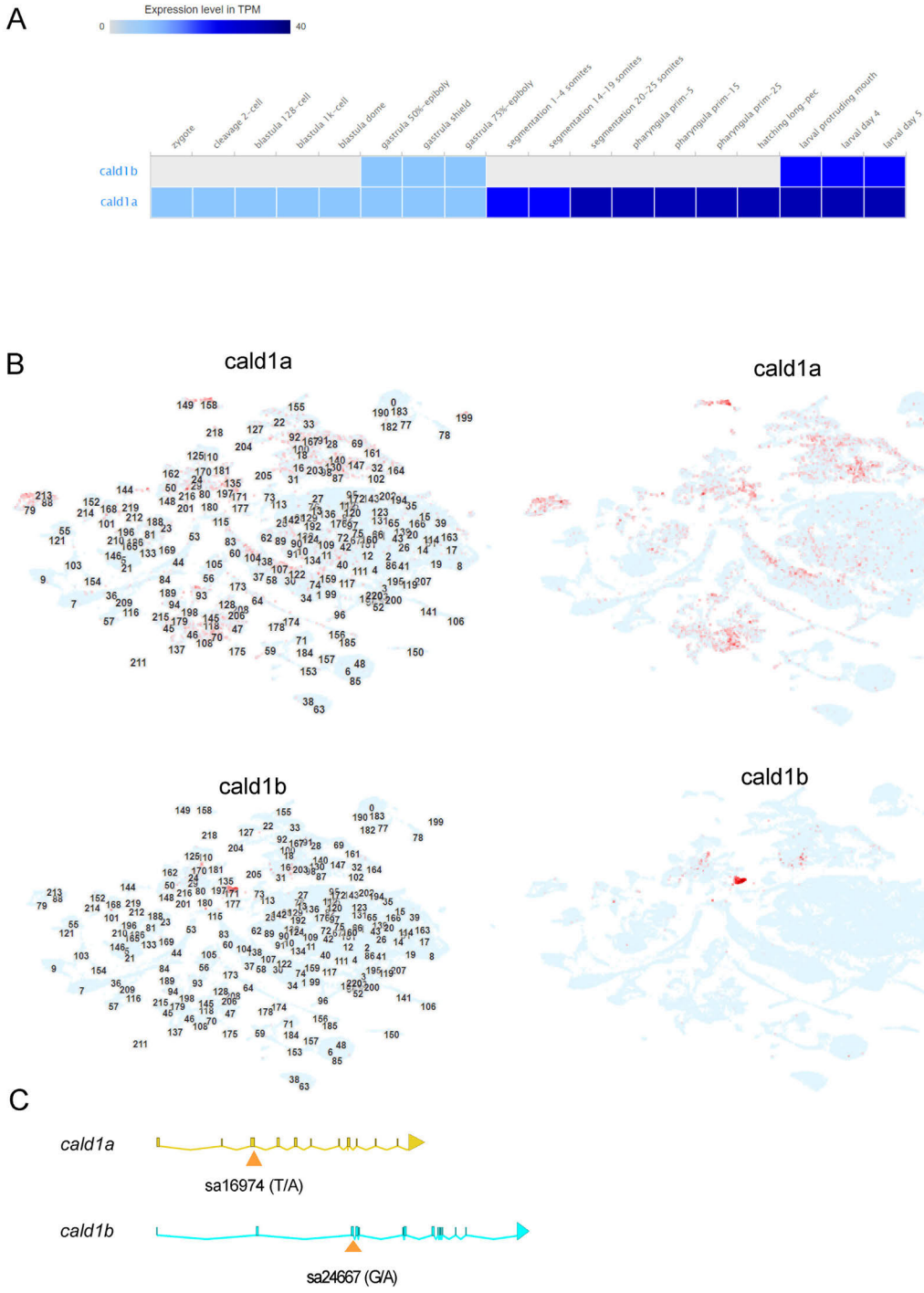

Fig. 1. The in silico analysis of cald1a and cald1b mRNA expression, and the mutations (A) Whole-embryo RNA-seq data for *cald1a* and *cald1b* from zebrafish embryo developmental time series. Data obtained from Expression Atlas (www.ebi.ac.uk/gxa/home, dataset E-ERAD-475, data downloaded January 3rd, 2023). (B) Single-cell RNA-seq data for developing

double-mutant zebrafish, which we then assessed for changes in morphology and in behavior during early development.

2. Materials and methods

2.1. Zebrafish husbandry

Analyses of zebrafish embryos were carried out under the licenses MMM/465/712–93 (issued by the Finnish Ministry of Agriculture and Forestry) and ESAVI/9339/04.10.07/2016 and ESAVI/31414/2020 (granted by Project Authorization Board of Regional State Administrative Agency for Southern Finland) according to the regulations of the Finnish Act on Animal Experimentation (62/2006). The study was carried out in compliance with the ARRIVE guidelines.

2.2. Zebrafish cald1a and cald1b mutants and genotyping

Zebrafish lines carrying *cald1a*^{sa16974} (*cald1a*$^{-/-}$) and *cald1b*^{sa24667} (*cald1b*$^{-/-}$) mutant alleles were obtained from European Zebrafish Resource Centre, Karlsruhe, Germany, and provided by Dr. Derek Stemple, Wellcome Trust Sanger Institute, Genome Research Limited, Hinxton, UK. The breeding stocks of these fish were kept as heterozygotes and intercrossed to generate homozygous embryos for the analyses. Zebrafish embryo DNA was extracted either using NucleoSpin TriPrep RNA, DNA, and protein extraction kit (Macherey-Nagel, Allentown, PA) (gene expression studies) or by using alkaline lysis (morphological and behavioural studies) dissolving the embryos in 50 mM NaOH 95 °C for 10 min. After alkaline lysis, 1 M Tris HCl pH 8 was used to neutralize the DNA solution. Genotyping PCR were done by using KASP genotyping assay (Biosearch Technologies, Hoddesdon, United Kingdom). A similar workflow was used in genotyping adult carrier fish.

2.3. Morphological analysis

The embryos were anesthetized and imaged using Nikon Eclipse Ti2 (Nikon). Data from images was extracted in ImageJ. Overall morphology was evaluated visually. Eye size, head size, body length and pericardium size were measured with ImageJ. All measurements were done independently by two investigators. Although formal blinding and randomization was not carried out, the measurements and analyses were essentially blinded as samples were genotyped after experimentation and phenotyping.

2.4. Quantitative real-time PCR

The RNA was extracted from zebrafish embryos using NucleoSpin TriPrep RNA, DNA, and protein extraction kit (Macherey-Nagel). RNA was further purified by using RNA Clean & Concentrator-25 kit (Zymo Research, Irvine, CA). After purification, RNA was reverse-transcribed with High-Capacity cDNA Reverse Transcription Kit (Thermo Fisher Scientific), and the cDNA was amplified with gene-specific primer pairs (*cald1a:* 5′ CACTTCGTTTGCCTCATCGC 3′, 5′ CGCCGATATGCCATCCTCTC 3′ and *cald1b*: 5′ CAGGAGGAAACAGTGCCAGA 3′, 5′ TCTTGCGGCTTTGTTGACAC 3′) using SYBR™ Green PCR Master Mix (Applied Biosystems, Bedford, MA). The quantities measured by real-time PCR were normalized to the *Rpl13* (5′GGCGGACCGATTCAATAAGGTTCTGATCATTG 3′, 3′CCAGAGATGTTGATACCCTCACACCTCAC 5′) expression level in each sample.

2.5. Behavior assays

Zebrafish behavioural assays were carried out using DanioVision (Noldus IT) instrument. Four 4dpf zebrafish embryos were placed in 96-well square bottom Whatman Uniplate multiwell plates (Sigma-Aldrich) in 300 μl of E3 medium. The plate was transferred to prewarmed DanioVision instrument (28.5 °C). After 30min adaptation phase in darkness, the embryos were subjected to three cycles of 5min light followed by 5min of darkness. After experimentation, the embryos were anesthesized with 200 mg/l tricaine and DNA was extracted for genotyping. The data analysis was carried out using EthoVisio XT and GraphPad Prism 9. Prior to statistical analysis, the first 20mins were removed (adaptation phase), then baseline was calculated from 20 to 30min time points, and it was subtracted from values to correct for potential differences in baseline values. 2-way ANOVA with Holm-Sidak post-hoc test for multiple testing correction was carried out. To increase statistical power, the different genotypes were pooled. *wt* (n = 52) = *wt* + *cald1a*$^{+/-}$ + *cald1b*$^{+/-}$; cald1a (n = 24) = *cald1a*$^{-/-}$ (*cald1b* either +/+ or +/−); *cald1b* (n = 38) = *cadl1b*$^{-/-}$ (*cald1a* either +/+ or +/−); *cald1a, cald1b* (n = 13) = homozygous mutant for both genes. In some experiments, the embryos were stimulated with 20 mM pentylene tetrazolium (PTZ), which was followed by similar adaptation and light-dark cycles. In these experiments neither pooling nor baseline subtraction was carried out.

3. Results

3.1. The in silico analysis of cald1a and cald1b mRNA expression

Zebrafish possess two caldesmon genes *cald1a* (ZFIN code: ZDB-GENE-030131-1629) located in chromosome 4 and *cald1b* (ZDB-GENE-090313-229) located in chromosome 25. To get insights into the potential role of caldesmon (*cald1a* and *cald1b*) in the developing zebrafish, we carried out in silico analysis of gene expression using published RNA-seq data set [15] using Gene Expression Atlas [16]. Both *cald1a* and *cald1b* were expressed during the development of zebrafish embryos (Fig. 1A, whole embryo RNA-seq data). The *cald1a* was expressed throughout development, with lower levels during earlier time points and with weak maternal contribution. Expression of *cald1b* was low in the earlier stages and showed weak activation during gastrulation, whereas more robust expression was evident only from protruding mouth stage (72 hpf) onwards. Besides being expressed during the development, the temporal whole animal expression patterns did not yield profound insights into role of *cald1* during development.

Recent advances in single-cell RNA-seq technology has enabled transcriptomic analysis of whole zebrafish embryos and single-cell level. We utilized pre-existing data set [17] using USCS Cell Browser [18] to analyze the spatio-temporal expression of cald1 transcripts during the development. *cald1a* was expressed broadly and especially in clusters associated with vasculature (clusters 79,88, 171, 213), heart (clusters 130, 147), neural crest (eg. 64, 87, 181), retina (30, 34, 58, 60, 83, 104, 138, 107, 122) and basal cells (47,145,70,108,118), whereas expression of *cald1b* was predominant

zebrafish embryos. Data obtained from USCS Cell Browser (http://cells.ucsc.edu/?ds=zebrafish-dev, data obtained January 3rd, 2023). The numbers in left panels refer to cell cluster ID numbers and in the right panels these are omitted for clarity. (C) Schematic illustration of the location of mutations in *cald1a* and *cald1b* genes. Exons are marked as bars and connected by lines representing introns. Mutation sa24667 locates in exon 3 of *cald1a*, disrupting the essential splice site. The first 67 amino acids of 778 amino acids in *cald1a* are predicted to be intact in *cald1a*(sa24667) mutant. Mutation sa16974 locates in exon 3 and creates a premature stop codon. The first 190 amino acids of 778 amino acids in *cald1b* are predicted to be intact in *cald1b*(sa16974) mutant.

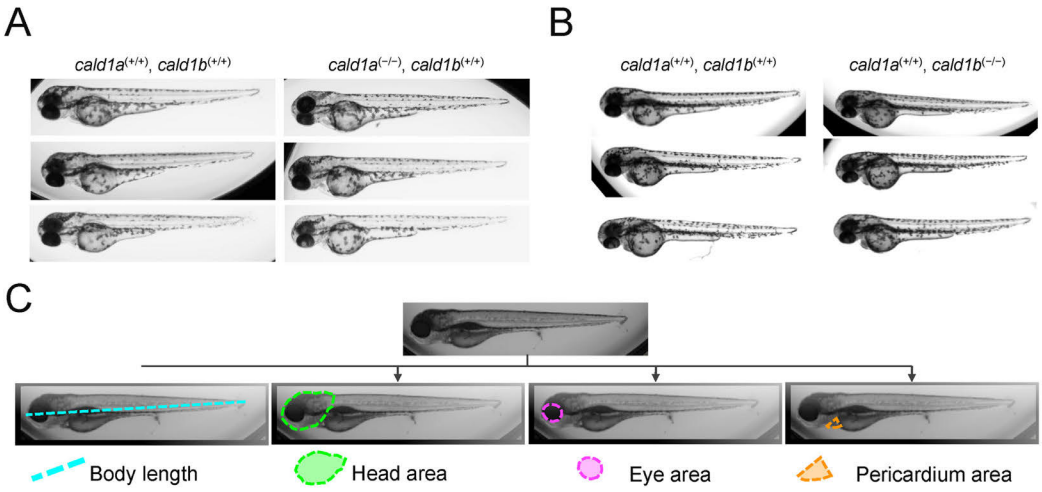
A
cald1a(+/+), cald1b(+/+)
cald1a(−/−), cald1b(+/+)
B
cald1a(+/+), cald1b(+/+)
cald1a(+/+), cald1b(−/−)
C
Body length
Head area
Eye area
Pericardium area

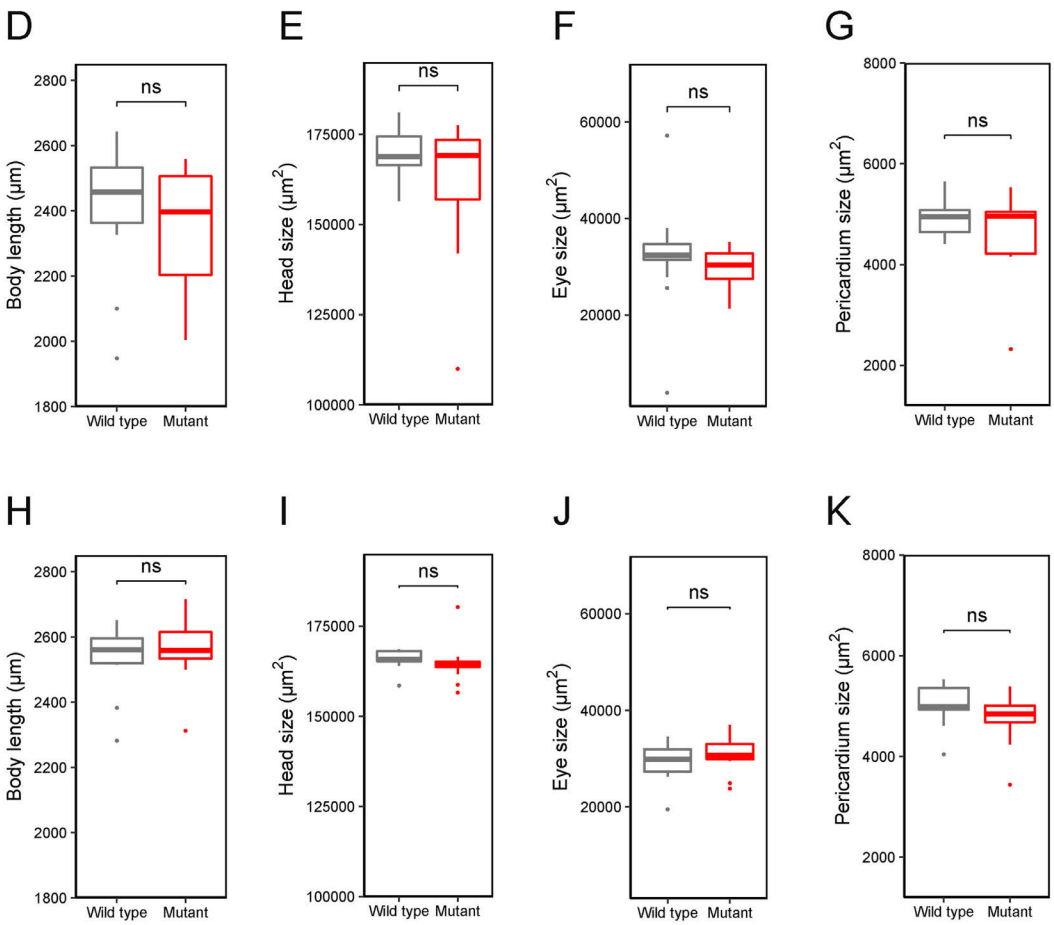
D
Body length (µm)
E
Head size (µm²)
F
Eye size (µm²)
G
Pericardium size (µm²)
H
Body length (µm)
I
Head size (µm²)
J
Eye size (µm²)
K
Pericardium size (µm²)
ns
Wild type
Mutant

in vascular smooth muscle cells (cluster 171) and neural crest (24,29, 31,170) (Fig. 1B).

To study caldesmon in vasculature development we searched for potentially existing *cald1a* and *cald1b* mutant fish lines. Indeed, suitable mutant alleles, *cald1a*^{sa16974} (named here as *cald1a*$^{-/-}$) and *cald1b*^{sa24667} (named here as *cald1b*$^{-/-}$), were generated in Zebrafish Mutation Project [19] (Fig. 1C) and they were available through European Zebrafish Resource Centre EZRC. Therefore, we used these mutant lines for analysis of the role of *cald1a* and *cald1b* in developing zebrafish.

3.2. No clear morphological phenotype for cald1a or cald1b single-mutant embryos

To investigate the effect of *cald1a* and *cald1b* on the morphology of developing zebrafish embryos (Fig. 2A and B), we measured standard length, area of the cephalic region, eye area, and pericardial area from brightfield images of *cald1a* or *cald1b* mutant embryos (Fig. 2C). To our surprise, no significant difference between the genotypes was detected in the body length, head size, eye size, or pericardium (Fig. 2D–K).

3.3. Regulation of cald1a and cald1b mRNA expression

To analyze *cald1a* and *cald1b* gene expression in mutant embryos we carried out qPCR analyses. In these qPCR analyses, *cald1a* mRNA was significantly reduced in the *cald1a*-mutant zebrafish larvae compared with the wild type (Fig. 3A). This was indicative of nonsense-mediated decay of mutated dysfunctional mRNAs [20]. Interestingly, *cald1b* mRNA expression was strongly increased in *cald1b*-mutant zebrafish larvae (Fig. 3B). This is consistent with a dysfunctional protein product in the case where a putative negative feedback loop regulates gene expression [21]. Previous work has indicated that mutant phenotypes could often be alleviated by compensatory mRNA expression from closely related genes upon nonsense-mediated decay of related transcripts [22]. To address this issue, we analyzed *cald1b* mRNA expression in *cald1a* mutants and vice versa. Neither *cald1a* mutants showed compensatory upregulation of *cald1b* mRNA (Fig. 3C) nor the *cald1b* mutants displayed increased compensatory expression of *cald1a* mRNA (Fig. 3D). Despite the lack of compensation response, the *cald1a* and *cald1b* could still have redundant functions and both genes might need to be mutated to see robust phenotypes.

3.4. No clear morphological phenotype for cald1a and cald1b double-mutant embryos

To investigate the effect of simultaneous mutation of both *cald1a* and *cald1b* on the morphology of developing zebrafish embryos, we measured standard length, area of the cephalic region, eye area, and pericardial area using manual segmentation of the brightfield images in ImageJ. No significant difference between the genotypes was detected in the body length, head size, eye size, or pericardium in double-mutant embryos (Fig. 4A–E).

3.5. Mutation of cald1a and cald1b genes is not lethal for zebrafish larvae

The lack of phenotype could be resulting from loss of strongly affected *cald1*-mutant embryos very early in the development. To identify potential early embryonic lethality, we analyzed the distribution of genotypes in the offspring of double heterozygote parents. The distribution of genotypes followed expected allele frequencies and also the Mendelian inheritance pattern of a dihybrid cross (Fig. 5A, B, C, D and E), indicating that there was no early embryonic lethality caused neither by single *cald1a* or *cald1b* mutation, nor by double homozygous mutation in *cald1a* and *cald1b*.

3.6. cald1-mutation has mild effects on the behavior of zebrafish embryos

Many gene effects are not evident at gross morphological level or survival, but have more subtle impact physiological functions of the organism. In zebrafish, the motility of larvae is widely used assay to measure effects on organismal locomotion and behavior [23]. Therefore, we analyzed the embryos from a *cald1a, cald1b* dihybrid cross for the ability to move and respond to stimulus.

The analysis of fish for the light-response indicated that the *cald1a, cald1b* double mutant fish displayed weaker responses to alternating light-dark illumination (Fig. 6A). This indicated that the *cald1a, cald1b* double mutant fish had mild neurological defect. *cald1a* gene mutation alone caused a milder phenotype (Fig. 6B), but the simultaneous mutation of also *cald1b* gene potentiated this effect. Mutation in *cald1b* gene did not have an effect (Fig. 6C). To further analyze if the effect was on visual detection of changes in lighting or the actual ability to move, we stimulated embryos with epileptogenic compound pentylenetetrazol (PTZ). The addition of PTZ induced embryo motility, and prevented light-responses. The *cald1a, cald1b* double mutants, however, did not differ from controls in this setting (Fig. 6D). This implied that the effect of *cald1* mutation was occurring at visual perception and neurological signal processing levels rather than due to better contraction capabilities of muscles.

4. Discussion

By constructing a *cald1a-cald1b*-mutant zebrafish model, we demonstrate that *cald1* mutations are not lethal, and no difference in the phenotype between the wild type and the double-mutant is present during early development. Our phenotype analysis was performed on dpf 4; therefore, potential later changes in the phenotype cannot be excluded. Previous work shows *cald1* knockdown in a zebrafish morphant model that presents with serious defects in vasculogenesis, angiogenesis and cardiac organogenesis observed at dpf 1.5–5 [24,25]. More recent zebrafish works put forward considerable criticism for morpholino studies, and therefore confirmation with an appropriate mutant model is recommended [26]. Morphant phenotypes are often more severe and can differ from mutant phenotypes for various reasons, including frequent off-target effects [26]. It is also possible that the

Fig. 2. Analyses of the anatomy of *cald1a* and *cald1b* single-mutant zebrafish. (A) Representative brightfield images of wild-type zebrafish larvae *cald1a* (+/+), *cald1b* (+/+) (left) and single-mutant zebrafish larvae *cald1a* (−/−), *cald1b* (+/+) (right) 4 dpf. (B) Representative brightfield images of wild-type zebrafish larvae *cald1a* (+/+), *cald1b* (+/+) (left) and single-mutant zebrafish larvae *cald1a* (+/+), *cald1b* (−/−) (right) 4 dpf. 19) (C) Schematic illustration of the measurements taken from the zebrafish larvae. Body length, head area, eye area and pericardium area are highlighted over the duplicates of the original image with teal, green, purple, and orange, respectively. (D–G) Morphological measurements and analyses display no statistically significant changes in body length, head size, eye size, and in pericardial area when compared wild-type *cald1a* (+/+), *cald1b* (+/+) (n = 22) larvae to single-mutant larvae *cald1a* (−/−), *cald1b* (+/+) (n = 12). All measurements were done by two independent investigators. (H–K) Morphological measurements and analyses display no statistically significant changes in body length, head size, eye size, and in pericardial area when compared wild-type *cald1a* (+/+), *cald1b* (+/+) larvae (n = 13) to single-mutant larvae *cald1a* (+/+), *cald1b* (−/−)(n = 19). All measurements were done by two independent investigators. (For interpretation of the references to colour in this figure legend, the reader is referred to the Web version of this article.)

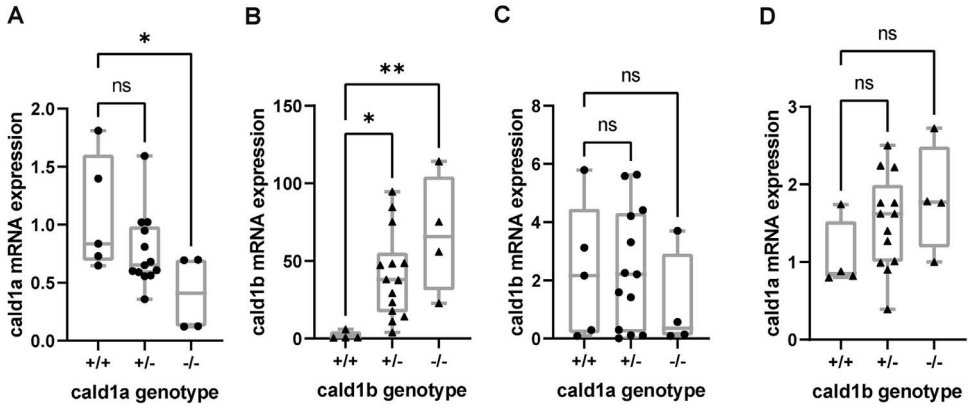

Fig. 3. *cald1a* and *cald1b* mutant mRNAs have abnormal expression levels. (A) Relative *cald1a* mRNA expressions in different genotypes of *cald1a* (left) ($n_{WT} = 5$, $n_{(\pm)} = 15$, and $n_{(-/-)} = 4$). (B) Relative *cald1b* mRNA expressions in different genotypes of *cald1b* (right) ($n_{WT} = 4$, $n_{(\pm)} = 14$, and $n_{(-/-)} = 4$) in zebrafish larvae (C) Relative *cald1b* mRNA expressions in different genotypes of *cald1a* (right) ($n_{WT} = 5$, $n_{(\pm)} = 13$, and $n_{(-/-)} = 4$). (D) Relative *cald1a* mRNA expressions in different genotypes of *cald1b* (left) ($n_{WT} = 4$, $n_{(\pm)} = 14$, and $n_{(-/-)} = 4$) in zebrafish larva. ns = not significant, $*p < 0.05$, $**p < 0.01$, and $***p < 0.001$ as determined by ANOVA.

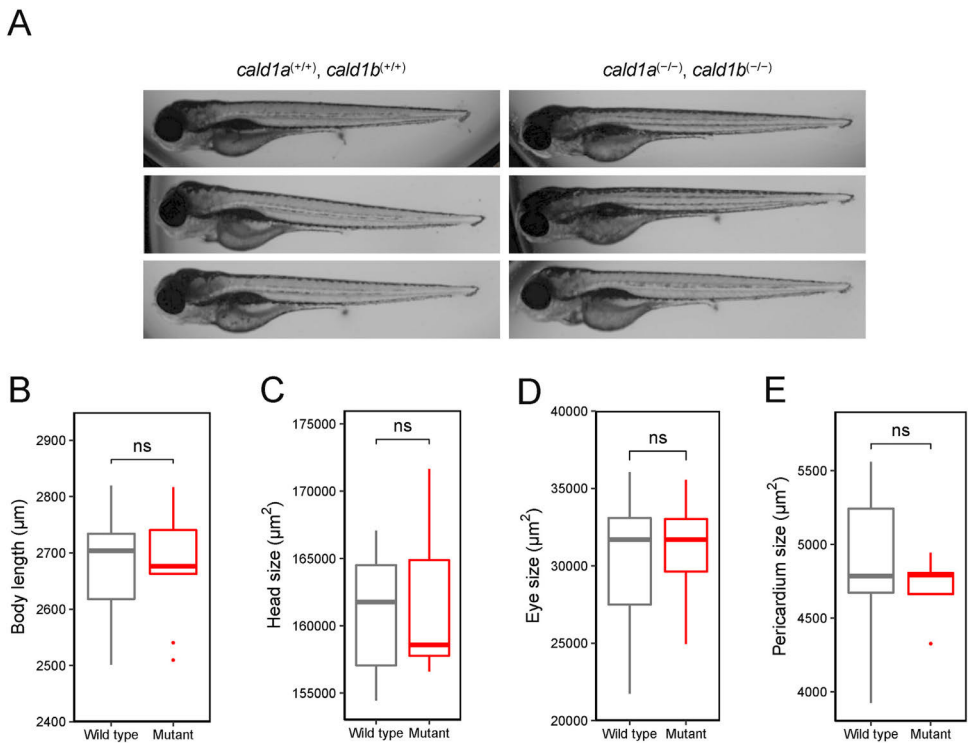

Fig. 4. *cald1a*, *cald1b* double-mutant zebrafish have no significant morphological phenotype (A) Representative brightfield images of wild type zebrafish larvae *cald1a* (+/+), *cald1b* (+/+) (left) and mutant zebrafish larvae *cald1a* (−/−), *cald1b* (−/−) (right) at 4 dpf. (B–E) Morphological measurements and analyses display no statistically significant changes (ns) in body length, head size, eye size, and in the pericardial area when compared wild type *cald1a* (+/+), *cald1b* (+/+) larvae (n = 15) to double-mutant *cald1a* (−/−), *cald1b* (−/−) larvae (n = 10).

mutant lines in our study are hypomorphic and not fully amorphic alleles.

In our studies, we observed effects of *cald1* mutation on light-dark cycle induced motility. As *cald1a* was clearly expressed in retinal and retinal progenitor cells but not in skeletal muscles, and there was no differences upon pharmacological stimulation with

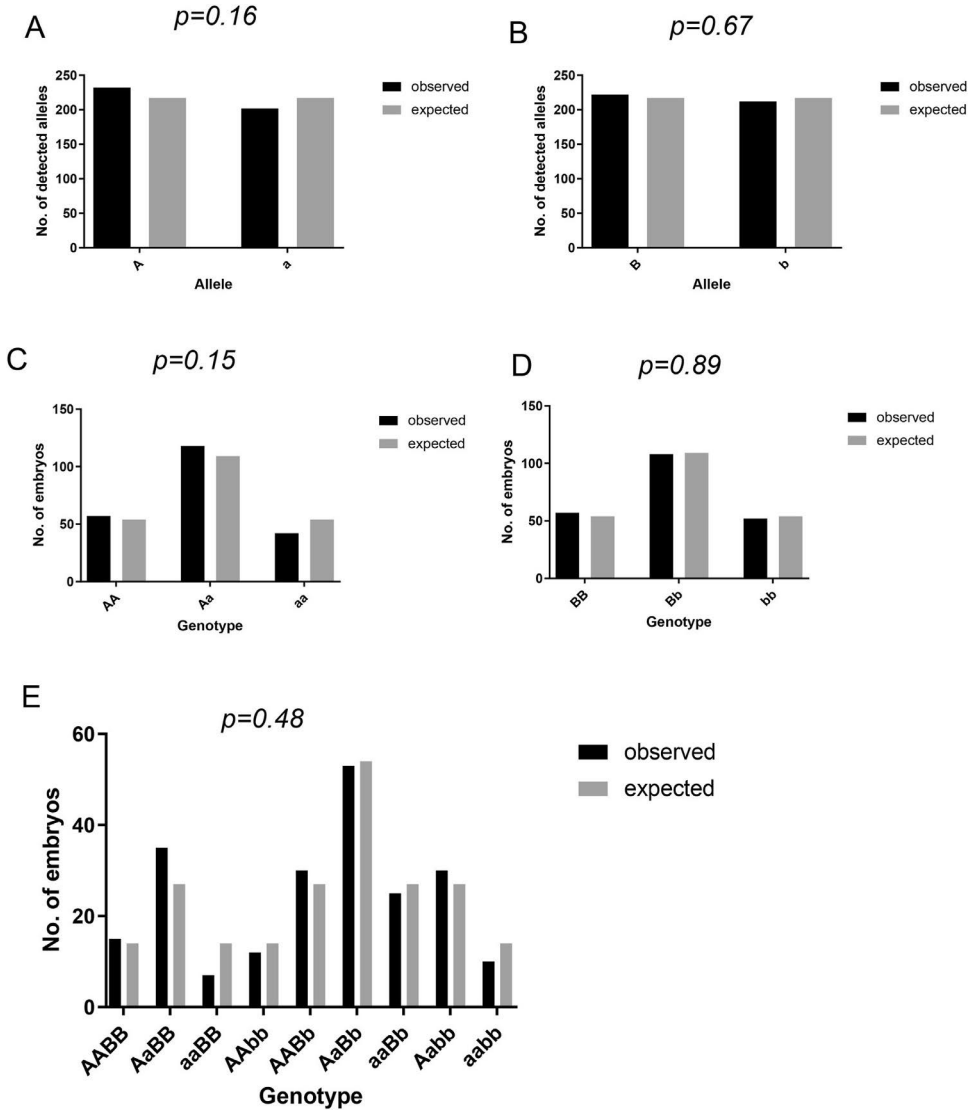

Fig. 5. Mutation of cald1a and cald1b genes is not lethal for zebrafish larvae Analyses of zebrafish allele frequencies and genotype of offspring. Fish heterozygous for both *cald1a* and *cald1b* mutation were incrossed in a dihybrid cross. All embryos were genotyped and observed counts (n = 217) were statistically compared to expected counts using binomial (A and B) or Chi-square (C, D, and E) test. (A) Count of detected alleles of *cald1a* wild-type (marked with A) and sa24667 mutant (a) allele. (B) Count of detected alleles of *cald1b* wild-type (marked with B) and sa16974 mutant (b) allele. (C) Distribution of *cald1a* genotypes. (D) Distribution of *cald1b* genotypes. (E) Distribution of *cald1a*, *cald1b* dihybrid genotypes.

PTZ, it seems plausible that the effect on light-dark cycle induced responses occurs at the visual perception and signal processing level. The embryos were still qualitatively responding correctly to the visual stimulus, but the magnitude of the response was affected. This data indicates that the mutations in *cald1a* and *cald1b* have functional effect. This doesn't fully reject possibility for hypomorphic mutation, but nevertheless indicates that at least some inhibition of cald1 could be tolerated reasonably well.

In the published knockout mice lacking both caldesmon isoforms (l-caldesmon and h-caldesmon), the mice die perinatally with an unresolved umbilical hernia [27]. However, in a model with homozygous loss of h-caldesmon, the loss is shown not to be lethal [28,29]. Another mouse model with mutations targeting a functional domain in both isoforms is lethal as a homozygote but reproduces normally as a heterozygote [30]. The severe cardiovascular defects are not described in *Cald1*-deficient mice, although the underlying causes of pre- and postnatal lethality are not fully understood [28–30]. More comprehensively the postnatal relevance of *Cald1*-deficiency could be evaluated in future studies by using conditional mouse models. Depletion of *cald1* in a xenopus

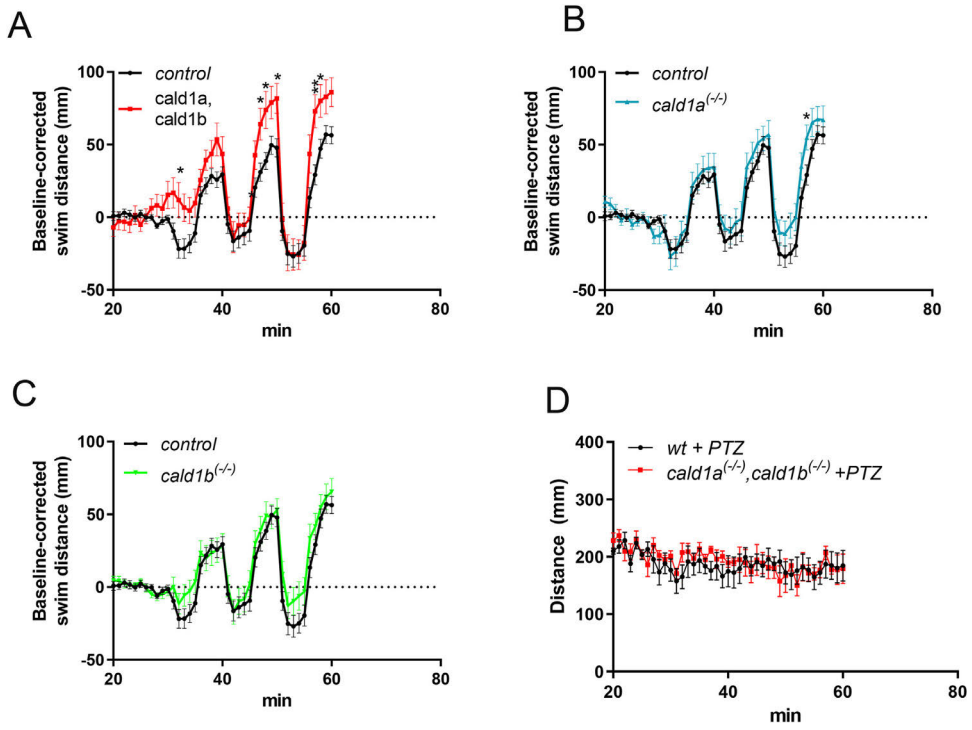

Fig. 6. Cald1 mutation has mild locomotory phenotype in zebrafish larvae Analyses of behavior and locomotion of *cald1a* and *cald1b* mutants in 96-well assay using DanioVision instrument. After the adaptation phase, an alternating light-dark cycles (5min light, 5min darkness) were used to stimulate movements. Some genotypes were pooled to increase statistical power. A) *control* (n = 52, genotypes *wt; cald1a*$^{+/-}$ *and cald1b*$^{+/-}$*)* vs *cald1a, cald1b* double-mutants (n = 13, genotypes, *cald1a*$^{-/-}$, *cald1b*$^{-/-}$), B) *control* vs *cald1a* mutants (n = 24, genotypes *cald1a*$^{-/-}$ and *cald1a*$^{-/-}$, *cald1b*$^{+/-}$*)*, C) *control* vs *cald1b* mutants (n = 38, genotypes *cald1b*$^{-/-}$ and *cald1b*$^{-/-}$,*cald1a*$^{+/-}$), D) Stimulation of wt (n = 5) or *cald1a,cald1b* mutants (n = 5) with pentylene tetrazolium (PTZ). In A-C the same control data are shown as reference.

morpholino model leads to severe cartilage defects due to reduced neural crest migration, suggesting its critical function in normal neural crest migration in xenopus [31]. Taken together, *Cald1* may have critical roles in cell migration during early development. However, our results show no strong phenotype in *cald1*-mutated zebrafish larvae, which suggests tolerability towards caldesmon inhibition to a certain degree in healthy tissues, which is a prerequisite for caldesmon being a therapeutic target.

Funding

This work was supported by grants from Academy of Finland, Finnish Medical Foundation, Finnish Cancer Foundations, Turku University Foundation, Turku University Hospital, TYKS Foundation, Finnish Cultural Foundation, and Turku Doctoral Programme of Molecular Medicine (TuDMM).

Contributions

VV, KP, IP, and MS designed the experiments; KP and IP carried out the zebrafish experiments; VV, KP, SN, and IP extracted measurements from the zebrafish; VV, KP, and IP prepared the figures; IP, KP, VV and MS prepared the original draft; VV, KP, IP, and MS reviewed and edited the article; IP and MS supervised the study; MS acquired funding; All authors have read and agreed to the published version of the manuscript.

Declaration of competing interest

Authors declare no competing financial interests.

Acknowledgements

We thank Zebrafish Core, Cell Imaging Core and Finnish Functional Genomics Centre (all in Turku Bioscience Centre and supported by Biocenter Finland) for services, instrumentation, and consultations. We thank Minna Santanen for excellent technical assistance.

References

[1] T. Svitkina, The actin cytoskeleton and actin-based motility, Cold Spring Harbor Perspect. Biol. 10 (2018), https://doi.org/10.1101/cshperspect.a018267.
[2] K. Ganesh, J. Massagué, Targeting metastatic cancer, Nat. Med. 27 (2021) 34–44, https://doi.org/10.1038/s41591-020-01195-4.
[3] D.X. Nguyen, P.D. Bos, J. Massagué, Metastasis: from dissemination to organ-specific colonization, Nat. Rev. Cancer 9 (2009) 274–284, https://doi.org/10.1038/nrc2622.
[4] K. Hayashi, H. Yano, T. Hashida, R. Takeuchi, O. Takeda, K. Asada, E.I. Takahashi, I. Kato, K. Sobue, Genomic structure of the human caldesmon gene, Proc. Natl. Acad. Sci. U. S. A 89 (1992) 12122–12126, https://doi.org/10.1073/pnas.89.24.12122.
[5] K. Sobue, Y. Muramoto, M. Fujita, S. Kakiuchi, Purification of a calmodulin-binding protein from chicken gizzard that interacts with F-actin, Proc. Natl. Acad. Sci. U. S. A 78 (1981) 5652–5655, https://doi.org/10.1073/pnas.78.9.5652.

[6] K. Sobue, T. Tanaka, K. Kanda, Purification and characterization of caldesmon77: a calmodulin-binding protein that interacts with actin filaments from bovine adrenal medulla, Proc. Natl. Acad. Sci. U. S. A 82 (1985) 5025–5029, https://doi.org/10.1073/pnas.82.15.5025.
[7] T. Manes, D.Q. Zheng, S. Tognin, A.S. Woodard, P.C. Marchisio, L.R. Languino, Avβ3 integrin expression up-regulates Cdc2, which modulates cell migration, J. Cell Biol. 161 (2003) 817–826, https://doi.org/10.1083/jcb.200212172.
[8] K.P. Chang, C.L.A. Wang, H.K. Kao, Y. Liang, S.C. Liu, L.L. Huang, C. Hseuh, Y.J. Hsieh, K.Y. Chien, Y.S. Chang, J.S. Yu, L.M. Chi, Overexpression of caldesmon is associated with lymph node metastasis and poorer prognosis in patients with oral cavity squamous cell carcinoma, Cancer 119 (2013) 4003–4011, https://doi.org/10.1002/cncr.28300.
[9] M.S. Lee, J. Lee, J.H. Kim, W.T. Kim, W.J. Kim, H. Ahn, J. Park, Overexpression of caldesmon is associated with tumor progression in patients with primary non-muscle-invasive bladder cancer, Oncotarget 6 (2015) 40370–40384, https://doi.org/10.18632/oncotarget.5458.
[10] S.B. Kokate, K. Ciuba, V.D. Tran, R. Kumari, S. Tojkander, U. Engel, K. Kogan, S. Kumar, P. Lappalainen, Caldesmon controls stress fiber force-balance through dynamic cross-linking of myosin II and actin-tropomyosin filaments, Nat. Commun. 13 (2022) 1–20, https://doi.org/10.1038/s41467-022-33688-w.
[11] M.D. Rawlins, Cutting the cost of drug development? Nat. Rev. Drug Discov. 3 (2004) 360–364, https://doi.org/10.1038/nrd1347.
[12] M.J. Waring, J. Arrowsmith, A.R. Leach, P.D. Leeson, S. Mandrell, R.M. Owen, G. Pairaudeau, W.D. Pennie, S.D. Pickett, J. Wang, O. Wallace, A. Weir, An analysis of the attrition of drug candidates from four major pharmaceutical companies, Nat. Rev. Drug Discov. 14 (2015) 475–486, https://doi.org/10.1038/nrd4609.
[13] N.E. Sharpless, R.A. DePinho, The mighty mouse: genetically engineered mouse models in cancer drug development, Nat. Rev. Drug Discov. 5 (2006) 741–754, https://doi.org/10.1038/nrd2110.
[14] G.J. Lieschke, P.D. Currie, Animal models of human disease: zebrafish swim into view, Nat. Rev. Genet. 8 (2007) 353–367, https://doi.org/10.1038/nrg2091.
[15] R.J. White, J.E. Collins, I.M. Sealy, N. Wali, C.M. Dooley, Z. Digby, D.L. Stemple, D.N. Murphy, K. Billis, T. Hourlier, A. Füllgrabe, M.P. Davis, A.J. Enright, E.M. Busch-Nentwich, A high-resolution mRNA expression time course of embryonic development in zebrafish, Elife 6 (2017) 1–32, https://doi.org/10.7554/eLife.30860.
[16] I. Papatheodorou, P. Moreno, J. Manning, A.M.P. Fuentes, N. George, S. Fexova, N.A. Fonseca, A. Füllgrabe, M. Green, N. Huang, L. Huerta, H. Iqbal, M. Jianu, S. Mohammed, L. Zhao, A.F. Jarnuczak, S. Jupp, J. Marioni, K. Meyer, R. Petryszak, C.A. Prada Medina, C. Talavera-López, S. Teichmann, J.A. Vizcaino, A. Brazma, Expression Atlas update: from tissues to single cells, Nucleic Acids Res. 48 (2020), https://doi.org/10.1093/nar/gkz947. D77–D83.
[17] D.R. Farnsworth, L.M. Saunders, A.C. Miller, A single-cell transcriptome atlas for zebrafish development, Dev. Biol. 459 (2020) 100–108, https://doi.org/10.1016/j.ydbio.2019.11.008.
[18] M.L. Speir, A. Bhaduri, N.S. Markov, P. Moreno, T.J. Nowakowski, I. Papatheodorou, A.A. Pollen, B.J. Raney, L. Seninge, W.J. Kent, M. Haeussler, UCSC Cell Browser: visualize your single-cell data, Bioinformatics 37 (2021) 4578–4580, https://doi.org/10.1093/bioinformatics/btab503.
[19] R.N.W. Kettleborough, E.M. Busch-Nentwich, S. a Harvey, C.M. Dooley, E. de Bruijn, F. van Eeden, I. Sealy, R.J. White, C. Herd, I.J. Nijman, F. Fényes, S. Mehroke, C. Scahill, R. Gibbons, N. Wali, S. Carruthers, A. Hall, J. Yen, E. Cuppen, D.L. Stemple, A systematic genome-wide analysis of zebrafish protein-coding gene function, Nature 496 (2013) 494–497, https://doi.org/10.1038/nature11992.
[20] T. Kurosaki, M.W. Popp, L.E. Maquat, Quality and quantity control of gene expression by nonsense-mediated mRNA decay, Nat. Rev. Mol. Cell Biol. 20 (2019) 406–420, https://doi.org/10.1038/s41580-019-0126-2.
[21] D.C. Marciano, R.C. Lua, C. Herman, O. Lichtarge, Cooperativity of negative autoregulation confers increased mutational robustness, Phys. Rev. Lett. 116 (2016) 1–6, https://doi.org/10.1103/PhysRevLett.116.258104.
[22] M.A. El-Brolosy, Z. Kontarakis, A. Rossi, C. Kuenne, S. Günther, N. Fukuda, K. Kikhi, G.L.M. Boezio, C.M. Takacs, S.L. Lai, R. Fukuda, C. Gerri, A.J. Giraldez, D.Y.R. Stainier, Genetic compensation triggered by mutant mRNA degradation, Nature 568 (2019) 193–197, https://doi.org/10.1038/s41586-019-1064-z.
[23] M. Granato, F.J. van Eeden, U. Schach, T. Trowe, M. Brand, M. Furutani-Seiki, P. Haffter, M. Hammerschmidt, C.P. Heisenberg, Y.J. Jiang, D. a Kane, R.N. Kelsh, M.C. Mullins, J. Odenthal, C. Nüsslein-Volhard, Genes controlling and mediating locomotion behavior of the zebrafish embryo and larva, Development 123 (1996) 399–413. http://www.ncbi.nlm.nih.gov/pubmed/9007258.
[24] P.P. Zheng, L.A. Severijnen, M. Van Der Weiden, R. Willemsen, J.M. Kros, A crucial role of caldesmon in vascular development in vivo, Cardiovasc. Res. 81 (2009) 362–369, https://doi.org/10.1093/cvr/cvn294.
[25] P.P. Zheng, L.A. Severijnen, R. Willemsen, J.M. Kros, Caldesmon is essential for cardiac morphogenesis and function: in vivo study using a zebrafish model, Biochem. Biophys. Res. Commun. 378 (2009) 37–40, https://doi.org/10.1016/j.bbrc.2008.10.165.
[26] D.Y.R. Stainier, E. Raz, N.D. Lawson, S.C. Ekker, R.D. Burdine, J.S. Eisen, P.W. Ingham, S. Schulte-Merker, D. Yelon, B.M. Weinstein, M.C. Mullins, S.W. Wilson, L. Ramakrishnan, S.L. Amacher, S.C.F. Neuhauss, A. Meng, N. Mochizuki, P. Panula, C.B. Moens, Guidelines for morpholino use in zebrafish, PLoS Genet. 13 (2017), e1007000, https://doi.org/10.1371/journal.pgen.1007000.
[27] S. Pütz, L.S. Barthel, M. Frohn, D. Metzler, M. Barham, G. Pryymachuk, O. Trunschke, L.T. Lubomirov, J. Hescheler, J.M. Chalovich, W.F. Neiss, M. Koch, M.M. Schroeter, G. Pfitzer, Caldesmon ablation in mice causes umbilical herniation and alters contractility of fetal urinary bladder smooth muscle, J. Gen. Physiol. 153 (2021), https://doi.org/10.1085/jgp.202012776.
[28] H. Guo, R. Huang, S. Semba, J. Kordowska, Y.H. Huh, Y. Khalina-Stackpole, K. Mabuchi, T. Kitazawa, C.L.A. Wang, Ablation of smooth muscle caldesmon affects the relaxation kinetics of arterial muscle, Pflugers Arch. Eur. J. Physiol. 465 (2013) 283–294, https://doi.org/10.1007/s00424-012-1178-8.
[29] H. Guo, C.L.A. Wang, Specific disruption of smooth muscle caldesmon expression in mice, Biochem. Biophys. Res. Commun. 330 (2005) 1132–1137, https://doi.org/10.1016/j.bbrc.2005.03.089.
[30] M. Deng, E. Boopathi, J.A. Hypolite, T. Raabe, S. Chang, S. Zderic, A.J. Wein, S. Chacko, Amino acid mutations in the caldesmon COOH-terminal functional domain increase force generation in bladder smooth muscle, Am. J. Physiol. Ren. Physiol. 305 (2013) 1455–1465, https://doi.org/10.1152/ajprenal.00174.2013.
[31] S. Nie, Y. Kee, M. Bronner-Fraser, Caldesmon regulates actin dynamics to influence cranial neural crest migration in Xenopus, Mol. Biol. Cell 22 (2011) 3355–3365, https://doi.org/10.1091/mbc.E11-02-0165.

TURUN
YLIOPISTO
UNIVERSITY
OF TURKU

Painosalama, Turku, Finland 2026

ISBN 978-952-02-0582-9 (PRINT)
ISBN 978-952-02-0583-6 (PDF)
ISSN 0355-9483 (Print)
ISSN 2343-3213 (Online)